



UNIL | Université de Lausanne

Unicentre

CH-1015 Lausanne

<http://serval.unil.ch>

---

Year : 2022

## Oxysterols as drivers of inflammatory diseases

Ruiz Florian

Ruiz Florian, 2022, Oxysterols as drivers of inflammatory diseases

Originally published at : Thesis, University of Lausanne

Posted at the University of Lausanne Open Archive <http://serval.unil.ch>

Document URN : urn:nbn:ch:serval-BIB\_7B33203F51495

### **Droits d'auteur**

L'Université de Lausanne attire expressément l'attention des utilisateurs sur le fait que tous les documents publiés dans l'Archive SERVAL sont protégés par le droit d'auteur, conformément à la loi fédérale sur le droit d'auteur et les droits voisins (LDA). A ce titre, il est indispensable d'obtenir le consentement préalable de l'auteur et/ou de l'éditeur avant toute utilisation d'une oeuvre ou d'une partie d'une oeuvre ne relevant pas d'une utilisation à des fins personnelles au sens de la LDA (art. 19, al. 1 lettre a). A défaut, tout contrevenant s'expose aux sanctions prévues par cette loi. Nous déclinons toute responsabilité en la matière.

### **Copyright**

The University of Lausanne expressly draws the attention of users to the fact that all documents published in the SERVAL Archive are protected by copyright in accordance with federal law on copyright and similar rights (LDA). Accordingly it is indispensable to obtain prior consent from the author and/or publisher before any use of a work or part of a work for purposes other than personal use within the meaning of LDA (art. 19, para. 1 letter a). Failure to do so will expose offenders to the sanctions laid down by this law. We accept no liability in this respect.



**UNIL** | Université de Lausanne

Faculté de biologie  
et de médecine

**Département des neurosciences cliniques**

# **Oxysterols as drivers of inflammatory diseases**

**Thèse de doctorat en médecine et ès sciences (MD-PhD)**

présentée à la

Faculté de biologie et de médecine  
de l'Université de Lausanne

par

**Florian Ruiz**

Médecin diplômé de la Confédération Helvétique

## **Jury**

Prof. Lorenz Hirt, Président·e et répondant MD-PhD  
Prof. Caroline Pot, Directrice de thèse  
Prof. Delaviz Golshayan, Experte  
Prof. Britta Engelhardt, Experte

Lausanne  
(2022)



UNIL | Université de Lausanne  
Ecole doctorale

**Ecole Doctorale**  
Doctorat MD-PhD

# Imprimatur

Vu le rapport présenté par le jury d'examen, composé de

Président·e	Monsieur Prof. Pedro	<b>Marques-Vidal</b>
Directeur·trice de thèse	Madame Prof. Caroline	<b>Pot Kreis</b>
Répondant·e	Monsieur Prof. Lorenz	<b>Hirt</b>
Expert·e·s	Madame Prof. Déla	<b>Golshayan</b>
	Madame Dre Britta	<b>Engelhardt</b>

le Conseil de Faculté autorise l'impression de la thèse de

## **Monsieur Florian RUIZ**

Master - Diplôme fédéral de médecin Université de Genève

intitulée

### **Le rôle des oxystérols dans les maladies inflammatoires**

Lausanne, le 15 juin 2022

pour Le Doyen  
de la Faculté de Biologie et de Médecine



Prof. Pedro Marques-Vidal

## Acknowledgements

I would like to start by giving a special thanks to my thesis supervisor, Professor Caroline Pot, who gave me the opportunity to work on this fascinating project, helped me to grow as a scientist, guided me and progressively enabled me to gain some autonomy. I am also grateful to my former and current colleagues, Aurélie, Donovan and Yannick, for introducing me to the bench work, Solenne for her help in managing technical issues and her scientific inputs and Benjamin, Jessica and Valentine for their assistance in the experiments. Additionally, I would like to thank Caroline Pot and the entire team again as they enabled me to create a healthy, fun and stimulating work environment. Thanks to them, I will remember my thesis as one of the happiest periods of my life.

I also want to thank Professor Tatiana Petrova, Professor Stéphanie Hugues, Professor Muccioli and Professor Misselwitz for their collaboration. Also a special thanks to Sylvain for all the scientific conversations that we had when we met in the hallway and the entire team of Professor Renaud Dupasquier, including him, for their help to navigate in the fascinating world of neuroimmunology. I am also grateful to the Swiss National Science Foundation for their financial support during the last 3 years of my thesis and for renewing their trust in me for a postdoc mobility. A big thanks also to Francis Derouet and the entire staff of the Epallinges animal facility.

From a more personal standpoint, I would like to thank my Mother, Viviane who is a fantastic human being and who accepted to support me when I decided to get back to my studies after finishing my apprenticeship. I also want to thank Zoé for her support and for being one of the most important people in my life. Finally, I am grateful to my sisters Caroline and Charlotte, my entire family and my friends for their support and for never blaming me for my lack of availability.

## **Acknowledgments**

### **Thesis abstract (English)**

### **Thesis abstract (French)**

#### **1. Introduction**

##### **1.1 Inflammatory diseases and immune imbalance**

##### **1.2 Oxysterols**

###### 1.2.1 Introduction

###### 1.2.2 Ch25h, 25-OHC and 7 $\alpha$ ,25-OHC

###### 1.2.3 Function of the Ch25h pathway in cholesterol homeostasis and lipid metabolism

##### **1.3 Ch25h and 25-OHC in the immune system**

###### 1.3.1 Introduction

###### 1.3.2 Function 25-OHC and Ch25h in the innate immune system

###### 1.3.3 Function 25-OHC and Ch25h in the adaptive immune system

##### **1.4 The chemotactic receptor GPR183**

###### 1.4.1 Introduction

###### 1.4.2 Function in secondary lymphoid organs: adaptive immune response

###### 1.4.3 Function in secondary and tertiary lymphoid organs: development

##### **1.5 Inflammatory bowel disease**

###### 1.5.1 Introduction

###### 1.5.2 Intestinal homeostasis

###### 1.5.3 Risk factors

###### 1.5.4 The role of dysbiosis and bacterial products

###### 1.5.5 The role of innate immune cells

###### 1.5.6 The role of T cells and B cells

1.5.7 Treatment

## **1.6 Multiple sclerosis**

1.6.1 Introduction

1.6.2 Relapsing and progressive multiple sclerosis

1.6.3 Physiopathology of a MS relapse

1.6.4 Treatment

## **1.7 Role of the vasculature in multiple sclerosis**

1.7.1 Endothelial cells

1.7.2 Regulation of inflammatory immune cell trafficking by endothelial cells

1.7.3 Endothelial cells of the central nervous-system: the blood-brain barrier(BBB)

1.7.4 Vascular pathology in MS and EAE

1.7.5 Regulation of leukocytes trafficking in the CNS by endothelial cells

## **2. Aim of the thesis and summary of the results**

**3. Manuscript N°1: The EBI2-oxysterol axis promotes the development of intestinal lymphoid structures and colitis**

**4. Manuscript N°2: A single nucleotide polymorphism in the gene for GPR183 increases its surface expression on blood lymphocytes of patients with inflammatory bowel disease**

**5. Manuscript N°3: Resolution of inflammation during multiple sclerosis**

**6. Manuscript N°4: Endothelial-derived oxysterols regulate myeloid-derived suppressor cell at the blood-brain barrier**

**7. Discussion and perspectives**

**8. References**

## List of figures

- Figure 1. Side chain vs ring-modified oxysterols.
- Figure 2. The Ch25h pathways.
- Figure 3. 25-OHC cellular targets.
- Figure 4. Function of the GPR183/7 $\alpha$ ,25-OHC axis in the germinal center response.
- Figure 5. Comparison of CD and UC, adapted from Robbins basic pathology 10<sup>th</sup> edition.
- Figure 6. IBD pathogenesis, made with Biorender (Biorender.com).
- Figure 7. Acute MS lesions, adapted from Greenfield's Neuropathology, 9<sup>th</sup> edition.
- Figure 8. Model of MS relapses, adapted from manuscript N°3.
- Figure 9. Leukocyte migration across the endothelium, made with Biorender (Biorender.com).
- Figure 10. Graphic representation of the neurovascular unit, made with Biorender (Biorender.com).

## **Abstract (English): Oxysterols as drivers of inflammatory diseases**

Florian Ruiz, MD-PhD student in the laboratory of Professor Pot, Department of clinical neurosciences, Lausanne University Hospital.

A dysregulation of the immune system is at the forefront of multiple sclerosis (MS) and inflammatory bowel disease (IBD). Oxysterols are oxygenated metabolites of cholesterol that display immuno-modulatory functions. In particular, the oxysterols downstream Cholesterol-25-hydroxylase (Ch25h) have been implicated in both IBD and MS.

A single nucleotide polymorphism (SNP) in the GPR183 gene locus, coding for a receptor for an oxysterol downstream Ch25h, is associated with IBD. We therefore interrogated GPR183 expression in peripheral blood mononuclear cells from healthy volunteers (HV) and IBD patients carrying or not the SNP. We found that GPR183 was co-expressed with chemokine receptor implicated in leukocyte trafficking in the inflamed gut. Patients carrying the SNP display an increased GPR183 expression in B cells and increased psoriasis rates.

In addition, Ch25h-deficient mice (Ch25 KO) display an attenuated form of an experimental model of MS, the experimental autoimmune encephalomyelitis (EAE). However, the cellular source of oxysterols during neuroinflammation remains unclear. We thus developed a floxed-reporter Ch25h-Knock-in mouse and demonstrated that ablation of Ch25h in central nervous system endothelial cells (CNS ECs) is sufficient to attenuate EAE. Mechanistically, ablation of Ch25h in inflamed CNS ECs activates a transcriptomic program inducing a “glioblastoma-associated endothelial cell-like” profile and a lipid remodeling that favored the expansion of immune-suppressive cells associated with cancer: myeloid-derived suppressor cells (MDSC). Accordingly, deletion of Ch25h in ECs favored the accumulation of MDSC in the CNS during EAE and reduced CD4 T cell proliferation.

Overall, the results of this thesis indicate that the Ch25h pathway is implicated in inflammatory diseases. Our results suggest that Ch25h favors CD4 T cell infiltration into the intestine and restricts MDSC accumulation in the CNS. Additional studies are necessary to confirm the relevance of these findings but the results of this thesis suggest that Ch25h might be an attractive therapeutic target for inflammatory diseases.

## **Abstract (French) : Le rôle des oxystérols dans les maladies inflammatoires**

Florian Ruiz, Etudiant MD-PhD dans le laboratoire de la Pre Pot, Département des neurosciences cliniques, Centre hospitalier universitaire vaudois.

Un dérèglement du système immunitaire est au premier plan de la sclérose en plaques (SEP) et des maladies inflammatoires de l'intestin (MICI). Les oxystérols sont des métabolites oxygénés du cholestérol qui présentent des fonctions immuno-modulatrices. En particulier, les oxystérols en aval de la cholestérol-25-hydroxylase (Ch25h) ont été impliqués à la fois dans les MICI et la SEP.

Un polymorphisme nucléotidique (PN) dans le locus du gène GPR183, codant pour un récepteur à un oxystérol dérivé de Ch25h est associé aux MICI. Nous avons donc évalué l'expression de GPR183 dans les cellules du sang périphérique de volontaires sains (VS) et de patients atteints de MICI porteurs ou non du PN. Nous avons découvert que GPR183 était co-exprimé avec des récepteurs de chimiokines impliqué dans le trafic de leucocytes dans l'intestin inflammé. Les patients porteurs du PN ont une expression augmentée GPR183 dans les cellules B et un taux augmenté de psoriasis.

De plus, les souris Ch25h KO, présentent une forme atténuée d'un modèle expérimental de SEP, l'encéphalomyélite auto-immune expérimentale (EAE). Cependant, la source cellulaire des oxystérols dans la neuroinflammation reste floue. Nous avons donc développé des souris Ch25h floxée et démontré que l'ablation de Ch25h dans les cellules endothéliales du système nerveux central (CE du SNC) est suffisante pour atténuer l'EAE. L'ablation de Ch25h dans les CE enflammées du SNC active un programme transcriptomique induisant un profil ressemblant aux CE du glioblastome et un remodelage lipidique qui favorise l'expansion des cellules immunosuppressives associées au cancer : les cellules myéloïdes suppressive (CMS). En conséquence, la suppression de Ch25h dans les CE favorise l'accumulation de CMS dans le SNC pendant l'EAE et réduit la prolifération des cellules T CD4. Les résultats de cette thèse indiquent que la voie Ch25h est impliquée dans les maladies inflammatoires. Nos résultats suggèrent que Ch25h favorise l'infiltration des lymphocytes T CD4 dans l'intestin et limite l'accumulation des CMS dans le SNC et que Ch25h pourrait être une cible thérapeutique intéressante pour les maladies inflammatoires.

## 1.1 Inflammatory diseases and immune imbalance

Inflammatory diseases are a group of incurable pathologies characterized by a dysregulation of the immune system leading to chronic inflammation and tissue damages that can be organ-specific or systemic<sup>1</sup>. It is estimated that they affect 3 to 7% of the population<sup>3</sup>. Our understanding of their pathophysiology remains limited, however, we consider that they are the result of specific environmental triggers in genetically susceptible individuals<sup>4</sup>.

Exogenous triggers, such as invading pathogens or foreign bodies, or endogenous triggers, such as abnormal cells can activate the inflammatory response. The removal of the causative agent is an active process that is limited by counter-regulatory mechanisms preventing excessive inflammation and, resolving mechanisms enabling wound healing and cessation of the response once the harmful stimulus has been cleared<sup>5</sup>.

The inflammatory response results from a cross-talk between organ-specific resident cells, stromal cells, and tissue-infiltrating cells<sup>5</sup>. Cell-to-cell communication is regulated by different molecular cues, including cytokines, growth factors, and bioactive lipids. Deregulation of this cross-talk can lead to a pathologic state, where the inflammatory reaction is inappropriate or fails to resolve. This state of immune imbalance is considered crucial for the pathogenesis of inflammatory diseases and may originate from a defective function of anti-inflammatory signals, excessive activity of pro-inflammatory signals, or a combination of both<sup>2</sup>.

One caveat to this notion could be summarized by a statement of a French epistemologist in his book "The formation of the scientific mind": "A knowledge that

lacks precision, or, to put it better, a knowledge that is not given with its precise conditions of determination is not a scientific knowledge”.

Even though Gaston Bachelard was not referring to the cellular and molecular networks involved in the inflammatory response, the specific context (i.e. the conditions of determination) in which a molecular signal is present can determine whether it acts as a pro or an anti-inflammatory signal. It is therefore not always appropriate (i.e. not a scientific statement or a truth per se) to present one cytokine or one bioactive lipid as pro or anti-inflammatory as these molecular cues are always working in coordination with other signals and can have different effects depending on the cell on which they act. Therefore, it should be noted that the pro or anti-inflammatory role of the main pathway studied in this thesis, the Ch25h pathway, is context-dependent even though for inflammatory bowel diseases and multiple sclerosis, our data indicate a pro-inflammatory function.

## **1.2 Oxysterols**

### 1.2.1 Introduction

The acquisition of the ability to synthesize sterols is an early event in eukaryogenesis<sup>6</sup>, indicating a crucial role of these compounds in cellular functions. Sterols, in particular cholesterol, are essential for the regulation of membrane fluidity. They are also critically involved in inter and intra-cellular communication. Oxidation of sterols, generally cholesterol, gives rise to oxysterols<sup>7</sup>. Oxysterols are subdivided into **primary** and **secondary** oxysterols (Figure 1).

**Primary oxysterols** carry only one modification compared with the native cholesterol molecule and can be further subdivided into:

- i) side-chain oxysterols, namely: 24(S)-hydroxycholesterol (24-(S)OHC), **25-hydroxycholesterol (25-OHC)**, and 27-hydroxycholesterol (27-OHC)
- ii) ring-modified oxysterols, namely: 7-hydroperoxycholesterol (7OOHC), 7 $\alpha$ -hydroxycholesterol (7 $\alpha$ -OHC), 7 $\beta$ -hydroxycholesterol (7 $\beta$ -OHC), and 7-ketocholesterol (7K-OHC).

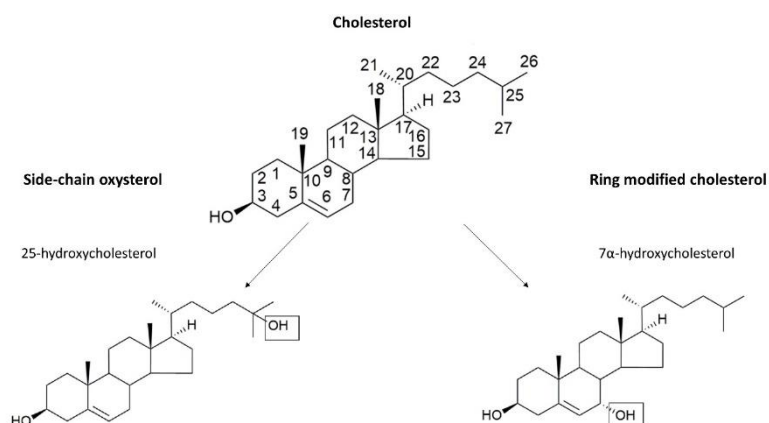


Figure 1. Comparison of the structural formula of cholesterol, 25-hydroxycholesterol, and 7 $\alpha$ -hydroxycholesterol. Structural formulas from Wang et al<sup>8</sup> were used.

**Secondary oxysterols** (e.g. **7 $\alpha$ ,25-dihydroxycholesterol (7 $\alpha$ ,25-OHC)** and **7K,25-dihydroxycholesterol (7K,25-OHC)**) contains more than one modification. Oxysterol concentrations compared to cholesterol are low, ranging usually from nM to  $\mu$ M<sup>9</sup> but can be substantially altered in various pathological conditions such as inflammatory or neurodegenerative diseases<sup>10, 11, 12</sup>.

Oxysterols are generated by either non-enzymatic oxidation (mainly by free radical attacks) or through enzymatic oxidation. The vast majority of oxysterol-producing enzymes belong to the cytochrome P450 family<sup>13</sup> and are located in the endoplasmic reticulum or the mitochondria<sup>14</sup>. A full description of oxysterols metabolizing enzymes and the biological function of their products is out of the scope of this thesis. Hence, we are going to mainly focus on the principal pathway explored during this project, which is the Cholesterol-25-hydroxylase (Ch25h) pathway.

### 1.2.2 Ch25h, 25-OHC, and 7 $\alpha$ ,25-OHC

Cholesterol-25-hydroxylase (Ch25h) is a peculiar oxysterol metabolizing enzyme since it does not belong to the cytochrome P450 family. It is encoded by an intronless gene and is an enzyme that utilizes diiron cofactors to catalyze the hydroxylation of cholesterol<sup>15</sup>. It is the rate-limiting enzyme for the conversion of cholesterol into 25-OHC. It also catalyzes the conversion of 7K-OHC into 7K, 25-OHC<sup>16</sup>. Additionally, 25-OHC can be metabolized into 7 $\alpha$ ,25-OHC by Cyp7b1, an enzyme belonging to the cytochrome P450 family. 7 $\alpha$ ,25-OHC can be further metabolized by Hydroxy-Delta-5-Steroid Dehydrogenase, 3 Beta- And Steroid Delta-Isomerase 7 (HSD3B7) into bile acid precursors (Figure 2).

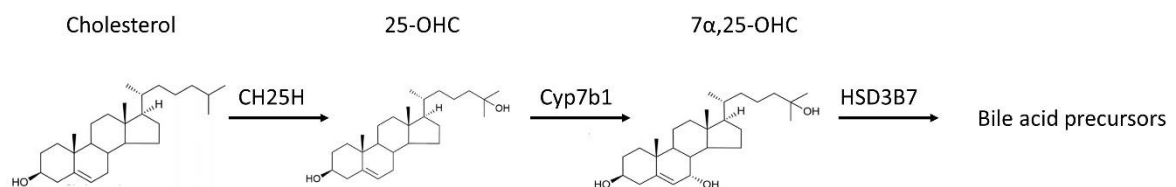


Figure 2. The Ch25h pathway.

### 1.2.3 Function of the Ch25h pathway in cholesterol homeostasis and lipid metabolism

Historically, the impact of oxysterols on metabolism attracted most of the attention. This is in part, due to the emergence of the "Oxysterol Hypothesis of Cholesterol Homeostasis"<sup>7, 17</sup>. Landmark studies revealed that cholesterol is capable of suppressing its synthesis<sup>18</sup>. It was then proposed that the feedback regulation of cholesterol biosynthesis is not mediated by cholesterol itself but rather achieved by an oxygenated form of cholesterol, oxysterols<sup>19</sup>. Later, it became clear that cholesterol is also playing a role in the regulation of its metabolism<sup>20, 21</sup>. Since then, the molecular mechanisms toward which cholesterol can restrain its synthesis have been deciphered<sup>22</sup>.

Sterol Regulatory Element Binding Protein 2 (SREBP2) is a key transcription factor in the regulation of cholesterol homeostasis. SREBP2 is synthesized as an endoplasmic reticulum-anchored precursor<sup>22</sup>. To become active, it needs to be translocated first to the Golgi apparatus to be cleaved by specific proteases (Site protease 1 and 2)<sup>22</sup>. It is then further exported to the nucleus where it induces the transcription of genes associated with cholesterol homeostasis, most notably hydroxy-3-methylglutaryl-CoA (HMG-CoA reductase) the rate-limiting enzyme for cholesterol biosynthesis<sup>22</sup>. SREBP cleavage-activating protein (SCAP) escorts SREBP2 from the endoplasmic reticulum (ER) to the Golgi apparatus. It also acts as a cholesterol sensor; high cholesterol concentration induces a conformational change of SCAP, favoring its interaction with insulin-induced genes (INSIG) resulting in SREBP2 retention in the ER. 25-OHC acts in a similar fashion by altering INSIG conformation and favoring its interaction with

SCAP, eventually inhibiting SREBP2 processing<sup>18</sup>. *In-vitro*, 25-OHC is more potent than cholesterol to suppress SREBP2 nuclear translocation<sup>23</sup>.

25-OHC is also an agonist of Liver X Receptors (LXRs) along with other oxysterols<sup>24</sup>,<sup>25</sup>. LXRs belong to the superfamily of nuclear receptors and are master regulators of lipid homeostasis<sup>26</sup>. They exist in two isoforms, LXR $\alpha$  and LXR $\beta$ <sup>26</sup>. To become active, they need to form heterodimers with Retinoid-X-Receptor- $\alpha$  (RXR $\alpha$ )<sup>26</sup>. LXRs and SREBP2 collaborate to regulate cholesterol homeostasis. LXRs activation promote the expression of genes implicated in cholesterol efflux and also prevent SREBP2 translocation to the Golgi apparatus<sup>26</sup>.

Retinoic acid-related Orphan Receptor  $\alpha$  (ROR $\alpha$ ) is another nuclear receptor involved in the regulation of immune response, cellular differentiation, cerebellum development, and lipid metabolism<sup>27, 28, 29, 30, 31</sup>. 25-OHC has been shown to work as an inverse agonist for this receptor<sup>32</sup>. Recent data indicates that ROR $\alpha$  activation restrains the expression of genes implicated in cholesterol efflux and that its inhibition reduces the expression of HMG-CoA reductase and SREBP2<sup>29</sup>.

Thus in case of high intracellular cholesterol concentrations, cholesterol is converted into 25-OHC which could reduce intracellular levels of cholesterol by restraining cholesterol synthesis and favoring cholesterol efflux by inhibiting SREBP2 and ROR $\alpha$  and by activating LXRs (Figure 3).

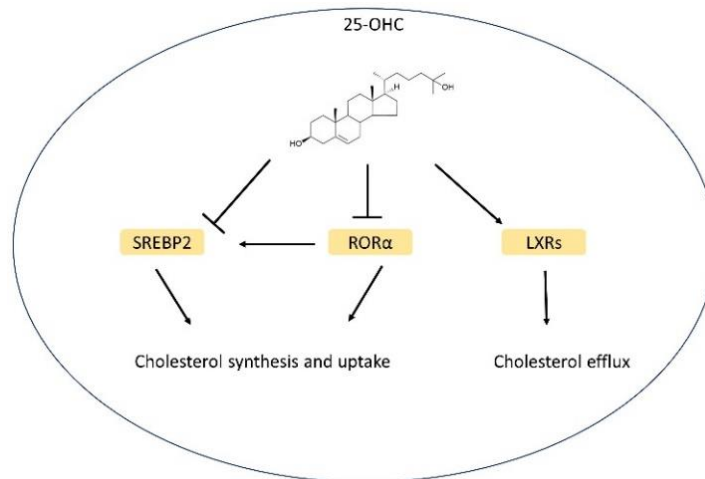


Figure 3. 25-OHC cellular targets regulating intracellular cholesterol homeostasis. SREBP2: sterol regulatory element binding protein 2, ROR $\alpha$ : retinoic acid-related orphan receptor. LXRs: liver X receptor.

The identification of 25-OHC cellular targets enabled us to predict its involvement in cholesterol homeostasis. However, previous reports suggest that germline Ch25h knockout (Ch25h KO) mice display normal cholesterol levels. It should be noted that these results are unpublished and only reported without any mention of the experimental approaches employed to address this question<sup>33, 34</sup>. Additionally, other enzymes display a 25-hydroxylase activity and hence could compensate for the lack of Ch25h<sup>35</sup>. Interestingly, Hereditary Spastic Paraplegia type 5 (SPG5), a rare autosomal recessive neurodegenerative disease caused by a loss-of-function mutation of Cyp7b1 is associated with a dramatic increase in circulating 25-OHC<sup>36</sup>. Despite that, these patients display normal cholesterol levels in the plasma<sup>36</sup>, questioning the *in-vivo* relevance of 25-OHC in the regulation of systemic cholesterol levels. Similarly, the vast majority of studies implicating 25-OHC as an activator of

LXRs were performed *in-vitro*, with low evidence that 25-OHC is indeed an important modulator of LXRs activity *in-vivo*<sup>37</sup>. This raises the question of the function of 25-OHC in other biological processes.

### **1.3 Ch25h and 25-OHC in the immune system**

#### **1.3.1 Introduction**

While performing screening of genes upregulated by Lipopolysaccharide (LPS) in mouse bone marrow-derived macrophages, Diczfalusy and colleagues identified a strong upregulation of Ch25h<sup>38</sup>. It was also demonstrated that Ch25h KO mice displayed increased serum IgA levels while Cyp7b1 KO mice showed decreased levels compared with their wild type (WT) counterparts<sup>39</sup>. Those seminal findings paved the way for investigations of the role of Ch25h in the immune system.

Since then, multiple studies evaluated the function of Ch25h in inflammatory conditions affecting various cell compartments and organs<sup>40, 41, 42, 43, 44, 45, 46, 47</sup>, indicating a pro or an anti-inflammatory role depending on the model. The multiple cellular targets of 25-OHC could partially explain those discrepancies. In addition, the downstream metabolite of 25-OHC, 7 $\alpha$ ,25-OHC also display immunomodulatory functions, however, its only described cellular target is the chemotactic receptor GPR183<sup>10</sup>. The role of this receptor in the immune system will be described below. It should also be noted that 25-OHC is an anti-viral molecule and can also limit the proliferation of some intracellular bacterias through non-immune mechanisms<sup>48</sup>.

### 1.3.2 Function 25-OHC and Ch25h in the innate immune system

LPS-induced upregulation of Ch25h is dependent on type I interferon signaling<sup>49</sup> and myeloid cells were the first source of 25-OHC identified<sup>38</sup>. In addition, Ch25h is upregulated in myeloid cells by other Toll-like receptor agonists<sup>42</sup>, pro-inflammatory cytokines including interleukin-6 (IL-6), interleukin-1 $\beta$  (IL-1 $\beta$ ), and tumor necrosis factors  $\alpha$  (TNF- $\alpha$ ) in a signal transducer and activator of transcription 1 (Stat1) dependent manner<sup>50</sup>. Functionally, 25-OHC restrains interleukin-1 $\beta$  (IL-1 $\beta$ ) production in macrophages through SREBP2 inhibition and by maintaining mitochondrial integrity<sup>40, 44</sup>, suggesting an anti-inflammatory function. Moreover, LXRs activation suppresses the production of IL-6, IL-1 $\beta$ , TNF- $\alpha$ , and inducible nitric oxide synthase (iNOS) which are considered pro-inflammatory signals<sup>51, 52, 53, 54</sup>. In line with this, intratracheal infusion of 25-OHC reduces leukocyte infiltration and TNF- $\alpha$  production in a mouse model of acute lung injury<sup>55</sup>. Still in lung inflammation, Ch25h expression by alveolar macrophages enables clearance of apoptotic neutrophils (efferocytosis)<sup>56</sup>, an essential mechanism of inflammation resolution. 25-OHC has recently been shown to suppress Interferon- $\gamma$  (IFN- $\gamma$ ) signaling in microglia<sup>57</sup>.

Alternatively, in macrophages and microglia, 25-OHC at  $\mu$ molar concentration can promote inflammasome assembly and favor IL-1 $\beta$  secretion<sup>58, 59</sup>. Intracerebral injection of 25-OHC induces recruitment and activation of microglia/macrophages<sup>58</sup>. Other groups have shown that 25-OHC potentiates IL-6 and colony-stimulating factor 1 (CSF1 or M-CSF) productions and that 25-OHC exacerbates lung inflammation in a mouse model of influenza infection<sup>42</sup>. By acting as an inverse agonist of ROR $\alpha$ , 25-OHC favors lipid droplet accumulation in macrophages<sup>60</sup>. Furthermore lipid droplet

accumulation favors macrophage infiltration and activation in tissues<sup>61</sup>. In addition, 25-OHC production promotes the transition of macrophages from a so-called M1 pro-inflammatory state to an M2 anti-inflammatory phenotype<sup>62</sup>.

Therefore, Ch25h and 25-OHC can activate or amplify pro and anti-inflammatory programs on monocytes/macrophages. The reasons for these contradictory findings remain a conundrum. The fact that 25-OHC can be metabolized in 7 $\alpha$ ,25-OHC, that Ch25h can produce 7K,25-OHC, and that these three oxysterols have different cellular targets complicate the picture. In addition, monocytes are highly plastic and can become “tolerant” to endotoxin stimulation, and therefore, their response to LPS can differ if they were previously exposed to it<sup>63, 64</sup>. They have a form of “innate memory”<sup>65</sup> and tissue-resident macrophages display an impressive diversity in different organs<sup>64</sup>. In addition, some authors have proposed that nanomolar concentrations of 25-OHC could be anti-inflammatory while micromolar concentrations could be pro-inflammatory, suggesting a bi-modal signaling of 25-OHC<sup>66</sup>. Therefore, the impact of 25-OHC and Ch25h downstream signaling might be influenced by its concentration, the state or the organ in which macrophages reside and by the influence of previous exposure to microorganism and their products.

### 1.3.3 Function 25-OHC and Ch25h in the adaptive immune system

Compared to myeloid cells, the function of 25-OHC in the regulation of the adaptive immune system is less studied. In Peyer’s patches, 25-OHC produced by follicular dendritic cells suppresses the differentiation of germinal center B cells into IgA producing plasma cells through inhibition of SREBP2<sup>67</sup>.

Ch25h is also upregulated in IL-27 induced Type 1 regulatory T cells in a Stat1 and IRF1 dependent manner<sup>68, 69</sup>. In that context, 25-OHC negatively regulates IL-10 production through LXR signaling<sup>69</sup>, inhibits T cell proliferation, and favors cell death through nutrient deprivation<sup>68, 69</sup>.

25-OHC is also a ligand of retinoic acid receptor-related orphan receptor- $\gamma$ <sup>70</sup> (ROR- $\gamma$ ) the master regulator for Th17 cell differentiation. However, evidence of the role of Ch25h in Th17 cell development is lacking.

## **1.4 The chemotactic receptor GPR183**

### 1.4.1 Introduction

As mentioned above, 25-OHC can be further hydroxylated to form 7 $\alpha$ ,25-OHC. 7 $\alpha$ ,25-OHC is the strongest ligand of the chemotactic receptor GPR183 also known as Epstein-Bar Virus-induced G-protein coupled receptor 2 (EBI2)<sup>71, 72</sup>. 7 $\alpha$ ,27-OHC, and 25-OHC can activate GPR183 but are less potent than 7 $\alpha$ ,25-OHC<sup>71, 72</sup>. GPR183 is a 7 transmembrane G- $\alpha$ i coupled receptor<sup>73</sup> that was first discovered as an Epstein-Bar virus-induced gene<sup>74</sup>. A role for this receptor in immune cell chemotaxis was then identified<sup>71, 72, 75</sup>. Since, GPR183 expression has been described in B cells<sup>71, 72</sup>, T cells<sup>76</sup>, dendritic cells<sup>77</sup>, monocyte/macrophages<sup>78</sup>, neutrophils<sup>72</sup>, innate lymphoid cells type 3 (ILC3s)<sup>41</sup>, eosinophils<sup>79</sup>, platelets<sup>80</sup>, astrocytes<sup>81</sup>, microglia<sup>82</sup>, osteoclast<sup>83</sup> and endothelial cells<sup>84</sup>. Thus, the biological function of GPR183 is not limited to the regulation of immune cell chemotaxis. However, in this thesis, we are going to focus on its function on the immune system. To describe its function, we will consider its dependence on the presence of its ligand, whose production is regulated by the

enzymatic cascade described in Figure 2. Thus, this pathway will be now referred to as the GPR183/7 $\alpha$ ,25-OHC axis.

#### 1.4.2 Function in secondary lymphoid organs: adaptive immune response

Secondary lymphoid organs (SLOs), the site where lymphocytes encounter their cognate antigen, are central to the adaptive immune response. They display a remarkable organization with multiple microenvironmental niches favoring efficient antigen presentation, lymphocyte proliferation, and cell-fate commitment<sup>85</sup> (e.g. long-term memory B cells or antibody-producing plasma cells).

B cells, T cells, and different subsets of antigen presenting cells (APCs, e.g. dendritic cells) are present in distinct compartments within SLOs (Figure 4). This compartmentalization is regulated by a network of chemotactic receptors and their ligands<sup>86, 87</sup>. The GPR183/7 $\alpha$ ,25-OHC axis is a part of this chemotactic network, where it fine-tunes immune cell positioning within specific SLO's compartments.

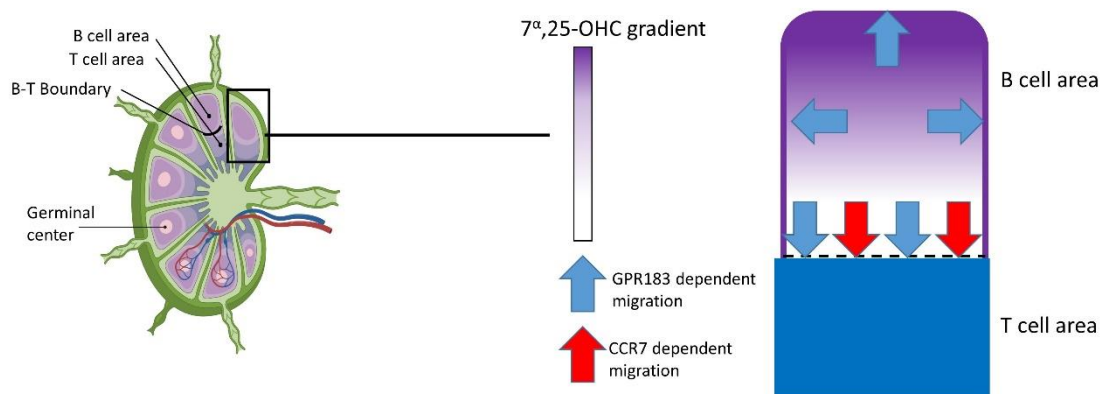


Figure 4. The function of the GPR183/7 $\alpha$ ,25-OHC axis in the germinal center response. Left panel: B cells and T cells location in lymph nodes. Right panel: Activation of B cells through BCR signaling quickly upregulates GPR183 which induces B cell migration to the outer follicular region (dark violet, blue arrows) where 7 $\alpha$ ,25-OHC concentration is supposedly the highest. This happens 2-3h after an antigenic challenge. 6h after the challenge, B

*cells upregulate CCR7 and move to the B-T boundary where CCL19 and CCL21 are produced to receive T cell help (red arrows). At this step, CCR7 and GPR183 collaborate to uniformly distribute B cells at the B-T boundary.*

Functionally, alteration of GPR183/  $7\alpha,25\text{-OHC}$ -mediated positioning will result in a defective T-dependent antibody response through multiple mechanisms. In the lymph nodes, GPR183, in collaboration with CCR7, favors the positioning of B cells at the T-B boundary<sup>75, 88</sup>, enabling T cells to induce B cell proliferation and differentiation during germinal center responses<sup>89, 90</sup>. GPR183 is also involved in T lymphocyte differentiation into T follicular helper cells<sup>91</sup>, a subset of leukocytes essential to the T-dependent humoral response<sup>92</sup>. In the spleen, GPR183 favors the positioning and development of CD4<sup>+</sup> dendritic cells<sup>77, 93</sup>, which are involved in extrafollicular T-dependent antibody response<sup>94</sup>.

In addition, GPR183/ $7\alpha,25\text{-OHC}$  mediated positioning of naïve CD4<sup>+</sup> T cells at the periphery of the T cell area favors their activation, expansion, and differentiation<sup>95</sup>. GPR183 KO mice display an impaired CD4-dependent helminth infection clearance<sup>95</sup>. They also fail to mount a CD4-dependent CD8 memory response against plasmodium<sup>95</sup>.

Therefore, the GPR183/ $7\alpha,25\text{-OHC}$  axis could be seen as a fine tuner of immune cell positioning within SLOs that optimize the adaptive immune response to favor pathogen clearance.

#### 1.4.3 Function in secondary and tertiary lymphoid organs: development

Besides its involvement in the optimization of the adaptive immune response, GPR183 participates in the formation of tertiary lymphoid organs (TLOs). Histologically and

functionally speaking, these lymphoid structures closely resemble SLOs<sup>96</sup>, however, in contrast to SLOs, TLOs arise after birth<sup>97</sup> and usually develop in diseases associated with chronic inflammation such as cancer or autoimmunity<sup>98</sup>.

As mentioned above, GPR183 is expressed by ILC3s<sup>41</sup>. Innate lymphoid cells are derived from the same committed progenitor as lymphocytes during hematopoiesis, but they lack a recombination-activating gene (RAG)-dependent rearranged antigenic receptor<sup>99, 100</sup>. As for T helper cells, they are subdivided into three subtypes (ILC1s, ILC2s, and ILC3s) based on their production of type 1, type 2, and Th17 cell-derived cytokines<sup>100</sup>. Like Th17 cells, ILC3 development depends on the master regulator ROR $\gamma$ t that is a key inducer of IL-17 and IL-22<sup>101</sup>. These cells are important for lymphoid tissue organogenesis<sup>102</sup>. In the gut, the GPR183/7 $\alpha$ ,25-OHC axis is responsible for ILC3 accumulation in TLOs such as cryptopatches (CPs) and isolated lymphoid follicles (ILF) and is essential for the formation of these structures in the colon<sup>41, 47</sup>. It might also be involved in the formation of CPs in the small intestine<sup>103</sup>, however, these results are controversial<sup>41</sup>. GPR183 expression by ILC3s is important for their capacity to clear enteric pathogen<sup>103</sup> and enhances inflammation in a mouse model of immune-mediated colitis<sup>41</sup>.

Furthermore, the GPR183/7 $\alpha$ ,25-OHC axis-dependent B cell migration has also been implicated in the formation of TLOs in a mouse model of chronic obstructive pulmonary disease (COPD)<sup>43</sup> and a mouse model of lymphocytic bronchiolitis post-lung transplantation<sup>104</sup>. In these two models, a dampening of the GPR183/7 $\alpha$ ,25-OHC axis resulted in a reduced formation of TLOs and lung inflammation<sup>43, 104</sup>. In contrast, intestinal SLOs, (e.g. mesenteric lymph nodes, Peyer's patches (PP), and colonic patches (CLP)) that are formed in-utero<sup>97</sup> develop normally in GPR183 KO or Ch25h KO mice<sup>41, 47</sup>. All those results suggest that the GPR183/7 $\alpha$ ,25-OHC axis is implicated

in the formation of TLOs and not SLOs. The function of this axis might be redundant for the homeostatic or “normal” development of lymphoid organs. However, it might be essential for the emergence of tertiary lymphoid organs, which are usually associated with chronic inflammation.

<b>Organ and model</b>	<b>Genotype</b>	<b>Phenotype</b>	<b>Reference</b>
Lungs, cigarette smoke exposure-induced emphysema	Ch25h KO, GPR183 KO	Reduced number of B cell-dependent iBALT and inflammation	Jia et al. 2018 <sup>43</sup>
Small intestine, steady state  Colon, steady state	GPR183 KO	Reduced number of CPs  Reduced number of ILFs and CPs	Chu et al. 2018 <sup>103</sup>
Small intestine, steady state  Colon, steady state	RAG-1 deficient GPR183 KO	Normal number of CPs and ILFs  Reduces the number of CPs and ILFs	Emgard et al., 2018 <sup>41</sup>
Colon, steady state	GPR 183 KO	Reduced number of ILFs	Wyss et al.2019 <sup>47</sup>
Colon, DSS-induced colitis  Colon, IL-10 KO colitis model	Ch25h KO, GPR 183 KO  IL-10 KO and GPR183 KO	Reduced number of lymphoid structures, normal inflammation  Reduced number of lymphoid structures and inflammation	Wyss et al.2019 <sup>47</sup>
Lungs, post lung transplantation lymphocytic bronchiolitis	GPR183 KO	Reduced number of TLOs	Smirnova et al.2019 <sup>104</sup>

Table 1. Overview of the impact of defects in the GPR183/7α,25-OHC axis in TLOs formation. iBALT: inducible bronchus-associated lymphoid tissue, CP: cryptopatches, ILF: isolated lymphoid follicle. Wyss et al. is our collaborative work with B. Misselwitz's research group.

## 1.5 Inflammatory bowel diseases

### 1.5.1 Introduction

Inflammatory bowel diseases (IBD) include two clinical entities: Ulcerative Colitis (UC) and Crohn's disease (CD). They are both chronic relapsing inflammatory diseases primarily affecting the gastrointestinal tract and display similar clinical features<sup>105, 106</sup>. However, they are considered to be separate diseases. The clinical presentation of these two pathologies is highly overlapping, with patients presenting bloody diarrhea, hematochezia, abdominal pain, and fatigue<sup>105, 106</sup>. Patients suffering from IBD often develop extra-intestinal symptoms that can affect skin, eyes, urinary and respiratory tracts, bile duct and joints<sup>107</sup>.

The prevalence and incidence of these diseases are increasing<sup>108</sup> with the incidence of CD ranging from 0.4 to 22.8 per 100 000 person-years and UC ranging from 2.4 to 44.0 per 100 000 person-years in Europe<sup>109</sup>. Gender-specific prevalence is less striking than in other immune-mediated diseases such as multiple sclerosis and differs between CD and UC and with age<sup>110</sup>. CD can virtually affect all segments of the gastrointestinal tract from the mouth to the anus. The histopathology is characterized by discontinuous lesions displaying transmural inflammatory lymphoid aggregates<sup>111</sup>. Moreover, granulomas are hallmark findings of this disease even though they are not identified in all patients<sup>111</sup>. By opposition, UC is usually restricted to the colon and rectum and lesions are confined to the mucosal and submucosal layers and do not display granulomas<sup>111</sup>.

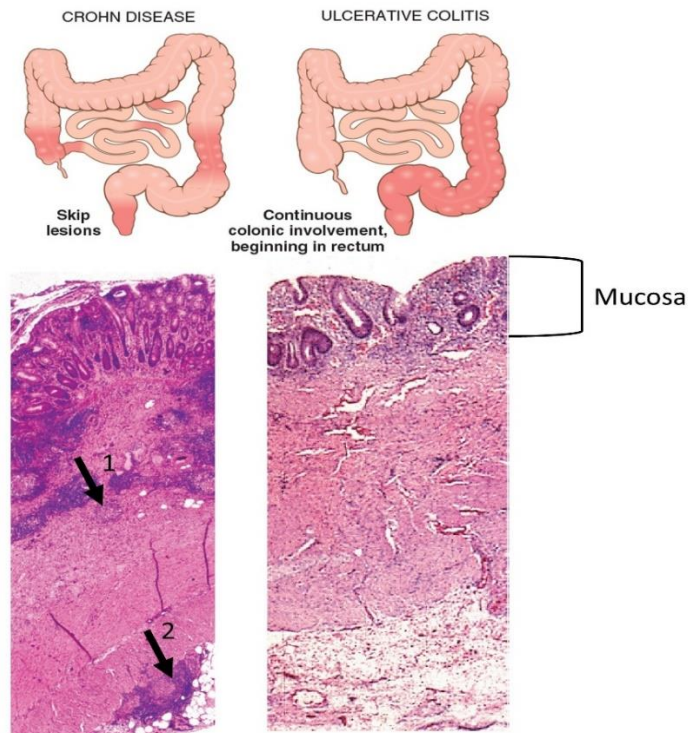


Figure 5. Comparison of CD and UC. Top left: Discontinuous (skip) lesions are illustrated. Bottom left: Transverse section of CD affected intestine showing the transmural aspect of CD. Arrow 1 indicate a submucosal granuloma and arrow 2 indicate serosal granuloma. Top right: continuous lesions of UC restricted to the colon. Bottom right: inflammatory infiltrate restricted to the mucosal layer can be seen. Adapted from Robbins basic pathology 10th edition.

### 1.5.2 Intestinal homeostasis

The gastrointestinal tract is constantly exposed to dietary antigens, commensal bacteria, and pathogenic micro-organisms. Hence, to maintain homeostasis, the intestinal immune system needs to be at the same time tolerant to non-harmful antigens while preserving its capacity to clear pathogens <sup>112</sup>.

It is postulated that IBD emergence results from an altered mucosal immune response to gut microbiota in patients presenting genetic predisposition <sup>113</sup>. Intestinal homeostasis relies on a complex cross-talk between the immune system, the intestinal epithelium, and the microbiota, and alterations in this cross-talk result in intestinal inflammation and IBD<sup>114</sup> (Figure 6).

## Homeostasis

## IBD

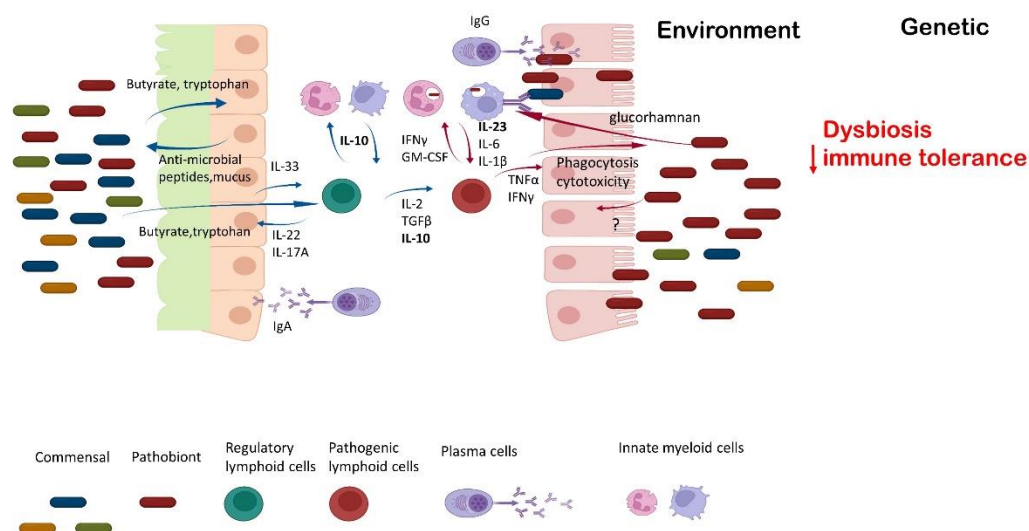


Figure 6. Simplified model of IBD pathogenesis. Left: During homeostasis, a thick layer of mucus (green) and anti-microbial peptides produced by intestinal epithelial cells protects the epithelium and the lamina propria and maintain an eubiotic state with a high diversity of bacteria and a dominance of commensal microorganism. IgA producing plasma cells are also involved in this process. Microbial or diet derived products, such as butyrate and tryptophan favor immune tolerance through induction of regulatory lymphocytes and promote epithelial barrier function. Regulatory lymphocytes produce cytokines (IL-22 and IL-17A) favoring epithelial barrier function while epithelial cells produce IL-33 inducing a regulatory phenotype. IL-10 plays a key role in maintaining intestinal homeostasis and in the cross-talk between myeloid and lymphoid cells. Right: During IBD a combination of environmental and genetic factors will alter intestinal homeostasis. A dysbiosis, characterized by a reduced bacterial diversity and a potential excessive proliferation of pathobionts is observed. Microbial derived products (e.g. glucorhamnan) induce pro-inflammatory myeloid cells. Increased epithelial permeability induced by pro-inflammatory signals (e.g TNF- $\alpha$  and INF $\gamma$ ) derived from innate and adaptive immune will results in leakage of the gut luminal content and bacterial infiltration. A reduction in the mucus layer is observed. Myeloid cell will engulf bacteria, become activated and stimulate adaptive immune cells. IL-23 plays a key role in this process. INF $\gamma$  and GM-CSF derived from activated lymphoid cells enhance myeloid cell activation. IgG-opsonized bacteria can further activate mononuclear phagocytes promoting tissue damage.

The lamina propria of the intestine is separated from the luminal resident microbiota by a thick layer of mucus and a single layer of epithelial cells. In addition, IgA, cytokines, and anti-microbial peptides produced by gut-resident immune and non-immune cells further control the integrity of the intestinal barrier and prevent leakage of the luminal content on the lamina propria<sup>115</sup>. To complicate the picture, the microbiome and its products participate in the regulation of the intestinal barrier

integrity and intestinal immune homeostasis<sup>116</sup> as microbial sensing controls cytokine, anti-microbial peptides, and growth factor production by intestinal resident cells<sup>117</sup>.

### 1.5.3 Risk factors

IBD environmental risk factors include low vitamin D status, smoking, antibiotic exposure during infancy, appendectomy, and diet<sup>118</sup>.

Moreover, genome-wide association studies (GWAS) have identified 163 loci associated with IBDs, among them, 30 are specific to CD and 23 to UC, and the other 110 are associated with both diseases<sup>119</sup>. They display an enrichment for immune-related pathways, host response to mycobacterial infection, and preservation of intestinal barriers<sup>120, 121 119</sup>. In particular, mutations in the nucleotide-binding oligomerization domain containing 2 (NOD2) locus are associated with CD<sup>122, 123</sup>. NOD2 is an intracellular pattern recognition receptor (PRR) expressed by hematopoietic and intestinal epithelial cells<sup>124</sup>. Most of the mutations in its locus associated with CD induce a loss-of-function<sup>125</sup>. It is therefore proposed that the increased risk of CD associated with NOD2 is due to defective clearance of pro-inflammatory bacteria but it remains to be clarified<sup>125</sup>. Besides, NOD2 is an inducer of autophagy in myeloid cells<sup>126</sup> and other mutations in genes involved in autophagy have been associated with CD<sup>127, 128</sup>. Autophagy is an important component of intestinal homeostasis, as it is involved in microbial sensing and antigen presentation<sup>126</sup> and can also protect intestinal epithelial cells from pro-apoptotic signals such as tumor necrosis factor  $\alpha$  (TNF- $\alpha$ )<sup>129</sup>. Therefore, autophagy is considered to be implicated in IBD pathophysiology through its involvement in the regulation of gut microbiota and intestinal barrier.

#### 1.5.4 The role of dysbiosis and bacterial products

The gut microbiota is a key element of intestinal homeostasis<sup>130</sup> as it is implicated in

- i) metabolism of nutrients, xenobiotics, and drugs
- ii) regulation of the immune system
- iii) antimicrobial functions
- iv) maintenance of the intestinal epithelium barrier function

Many IBD risk factors, discussed above can alter its composition. Even though a normal microbiota is hard to define, functional and compositional alterations of microbial communities observed in pathogenic states are defined as dysbiosis<sup>131</sup>. The dysbiosis seen in IBD is characterized by reduced diversity of bacteria and Table 2 summarizes alterations found in the IBD microbiome.

Increased	Decreased
<p>Bacteria:</p> <ul style="list-style-type: none"> <li>● <i>Fusobacterium</i> species</li> <li>● Pasteurellaceae</li> <li>● Proteobacteria (adherent invasive <i>Escherichia coli</i>)</li> <li>● <i>Ruminococcus gnavus</i></li> <li>● Veillonellaceae</li> </ul> <p>Fungi:</p> <ul style="list-style-type: none"> <li>● <i>Candida albicans</i></li> <li>● <i>Candida tropicalis</i></li> <li>● <i>Clavispora lusitaniae</i></li> <li>● <i>Cyberlindnera jadinii</i></li> <li>● <i>Kluyveromyces marxianus</i></li> </ul> <p>Viruses:</p> <ul style="list-style-type: none"> <li>● Caudivirales</li> </ul>	<p>Bacteria:</p> <ul style="list-style-type: none"> <li>● <i>Bacteroides</i> species</li> <li>● <i>Bifidobacterium</i> species</li> <li>● <i>Clostridium</i> XIVa, IV</li> <li>● <i>Faecalibacterium prausnitzii</i></li> <li>● <i>Roseburia</i> species</li> <li>● <i>Suterella</i> species</li> </ul> <p>Fungi:</p> <ul style="list-style-type: none"> <li>● <i>Saccharomyces cerevisiae</i></li> </ul>

Table 2: Summary of alterations in the gut microbiota observed in IBD. Adapted from Glassner et al.2021<sup>132</sup>

If dysbiosis is a cause or consequence of IBD is unclear. Murine studies indicate however that a spontaneous model of colitis does not occur in microbiome absence (i.e germ-free mice)<sup>133</sup>. Moreover, microbial-derived products are implicated in intestinal homeostasis. Specifically, Short-chain fatty acid (SCFA), tryptophan metabolites, and secondary biliary acids (SBAs) can induce Tregs and promote intestinal epithelium barrier properties<sup>134, 135, 136, 137, 138</sup>. Interestingly, a reduction in SCFA-producing bacteria is observed during CD<sup>139</sup>.

Several studies indicate that increased intestinal permeability is an important feature of IBD physiopathology<sup>140, 141, 142</sup> and that dysbiosis and breakdown of the intestinal barrier are key events for IBD initiation<sup>143</sup>. The exact pathogenic role of the leakage of the luminal content into the subjacent lamina propria is unclear<sup>115</sup>, but some authors have proposed that translocation of bacteria and their products activate immune cells that will trigger intestinal inflammation<sup>144</sup>. In line with this, an increase of a bacterial

clade called *Ruminococcus gnavus* was observed during CD<sup>145</sup> and associated with exacerbations<sup>146</sup>. A product of this same bacteria (a glucorhamnan polysaccharide) has been shown to induce TNF- $\alpha$  secretion in mouse bone marrow-derived dendritic cells through TLR4 signaling<sup>147</sup>, suggesting a pro-inflammatory role.

Therefore, alterations in relative abundance of bacteria can alter the levels of their products. These alterations might disturb intestinal homeostasis by increasing epithelial permeability and inducing an inflammatory imbalance of the immune system. It is interesting to note that bacteria that are increased during IBD are also present in the normal flora and could be implicated in the pathogenesis through their excessive expansion. Such a type of bacteria can be defined as pathobiont<sup>148</sup>. Therefore, some authors have proposed a model for IBD in which genetic alterations (such as NOD2 mutations) and environmental factors result in an expansion of pathobiont and a decrease of symbiont favoring intestinal inflammation<sup>149, 150</sup>. However, some authors consider that virtually all gut resident bacteria could have a pathogenic potential and therefore, that the concept of pathobiont is questionable<sup>151</sup>. In addition, no pathobiont has been consistently identified as a trigger of IBD and the functional consequences of the increased abundance of bacteria species observed during the disease on intestinal homeostasis necessitate further investigation<sup>149</sup>.

#### 1.5.5 The role of innate immune cells

The histological hallmark of CD (i.e. granulomas) and UC (crypt abscess with a predominance of granulocytes)<sup>111</sup> is suggestive of a crucial role for innate immune cells in IBD pathogenesis. Several lines of evidence indicate that pathogenic activation of myeloid cells is of paramount importance for IBD initiation. First, GR1<sup>+</sup> cells (that

include principally monocytes and neutrophils) depletion exacerbates an experimental model of colitis<sup>152</sup> while macrophage depletion is protective in the same model<sup>153</sup>. The gene of the IL-23 receptor (IL-23R) is associated with IBD<sup>154</sup>. IL-23 is a heterodimeric cytokine from the IL-12 family and is principally produced by activated myeloid cells<sup>155, 156</sup>. It is a key signal for the survival and acquisition of effector functions of IL-17-producing lymphoid cells<sup>157, 158</sup>. They include ILC3s and Th17 CD4<sup>+</sup> T cells, which are particularly important for the host defense at mucocutaneous surfaces (e.g. gut, lung, and skin) but also play a key role in inflammatory diseases<sup>159</sup>. Loss-of-function mutations in the IL-23R genes are protective in IBDs<sup>160</sup> while gain-of-function mutations might be detrimental<sup>161</sup>, suggestive of the pathogenic role of the IL-23 axis in these diseases. In line with this, IL-23 deficiency is protective in murine models of IBD<sup>113, 162</sup>, and treatment with an antibody blocking IL-23 and IL-12 (Ustekinumab) signaling attenuate both CD and UC<sup>163, 164</sup>. IL-1 $\beta$  and IL-6 are also produced by activated myeloid cells and favor the pro-inflammatory function of IL-17-producing and IFN- $\gamma$ -producing lymphoid cells in the context of intestinal inflammation<sup>165, 166, 167, 168, 169, 170</sup>. TNF- $\alpha$  is also a key cytokine in intestinal inflammation that is produced by activated myeloid cells. Mice displaying an innate immune cell over-production of TNF- $\alpha$  spontaneously develop a CD-like disease<sup>171</sup> and its importance is highlighted by the clinical benefits of anti-TNF- $\alpha$  therapy in IBD<sup>169, 170</sup>. As mentioned, IL-23, IL-1 $\beta$ , IL-6, and TNF- $\alpha$  are produced by myeloid cells and contribute to intestinal inflammation through the activation of lymphoid cells. However, some of these cytokines are also produced by epithelial cells and directly participate in tissue damage by inducing epithelial cell apoptosis and altering the intestinal barrier<sup>129, 172</sup>. ILCs could also be implicated in IBD. IFN- $\gamma$  producing ILC1s have been shown to accumulate in the intestine of CD patients<sup>173</sup> and to drive colitis in experimental

models<sup>174, 175</sup>. IL-23-dependent ILC3s are also increased in the intestine of CD patients<sup>176</sup> and promote intestinal inflammation by favoring mononuclear phagocyte infiltration<sup>177, 178, 179</sup>. Overall, a network of cytokines produced by activated myeloid cells, innate lymphoid cells, and epithelial cells are considered to initiate IBD.

#### 1.5.6 The role of T and B cells

T cells are thought to be important for IBD physiopathology, as patients suffering from lymphopenia can experience improvement of these diseases,<sup>180</sup> both CD and UC lesions display lymphoid infiltrations<sup>111</sup> and adoptive transfer of naïve CD4 T cells in immune-deficient mice induces colitis<sup>181</sup>. In addition, treatment with immune checkpoint inhibitors can lead to colitis<sup>182</sup>. Both Th1 and Th17 cells are implicated in IBD pathophysiology. IFN- $\gamma$  and TNF- $\alpha$  are the main cytokines produced by Th1 cells and induce intestinal inflammation by promoting epithelial cell apoptosis and favoring inflammatory cells recruitment and activation<sup>183, 184, 185, 186</sup>. IL-17<sup>+</sup> cells are also increased in the intestine of both CD and UC<sup>187</sup> but the role of Th17 cells in IBD is controversial as anti-IL-17A antibodies have been shown to exacerbate CD<sup>188</sup>. Moreover, IL-17A promote barrier functions of intestinal epithelial cells and is protective in an adoptive transfer model of colitis<sup>189, 190</sup>. On the other hand, sustained IL-23 signaling in Th17 cells enables them to acquire a pathogenic phenotype, notably through the production of IFN- $\gamma$  and granulocyte-macrophage colony-stimulating factor (GM-CSF)<sup>157, 191, 192</sup>. Th17 cells are highly plastic and thus can be protective or pathogenic depending on the cytokine milieu encountered<sup>193, 194</sup> which might explain these contradictory findings.

CD8 T cells also infiltrate the gut during IBD<sup>195</sup> and, as Th17 cells, have been shown to be both beneficial<sup>196, 197</sup> or detrimental<sup>198, 199</sup>. Single-cell technologies have enabled the identification of IBD-associated expansion of a particular CD8 T cell population in the intestine displaying a pro-inflammatory phenotype<sup>200, 201</sup>, and activation of circulating CD8 T cells is associated with an increased disease activity<sup>202</sup>. CD8 T cells that infiltrate the gut favor intestinal inflammation and tissue damage through the release of pro-inflammatory signals such as IFN- $\gamma$  and TNF- $\alpha$  and the secretion of cytotoxic granules<sup>203</sup>.

B cells are also present in IBD lesions and plasma cell infiltration at the basis of the crypts (basal plasmacytosis) is the strongest predictor of positive diagnosis for IBD<sup>111</sup>. A subset of B cells (CD45RO<sup>+</sup>B cell), representing antigen-activated B cells correlates with increased CD activity and intestinal permeability<sup>204, 205</sup>. IgA is the dominant immunoglobulin of the healthy intestinal mucosa, but IBD patients display increased production of IgG<sup>206, 207, 208</sup>. Furthermore, IgG-producing plasma cells can favor UC by inducing activation of mononuclear phagocytes and enhancing Th17 cell activity<sup>209, 210</sup>. UC patients display a deep remodeling of the B cell compartment in the inflamed mucosa and an expansion of circulating gut homing plasma cells that correlate with disease activity<sup>208</sup>. Furthermore, CD patients displaying resistance to anti-TNF therapy compared to responders display a specific cellular signature including IgG producing plasma cells<sup>211</sup>. Finally, autoantibodies or antibodies reactive to commensal bacteria participate in IBD pathogenesis and could be used as biomarkers for diagnosis and prognosis<sup>209, 212, 213</sup>.

On the other hand, CD8 and CD4 regulatory T cells are abundant in mucosal tissue of the intestine and increase during IBD<sup>200, 214</sup>. The anti-inflammatory cytokines that they produce are of paramount importance in maintaining an immuno-tolerant environment

in the intestine, in particular IL-10, an anti-inflammatory cytokine produced by regulatory lymphocytes and myeloid cells<sup>215</sup>. Loss-of-function mutations in the gene coding for IL-10 lead to infantile IBD<sup>216</sup> and IL-10 deficient mice develop spontaneous colitis<sup>217</sup>. IL-22 is another cytokine of the IL-10 family produced by Th17 cells and ILCs that favors epithelial cell proliferation and intestinal wound-healing and hence that might be protective during IBD<sup>218, 219</sup>. IL-2 and TGF- $\beta$  are also important in the maintenance of intestinal homeostasis as a defect of their signaling induce colitis in mice<sup>220, 221</sup>. They are produced by CD4 T cells and maintain intestinal immune tolerance through induction regulatory CD4 T cells<sup>222, 223</sup>. IL-33 is a cytokine that is produced by intestinal epithelial cells whose production increases during inflammation and that can also induce regulatory T cells<sup>224</sup>.

Overall, there is a strong level of evidence implicating the adaptive immune system in IBD pathophysiology. An imbalance between anti-inflammatory and pro-inflammatory mediators triggers uncontrolled inflammation that either initiates or perpetuates the disease. However, the respective roles of the different leukocyte subsets, epithelial cells, and gut microbiota, their effector molecules, and the sequence of events leading to the dysregulation of intestinal homeostasis need to be better defined to clarify mechanisms at the origin of the disease.

### 1.5.7 Treatment

Since the physiopathology of IBD is incompletely understood, no cure is available. Pharmacological interventions are at the frontline of patient care but surgery is still an

important part of the management of the disease<sup>225</sup>. Clinical management of CD and UC are different and complex. It will depend on a variety of factors including the severity and location of the disease, the age of the patient, its comorbidities, and the presence of extra-intestinal manifestation<sup>226, 227</sup>. The aim is to achieve complete remission, prevent relapses and reach “mucosal healing”, the latter being the restoration of the normal mucosal cyto-architecture<sup>225</sup>. A full description of the management of these two diseases is beyond the scope of this thesis and beyond my field of expertise. However, given their relevance for the understanding of IBD pathophysiology, the mechanisms of action of some drugs employed to treat CD and UC will be briefly discussed.

Pharmacological treatments for IBD include 4 categories<sup>226, 227</sup>: anti-inflammatory drugs, immunosuppressive, biological, and Janus kinase inhibitors.

Anti-inflammatory drugs are usually used as first-line therapy and include corticosteroids and aminosalicylates<sup>226, 227</sup>. They are both capable of suppressing NF- $\kappa$ B downstream signaling<sup>228,229</sup> and NF- $\kappa$ B induces IL-23 production<sup>230</sup>. In the biological category, as mentioned, anti-IL-12/IL-23 antibodies and anti-TNF- $\alpha$  are also effective in treating IBD<sup>163, 164, 169, 170</sup> which further highlights the importance of innate-derived cytokines in IBD pathophysiology. A recently developed approach is reminiscent of the therapeutic strategy employed in MS and consists of preventing leukocyte infiltration in the intestine. Indeed, ozanimod, a selective S1p1 modulator that entraps lymphocytes in lymph nodes has shown some clinical benefit in both MS and UC<sup>231, 232</sup>. Vedolizumab, an anti- $\alpha$ 4 $\beta$ 7 integrin antibody preventing interaction between leukocytes and MADCAM-1 and thereby preventing infiltration of immune cells in the intestine is also an effective therapy against both CD and UC<sup>233, 234</sup>. The effectiveness of these therapies suggests a key role for lymphocyte infiltration in the

intestine during IBD. Overall, drugs interfering with leukocyte migration are progressively becoming a pillar in IBD management<sup>235, 236</sup>. It is therefore relevant to study the molecular determinant of lymphocyte trafficking into the gut and therefore, the implication of GPR183 in this process as results from our group and others indicate its importance in experimental models<sup>41, 47, 103, 237</sup> and possibly in IBD<sup>47, 237, 238</sup>.

## 1.6 Multiple sclerosis

### 1.6.1 Introduction

Multiple sclerosis (MS) is an inflammatory demyelinating neurodegenerative disease of the central nervous system (CNS). As IBD, the exact cause of MS remains elusive, but it is a multifactorial disease. Studies in families and monozygotic twins indicate that genetics contribute to MS development and that environment is also a key factor<sup>239, 240</sup>.

Genetic variants associated with MS display an enrichment for immune-related genes<sup>241, 242</sup>. Moreover, a recent study indicates that MS-associated variants implicate genes particularly expressed in peripheral immune cells and microglia<sup>241</sup>. In particular, the HLA variant HLA-DRB1\*15:01 is the strongest genetic factor identified so far<sup>242</sup>. Environmental risk factors include low vitamin D status, low sun exposure, smoking, obesity during adolescence, and viral infections<sup>243</sup>. Epstein-Barr virus (EBV) infection, in particular, infectious mononucleosis during adolescence strongly increases the risk of developing MS<sup>244</sup>. Moreover, two recent studies indicate that EBV seroconversion is a necessary (but not sufficient) condition to trigger the disease<sup>245</sup> and that an antibody targeting an EBV viral protein cross-reacts with a glial protein<sup>246</sup>. It is therefore clear that EBV is a major risk factor and that alterations of the immune system are at the forefront of MS development.

MS display three distinct clinical presentations. The most frequent is the relapsing-remitting MS (RRMS) characterized by flares of neurological symptoms (such as focal sensory and motor deficit, cerebellar ataxia, and optic neuritis) virtually affecting the

entire CNS<sup>247</sup>. Around 20% of the patients will then convert to a secondary progressive form (SPMS) where disability starts to accumulate<sup>248</sup>. The primary progressive form of

No. of clinical attacks	No. of MRI lesions with objective clinical evidence <sup>a</sup>	Additional data needed for diagnosis of multiple sclerosis
<b>Relapsing-remitting multiple sclerosis</b>		
≥2	≥2	None <sup>b</sup>
≥2	1 <sup>c</sup>	None
≥2	1	DIS demonstrated by an additional clinical attack implicating a different CNS Site or by MRI
1	≥2	DIT demonstrated by additional clinical attack, MRI, or CSF-specific oligoclonal bands
1	1	DIS demonstrated by additional clinical attack implicating a different CNS site or by MRI and DIT demonstrated by an additional clinical attack or by MRI or demonstration of CSF-specific oligoclonal bands
<b>Primary progressive multiple sclerosis</b>		
Required: 1 year of disability progression (retrospectively or prospectively determined) independent of clinical relapse Plus 2 of the following: 1 or more T2-hyperintense lesions characteristic of multiple sclerosis in 1 or more of the following brain regions: periventricular, cortical or juxtacortical, or infratentorial; 2 or more T2-hyperintense lesions in the spinal cord; presence of CSF-specific oligoclonal bands		

Table 3. McDonald criteria 2017 for MS diagnosis. CSF: cerebrospinal fluid, DIS: diffusion in space, DIT: diffusion in time, MRI : magnetic resonance imaging. Adapted from McGinley et al., 2021<sup>303</sup>.

MS (PPMS), where neurological disability increases without any superimposed relapses affects approximately 10-15% of patients diagnosed with MS<sup>249</sup>. MS diagnosis is based on McDonald criteria 2017 summarized in table 3. In 2016, MS was affecting 2.22 million people worldwide showing a north to the south gradient of prevalence<sup>250</sup>, with north hemisphere countries being more affected. At the adult age, the disease more frequently affects females with a sex ratio of 2:1, but the incidence between genders is similar in pre-teen children<sup>250</sup>. The mean age of onset ranges from 25 to 29 years for RRMS and 39 to 41 years for PPMS<sup>251</sup>.

### 1.6.2 Relapsing and progressive multiple sclerosis

The hallmarks of an MS-affected CNS are multiple focal demyelinated lesions induced by oligodendrocytes cell death (also called plaques) with variable levels of gliosis and inflammation and with relative axonal sparing<sup>252</sup>. However, with progression, the axonal and neuronal loss will occur<sup>253</sup>. Acute lesions are characterized by a disruption

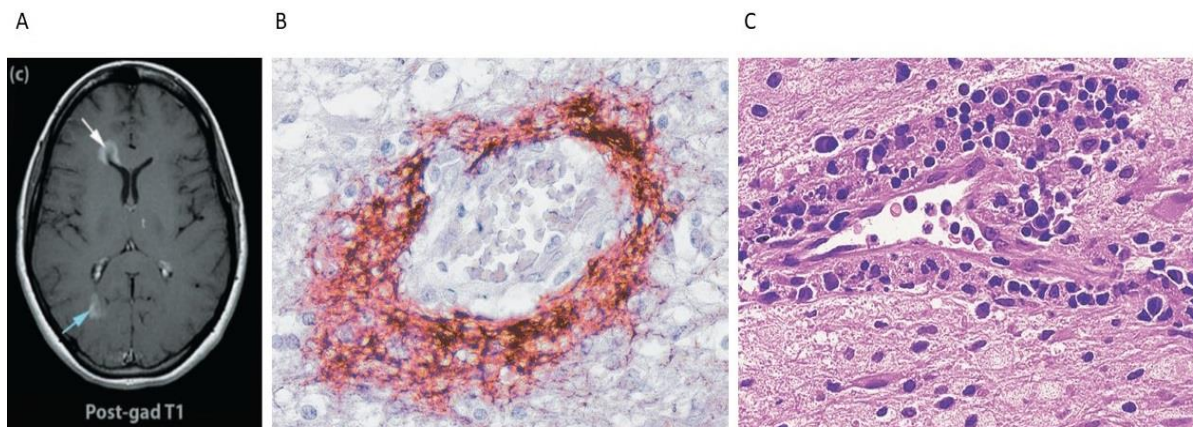


Figure 7. Acute MS lesions. A) Axial slice of a MS brain with T1-weighted magnetic resonance imaging. Arrow indicates gadolinium (gad) enhancing lesions. B) Brain biopsy of an acute MS lesion. Immunohistochemistry for fibrinogen (red) without counter-stain showing perivascular leakage in the CNS parenchyma. C) Brain biopsy of a patient with a 3 months history of MS. Mononuclear cells (lymphocytes and monocytes/macrophages) can be seen in the perivascular space. Adapted from Greenfield's Neuropathology, 9<sup>th</sup> edition, 2015.

of the blood-brain barrier (BBB) that can be identified by gadolinium-enhancing lesions at the T1-weighted imaging with magnetic resonance imaging (Figure 7A). Increased vascular permeability will result in the leakage of the plasma content into the CNS parenchyma (Figure 7B). Perivascular inflammatory infiltrates (perivascular cuffs) are seen at the histology and will contain mononuclear cells, principally lymphocytes, monocytes/macrophages, and plasma cells (Figure 7C). CNS infiltrating autoreactive lymphocytes, supposedly against myelin<sup>254</sup> or other CNS antigens<sup>255, 256</sup> will collaborate with the myeloid compartment to trigger inflammation and demyelination<sup>257</sup>. Neurodegeneration can occur subsequently to demyelination but in myelocortical MS, a cortical neuronal loss can also be observed in the absence of demyelination of its associated white matter<sup>258</sup>.

The efficacy of treatments blocking the entry of leukocytes in the CNS for preventing relapses indicates a key role of this process in RRMS pathophysiology<sup>257</sup>. However, for the progressive forms, therapeutic approaches used in RRMS are inefficient, except for the B cell-depleting antibody (Ocrelizumab) and Siponimod (an S1P receptor modulator) which have shown some moderate benefits in specific patient subgroups<sup>259, 260</sup>. In addition, BBB disruption is less visible to absent in the progressive

forms<sup>261</sup>, the presence of lymphocytes markedly reduced and the presence of macrophages/microglia increased compared to acute lesions<sup>262</sup>. Macrophages/microglia are containing myelin fragments and display an activated profile at the edge of the active lesions of progressive MS<sup>263</sup>. It is therefore thought that inflammation is compartmentalized to the CNS in the progressive forms of the disease and that the pathological process driving acute relapses and progressive neurodegeneration are different<sup>264</sup>. Specifically, aberrant activation of macrophages/microglia might be a key aspect of PPMS and SPMS<sup>265</sup>.

The trigger of MS is unknown, but two theories have been proposed. The outside-in hypothesis is that over-activation of leukocytes takes place in the periphery and enables subsequent infiltration of immune cells in the CNS<sup>266</sup>. On the other hand, the inside-out theory consider that MS “primum movens” is a neurodegenerative process that subsequently activates peripheral leukocytes and triggers immune cell infiltration in the CNS parenchyma<sup>267</sup>.

The lack of experimental models for progressive MS has limited our ability to understand its underlying pathophysiology and the experimental model used in this thesis, experimental autoimmune encephalomyelitis (EAE) more closely mimics RRMS. Therefore, the cellular and molecular mechanisms driving relapses will be described in more detail than the ones of the progressive forms.

### 1.6.3 Physiopathology of an MS relapse

As mentioned, immune cell infiltration in the CNS is a key aspect of MS relapses. The molecular mechanisms driving leukocyte transmigration across the BBB are described in section 1.7.5 and the knowledge on the resolution of MS inflammation is described

in our review in manuscript N°3. For this subsection, we are going to mainly focus on the pro-inflammatory mechanisms driving MS relapses (Figure 8).

In peripheral blood mononuclear cells (PBMC) of twins discordant for MS, naïve CD4 T from the MS twin display a more activated profile and monocytes display a shift toward a pro-inflammatory phenotype<sup>239</sup> compared with the non-MS twin. This highlights the importance of these two leukocyte subsets in MS.

In mice, adoptive transfer of myelin reactive CD4 T cells is sufficient to trigger demyelination, and Th1, Th9, and Th17 cells can induce EAE but with different clinical manifestation<sup>268</sup>. Myelin-reactive CD4 T cells from RRMS patients overproduce IL-17, IFN- $\gamma$ , and GM-CSF compared with healthy controls<sup>269</sup>. In addition, Th17 cells from MS patients produce less IL-10<sup>270</sup>, and an MS-specific CD4 T cell signature (co-expression of CXCR4, VLA-4, and GM-CSF) has been found in peripheral blood and MS lesions<sup>271</sup>. In mice, overexpression of GM-CSF in CD4 T cells induces spontaneous myeloid cell infiltration and CNS inflammation<sup>272</sup>. Adoptive transfer of myelin reactive CD4 T cells deficient for GM-CSF fails to induce EAE<sup>273</sup> and ablation of the GM-CSF receptor (CSFR2) on CCR2 expressing monocytes also induces complete EAE protection<sup>274</sup>. GM-CSF activated myeloid cells that display a pro-inflammatory phenotype with increased reactive oxygen species and pro-inflammatory mediator production, are thereby licensed to induce tissue damages<sup>275, 276, 277</sup>. In acute MS lesions, macrophage/microglia infiltration correlates well with axonal damage<sup>278</sup>, further suggesting a tissue-damaging role for these cells. Of note, in MS lesions, some CD4 T cells are found in close contact with oligodendrocytes and Th17 cells could induce direct cell death through the release of glutamate<sup>279</sup>.

In addition, reactivation of CD4 T cells by infiltrating myeloid cells in the CNS is essential to induce EAE<sup>280</sup>. Therefore, the myeloid/CD4 T cell cross-talk plays a key

role in EAE pathophysiology, and possibly MS and GM-CSF might be a key factor in neuroinflammation. The recent success of B cell depleting therapies in RRMS also highlights the importance of these cells in promoting the disease<sup>281</sup>, and GM-CSF producing B cells are increased in the peripheral blood of MS patients<sup>282</sup>. B cell depleting therapies employed to treat MS do not target plasma cells<sup>283</sup>. Therefore it is thought that the pathogenic role of B cells in MS relapses is due to their function as APCs or through cytokine production rather than via an antibody-mediated effect<sup>283</sup>. In MS lesions, CD4 T cells are mainly found in perivascular cuffs while CD8 T cells, that generally outnumber them, are found diffusely across the lesions, and are clonally expanded<sup>284</sup>. In addition, adoptive transfer of myelin reactive CD8 T cells can also induce EAE<sup>285</sup> and CD8 T cell infiltration correlates well with axonal damages in MS lesions<sup>286</sup>. Therefore, the adaptive immune system is supposed to play a key role in MS relapses, in particular in their initiation while myeloid cells and lymphocytes collaborate to induce demyelination and tissue damage.

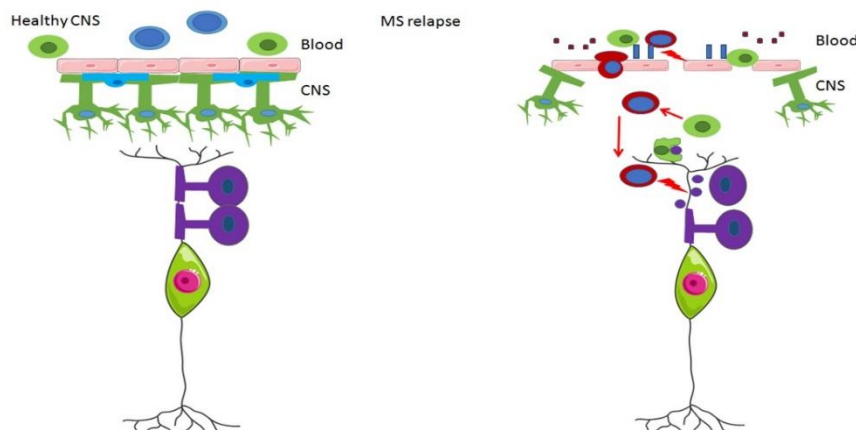


Figure 8. Model of MS relapse at the level of CNS capillaries. Left panel: At steady, the BBB is sealed, astrocyte end-feet ensheet the basolateral surface of endothelial cells, and leukocytes are excluded from the CNS parenchyma. Right panel: during MS relapses, the blood-brain barrier is disrupted, astrocytic end-feet will get detached, and endothelial cells will display an increased expression of adhesion molecules and produce chemokine. This will enable encephalitogenic lymphocytes to reach the CNS parenchyma. Here they will be reactivated by APCs presenting CNS antigen. Lymphocytes will further recruit mononuclear phagocytes. Adapted from Ruiz et al<sup>2</sup>.

#### 1.6.4 Treatment

MS management is rather complex and involves a multidisciplinary approach<sup>247</sup>. It consists of managing acute relapses, reducing their frequency, and decreasing the disability that they induce<sup>247</sup>. As mentioned, therapeutic options for the progressive forms are limited and thus we are going to mainly focus on RRMS.

Acute exacerbations are treated with high doses of corticosteroids and when refractory, can be managed by plasma exchanges or apheresis<sup>287</sup>. Corticoid treatment does not prevent the occurrence of new relapses or improve long-term disability<sup>288</sup>. Therefore, long-term management necessitates the introduction of disease-modifying therapy (DMT).

Regarding the choice of DMT, there are two schools of thought. Some authors consider that MS should be treated with high efficacy therapy first<sup>289</sup>. This is based on the notion that the disease is more active at onset<sup>290</sup> and that patients are usually younger at time of diagnosis and thus tolerate more aggressive treatment<sup>289</sup>. Examples of high efficacy treatments are Natalizumab whose mechanisms of action will be discussed in section 1.7.5 and B cell depleting therapies (e.g. Ocrelizumab). Autologous hematopoietic stem cell transplantation is effective in cases of RRMS refractory to other therapies<sup>291</sup>.

Another approach is the escalation strategy, where a low-risk therapy (e.g.  $\beta$ -interferons, glatiramer acetate) is first introduced. Then in case of new relapses or MRI enhancing lesions an escalation to intermediate or high efficacy DMT is performed<sup>289</sup>. This approach is less recommended as several recent studies have shown the long-term benefit of the early introduction of highly efficacious treatments<sup>292, 293</sup>.

## 1.7 Role of the vasculature in multiple sclerosis

### 1.7.1 Endothelial cells

Endothelial cells are highly specialized cells derived from the mesoderm. They form a monolayer lining the luminal side of blood and lymphatic vessels.

Blood endothelial cells (BECs) are essential regulators of homeostasis and exert both systemic and tissue-specific function<sup>294</sup>. They display a remarkable inter- and intra-organ heterogeneity<sup>295, 296</sup> and fulfill many essential functions for multicellular organisms.

Endothelial cells (ECs) are not part of the immune system; however, they are key regulators of immune cell trafficking and thus are immunologically active.

### 1.7.2 Regulation of inflammatory immune cell trafficking by endothelial cells

Endothelial cells enable the recruitment of leukocytes into inflamed tissues through a multi-step cascade characterized by two different phases<sup>297</sup> (Figure 9):

- i) the leukocyte adhesion cascade that enables the vasculature to capture free-flowing leukocytes from the blood circulation
- ii) the transendothelial migration (TEM) or diapedesis where leukocytes cross the vasculature to reach the target organ or tissue.

These steps are regulated by different molecular cues and take place at the level of postcapillary venules in most organs<sup>298</sup>.

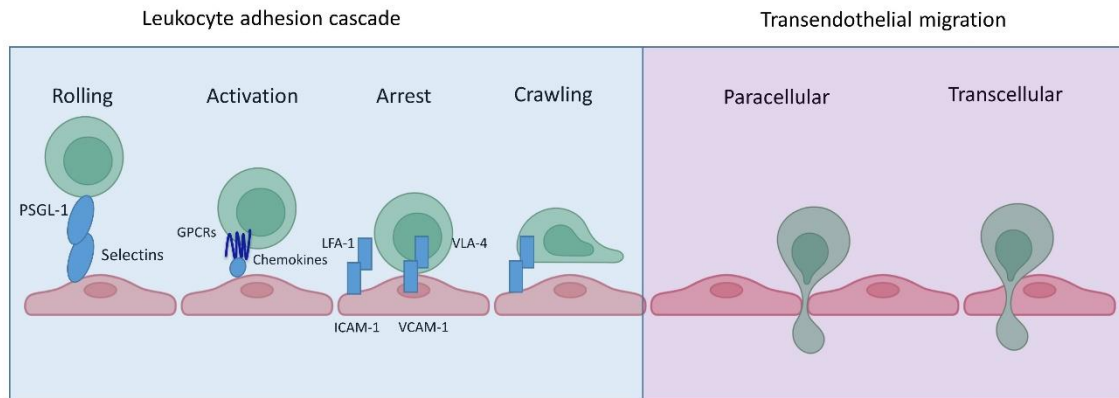


Figure 9. Leukocyte migration across the endothelium. See the text for the description of the different steps.

The cascade starts with the **rolling** phase. Inflammatory signals, such as TNF- $\alpha$  or IL-1 $\beta$  increase the expression of **selectins** (e.g. E- and P-selectin) and adhesion molecules (i.e. Vascular cell adhesion molecule (VCAM-1) and Mucosal addressin cell adhesion molecule 1 (MADCAM-1)) on the luminal surface of ECs<sup>299, 300</sup>. Interactions of selectins and adhesion molecules with their ligand expressed at the surface of circulating leukocytes (P-selectin glycoprotein ligand 1(PSGL-1) and integrins respectively) reduce their velocity<sup>300</sup>. Chemotactic signals (mainly chemokines) present at the luminal surface of ECs<sup>297</sup> will **activate** rolling leukocytes via their cognate chemotactic receptor which are G protein-coupled receptors (GPCRs)<sup>298</sup>. Activation of these receptors will induce conformational changes and clustering of integrins (e.g. lymphocyte function-associated antigen 1 (LFA-1) and very late antigen 4 (VLA-4)), increasing their affinity and avidity for their cognate ligands present on the luminal surface of ECs (Intercellular cell adhesion molecule 1 (ICAM-1) and VCAM-1 respectively))<sup>300</sup>. Leukocytes will thus become resistant to shear-stress mediated detachment and become **arrested**. They will then start to **crawl** against or perpendicularly to the blood flow looking for a site permissive for **transendothelial**

**migration**<sup>298</sup>. This step is also regulated by integrins and their cognate ligand<sup>298</sup>. Finally, leukocytes will cross the vascular endothelium, supposedly mainly through the paracellular route by a remodeling of endothelial junctions and less often through the formation of a transcellular pore<sup>301, 302, 303</sup>. It should be noted that the molecular determinants of the leukocyte adhesion cascade and TEM might vary depending on the leukocyte subset (e.g. Neutrophils vs CD4<sup>+</sup>T cells) and the target organ. Leukocyte migration across the blood-brain barrier will be described in more detail in the designated chapter.

### 1.7.3 Endothelial cells of the central nervous-system: the blood-brain barrier (BBB)

To maintain proper neuronal function, the exchanges of oxygen, nutrients, molecules, and immune cells between the CNS parenchyma and the peripheral blood need to be tightly controlled. Thus, endothelial cells of capillaries and postcapillary venules at the interface between blood and CNS parenchyma display specific characteristics compared with peripheral ECs<sup>304</sup>:

- i) They lack fenestrations and restrain paracellular diffusion of water-soluble molecules through the expression of tight junction proteins
- ii) They display a low basal transcytotic activity
- iii) They display intense and polarized expression of specific transporters
- iv) They limit leukocyte migration in the CNS parenchyma

These properties are not intrinsic to CNS ECs but are the result of their interaction with CNS resident cells mainly brain pericytes, neurons, and astrocytes<sup>304, 305, 306, 307</sup>. Together, these cells form the Neuro-vascular unit (NVU) (Figure 10).

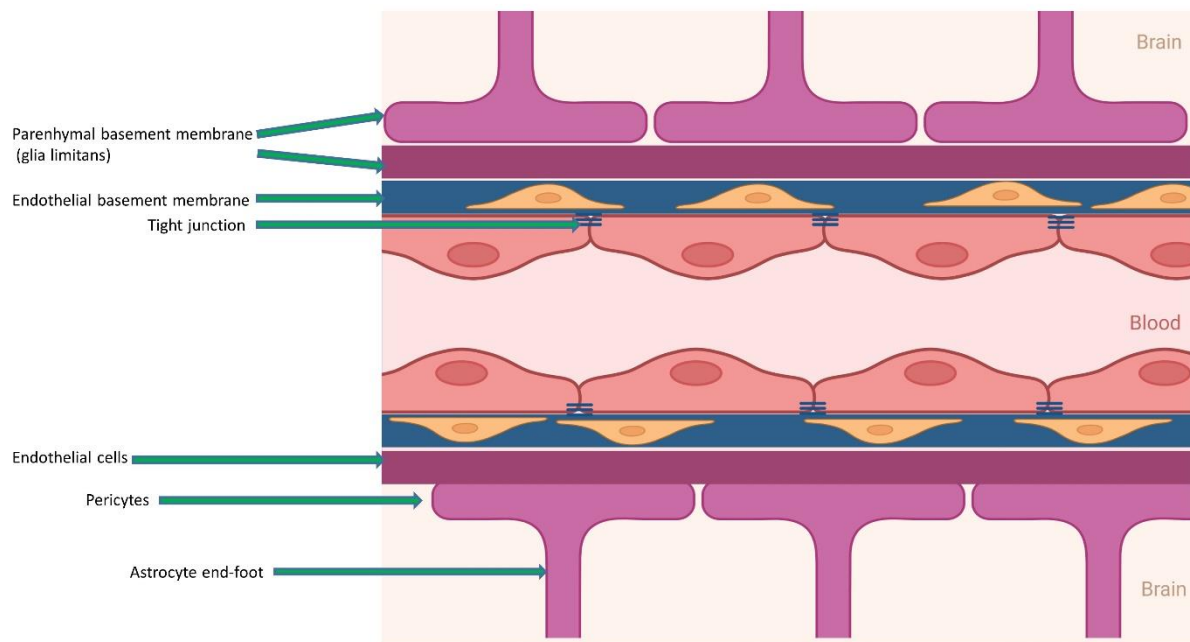


Figure 10. Graphic representation of the neurovascular unit showing a capillary.

Pericytes are important for the induction of barrier properties of CNS ECs including suppression of transcytosis and regulation of tight junction formation<sup>306, 308</sup>. This is true during development, but pericytes might also be involved in the maintenance of barrier properties during the post-natal phase<sup>309</sup>. A lipid transporter called major facilitator superfamily domain containing 2a (MFS2Da) is specifically expressed by CNS ECs and suppresses caveolae-mediated transcytosis and is thus critical for the regulation of BBB permeability<sup>310, 311</sup>. Pericytes might suppress transcytosis in CNS ECs by inducing the expression of this transporter<sup>310</sup>. In addition, they also reduce the expression of ICAM-1 and VCAM-1 in brain vessels<sup>312</sup>. In collaboration with ECs, they regulate the production of one of the two basement membranes of the CNS vasculature which is the endothelial basement membrane<sup>313</sup>.

Astrocytes are also thought to play a key role in CNS barrier genesis. First, as their end-feet cover the abluminal surface of blood vessels they produce the second basement membrane of CNS vasculature: the parenchymal basement membrane<sup>314</sup> (or glia limitans) and could act as a physical barrier<sup>315</sup>. In addition, astrocyte-derived soluble factors including sonic hedgehog and WNT ligands are key signals to the acquisition and maintenance of CNS EC BBB phenotype<sup>316, 317, 318</sup>. They induce the expression of key BBB transporters (e.g. glut-1) and tight junction proteins such as claudin-5, which is essential for the paracellular barrier properties of CNS endothelium<sup>319</sup>.

Another remarkable feature of CNS vasculature is the neurovascular coupling which is the capacity to adapt the cerebral blood flow to neuronal activity. The molecular mechanisms of this process are poorly understood but it is considered that it involves a cross-talk between astrocytes, ECs, neurons, and mural cells<sup>320</sup>.

#### 1.7.4 Vascular pathology in MS and EAE

The very first descriptions of MS lesions were suggesting a link between vascular pathology and MS. In 1880, Charcot observed that the inflammatory reaction initiating MS lesions was located around veins. In 1916, Dawson further described that the demyelination process was displaying a perivenous location, giving rise to the so-called "Dawson fingers"<sup>263</sup>. In addition to those historic observations, more recent data suggest an involvement of vascular pathology in MS.

In comparison to the general population, MS patients could have a greater risk to develop ischemic stroke<sup>321</sup>. Furthermore, some studies indicate that compared with healthy individuals, patients displaying a clinically isolated syndrome, relapsing-

remitting, or primary progressive multiple sclerosis present a reduced cerebral blood flow (CBF)<sup>322, 323, 324</sup>. In addition, chronic MS lesions are often localized in watershed areas (i.e. regions at the interface between the territories of large arteries more sensitive to ischemia/hypoxia) of the brain<sup>325</sup> and endothelial cell proliferation has been observed in the brain of MS patients and during EAE<sup>326, 327, 328</sup>. Several studies indicate that pharmacological inhibition of angiogenesis reduces EAE severity<sup>329, 330, 331</sup>, although the efficacy of the treatment might depend on the timing of administration<sup>331</sup>. On the other hand, ischemic preconditioning has been shown to attenuate EAE<sup>332</sup>. The authors have proposed that the observed attenuation was due to vascular remodeling induced by hypoxia<sup>333</sup>, however, no causal link between the two was directly established. A recent study also indicates that microvascular endothelial cells can phagocytose myelin fragments during CNS injuries, including EAE, and that this process triggers angiogenesis and endothelial-to-mesenchymal transition (EndoMT)<sup>334</sup>. Interestingly, EndoMT, a process throughout which ECs partially or completely lose their differentiated state and acquire a mesenchymal phenotype has been observed in CNS ECs during EAE by another study<sup>335</sup> and has also been described in MS lesions<sup>336</sup>. During endoMT, microvascular ECs lose their BBB phenotype, which could be a mechanism of endothelial dysfunction favoring leukocyte infiltration in the CNS in MS<sup>337</sup>. EndoMT is also proposed to play a role in several cardiovascular diseases<sup>338</sup>. Finally, a recent study suggests that BBB-like endothelial cells of MS patients display intrinsic alterations compared with healthy individuals<sup>339</sup>. Hence, several lines of evidence suggest a link between MS and vascular alterations, which prompted some authors to speculate that “vascular changes”<sup>340</sup> and hypoxia<sup>341</sup> instead of being epiphenomenon of inflammation might play a key role in the disease pathogenesis.

### 1.7.5 Regulation of leukocyte trafficking in the CNS by endothelial cells

Leukocyte infiltration in the CNS parenchyma is a key event for the initiation of MS relapses and EAE<sup>266</sup>. A combination of *in-vitro* studies, intravital microscopy, EAE, and analysis of MS lesions have enabled us to better understand the sequence of events allowing leukocytes to cross the BBB and the molecular players involved<sup>300, 342</sup>.

Compared with peripheral endothelial cells, CNS ECs display a low expression of genes associated with immune response and leukocyte chemotaxis at a steady state<sup>335, 343</sup>. Thus, in healthy conditions, leukocytes are almost completely excluded from the CNS parenchyma<sup>300</sup>. However, during MS relapses and EAE, the CNS endothelium becomes activated, expression of adhesion molecules is increased<sup>344, 345</sup> as BBB permeability<sup>346</sup>. Selectin expression in the luminal surface of CNS ECs is increased and will promote leukocyte rolling<sup>347</sup>. However, at least in mice, this step is dispensable for invasion of CD4<sup>+</sup> T cells in the brain and spinal cord parenchyma,<sup>347, 348, 349</sup>. In contrast,  $\alpha 4\beta 1$  integrin interaction with VCAM-1 is essential for EAE<sup>350, 351</sup>. This has led to the development of a mouse humanized anti- $\alpha 4$  integrin antibody (Natalizumab)<sup>352</sup> which has been proven to be effective in preventing MS relapses by two phase III clinical trials<sup>353, 354</sup>, and is now used as a DMT. GPCR activation by chemotactic signals is essential to mediate a firm attachment between integrins expressed by leukocytes and adhesion molecules present at the endothelial surface<sup>300</sup> and GPCR inhibition by pertussis toxin protects mice from EAE<sup>268, 355, 356</sup>. Under inflammatory conditions, the CNS endothelium produces a wide array of chemokines that can regulate leukocyte infiltration<sup>357, 358</sup>. *In-vitro* data indicate that the atypical chemokine receptor 1 (ACKR1 formerly known as DARC), whose expression is

induced in CNS ECs in both MS and EAE<sup>359, 360</sup>, can act as a transporter for pro-inflammatory chemokine<sup>359</sup>. It could thus transport chemokines produced by CNS resident cells and increase their bioavailability on the luminal surface of the BBB. However, ACKR1 KO mice are not completely protected from EAE<sup>359</sup>; indicating that additional mechanisms might be implicated in the activation phase of the cascade during neuroinflammation. Of note, the nature of the exact chemotactic signals responsible for the firm arrest of leukocytes on the BBB is not identified yet<sup>342</sup>.

Interaction of  $\alpha$ L $\beta$ 2 integrin on leukocytes with endothelial ICAM-1 and ICAM-2 regulate the arrest and the crawling phases of the adhesion cascade<sup>361, 362, 363</sup>. Furthermore, ICAM-1 deficient mice display an attenuated active EAE disease course<sup>364</sup>, and the absence of both ICAM-1 and ICAM-2 reduces EAE severity in the adoptive transfer model<sup>363</sup>. Reelin and Apolipoprotein E receptor 2 have been shown to promote rolling and CNS parenchymal infiltration of macrophages and mice KO for these 2 genes are partially protected against EAE<sup>365, 366</sup>.

In addition to participating in the adhesion cascade, endothelial cell surface receptors are also involved in the regulation of diapedesis. Hence, *in-vitro*, while CD99 and CD31 (PECAM-1) seem to favor the paracellular route<sup>367, 368</sup>, the absence of expression of ICAM-1 and ICAM-2 in CNS ECs or high surface levels of ICAM-1 favor the transcellular route of diapedesis<sup>369</sup>. In CNS ECs, the expression of a scaffolding protein of caveolae (Caveolin-1, CAV-1), increases during EAE and is required for CD4<sup>+</sup> transcellular diapedesis<sup>370, 371</sup>.

Most of the above-mentioned pathways act as pro-migratory signals for leukocytes. On the other hand, alterations in pathways preventing leukocyte entry into the CNS parenchyma might also be involved in EAE and MS pathophysiology. The Sonic Hedgehog pathway (Shh) is important in maintaining BBB integrity<sup>305</sup> and might be

dysregulated in both EAE and MS<sup>305, 372, 373</sup>. Notably, the expression of the Shh downstream effector Netrin-1 is increased in CNS ECs of MS lesions<sup>374</sup>. Furthermore, Netrin-1 can reduce pro-inflammatory cytokine production by inflamed CNS ECs *in-vitro* and is protective during EAE<sup>374</sup>, and alterations in serum levels of Netrin-1 have been described in MS patients compared with healthy controls<sup>374 375</sup>. Developmental Locus 1 (DEL-1) is a glycoprotein secreted by ECs that can inhibit  $\alpha$ L $\beta$ 2 integrin-dependent leukocytes adhesion<sup>376</sup>. Its expression is reduced during both MS and EAE and DEL-1 KO mice display a slightly exacerbated EAE disease course<sup>377</sup>. In addition, a mutation in the DEL-1 gene locus (EDIL-3) , has been associated with MS <sup>378</sup>. The chemokine CXCL12, which is the ligand of CXCR4 and is a potent chemotactic signal for leukocytes, displays interesting functions in MS and EAE. During homeostasis, CXCL12 expression is polarized to the basolateral surface of the BBB and this polarization is lost during EAE <sup>379</sup> and MS<sup>380</sup>. Some studies indicate that antagonizing CXCR4 exacerbates EAE and that CXCL12 may prevent the entry of leukocytes in the CNS parenchyma by retaining them in the perivascular space <sup>379</sup>. However, other groups describe opposite findings of CXCR4 antagonism on EAE disease course<sup>381, 382</sup>. Those discrepancies could be explained by the use of different EAE models or of CXCR4 antagonists with different specificity. Indeed, CXCL12 is the ligand of CXCR4 and ACKR3 (also known as CXCR7). Interestingly, increased expression of ACKR3 in CNS ECs during EAE might favor leukocyte parenchymal infiltration by quenching CXCL12<sup>383</sup> and, hence reducing its bioavailability. In line with this, ACKR3 antagonism attenuates EAE<sup>383, 384</sup>.

Overall, the regulation of immune cell infiltration in the CNS parenchyma by BBB endothelial cells is a tightly regulated process with many molecular players involved.

It thus tempting to speculate that, leukocyte infiltration in the CNS parenchyma or retention in the blood is determined by the balance between pro and anti-migratory signals. This is reminiscent of leukocyte activation that depends on the sum of co-stimulatory and co-inhibitory signals.

## 2. Aim of the thesis and summary of the results

The principal aim of this thesis was to increase the knowledge about Ch25h function during inflammatory diseases. The laboratory of Professor Pot being primarily interested in neuroinflammation, the vast majority of my work was dedicated to this field. However, I also worked on the impact of the Ch25h pathway on IBD as a side project.

I had the opportunity to collaborate with Professor Misselwitz who is a gastroenterologist working at the Inselspital (Bern). The aim of this collaboration was exploratory. We collected lamina propria mononuclear cells (LMPCs) and peripheral blood mononuclear cells (PBMCs) from IBD patients and healthy volunteers (for the PBMCs) to perform an in-depth immuno-phenotyping of GPR183 expressing cells in IBD. Additionally, the IBD cohort contained patients carrying or not a GPR183 IBD-associated SNP to study the effect of this SNP on disease outcome and immune cells phenotype. All the LPMCs were collected, and some PBMCs were finally used for the revisions of manuscript N°1. This paper described the pro-inflammatory role of GPR183 (EBI2) and Ch25h in IBD and its experimental models.

Therefore, the aim of this collaboration slightly changed and we focused our attention on immuno-phenotyping of GPR183 expressing lymphocytes in the peripheral blood. We also evaluated the impact of the SNP on disease outcome and circulating lymphocytes. The outcomes of this aim are described in manuscript N°2.

For the main subject of my thesis, one of the key aims was the establishment and validation of a new mouse model, the *Ch25h<sup>fl/fl</sup>* mice. The purpose of this model was to determine the cellular source of Ch25h during EAE and to better understand the

molecular mechanism through which Ch25h promotes neuroinflammation during EAE.  
For a more detailed description of this model and the outcomes of this aim, the reader is referred to manuscript n° 4.

### **3. Manuscript N°1: The EBI2-oxysterol axis promotes the development of intestinal lymphoid structures and colitis**

This manuscript was published in *Mucosal Immunology* (2019).

DOI:<https://doi.org/10.1038/s41385-019-0140-x>

It demonstrates that the activity of the GPR183/7 $\alpha$ ,25-diOHC axis is increased during intestinal inflammation in both humans and mice and, that it promotes the formation of colonic lymphoid structures at steady state and during inflammation. It also promotes colonic inflammation in the IL-10  $-/-$  spontaneous model of colitis.

My contribution to this manuscript, under the supervision of Professor Pot, is fig. 1a and b. I performed the preparation, acquisition, and analysis of the PMBCs and LPMCs samples by flow cytometry. I found that on the 4 samples analyzed, the CD4 memory T cells from the lamina propria of the colon display a higher expression of GPR183 than CD4 memory T cells from the peripheral blood. It should be noted that the donors of PMBCs and LPMCs were not matched and that the underlying conditions of the patients undergoing colonic surgery (colonic cancer and in one IBD patients) might also result in increased infiltration of GPR183<sup>+</sup> CD4 memory T cells. In addition, as TNF- $\alpha$  mRNA levels were positively correlated with GPR183 transcripts (Table S3), I assessed the impact of TNF- $\alpha$  stimulation of PMBCs on GPR183 expression. We did not observe any effect of the treatment on GPR183 expression on lymphocytes (Fig S1c-d).



## ARTICLE OPEN

## The EBI2-oxysterol axis promotes the development of intestinal lymphoid structures and colitis

Annika Wyss<sup>1</sup>, Tina Raselli<sup>1</sup>, Nathan Perkins<sup>2</sup>, Florian Ruiz<sup>3</sup>, Gérard Schmelzner<sup>1</sup>, Glynis Klinke<sup>2,6</sup>, Anja Moncsek<sup>1</sup>, René Roth<sup>1</sup>, Marianne R. Spalinger<sup>1</sup>, Larissa Hering<sup>1</sup>, Kirstin Atrott<sup>1</sup>, Silvia Lang<sup>1</sup>, Isabelle Frey-Wagner<sup>1</sup>, Joachim C. Mertens<sup>1</sup>, Michael Scharl<sup>1</sup>, Andreas W. Sailer<sup>4</sup>, Oliver Pabst<sup>5</sup>, Martin Hersberger<sup>2</sup>, Caroline Pot<sup>3</sup>, Gerhard Rogler<sup>1</sup> and Benjamin Misselwitz<sup>1,7</sup>

The gene encoding for Epstein-Barr virus-induced G-protein-coupled receptor 2 (EBI2) is a risk gene for inflammatory bowel disease (IBD). Together with its oxysterol ligand 7 $\alpha$ ,25-dihydroxycholesterol, EBI2 mediates migration and differentiation of immune cells. However, the role of EBI2 in the colonic immune system remains insufficiently studied. We found increased mRNA expression of EBI2 and oxysterol-synthesizing enzymes (CH25H, CYP7B1) in the inflamed colon of patients with ulcerative colitis and mice with acute or chronic dextran sulfate sodium (DSS) colitis. Accordingly, we detected elevated levels of 25-hydroxylated oxysterols, including 7 $\alpha$ ,25-dihydroxycholesterol in mice with acute colonic inflammation. Knockout of EBI2 or CH25H did not affect severity of DSS colitis; however, inflammation was decreased in male EBI2<sup>-/-</sup> mice in the IL-10 colitis model. The colonic immune system comprises mucosal lymphoid structures, which accumulate upon chronic inflammation in IL-10-deficient mice and in chronic DSS colitis. However, EBI2<sup>-/-</sup> mice formed significantly less colonic lymphoid structures at baseline and showed defects in inflammation-induced accumulation of lymphoid structures. In summary, we report induction of the EBI2-7 $\alpha$ ,25-dihydroxycholesterol axis in colitis and a role of EBI2 for the accumulation of lymphoid tissue during homeostasis and inflammation. These data implicate the EBI2-7 $\alpha$ ,25-dihydroxycholesterol axis in IBD pathogenesis.

*Mucosal Immunology* (2019) 12:733–745; <https://doi.org/10.1038/s41385-019-0140-x>

## INTRODUCTION

Inflammatory bowel diseases (IBD), with the main forms Crohn's disease (CD) and ulcerative colitis (UC), are chronic inflammatory conditions of the human gut. The pathogenesis of IBD is incompletely understood, but genetic and environmental factors were shown to contribute to disease development and progression. Genome wide association studies (GWAS) have identified more than 240 genetic regions in the human genome affecting the risk for IBD.<sup>1,2</sup> The majority of IBD-specific single nucleotide polymorphisms (SNPs) confer an increased risk for both, CD and UC.<sup>1</sup> Genes identified by GWAS provide a framework for future scientific studies addressing IBD pathogenesis.

Epstein-Barr virus-induced G-protein-coupled receptor 2 (EBI2, also known as GPR183), is an IBD risk gene identified by GWAS.<sup>1</sup> EBI2 exerts a crucial function for the correct activation and maturation of naïve B cells in secondary lymphoid organs.<sup>3–5</sup> Oxysterols are ligands for EBI2, the most potent being 7 $\alpha$ ,25-dihydroxycholesterol (7 $\alpha$ ,25-diHC).<sup>6,7</sup> 7 $\alpha$ ,25-diHC acts as a chemoattractant, directing migration of EBI2 expressing B cells, T cells, and DCs.<sup>6–9</sup> A 7 $\alpha$ ,25-diHC gradient in secondary lymphoid organs seems to be important for correct positioning of immune cells and

a rapid and efficient antibody response.<sup>10</sup> 7 $\alpha$ ,25-diHC is produced from cholesterol via two hydroxylation steps, at position 25 and 7 $\alpha$ , by the enzymes cholesterol 25-hydroxylase (CH25H) and cytochrome P450 family 7 subfamily member B1 (CYP7B1), respectively.

Besides B cells and DCs, EBI2 is also expressed in macrophages and natural killer cells,<sup>6</sup> and CH25H and CYP7B1 are expressed in immune cells and many tissues including lymph nodes, lung, and colon.<sup>6,11</sup> Therefore, the oxysterol-EBI2 axis might constitute a fundamental mechanism in the regulation of the immune system and tissue homeostasis.

Intestinal immune responses are orchestrated in lymphoid tissue localized directly in the intestinal tract and draining lymph nodes. Local lymphoid tissues show considerable plasticity, varying in organization and cellular composition depending on the segments of the gut and the immune status. The colonic immune system comprises two types of secondary lymphoid organs: large colonic patches (CLP), similar to Peyer's patches (PP) in the small intestine, and smaller structures referred to as solitary intestinal lymphoid tissue (SILT).<sup>12</sup> CLP and PP develop before birth, whereas SILT develop strictly postnatally. SILT comprise a

<sup>1</sup>Department of Gastroenterology and Hepatology, University Hospital Zurich, University of Zurich, Zurich, Switzerland; <sup>2</sup>Division of Clinical Chemistry and Biochemistry, University Children's Hospital Zurich, University of Zurich, Zurich, Switzerland; <sup>3</sup>Laboratories of Neuroimmunology, Division of Neurology and Neuroscience Research Center, Department of Clinical Neurosciences, Lausanne University Hospital, Epalinges, Switzerland; <sup>4</sup>Chemical Biology & Therapeutics, Novartis Institutes for BioMedical Research, Basel, Switzerland and <sup>5</sup>Institute for Molecular Medicine, RWTH Aachen University, Aachen, Germany

Correspondence: Benjamin Misselwitz ([benjamin.misselwitz@usz.ch](mailto:benjamin.misselwitz@usz.ch))

<sup>6</sup>Present address: Department of General Pediatrics, Division of Neuropediatrics and Metabolic Medicine, Center for Pediatric and Adolescent Medicine, University Hospital Heidelberg, Heidelberg, Germany

<sup>7</sup>Present address: University Clinic for Visceral Surgery and Medicine, Inselspital, University of Bern, Bern, Switzerland

Received: 25 January 2018 Revised: 9 December 2018 Accepted: 16 December 2018

Published online: 11 February 2019



continuum of lymphoid structures ranging from nascent small immature cryptopatches (CP) to mature isolated lymphoid follicles (ILF) containing B cells.

General principles of secondary lymphoid tissue formation are shared between mesenteric lymph nodes and intestinal lymphoid tissues including CLP/PP and SILT (reviewed in ref. <sup>13</sup>). Development of these lymphoid tissues includes clustering of lymphoid tissue inducer (LTi) cells, a subclass of innate lymphoid cells (ILC), and requires an intact lymphotoxin signaling pathway. Most previous studies focused on the development of lymphoid tissue in the small intestine; in contrast, formation of SILT in the colon has been studied to a lower extent and specific factors required beyond lymphotoxin remain unknown. While in the small intestine, maturation of SILT depends on CXCL13, RANKL, and CCR6/CCL20, these chemokines are not essential in the colon.<sup>12,14</sup> Furthermore, while the gut microbiota stimulates small intestinal SILT, the microbiota dampens SILT formation in the colon, an effect mediated by IL-25 and IL-23.<sup>15</sup> Therefore, additional molecular factors besides those cytokines seem to be required, and very recently, a role of EBI2 expressing ILCs for the development of colonic lymphoid structures has been demonstrated.<sup>16</sup>

In the colon, adaptation to inflammation includes formation of additional lymphoid structures. Induction of newly formed lymphoid structures upon inflammation requires the presence of microbiota and lymphotoxin signaling but was independent from the nuclear hormone receptor ROR- $\gamma$ t,<sup>17</sup> suggesting that ILCs and LTi cells are not strictly necessary. SILT were proposed to host a flexible pool of B cells for the formation of an IgA response complementing PP and CLP with a fixed B cell pool size.<sup>18</sup> However, the role of SILT in colon inflammation has not been clarified.

Given the function of EBI2 in immune cell migration, we aimed at investigating the role of EBI2 and oxysterols in the pathogenesis of intestinal inflammation and the development of colonic lymphoid tissues. Our results implicate the EBI2-oxysterol axis in colonic SILT development and inflammatory responses in the colon.

## RESULTS

### Human intestinal lymphocytes express EBI2

To test for surface expression of EBI2 on intestinal immune cells, colon lamina propria mononuclear cells (LPMC) from patients undergoing intestinal surgery were analyzed by flow cytometry. We observed robust EBI2 expression on various subsets of B and T cells. As reported previously, expression levels were highest in memory CD4<sup>+</sup> T cells (Fig. 1a) in human peripheral blood mononuclear cells (PBMC).<sup>19</sup> EBI2 expression was also observed in PBMCs without significant differences between healthy volunteers and IBD patients (CD and UC, Fig. 1b). Direct comparison of LPMCs with identical cellular subsets of PBMCs revealed significantly higher EBI2 expression in the gut ( $p = 0.0001$ ).

### Upregulation of gene expression of EBI2 and oxysterol-synthesizing enzymes in inflamed tissue of UC patients

We found an inflammation dependent upregulation of the EBI2-oxysterol axis in the gut. Results of a whole human genome microarray performed with total RNA isolated from inflamed and non-inflamed intestinal tissue from UC patients (GEO data sets: GDS3268)<sup>20</sup> were analyzed. RNA expression levels of the oxysterol-synthesizing enzymes CH25H, CYP7B1, and CYP27A1 from inflamed tissue of UC patients were significantly higher compared to non-inflamed tissue of UC patients ( $p < 0.05$  and  $p < 0.001$ ) and tissue of healthy controls ( $p < 0.001$  and  $p < 0.0001$ ; Fig. 1c and Supplementary Figure S1a). A similar increase was observed for the oxysterol receptor EBI2 ( $p < 0.001$  for inflamed vs. healthy).

Expression levels of *HSD3B7* remained unchanged in all three sample groups (Supplementary Figure S1a).

To validate these results, we analyzed colon biopsy samples from inflamed and non-inflamed tissue of UC patients from the Swiss IBD cohort study (SIBDCS). Biopsy samples were obtained from patients with moderate to severe or quiescent UC disease activity, respectively (Supplementary Table S1).

SIBDCS samples confirmed an upregulation of *CH25H* ( $p < 0.01$ ), *CYP7B1* ( $p < 0.0001$ ), and *EBI2* ( $p < 0.0001$ ) mRNA levels in inflamed tissue (Fig. 1d). mRNA expression levels of genes encoding proinflammatory cytokines (*TNF*, *IFNG*, and *IL1B*) were used to confirm the severity of colonic inflammation (Supplementary Figure S1b). Expression of genes of the EBI2-oxysterol axis also depended on clinical parameters: In a multivariate analysis, EBI2 expression was related to UC activity (modified Truelove and Witts activity index) while expression of *CH25H* and *CYP7B1* was related to endoscopic activity and a history of past or current TNF treatment ( $p < 0.05$ ; Supplementary Table S2).

Expression levels of *CYP7B1*, *EBI2*, and *TNF* strongly correlated ( $r \geq 0.6$ ,  $p < 0.001$  for all correlations) and *CYP7B1* expression correlated with *CH25H* ( $r = 0.46$ ,  $p < 0.05$ ), suggesting an upregulation of the EBI2-oxysterol system in active UC in parallel with the critical cytokine *TNF* (Supplementary Table S3). However, TNF does not seem to directly affect EBI2 expression since treatment of PBMCs with TNF did not affect EBI2 surface expression (Supplementary Figure S1c-d).

### Increased gene expression of EBI2 and oxysterol-synthesizing enzymes in murine DSS colitis

To further study the function of the EBI2-oxysterol system in gut inflammation, we induced acute and chronic dextran sulfate sodium (DSS) colitis in mice. In acute colitis, expression levels of *Ebi2*, *Ch25h*, and *Cyp7b1* were significantly increased ( $p < 0.001$ ; Fig. 2a). This increase was more pronounced than in human samples (Fig. 1c, d), potentially reflecting the more acute and severe inflammation in DSS colitis. In chronic DSS colitis, robust upregulation of *Ebi2* ( $p < 0.05$ ), *Ch25h* ( $p < 0.05$ ), and *Cyp7b1* ( $p < 0.0001$ ) was evident even though the increase was weaker in chronic than in acute inflammation, reminiscent of the human situation (Fig. 2b). No significant changes were observed in *Cyp27a1* and *Hsd3b7* expression in both acute and chronic colitis (Supplementary Figure S2a, b).

### Increased oxysterol levels in murine colitis

To determine the functional outcome of altered CH25H and CYP7B1 expression during inflammation, we compared oxysterol concentrations between mice with acute DSS colitis and controls. Eight oxysterol derivatives (hydroxycholesterol: HC; dihydroxylated cholesterols: diHC) were measured by mass spectrometry: 7 $\alpha$ ,25-diHC, 7 $\beta$ ,25-diHC, 25-HC, 7 $\alpha$ ,27-diHC, 7 $\beta$ ,27-diHC, 27-HC, 24S-HC, and 7 $\alpha$ ,24-diHC (Fig. 2c, d and Supplementary Figure S2c-f).

We found a trend for higher levels of 25-HC, 7 $\alpha$ ,25-diHC, and 7 $\alpha$ ,27-diHC in colon tissue of DSS-treated mice with acute colitis compared to untreated controls (Fig. 2c, upper panel) and significantly higher levels of 25-HC and 7 $\alpha$ ,25-diHC in liver tissue of inflamed versus untreated mice (Fig. 2c, lower panel). In both, colon and liver tissue knockout of CH25H led to lower levels of 25-hydroxylated oxysterols whereas lack of EBI2 did not influence any of the liver oxysterols (Fig. 2c and Supplementary Table S4).

In a multivariate linear regression analysis of liver oxysterol levels (Supplementary Table S4) controlling for DSS, CH25H, and EBI2 genotype, DSS treatment increased the levels of all 25-hydroxylated oxysterols (25-HC, 7 $\alpha$ ,25-diHC, 7 $\beta$ ,25-diHC) and all 24-hydroxylated oxysterols (24S-HC, 7 $\alpha$ ,24-diHC;  $p \leq 0.0015$  for all compounds). In contrast, inflammation did not seem to change 7 $\alpha$ - or 27-hydroxylation activity. In the same multivariate regression analysis, CH25H knockout significantly decreased all 25-hydroxylated oxysterols (7 $\alpha$ ,25-diHC, 7 $\beta$ ,25-diHC, and 24S-HC,

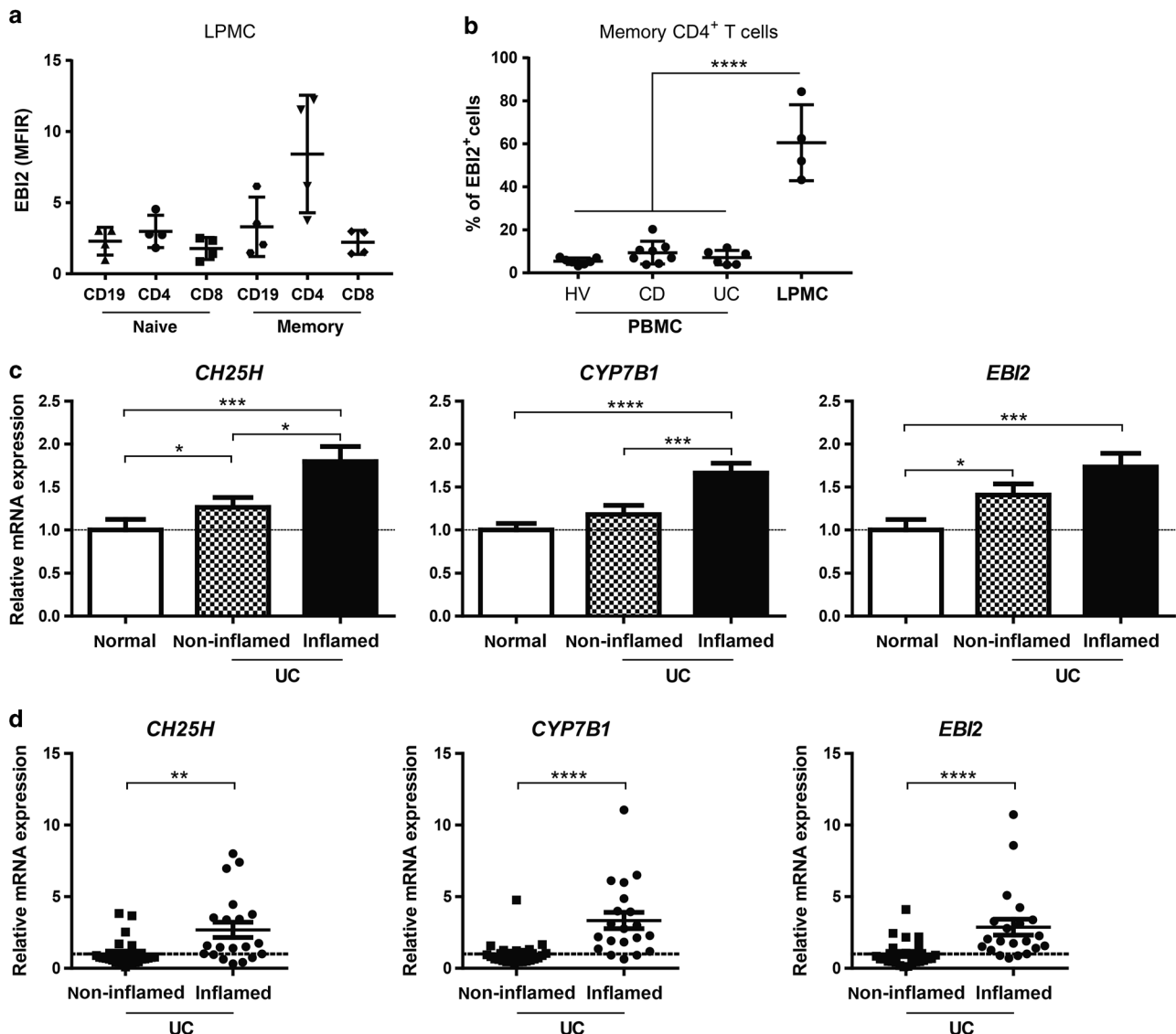


**Fig. 1** High EBI2 surface expression in human intestinal lymphocytes and upregulated gene expression of EBI2 and oxysterol-synthesizing enzymes in inflamed intestinal tissue. **(a)** EBI2 expression on human LPMCs of colon resections shown as mean fluorescence intensity ratio (MFIR) in naïve (CD19<sup>+</sup>CD27<sup>-</sup>) and memory (CD19<sup>+</sup>CD27<sup>+</sup>) subsets of B cells and in naïve (CD45RA<sup>+</sup>) and memory (CD45RA<sup>-</sup>) CD4<sup>+</sup> and CD8<sup>+</sup> T cells determined by FACS analysis. **(b)** Percentages of memory CD4<sup>+</sup> T cells expressing EBI2 on human PBMCs from healthy volunteers (HV) and CD and UC patients and on human LPMCs of colon resections determined by FACS analysis. **(c)** Data from a human whole genome microarray (GEO data sets: GDS3268) was analyzed regarding mRNA expression levels of *EBI2*, *CH25H* and *CYP7B1* in non-inflamed colon tissue of healthy volunteers ( $n = 63$ ) and non-inflamed ( $n = 61$ ) and inflamed ( $n = 62$ ) colon tissue of UC patients. The dotted line represents the mean of healthy tissue (set to 1). **(d)** mRNA expression levels from rectal biopsies of UC patients, either non-inflamed from patients with quiescent disease activity ( $n = 24$ ) or inflamed from patients with moderate to severe disease activity ( $n = 20$ ) from the Swiss IBD cohort study were determined by RT-PCR and normalized to GAPDH using the  $\Delta\Delta C_t$  method. Data shown as mean  $\pm$  SEM. Statistical analysis: **(a)**: One-way ANOVA with Dunnetts test; **(b-d)**: Mann-Whitney U test; \* $p < 0.05$ , \*\*\* $p < 0.001$ , \*\*\*\* $p < 0.0001$

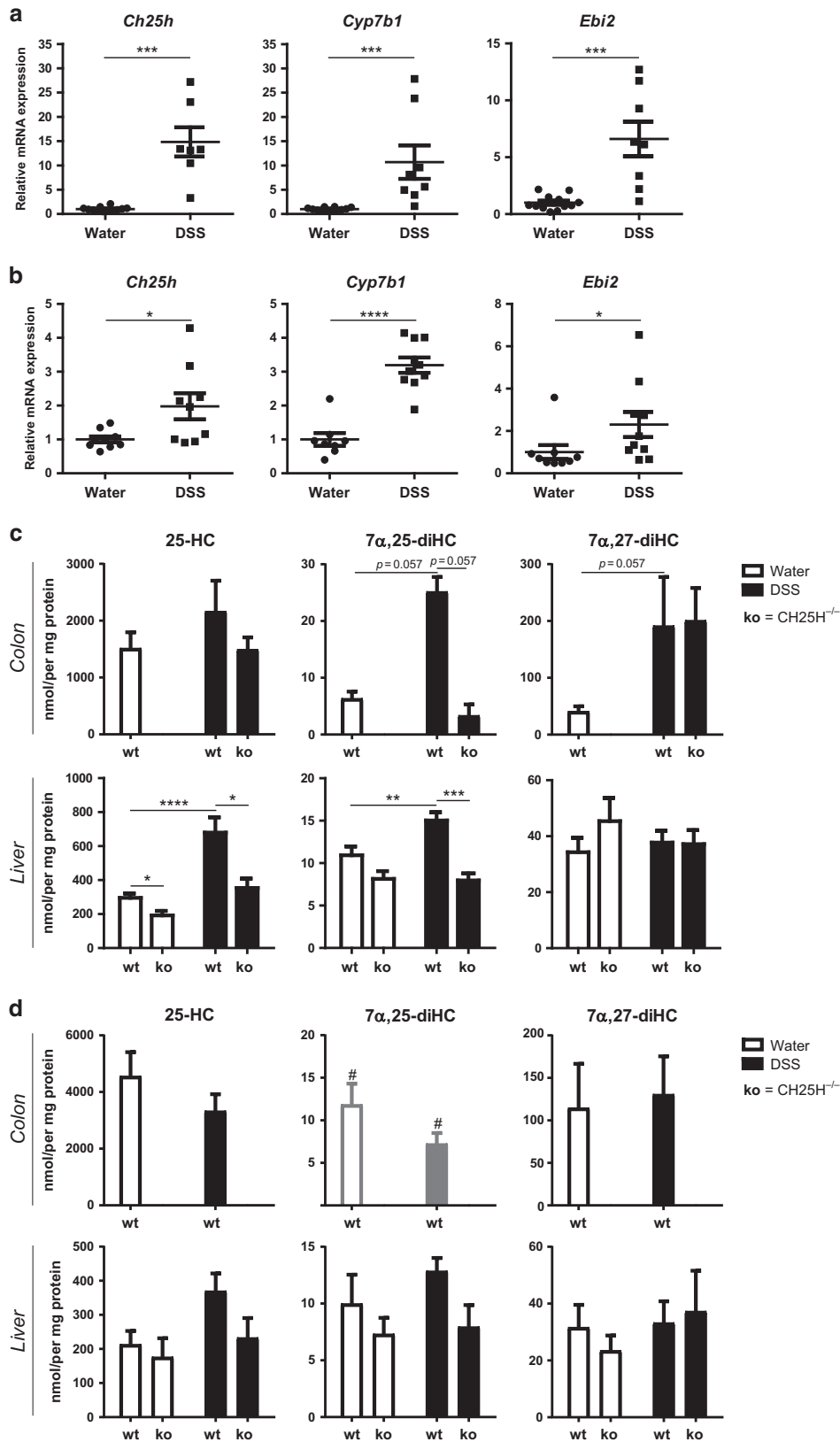
$p \leq 0.01$  for all compounds). However, as expected, the effect of CH25H knockout was not absolute and high levels of all 25-hydroxylated oxysterols remained, most likely due to the 25-hydroxylation activity of other enzymes including CYP27A1, CYP46A1, and CYP3A4.<sup>21</sup> Intestinal and liver gene expression levels of all analyzed oxysterol-related enzymes did not increase predictive value of the analysis (data not shown). A multivariate analysis for colon oxysterol measurements was not possible due to a low number of observations.

Our data thus indicate pronounced changes in liver oxysterol levels upon induction of acute colitis and CH25H knockout. Of note, inflammation increased levels of the EBI2 ligand 7 $\alpha$ ,25-diHC ( $p = 0.0015$ ) while CH25H knockout decreased its concentration ( $p < 0.0001$ ).

In chronic DSS colitis, oxysterol levels were not significantly elevated in colon or liver tissue (Fig. 2d), in agreement with only mild upregulation of oxysterol-producing enzymes (Fig. 2b).

Lack of EBI2 and CH25H does not affect severity of inflammation in the DSS colitis model

Despite the upregulation of the EBI2-oxysterol system in acute and chronic DSS colitis, knockout of neither EBI2 nor CH25H substantially decreased histological or endoscopic scoring of inflammation (Fig. 3a–d, Supplementary Figure S3a–c, and submitted manuscript.<sup>22</sup>) For CH25H<sup>-/-</sup> mice we observed a trend towards slightly increased inflammation indicated by significantly higher endoscopic colitis scores in acute DSS colitis (affecting all sub-scores, Supplementary Figure S3b). Of note, in



chronic colitis we also observed slightly increased inflammation, but for unclear reasons only the histological score with all sub-scores was affected (submitted manuscript.<sup>22</sup>) Reboldi et al. reported a 25-HC dependent suppression of *I11b* expression and

inflammasome activity.<sup>23</sup> However, in our experiments, increased inflammation in CH25H<sup>-/-</sup> mice could not be explained by increased *I11b* mRNA expression (Supplementary Figure S3d, e). Similar to wild-type animals, CH25H and EBI2 knockout mice

**Fig. 2** Increased expression levels of oxysterol-synthesizing enzymes CH25H and CYP7B1 accompanied by elevated oxysterol levels in murine DSS colitis. Acute and chronic DSS colitis was induced; on day 8 (acute colitis) or 80 (chronic colitis) mice underwent colonoscopy and were sacrificed to obtain tissue samples. **(a)** mRNA expression levels of *Ch25h*, *Cyp7b1* and *Ebi2* from colon tissue of wild-type mice with acute colitis and **(b)** chronic colitis and water controls were determined by RT-PCR and normalized to GAPDH using the  $\Delta\Delta C_t$  method. **(c)** Oxysterol levels from acute DSS colitis experiments were measured by LC-MS/MS. **Upper panel:** Oxysterol levels in colon tissue of inflamed wild-type ( $n = 4$ ) and inflamed CH25H<sup>-/-</sup> mice ( $n = 3$ ) with wild-type water controls ( $n = 3$ ). **Lower panel:** Oxysterol levels in liver tissue of inflamed wild-type ( $n = 12$ ) and inflamed CH25H<sup>-/-</sup> mice ( $n = 6$ ) and respective water controls ( $n = 12/n = 6$ ). **(d)** Oxysterol levels from chronic DSS colitis. **Upper panel:** Colon tissue from wild-type mice (DSS:  $n = 6$ , water:  $n = 6$ ). # indicates measurements, which were on the limit of detection (grey). **Lower panel:** Liver tissue of inflamed wild-type ( $n = 6$ ) and inflamed CH25H<sup>-/-</sup> ( $n = 5$ ) mice and respective water controls ( $n = 5/n = 6$ ). Data from acute and chronic DSS colitis are pooled from two independent experiments each. Data shown as mean  $\pm$  SEM. Statistical analysis: Mann-Whitney U test; \* $p < 0.05$ , \*\* $p < 0.01$ , \*\*\* $p < 0.001$ , \*\*\*\* $p < 0.0001$

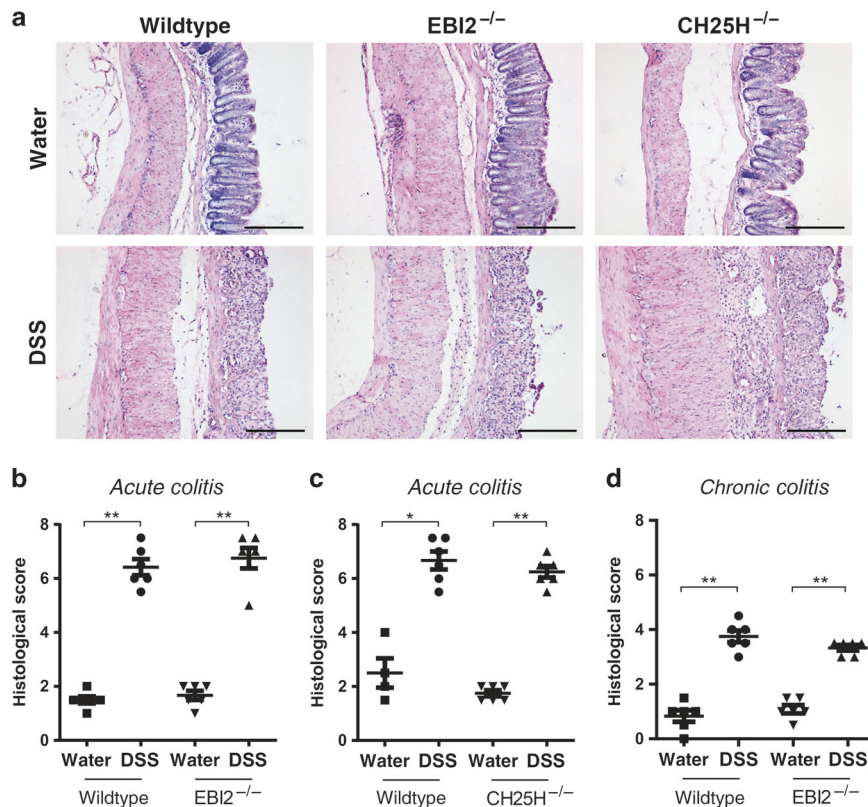


**Fig. 3** Lack of EB12 and CH25H does not affect severity of inflammation in the DSS colitis model. **(a)** Histological scores for acute DSS colitis were determined on HE-stained colon sections (scale bars: 200  $\mu$ m) in wild-type and EB12<sup>-/-</sup> mice **(b)**, and wild-type and CH25H<sup>-/-</sup> mice **(c)**. **(d)** Histological scores for chronic DSS colitis in EB12<sup>-/-</sup> mice were determined accordingly. Data from acute and chronic DSS colitis are pooled from two independent experiments each. Data shown as mean  $\pm$  SEM. Statistical analysis: Mann-Whitney U test; \* $p < 0.05$ , \*\* $p < 0.01$

showed increased expression levels of *Ch25h*, *Cyp7b1*, and *Ebi2* in acute and chronic DSS colitis (data not shown). Taken together, in the DSS-induced colitis model, the activity of EB12 and CH25H was not essential.

EB12 promotes colon inflammation in the IL-10 colitis model. Genetic defects of IL-10 or its receptor have been linked to human IBD,<sup>24</sup> hence we also addressed the role of EB12 in the IL-10 model of spontaneous colitis. For this aim, we generated EB12<sup>-/-</sup>IL10<sup>-/-</sup> mice and compared inflammatory activity to EB12<sup>+/+</sup>IL10<sup>-/-</sup> (in the following named IL10<sup>-/-</sup>) littermate controls. In 200-days-old mice, the histological colitis score of male EB12<sup>-/-</sup>IL10<sup>-/-</sup> mice was significantly reduced compared to IL10<sup>-/-</sup> controls ( $p < 0.01$ ; Fig. 4a, b). Reduced spleen weight in these EB12<sup>-/-</sup>IL10<sup>-/-</sup> animals ( $p < 0.05$ ) confirmed reduced systemic inflammation in EB12<sup>-/-</sup>IL10<sup>-/-</sup> males (Fig. 4c). Effects of EB12 on colon inflammation were restricted to male animals, in females no EB12-dependent changes were detected (Supplementary Figure S4a–c).

A minority of IL10<sup>-/-</sup> animals developed rectal prolapses due to colonic inflammation; however, time to develop prolapse did not differ between EB12<sup>-/-</sup>IL10<sup>-/-</sup> and IL10<sup>-/-</sup> in male and female animals (Fig. 4d, Supplementary Figure S4c). The genotype also did not affect colon inflammation of animals with prolapse (Fig. 4a).

Testing expression levels of a panel of immune regulatory genes in 200-days-old male EB12<sup>-/-</sup>IL10<sup>-/-</sup> and IL10<sup>-/-</sup> mice revealed similar expression of most cytokines and T cell regulatory genes except *Tbx21* and *Il23* for which expression was significantly higher in EB12<sup>-/-</sup>IL10<sup>-/-</sup> mice (Supplementary Figure S5a, b). Expression levels of enzymes regulating the concentration of EB12 ligands (CH25H, CYP7B1, CYP27A1, and HSD3B7) did not differ significantly between IL10<sup>-/-</sup> and EB12<sup>-/-</sup>IL10<sup>-/-</sup> mice (Supplementary Figure S5c, d).

EB12 is required for a normal number of colonic SILT. Since EB12 affects the localization of immune cells in secondary lymphatic organs, we speculated that EB12 knockout might also alter the distribution of immune cells in the colon. For

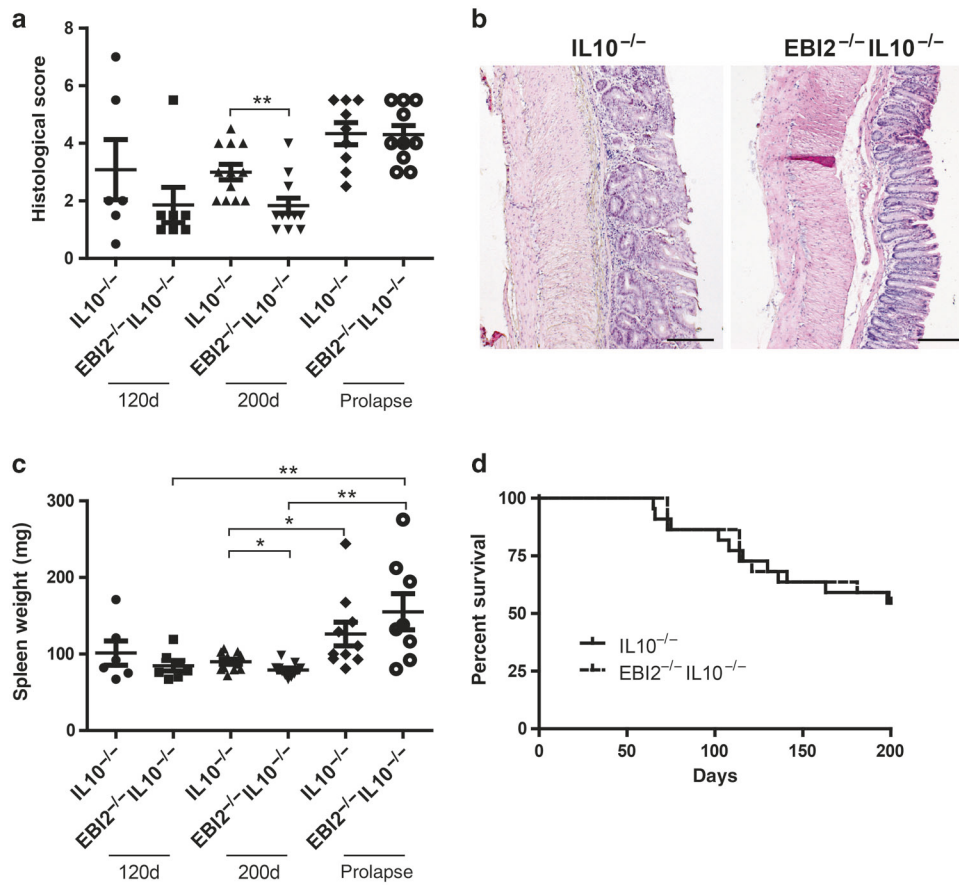


**Fig. 4** EB12 promotes inflammation in the IL-10 colitis model. EB12<sup>-/-</sup>IL10<sup>-/-</sup> and IL10<sup>-/-</sup> male mice were sacrificed after onset of rectal prolapse or at the age of 120 or 200 days. Histological scoring (a) and representative images (b) from HE-stained colon sections from 200 days old mice. Scale bars: 200 μm. (c) Spleen weight of animals from (a). (d) Onset of prolapse in EB12<sup>-/-</sup>IL10<sup>-/-</sup> and IL10<sup>-/-</sup> mice depicted in a survival curve. Each animal represents an independent observation from continuous breeding > 12 months. Data shown as mean ± SEM. Statistical analysis: Mann–Whitney U test; \*p < 0.05, \*\*p < 0.01

quantification of lymphoid structures in whole colons, B cells were visualized by B220 staining in a whole mount approach. The number of B220<sup>+</sup> structures was strongly reduced in EB12<sup>-/-</sup> mice in comparison to wild-type littermate controls ( $p < 0.05$ , Fig. 5a, b). This difference was much stronger than experimental variation (i.e., effects of cages). Stratifying B220<sup>+</sup> structures by size revealed a strongly reduced number of small and intermediate B220<sup>+</sup> structures ( $<20'000 \mu\text{m}^2$ ;  $p = 0.004$ ;  $<100'000 \mu\text{m}^2$ ;  $p < 0.0001$ ) while the number of large B220<sup>+</sup> structures ( $>100'000 \mu\text{m}^2$ ) remained unchanged (Fig. 5c). Furthermore, classification into multifollicular or single structures revealed lower numbers for both types in EB12<sup>-/-</sup> mice, but with a much stronger reduction for single structures, likely representing isolated lymphoid follicles (ILF) belonging to the group of SILT (Fig. 5d).

Lymphoid structures can also be identified on HE-stained colon “Swiss rolls”, where SILT are clearly distinguishable from CLP: SILT locate in the lamina propria, CLP between the two muscular layers and the muscularis mucosae<sup>12</sup> (Fig. 5e). This approach also allows for the visualization of small lymphoid structures including cryptpatches, largely devoid of B cells. While the number of SILT in EB12<sup>-/-</sup> animals was reduced ( $p < 0.05$ ), the number of large CLP remained unchanged (Fig. 5f).

Immunohistochemical stainings of the colon revealed normal structures of both SILT and CLP in EB12<sup>-/-</sup> animals with a normal distribution of B and T cells and c-kit<sup>+</sup> LTi cells recapitulating the situation of wild-type mice (Fig. 6). Taken together, our data suggest that EB12 does not seem to be required for maturation of SILT since the few detected lymphoid structures in EB12<sup>-/-</sup>

animals were indistinguishable from lymphoid structures in wild-types.

Development of intestinal lymphoid structures is a complex process involving ROR-γt-expressing ILCs, cytokines, and chemokines. However, colonic expression of RORC and chemokines important for lympho-organogenesis and lymphocyte recruitment including CCL20, CXCL13, and CCL19 were not altered in EB12<sup>-/-</sup> compared to wild-type mice (Supplementary Figure S6a) suggesting that the effect of EB12 is direct and not mediated via altered expression of any of the tested chemokines.

#### EB12 deficiency does not affect levels of B cells, IgA, and microbiota composition

To further assess effects of EB12 knockout on the colonic immune system, we quantified B and T cells by FACS. Overall, the fraction of B and T cells in the colon, mesenteric lymph nodes, and spleen of EB12<sup>-/-</sup> animals was similar to wild-types (Supplementary Figure S6b, c). Similarly, the substantial reduction of SILT numbers in EB12<sup>-/-</sup> mice did not significantly affect fecal IgA levels (Supplementary Figure S6d). Furthermore, overall microbiota composition of wild-type and EB12<sup>-/-</sup> animals was indistinguishable, and the microbiota of EB12<sup>-/-</sup> or wild-type animals resembled more strongly the microbiota of wild-type littermates from the same cage than animals of the same genotype housed in a different cage (data not shown). Finally, the fraction of colonic bacteria covered by IgA was similar in wild-type and EB12<sup>-/-</sup> animals (Supplementary Figure S6e). Overall, these experiments indicate an intact intestinal adaptive immune system and

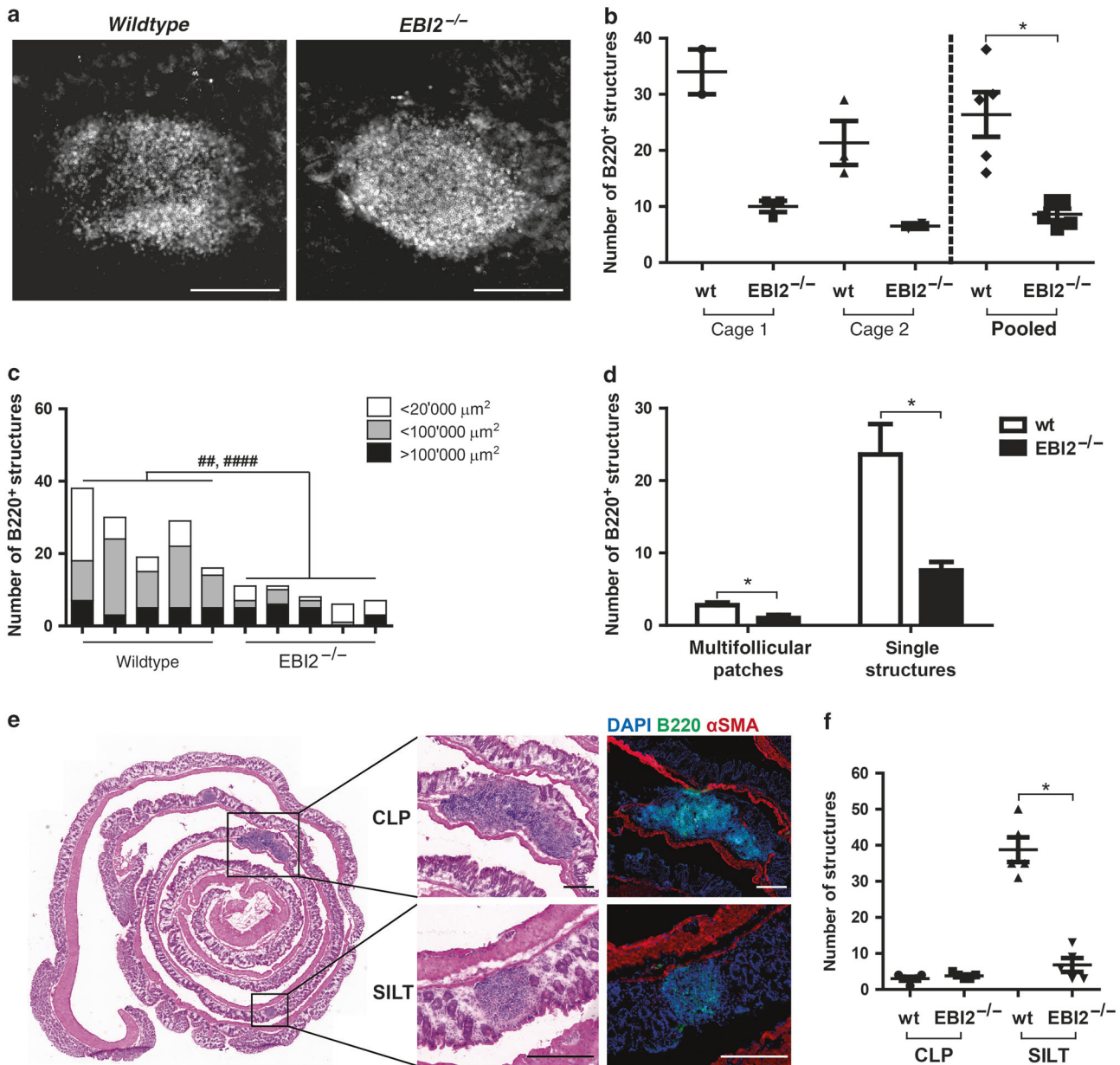


**Fig. 5** Lack of EB12 leads to a lower number of lymphoid structures in the colon. Colonic lymphoid structures of 12 weeks old female EB12<sup>-/-</sup> and wild-type littermate mice were assessed using complementary approaches. **(a)** B220 B cell staining in a whole mounted colon of wild-type and EB12<sup>-/-</sup> mice (B220: white). **(b)** Quantification of B cell follicles in B220-stained whole mounted colons. **(c)** Stratification of B220<sup>+</sup> structures from **(b)** by size (area). ## =  $p < 0.01$  and #### =  $p < 0.0001$  comparing structures  $< 20'000 \mu\text{m}^2$  and  $< 100'000 \mu\text{m}^2$  respectively with a multivariate Poisson regression using model-based t-tests. **(d)** Classification of B220<sup>+</sup> structures from **(b)** by presence or absence of multiple follicles per structure. **(e)** HE-stained colon Swiss rolls (left) and representative SILT and CLP structures stained with HE (middle) and B220 and  $\alpha\text{SMA}$  (right); scale bars: 200  $\mu\text{m}$ . **(f)** Lymphoid structures were quantified and categorized according to their location in 20 HE-stained colon Swiss roll sections per mouse. Scale bars: 200  $\mu\text{m}$ . Data shown as mean  $\pm$  SEM. Statistical analysis: Mann-Whitney U test; \* $p < 0.05$

microbiota composition in the non-inflamed colon of EB12<sup>-/-</sup> animals.

EB12 promotes an increase of the number of colonic lymphoid structures in intestinal inflammation

To test for effects of EB12 on the formation of lymphoid structures during inflammation, we quantified lymphoid structures in mice with chronic DSS colitis. As previously reported, in wild-type mice with DSS colitis, the number of colonic lymphoid structures was approximately two-fold higher compared to control animals ( $p < 0.05$ ; Fig. 7a, b). Furthermore, in EB12<sup>-/-</sup> animals the number of lymphoid structures did not significantly increase upon DSS

treatment ( $p = 0.07$ , Fig. 7a) and remained well below levels observed in inflamed wild-type colons even though severity of inflammation was comparable between wild-type and EB12<sup>-/-</sup> mice (Fig. 3b, d). In CH25H<sup>-/-</sup> mice the number of lymphoid structures at baseline was also lower compared to wild-type animals ( $p < 0.05$ ; Fig. 7b). However, DSS-induced colonic inflammation increased the number of lymphoid structures in CH25H<sup>-/-</sup> mice almost to wild-type levels. Therefore, CH25H activity seems necessary for normal development of lymphoid structures at baseline but not for an increase in chronic inflammation. No increase in lymphoid structures was observed in acute DSS colitis (Supplementary Figure S7a, b).

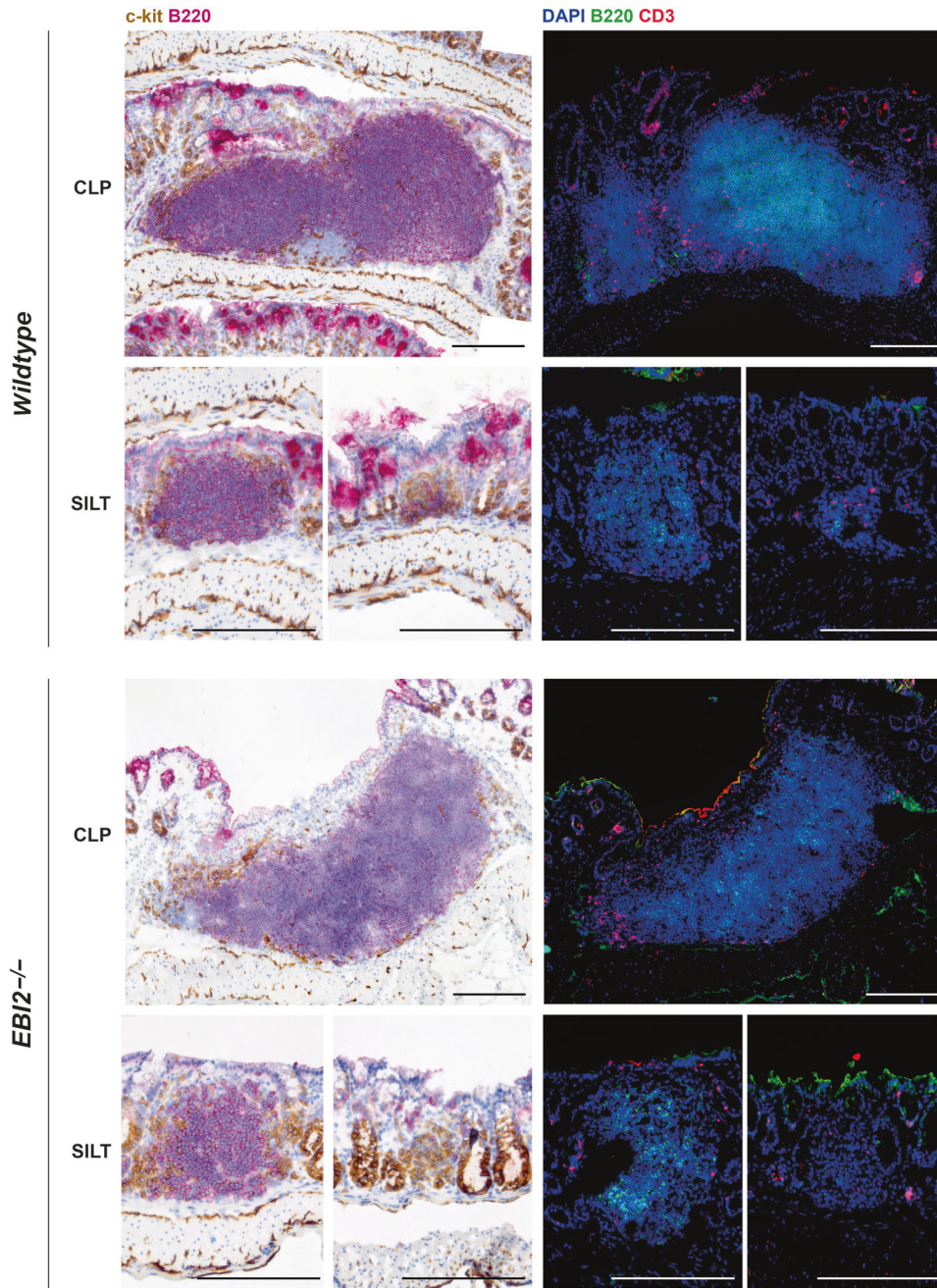


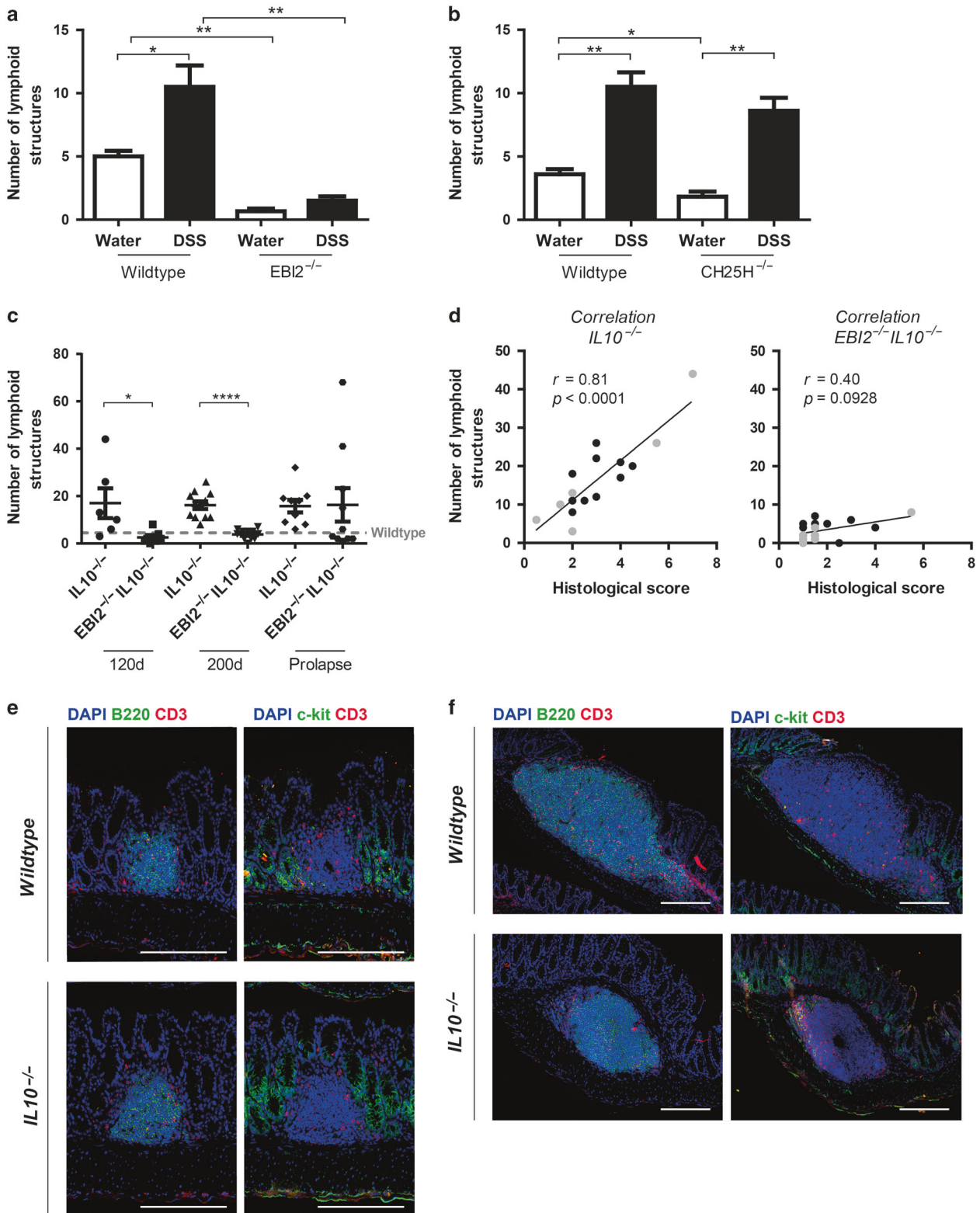
**Fig. 6** Similar lymphoid structures (CLP and SILT) in wild-type and EB12<sup>-/-</sup> mice. Cellular characterization of CLP and SILT with immunohistochemical staining of colon Swiss rolls for c-kit (brown) and B220 (pink; please note unspecific staining of alkaline phosphatase at the top of crypts) and with immunofluorescent staining for B220 (green) and CD3 (red). Scale bars: 200 μm, images are representative from at least 3 mice

Compared to untreated wild types, the number of lymphoid structures was increased in IL10<sup>-/-</sup> mice (>three-fold; Fig. 7c and Supplementary Figure S8a), and the number of lymphoid structures strongly correlated with the level of intestinal inflammation in IL10<sup>-/-</sup> animals (Fig. 7d). However, this was not the case in EB12<sup>-/-</sup>IL10<sup>-/-</sup> mice, which had clearly decreased numbers of colonic lymphoid structures compared to IL10<sup>-/-</sup> mice ( $p < 0.05$  and  $p < 0.0001$ , at day 120 and 200, respectively). Furthermore, inflammation did not significantly increase the number of lymphoid structures in EB12<sup>-/-</sup>IL10<sup>-/-</sup> animals, suggesting that EB12 is required for efficient accumulation of lymphoid structures during inflammation (Fig. 7c, d and Supplementary Table S5). The cellular composition of gut mucosal lymphoid structures in IL10<sup>-/-</sup> mice was very similar to the structures seen in wild-type mice (Fig. 7e, f).

In IL10<sup>-/-</sup> mice, accumulation of lymphoid structures was clearly accompanied by an increase in IgA levels in fecal colon extracts. However, this effect was much lower in EB12<sup>-/-</sup> animals (Supplementary Figure S8b-c), due to a reduced number of SILTs and/or other effects of missing EB12 function. Taken together, our data indicate an essential role of EB12 in the accumulation of lymphoid structures upon colonic inflammation.

## DISCUSSION

This study assessed the role of EB12 and oxysterols for the development of colonic lymphoid tissue and human and murine colitis. Key observations of our study include: i) The EB12-7α,25-diHC axis is upregulated in colitis, indicated by mRNA



measurements of EB12 and oxysterol-synthesizing enzymes in human and murine colon samples and oxysterol levels in mice. ii) EB12 is required for efficient formation of solitary intestinal lymphoid tissue (SILT) in the mouse colon. iii) EB12 is required for accumulation of lymphoid tissue in chronic mouse colitis. iv) EB12 increases the severity of colitis in the IL-10 colitis model but not in acute or chronic DSS colitis.

We show an activation of the EB12-oxysterol axis in colon inflammation using mRNA and direct oxysterol measurements. Analogous to previous studies, our results demonstrate that inflammation increased CYP7B1 and CH25H mRNA expression and levels of all 25-hydroxylated oxysterols tested, including the EB12 ligand 7 $\alpha$ ,25-diHC.<sup>11,25-28</sup> Inflammation did not affect concentrations of most 7 $\alpha$ -hydroxylated oxysterols, even though *Cyp7b1*

**Fig. 7** EB12 promotes an increase in the number of colonic lymphoid structures in chronic intestinal inflammation. Lymphoid structures were quantified in representative HE-stained colon sections. **(a)** Quantification of lymphoid structures in female wild-type ( $n = 6$ ) and EB12<sup>-/-</sup> mice ( $n = 6$ ) with chronic DSS colitis and water controls ( $n = 6$  each). **(b)** As in (a), but with wild-type ( $n = 6$ ) and CH25H<sup>-/-</sup> mice ( $n = 5$ ) and water controls ( $n = 5 / n = 6$ ). **(c)** Quantification of lymphoid structures in EB12<sup>-/-</sup>IL10<sup>-/-</sup> and IL10<sup>-/-</sup> male mice at the indicated ages or after occurrence of prolapse. The dotted line indicates the mean number of lymphoid structures in wild-type animals at the age of approximately 200 days. **(d)** Correlation of the numbers of lymphoid structures with histological scoring of 120 (grey) and 200 days old (black) EB12<sup>-/-</sup>IL10<sup>-/-</sup> and IL10<sup>-/-</sup> male mice. **(e, f)** Cellular characterization of lymphoid structures **(e)**: SILT and **(f)**: CLP with immunofluorescent staining of colon Swiss rolls for B220 (green; left panels) or c-kit (green; right panels), CD3 (red) and DAPI (blue) in wild-type and IL10<sup>-/-</sup> mice at the age of 200 days. Scale bars: 200  $\mu$ m. Data from chronic DSS colitis (a and b) are pooled from two independent experiments each. Data from IL-10 colitis: each animal represents an independent observation from continuous breeding > 12 months. Data shown as mean  $\pm$  SEM. Statistical analysis: Mann-Whitney U test; \* $p < 0.05$ , \*\* $p < 0.01$ , \*\*\*\* $p < 0.0001$ ; correlation analysis: Spearman R

mRNA levels were induced 10-fold. Effects of inflammation on enzyme expression and oxysterols levels were less pronounced in chronic DSS colitis. No oxysterol measurements for the IL-10 colitis models are available, which is a limitation of our study. Yet, very recently an independent study observed a similar increase of oxysterol levels both in other mouse models of colitis and in human colitis cohorts.<sup>29</sup>

Knockout of the 7 $\alpha$ ,25-diHC receptor EB12 decreased the number of colonic lymphoid structures approximately five-fold, as also demonstrated very recently.<sup>16</sup> Further, the number of lymphoid structures was reduced in CH25H<sup>-/-</sup> animals, independently confirming a role of the EB12-7 $\alpha$ ,25-diHC axis in colonic lymphoid tissue formation. SILT in EB12<sup>-/-</sup> and wild-type animals were morphologically indistinguishable, suggesting that EB12 promotes induction but is not essential for subsequent maturation of SILT. Further, our results indicate an intact IgA response with intact bacterial IgA coating in homeostasis in EB12<sup>-/-</sup> mice with a reduced number of SILTs.

Our results agree with the recent paper by Emgård et al., describing EB12-dependent lymphoid tissue formation during homeostasis.<sup>16</sup> Emgård et al. showed EB12 expression by ILC with a LTi phenotype. LTi cells migrate towards a 7 $\alpha$ ,25-diHC gradient in vitro and EB12 knockout reduced the number of cryptopatches and ILF (i.e., immature and mature SILT). Emgård et al. also demonstrated expression of CH25H and CYP7B1 by CD34<sup>+</sup>Podoplanin<sup>+</sup> fibroblasts as a likely source for 7 $\alpha$ ,25-diHC production, which would attract EB12<sup>+</sup> LTi-cells.<sup>16</sup>

There is agreement that chronic inflammation increases the number of intestinal lymphoid tissues in the DSS colitis model.<sup>17,30,31</sup> However, in a carefully performed study by Olivier et al., three large colonic lymphoid structures were induced in inflammation in three distinct locations in the colon.<sup>31</sup> In contrast, in a study by Lochner et al., up to 30 lymphoid structures were found in inflamed colonic tissue,<sup>17</sup> similar to our experiments. The reason for this discrepancy remains unclear but might be related to differences in the intestinal microbiota or different scoring systems used in these studies.

Our study shows that accumulation of lymphoid structures in chronic DSS colitis strongly depends on EB12 activity. Similarly, in IL-10 colitis, the level of inflammation increased the number of colonic lymphoid structures and EB12 knockout abolished accumulation of lymphoid structures in inflammation (Supplementary Table S5). In contrast, CH25H knockout did not significantly affect the number of lymphoid structures in inflammation, suggesting that CH25H activity is not limiting for immune cell recruitment. In inflammation, we found an increase of the other EB12 ligand 7 $\alpha$ ,27-diHC produced by CYP27A1 in colon tissue (Figure 2c). 7 $\alpha$ ,27-diHC might replace 7 $\alpha$ ,25-diHC as a chemoattractant in intestinal inflammation, as 7 $\alpha$ ,27-diHC has been shown to act as an efficient EB12 ligand for the positioning of dendritic cells in the spleen.<sup>32</sup> However, we cannot completely rule out that other enzymes with 25-hydroxylation activity can replace CH25H. In any case, future studies with CH25H/ CYP27A1 double knockouts are warranted. In previous studies, several requirements for induction of lymphoid tissue in inflammation,

including a role of lymphotoxin, IL-22, IL-23, and CXCL13 have been described.<sup>17,33,34</sup> Our study identifies EB12 as a further molecule promoting the accumulation of lymphoid tissue in chronic inflammation.

Even though lymphoid structures uniformly accompany colonic inflammation, it is unclear whether their accumulation promotes colon inflammation or whether it is a reaction to chronic inflammation, potentially enabling downregulation of inflammation, or induction of tolerance.<sup>35</sup> Some experimental evidence for proinflammatory effects of SILT in murine colitis has been published: ROR- $\gamma$ t deficient mice displayed more colonic SILT and more severe DSS colitis compared to wild-type. Vice versa, reduction of the number of SILT by lymphotoxin neutralization decreased colitis severity.<sup>17</sup> A similar correlation between intestinal lymphoid tissue accumulation and severity of inflammation was observed in the TNF <sup>$\Delta$ ARE</sup> model. Interference by anti-CCR7 treatment further increased lymphoid tissue formation and severity of inflammation.<sup>36</sup>

Our results argue against an essential proinflammatory role of lymphoid structures in the chronic DSS and IL-10 colitis model: Severity of inflammation in chronic DSS colitis was identical in EB12 wild-type and knockout animals. Further, EB12 knockout did not reduce inflammation in female IL10<sup>-/-</sup> animals even though the number of lymphoid structures was decreased to a similar level as in males.

In contrast to DSS colitis, EB12 knockout reduces inflammation in IL-10 colitis; however, EB12 deficiency only reduced inflammation in male mice. This gender dependent dimorphism of EB12<sup>-/-</sup>IL10<sup>-/-</sup> animals has parallels in the literature. Other sexual dimorphisms regarding colitis severity have been related to various factors including microbiota<sup>37</sup> and colon cellular infiltrate<sup>38</sup> or direct effects of estradiol.<sup>39</sup> Further, in a recent study with the murine TNF <sup>$\Delta$ ARE</sup> model, protection from ileitis was observed in male, but not female mice with a specific pathogen-free flora.<sup>40</sup> Strikingly, for a genetic polymorphism within the human *IL10* gene, a sexual dimorphism regarding the risk of ulcerative colitis has been described.<sup>41</sup> For the enzyme CYP7B1, producing the EB12 ligand 7 $\alpha$ ,25-diHC, differential expression in mouse livers (male > females) has been described;<sup>42</sup> however, our analysis did not reveal relevant gender specific differences of all oxysterol producing enzymes tested (Supplementary Figure S5c and data not shown). Further, the number of lymphoid structures was similar in both sexes. Taken together, the mechanism for the sexual dimorphism of the EB12 knockout in IL-10 colitis regarding inflammation cannot be explained by our experiments, which remains a further limitation of our study.

Further, EB12 knockout only affected IL-10 colitis but not acute or chronic DSS colitis, likely reflecting different mechanisms of inflammation.<sup>43</sup> In DSS colitis, pathogenesis comprises destruction of the epithelial barrier and primarily innate immune system activation. In contrast, IL-10 colitis results from lack of immunomodulatory effects of IL-10 on several immune cells.<sup>44</sup> To test whether EB12 knockout would reduce recruitment of proinflammatory T cells, we analyzed mRNA levels of several T cell markers but no clear difference was detected (Supplementary Figure S5a).

ILCs were shown to have high EB12 expression and ILCs lacking EB12 failed to localize into colonic lymphoid structures.<sup>16,45</sup> Impaired ILC recruitment might explain reduced inflammation in EB12<sup>-/-</sup>IL10<sup>-/-</sup> animals. The role of ILCs in IL-10 colitis has not been formally addressed; however, in a related infectious colitis model with *Campylobacter jejuni* infecting IL10<sup>-/-</sup> mice, colonic ILCs were increased and depletion of ILCs abrogated colitis.<sup>46</sup> ILCs have also been implicated in other models of colitis.<sup>47–49</sup> In CD40 colitis, ILCs within colonic cryptopatches increased their motility shortly after induction of inflammation, resulting in ILC accumulation at the tip of the villus.<sup>50</sup> The signal driving ILC movements is unclear but 7 $\alpha$ ,25-diHC produced immediately after onset of inflammation might stimulate EB12-dependent ILC motility.

Emgård et al. also demonstrated reduced colon inflammation upon EB12 knockout: In CD40 colitis, EB12 expressing ILCs and myeloid cells accumulated in inflammatory foci in the colon mucosa and colitis severity were much lower in EB12<sup>-/-</sup> animals.<sup>16</sup> These data, together with our data, suggest that the dependence of inflammation on EB12 varies regarding the colitis model. EB12 dependence would be expected for models with a critical role of ILCs including CD40 colitis,<sup>16,48</sup> TRUC colitis (spontaneous colitis in RAG2<sup>-/-</sup>TBX21<sup>-/-</sup> animals),<sup>49</sup> and some infectious colitis models.<sup>47</sup> In contrast, DSS colitis with breakdown of the physical barrier of the colon seems to develop independently of EB12. ILCs have also been implicated in human IBD since proinflammatory ILCs were found in intestinal samples.<sup>51</sup> In addition, a SNP associated with the EB12 gene increased the risk for both, UC and CD.<sup>1</sup>

In summary, we describe increased oxysterol synthesis in colon inflammation and a role of the EB12-7 $\alpha$ ,25-diHC axis for generation of colonic lymphoid structures in steady state and inflammation. Our results provide further insights to lymphoid tissue development in the colon, which has been substantially less studied than the small intestine. We also report a role of EB12 in IL-10 colitis, pointing to EB12 as a potential drug target in IBD since specific EB12 inhibitors are available.<sup>52</sup>

## MATERIALS AND METHODS

### Human samples

LPMCs were isolated from colon resections of patients undergoing intestinal surgery. PBMCs were isolated from healthy volunteers and IBD patients. Intestinal biopsies from IBD patients were obtained from the Swiss IBD Cohort Study (SIBDCS), a large, prospective nation-wide registry. The cohort goals and methodology are described elsewhere.<sup>53</sup> Sample and data collection was approved by local ethics committees (BASEC 2017-01868, EK-1316) and all patients provided written informed consent. Data from a whole human genome oligo microarray (GEO data sets: GDS3268)<sup>20</sup> were used as a complementary data set.

### Flow cytometric analysis of human samples

PBMCs and LPMCs (prepared as described in the supplementary methods) were thawed and resuspended in RPMI-PSG-10% FCS and plated for resting at 37 °C (PBMCs: overnight; LPMCs: 5 h). The cells were stained with LIVE/DEAD Fixable Dead Cell Stain Kit (Life technologies/ Thermo Fisher scientific, Waltham, USA) according to the manufacturer's instructions. For cell staining the following antibodies were purchased from BioLegend (San Diego, USA): CD8 (SK1), CD4 (SK3), CD45RA (HI100), CD27 (M-T271), CD19 (HIB19), and CCRR6 (G0343E3). The following antibodies were purchased from BD Biosciences (Franklin Lakes, USA): PE-Streptavidin and CD3 (SK7). The isotype control was purchased from R&D Systems (Minneapolis, USA): Mouse IgG2a control biotin conjugated (Cat: IC0038). The EB12 antibody (57C9B5C9) was provided by Andreas Sailer from Novartis and biotinylated. All patient samples were analyzed with an LSR II flow cytometer (BD Biosciences, Franklin Lakes,

USA) within the same month. The analysis was performed with FlowJo software (FlowJo LLC).

### Animals

All mice were kept in a specific pathogen-free (SPF) facility in individually ventilated cages. EB12<sup>-/-</sup> mice (C57BL/6 x C129) were originally purchased from Deltagen (San Mateo, USA) and CH25H-deficient mice (C57/BL6) were provided by David. W. Russell, University of Texas Southwestern.<sup>6</sup> Both strains were subsequently back-crossed to C57BL/6 for more than 10 generations.<sup>6</sup> In our facility, they were crossed with wild-type C57BL/6 mice and heterozygous offspring was mated to generate knockout and wild-type littermates. All animal experiments were conducted according to Swiss animal welfare law and approved by the local animal welfare authority of Zurich county (Tierversuchskommission Zürich, Zurich, Switzerland, License No. ZH256-2014).

### Colitis models

Acute dextran sulfate sodium (DSS) colitis was induced in age- and weight-matched females by administration of 3% DSS (MW: 36–50 kDa; MP Biomedicals/ Thermo Fischer Scientific, Waltham, USA) in the drinking water for 7 days. Mice were sacrificed after colonoscopy on day 8. To induce chronic colitis, animals underwent 4 DSS cycles, consisting of 2% DSS administration for 7 days followed by 10 days of normal drinking water, each. Mice were sacrificed after colonoscopy 3 weeks after the last DSS cycle. Colonoscopy was performed as described previously and scored using the murine endoscopic index of colitis severity (MEICS) scoring system.<sup>54</sup>

IL10<sup>-/-</sup> mice (C57BL/6) were crossed with EB12<sup>-/-</sup> mice; animals heterozygous for EB12 (EB12<sup>+/-</sup>IL10<sup>-/-</sup>) were used to generate EB12<sup>-/-</sup>IL10<sup>-/-</sup> and EB12<sup>+/-</sup>IL10<sup>-/-</sup> littermates. IL10<sup>-/-</sup> animals are highly susceptible to develop spontaneous colitis. As described in previous studies,<sup>55</sup> 1% DSS for 4 days in drinking water at the age of 90 days was used to trigger inflammation, as the spontaneous development of colitis is dependent on the gut microbiota and is drastically reduced under SPF conditions. Mice were sacrificed at 120 or 200 days of age or upon development of rectal prolapse.

### Histological score

Colons were dissected, fixed in 4% formalin, embedded in paraffin, and cut into 5- $\mu$ m sections. Deparaffinized sections were stained with hematoxylin and eosin (HE). Histological scoring for acute and chronic DSS colitis was performed as described;<sup>56</sup> a slightly adapted score was used for IL10<sup>-/-</sup> colitis (Supplementary Table S6).

### Oxysterol measurements

**Extraction of oxysterols from murine liver samples.** Frozen colon or liver samples from colitis experiments were pulverized using a CryoPrepTM CP02 (Covaris, Woburn, USA), weighed and lysed in homogenization buffer (0.9% sodium chloride) using a Qiagen TissueLyser II (Qiagen, Venlo, NL) at 4 °C. Oxysterols were extracted from the lysate by two liquid-liquid extractions using a methanol:dichloromethane (1:1) mix and a homogenization buffer:dichloromethane (1:2) mix, respectively. The organic phases from both extractions were pooled and dried under nitrogen. The residue was reconstituted with ethanol containing 0.1% formic acid and filtered before analysis on the liquid chromatography tandem-mass spectrometry (LC-MS/MS) system.

**LC-MS/MS analysis.** The LC-MS/MS analysis was performed on a Dionex UltiMate 3000 RS with HPG Pump (Thermo Scientific, Waltham, USA), coupled with a Sciex Triple QuadTM 5500 mass spectrometer (AB Sciex, Zug, CH).

Detailed protocols of oxysterol extraction and LC-MS/MS analysis are provided in the supplementary methods.



### Quantification of lymphoid structures

**Whole mount.** Colons were removed intact, flushed with cold PBS, opened along the mesenteric border, and mounted, lumen facing up. Colons were then incubated two times for 10 min with warmed HBSS containing 2 mM EDTA at 37°C on a shaker to remove epithelial cells. After washing with PBS, colons were fixed with 4% Paraformaldehyde (PFA) for 1 h at 4°C. Colons were washed five times with TBST (1 M Tris (pH 7.2), 1 M NaCl, 0.2% Triton X-100) and blocked with TBST containing 2% rat serum for 1 h at 4°C. Colons were incubated with Cy3-conjugated anti-mouse B220 antibody (clone TIB146; provided by Oliver Pabst: Institute for Molecular Medicine, RWTH Aachen University, Aachen, Germany) in the above solution overnight at 4°C. The next day, colons were washed with TBST and mounted on glass slides. B220<sup>+</sup> cell clusters were quantified under the microscope.

**Swiss rolls.** Colons were dissected and opened along the mesenteric border. Swiss rolls were prepared with the luminal side facing outwards and embedded in optimum cutting temperature (OCT) compound, and frozen in liquid nitrogen. Quantification of lymphoid structures was performed in 20 HE-stained cryosections (6 µm) per colon, ~100 µm apart (the protocol for immunofluorescent stainings is provided in the supplementary methods). Zeiss Axio Scan.Z1 with ZEN blue Software (Zeiss, Oberkochen, Germany) was used to scan and analyze sections. SILT and CLP were defined according to their size and localization; CLP: composed of large lymphoid follicles between the two external muscular layers and the muscularis mucosae, SILT: smaller clusters of lymphoid cells in the lamina propria.

Lymphoid structures in animals from colitis experiments were enumerated using one HE-stained section of the rolled-up colon per mouse.

If not indicated otherwise, a Zeiss Axio Imager Z2 Microscope with Axio Vision Software (Zeiss, Oberkochen, Germany) was used.

### Statistical analysis

If not indicated otherwise, Mann–Whitney U test was performed with GraphPad Prism software (GraphPad, San Diego, USA). For the multivariate linear regression analysis, appropriate modules of Matlab R2017b were used. To compare the number of B220<sup>+</sup> lymphoid structures of different sizes (Fig. 5c) we used R studio to generate a multivariate Poisson regression relating log(average counts) with the genotype using model-based *t*-tests. Data are presented as mean ± SEM. *P*-values less than 0.05 were considered significant (\**p* < 0.05, \*\**p* < 0.01, \*\*\**p* < 0.001, \*\*\*\**p* < 0.0001).

### ACKNOWLEDGEMENTS

The authors would like to thank Silvia Lang for technical support, Jean-Benoît Rossel, Nicolas Fournier, and Delphine Golay for help with SIBDC data and biosamples, Brian Lang for help with the multivariate linear regression analysis, and the scientific committee of SIBDC for generous support.

### AUTHOR CONTRIBUTIONS

A.W., G.R. and B.M. conceived, designed, and supervised the study. A.W., T.R., G.S., F.R., C.P., A.M., R.R., M.R.S., L.H., I.F.W., K.A. and S.L. performed experiments and/or were involved in data analysis. M.H., G.K. and N.P. performed oxysterol measurements. O.P. performed analysis of microbial IgA coating. A.W. and B.M. wrote the paper. M.R.S., A.W.S., I.F.W., O.P., M.H., C.P., M.S. and G.R. critically revised the manuscript for important intellectual content. All authors approved the final version of the manuscript.

### ADDITIONAL INFORMATION

The online version of this article (<https://doi.org/10.1038/s41385-019-0140-x>) contains supplementary material, which is available to authorized users.

**Competing interests:** This work was supported by grants from the Swiss National Science Foundation to BM (grant No. 32473B\_156525), CP (PP00P3\_157476), FR

(MD-PhD fellowship) and GR (for the Swiss IBD Cohort, grant no. 33CS30\_148422) and a grant from the Hartmann-Müller Foundation to BM. AWS is an employee of Novartis Pharma AG and does hold stock and stock options in this company. The remaining authors declare no competing interests.

### REFERENCES

- Jostins, L. et al. Host-microbe interactions have shaped the genetic architecture of inflammatory bowel disease. *Nature* **491**, 119–124 (2012).
- de Lange, K. M. et al. Genome-wide association study implicates immune activation of multiple integrin genes in inflammatory bowel disease. *Nat. Genet.* **49**, 256–261 (2017).
- Gatto, D., Paus, D., Basten, A., Mackay, C. R. & Brink, R. Guidance of B cells by the orphan G protein-coupled receptor EB12 shapes humoral immune responses. *Immunity* **31**, 259–269 (2009).
- Gatto, D., Wood, K. & Brink, R. EB12 operates independently of but in cooperation with CXCR5 and CCR7 to direct B cell migration and organization in follicles and the germinal center. *J. Immunol.* **187**, 4621–4628 (2011).
- Pereira, J. P., Kelly, L. M., Xu, Y. & Cyster, J. G. EB12 mediates B cell segregation between the outer and centre follicle. *Nature* **460**, 1122–1126 (2009).
- Hannedouche, S. et al. Oxysterols direct immune cell migration via EB12. *Nature* **475**, 524–527 (2011).
- Liu, C. et al. Oxysterols direct B-cell migration through EB12. *Nature* **475**, 519–523 (2011).
- Gatto, D. et al. The chemotactic receptor EB12 regulates the homeostasis, localization and immunological function of splenic dendritic cells. *Nat. Immunol.* **14**, 876 (2013).
- Li, J., Lu, E., Yi, T. & Cyster, J. G. EB12 augments Tfh cell fate by promoting interaction with IL-2-quenching dendritic cells. *Nature* **533**, 110–114 (2016).
- Yi, T. et al. Oxysterol gradient generation by lymphoid stromal cells guides activated B cell movement during humoral responses. *Immunity* **37**, 535–548 (2012).
- Bauman, D. R. et al. 25-Hydroxycholesterol secreted by macrophages in response to Toll-like receptor activation suppresses immunoglobulin A production. *Proc. Natl Acad. Sci. USA* **106**, 16764–16769 (2009).
- Baptista, A. P. et al. Colonic patch and colonic SILT development are independent and differentially regulated events. *Mucosal Immunol.* **6**, 511–521 (2013).
- Buettner, M. & Lochner, M. Development and function of secondary and tertiary lymphoid organs in the small intestine and the colon. *Front. Immunol.* **7**, 342 (2016).
- Knoop, K. A., Butler, B. R., Kumar, N., Newberry, R. D. & Williams, I. R. Distinct developmental requirements for isolated lymphoid follicle formation in the small and large intestine: RANKL is essential only in the small intestine. *Am. J. Pathol.* **179**, 1861–1871 (2011).
- Donaldson, D. S., Bradford, B. M., Artis, D. & Mabbott, N. A. Reciprocal regulation of lymphoid tissue development in the large intestine by IL-25 and IL-23. *Mucosal Immunol.* **8**, 582–595 (2015).
- Emgard, J. et al. Oxysterol sensing through the receptor GPR183 promotes the lymphoid-tissue-inducing function of innate lymphoid cells and colonic inflammation. *Immunity* **48**, 120–132 e128 (2018).
- Lochner, M. et al. Microbiota-induced tertiary lymphoid tissues aggravate inflammatory disease in the absence of RORγt and LTi cells. *J. Exp. Med.* **208**, 125–134 (2011).
- Knoop, K. A. & Newberry, R. D. Isolated lymphoid follicles are dynamic reservoirs for the induction of intestinal IgA. *Front. Immunol.* **3**, 84 (2012).
- Clottu, A. S. et al. EB12 expression and function: robust in memory lymphocytes and increased by natalizumab in multiple sclerosis. *Cell Rep.* **18**, 213–224 (2017).
- Noble, C. L. et al. Regional variation in gene expression in the healthy colon is dysregulated in ulcerative colitis. *Gut* **57**, 1398–1405 (2008).
- Honda, A. et al. Cholesterol 25-hydroxylation activity of CYP3A. *J. Lipid Res.* **52**, 1509–1516 (2011).
- Raselli, T. et al. The oxysterol synthesizing enzyme CH25H contributes to the development of intestinal fibrosis. <https://www.biorxiv.org/content/early/2018/09/23/424820>.
- Reboldi, A. et al. Inflammation. 25-Hydroxycholesterol suppresses interleukin-1-driven inflammation downstream of type I interferon. *Science* **345**, 679–684 (2014).
- Kotlarz, D. et al. Loss of interleukin-10 signaling and infantile inflammatory bowel disease: implications for diagnosis and therapy. *Gastroenterology* **143**, 347–355 (2012).
- Diczfalusy, U. et al. Marked upregulation of cholesterol 25-hydroxylase expression by lipopolysaccharide. *J. Lipid Res.* **50**, 2258–2264 (2009).
- Xiang, Y. et al. Identification of cholesterol 25-hydroxylase as a novel host restriction factor and a part of the primary innate immune responses against hepatitis C virus infection. *J. Virol.* **89**, 6805–6816 (2015).

27. Wu, J. et al. LC/MS/MS profiling of tissue oxysterols and its application in dextran sodium sulphate induced mouse colitis models. *Curr. Top. Med. Chem.* **17**, 2781–2790 (2017).
28. Blanc, M. et al. The transcription factor STAT-1 couples macrophage synthesis of 25-hydroxycholesterol to the interferon antiviral response. *Immunity* **38**, 106–118 (2013).
29. Guillemot-Legrès O., et al. Colitis alters oxysterol metabolism and is affected by 4beta-hydroxycholesterol administration. *J. Crohns Colitis* 2018. <https://doi.org/10.1093/ecco-jcc/jjy157>. Epub ahead of print.
30. Okayasu, I. et al. A novel method in the induction of reliable experimental acute and chronic ulcerative colitis in mice. *Gastroenterology* **98**, 694–702 (1990).
31. Olivier, B. J. et al. Vagal innervation is required for the formation of tertiary lymphoid tissue in colitis. *Eur. J. Immunol.* **46**, 2467–2480 (2016).
32. Lu, E., Dang, E. V., McDonald, J. G. & Cyster, J. G. Distinct oxysterol requirements for positioning naive and activated dendritic cells in the spleen. *Sci. Immunol.* **2**, 10 (2017).
33. Ota, N. et al. IL-22 bridges the lymphotoxin pathway with the maintenance of colonic lymphoid structures during infection with *Citrobacter rodentium*. *Nat. Immunol.* **12**, 941–948 (2011).
34. Marchesi, F. et al. CXCL13 expression in the gut promotes accumulation of IL-22-producing lymphoid tissue-inducer cells, and formation of isolated lymphoid follicles. *Mucosal Immunol.* **2**, 486–494 (2009).
35. McNamee, E. N. & Rivera-Nieves, J. Ectopic tertiary lymphoid tissue in inflammatory bowel disease: protective or provocateur? *Front. Immunol.* **7**, 308 (2016).
36. McNamee, E. N. et al. Ectopic lymphoid tissue alters the chemokine gradient, increases lymphocyte retention and exacerbates murine ileitis. *Gut* **62**, 53–62 (2013).
37. Kozik, A. J., Nakatsu, C. H., Chun, H. & Jones-Hall, Y. L. Age, sex, and TNF associated differences in the gut microbiota of mice and their impact on acute TNBS colitis. *Exp. Mol. Pathol.* **103**, 311–319 (2017).
38. Gao, Y., Postovalova, E. A., Makarova, O. V., Dobrynina, M. T. & Mikhailova, L. P. Sex-related differences in the morphology and subpopulation composition of colon lymphocytes in experimental acute colitis. *Bull. Exp. Biol. Med.* **165**, 503–507 (2018).
39. Babickova, J. et al. Sex differences in experimentally induced colitis in mice: a role for estrogens. *Inflammation* **38**, 1996–2006 (2015).
40. Schaubek, M. et al. Dysbiotic gut microbiota causes transmissible Crohn's disease-like ileitis independent of failure in antimicrobial defence. *Gut* **65**, 225–237 (2016).
41. Tedde, A. et al. Interleukin-10 promoter polymorphisms influence susceptibility to ulcerative colitis in a gender-specific manner. *Scand. J. Gastroenterol.* **43**, 712–718 (2008).
42. Li-Hawkins, J., Lund, E. G., Bronson, A. D. & Russell, D. W. Expression cloning of an oxysterol 7alpha-hydroxylase selective for 24-hydroxycholesterol. *J. Biol. Chem.* **275**, 16543–16549 (2000).
43. Jones-Hall, Y. L. & Grisham, M. B. Immunopathological characterization of selected mouse models of inflammatory bowel disease: Comparison to human disease. *Pathophysiology* **21**, 267–288 (2014).
44. Keubler, L. M., Buettner, M., Hager, C. & Bleich, A. A multihit model: colitis lessons from the interleukin-10-deficient mouse. *Inflamm. Bowel Dis.* **21**, 1967–1975 (2015).
45. Chu, C. et al. Anti-microbial functions of group 3 innate lymphoid cells in gut-associated lymphoid tissues are regulated by G-protein-coupled receptor 183. *Cell Rep.* **23**, 3750–3758 (2018).
46. Malik, A. et al. Contrasting immune responses mediate *Campylobacter jejuni*-induced colitis and autoimmunity. *Mucosal Immunol.* **7**, 802–817 (2014).
47. Buonocore, S. et al. Innate lymphoid cells drive interleukin-23-dependent innate intestinal pathology. *Nature* **464**, 1371–1375 (2010).
48. Vonarbourg, C. et al. Regulated expression of nuclear receptor RORgammat confers distinct functional fates to NK cell receptor-expressing RORgammat(+) innate lymphocytes. *Immunity* **33**, 736–751 (2010).
49. Powell, N. et al. The transcription factor T-bet regulates intestinal inflammation mediated by interleukin-7 receptor+ innate lymphoid cells. *Immunity* **37**, 674–684 (2012).
50. Pearson, C. et al. ILC3 GM-CSF production and mobilisation orchestrate acute intestinal inflammation. *elife* **5**, e10066 (2016).
51. Geremia, A. et al. IL-23-responsive innate lymphoid cells are increased in inflammatory bowel disease. *J. Exp. Med.* **208**, 1127–1133 (2011).
52. Gessier, F. et al. Identification and characterization of small molecule modulators of the Epstein-Barr virus-induced gene 2 (EBI2) receptor. *J. Med. Chem.* **57**, 3358–3368 (2014).
53. Pittet, V. et al. Cohort profile: the Swiss Inflammatory Bowel Disease Cohort Study (SIBDCS). *Int. J. Epidemiol.* **38**, 922–931 (2009).
54. Becker, C., Fantini, M. C. & Neurath, M. F. High resolution colonoscopy in live mice. *Nat. Protoc.* **1**, 2900–2904 (2006).
55. Michael, S. et al. Quantitative phenotyping of inflammatory bowel disease in the IL-10-deficient mouse by use of noninvasive magnetic resonance imaging. *Inflamm. Bowel Dis.* **19**, 185–193 (2013).
56. Hausmann, M. et al. In vivo treatment with the herbal phenylethanoid acteoside ameliorates intestinal inflammation in dextran sulphate sodium-induced colitis. *Clin. Exp. Immunol.* **148**, 373–381 (2007).



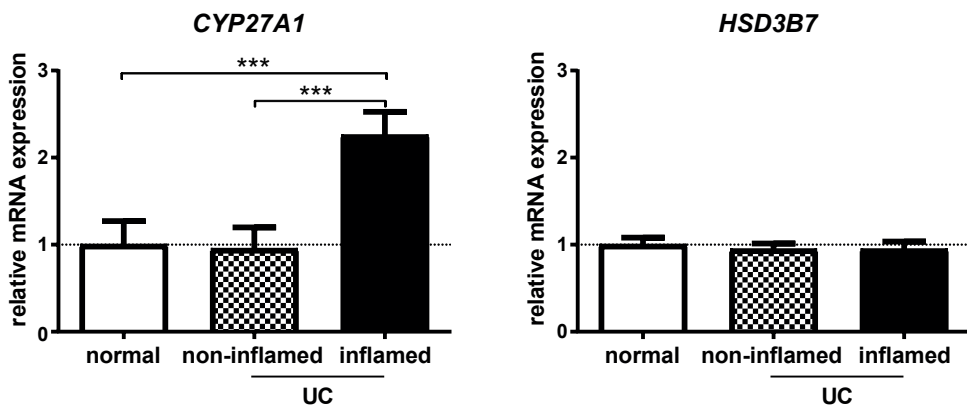
**Open Access** This article is licensed under a Creative Commons Attribution 4.0 International License, which permits use, sharing, adaptation, distribution and reproduction in any medium or format, as long as you give appropriate credit to the original author(s) and the source, provide a link to the Creative Commons license, and indicate if changes were made. The images or other third party material in this article are included in the article's Creative Commons license, unless indicated otherwise in a credit line to the material. If material is not included in the article's Creative Commons license and your intended use is not permitted by statutory regulation or exceeds the permitted use, you will need to obtain permission directly from the copyright holder. To view a copy of this license, visit <http://creativecommons.org/licenses/by/4.0/>.

© The Author(s) 2019

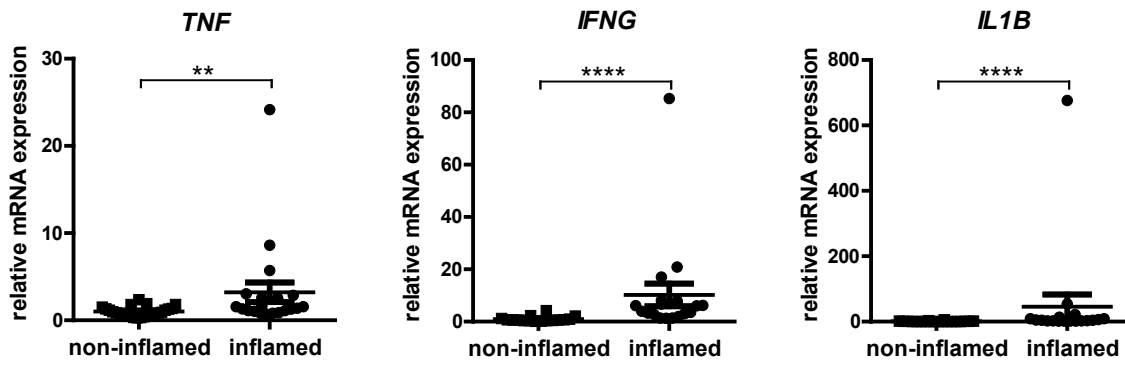


Supplementary Figure 1

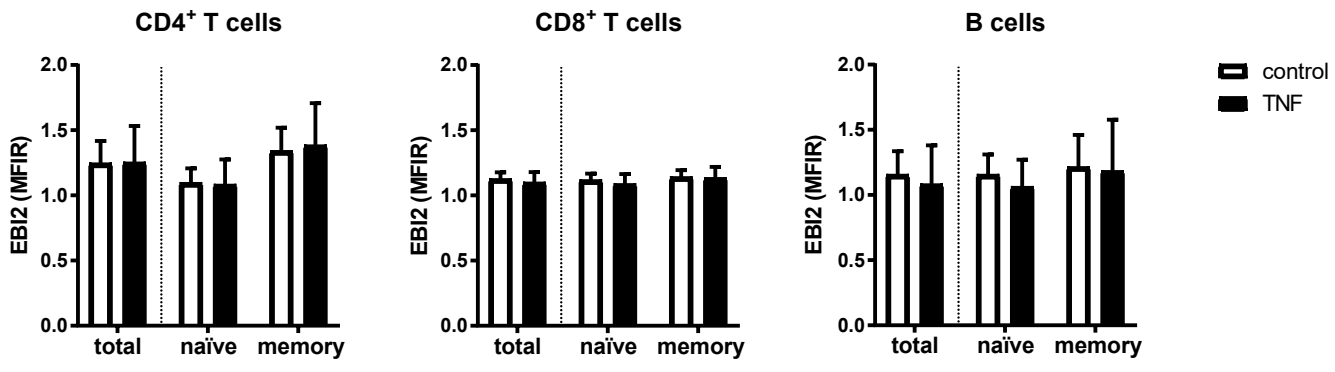
**a**



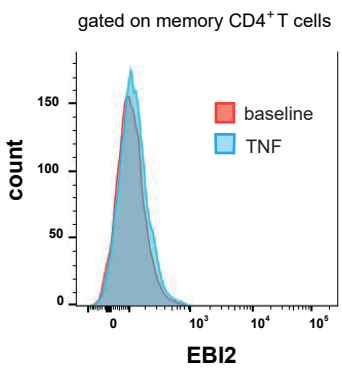
**b**



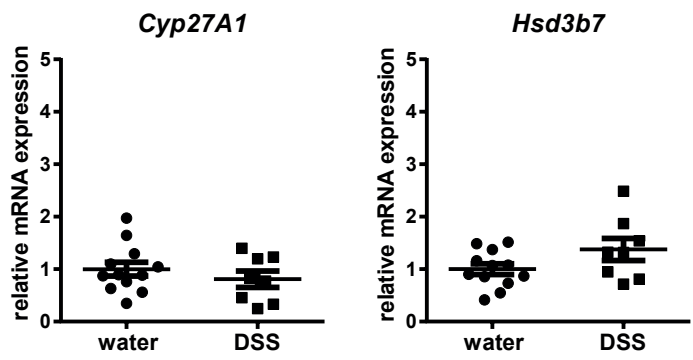
**c**



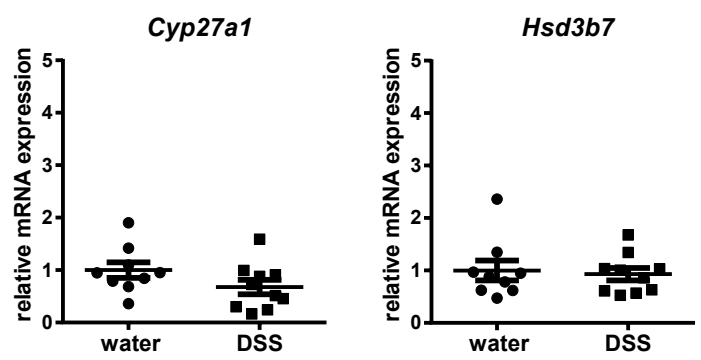
**d**



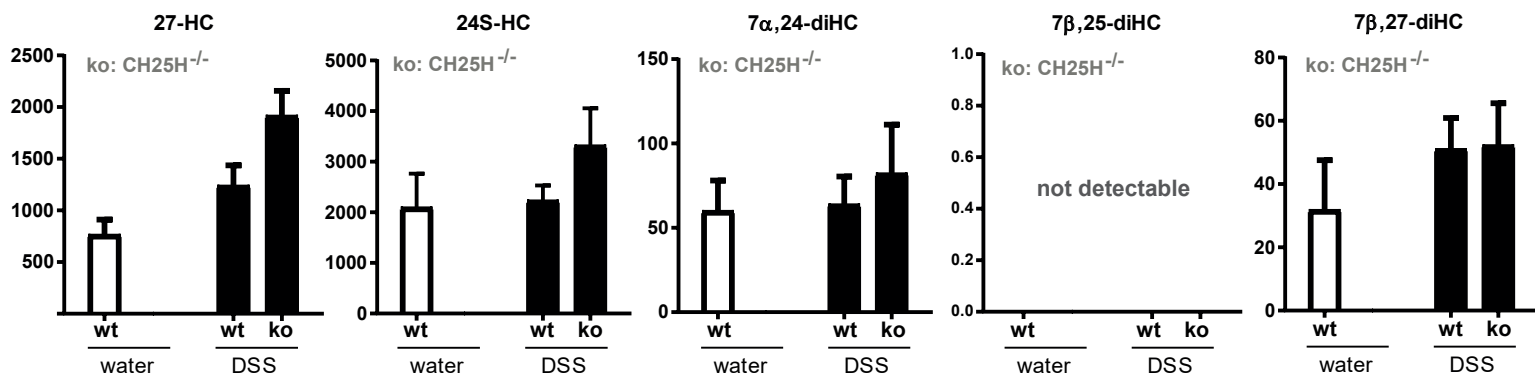
**a**



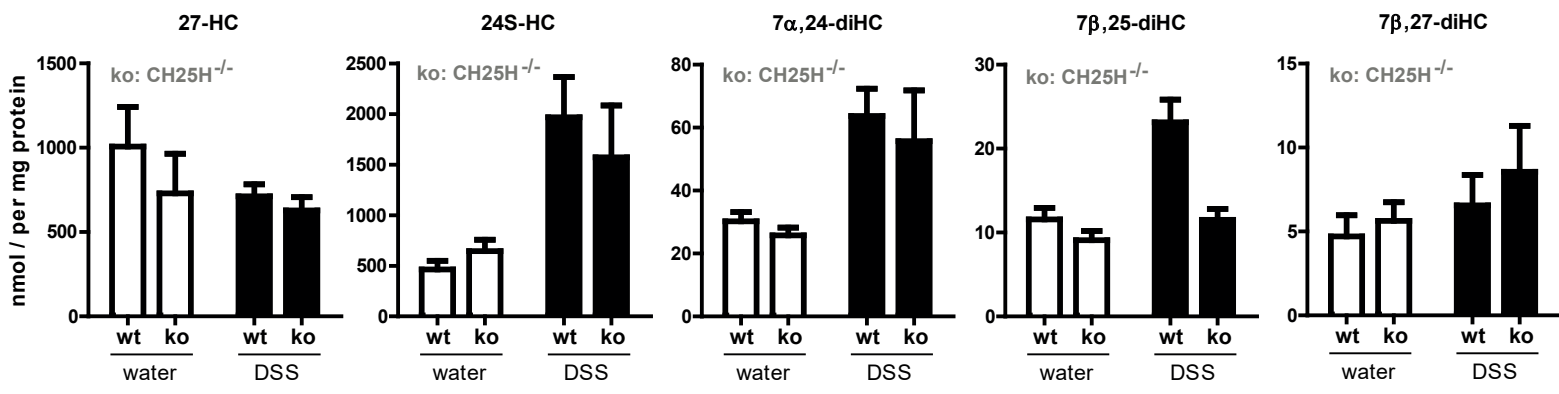
**b**



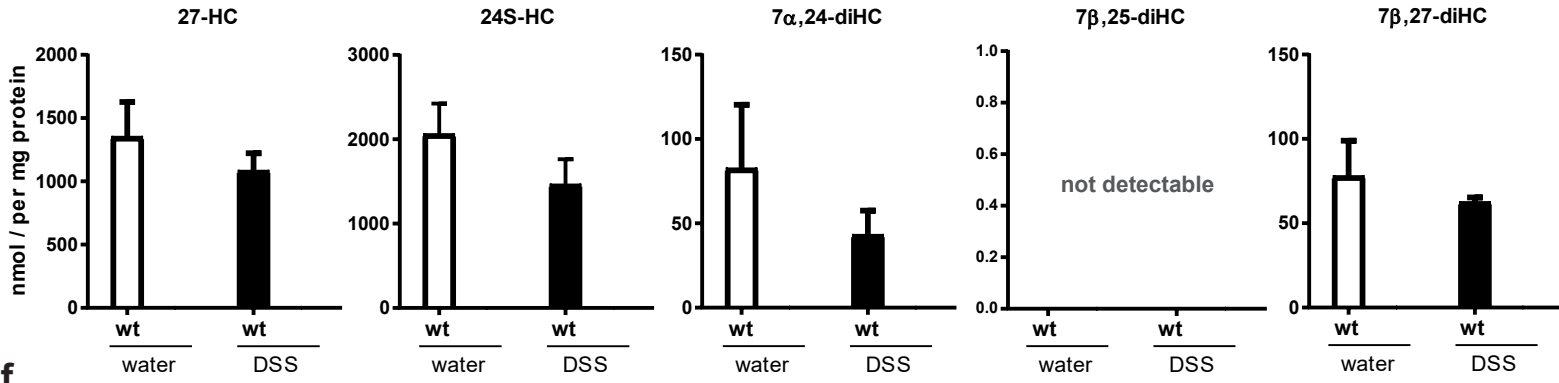
**c**



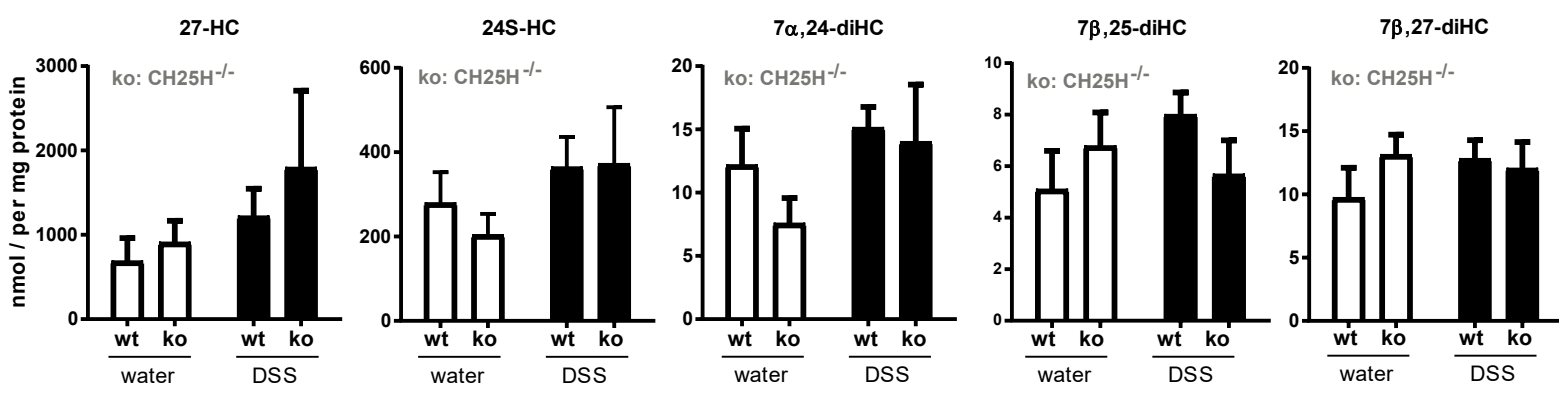
**d**



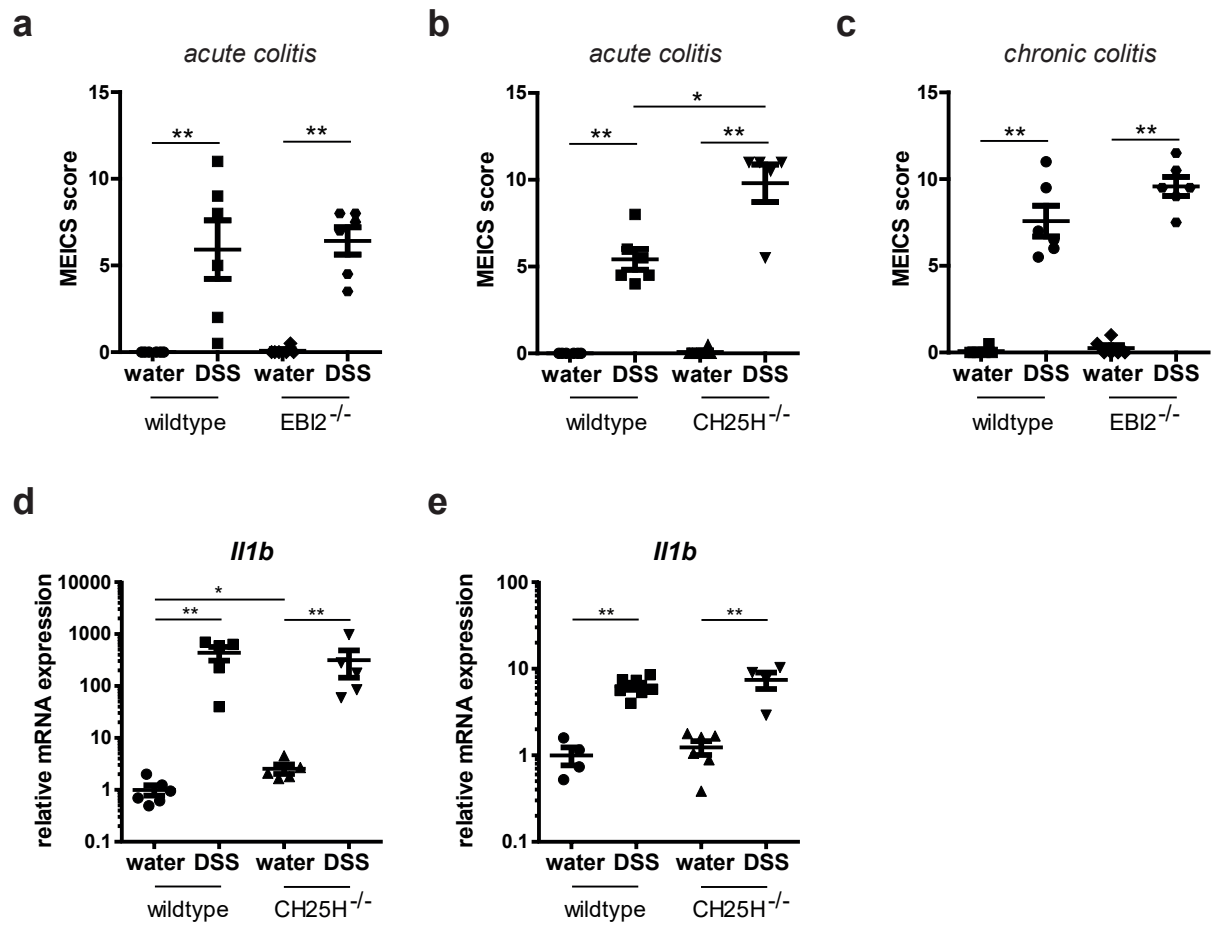
**e**



**f**

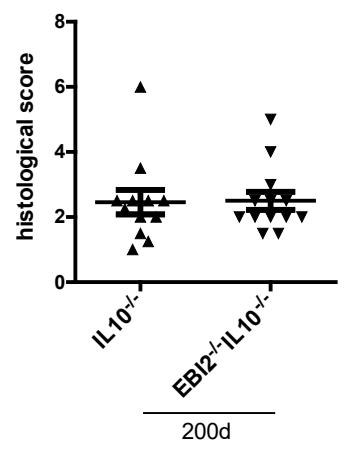


Supplementary Figure 3

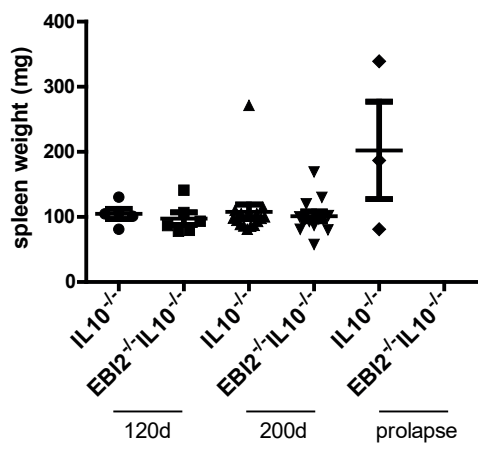


Supplementary Figure 4

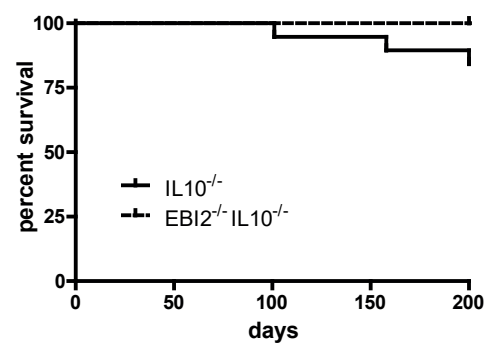
**a**



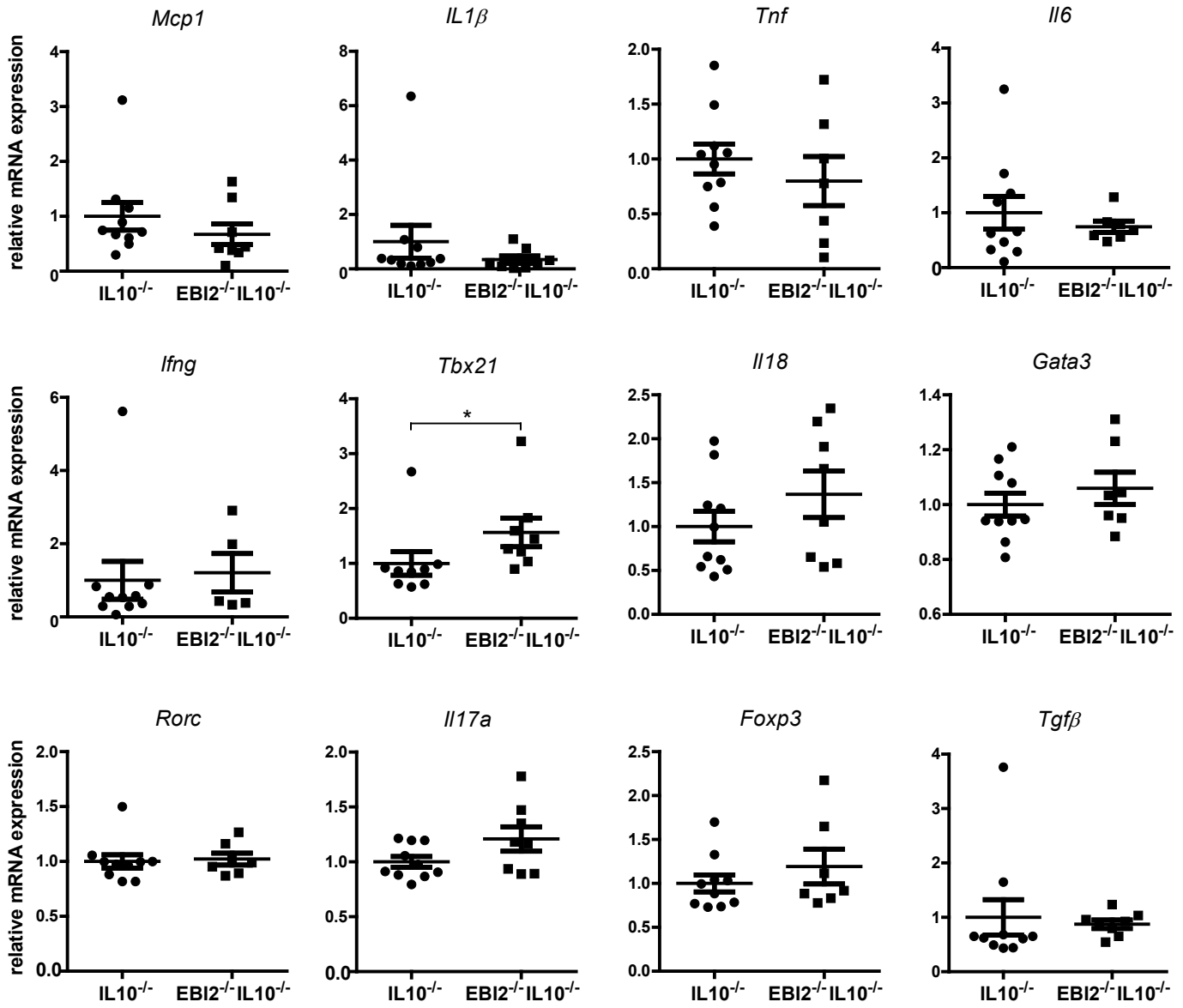
**b**



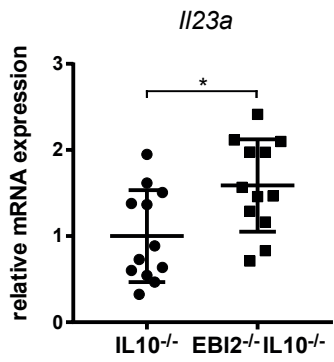
**c**



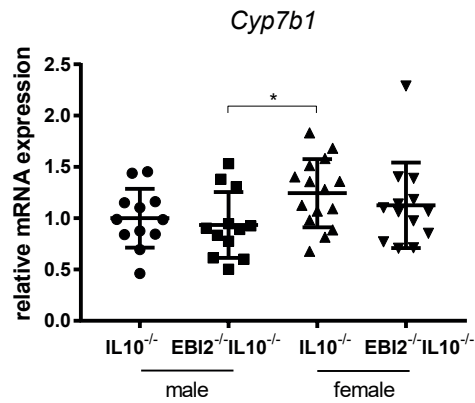
**a**



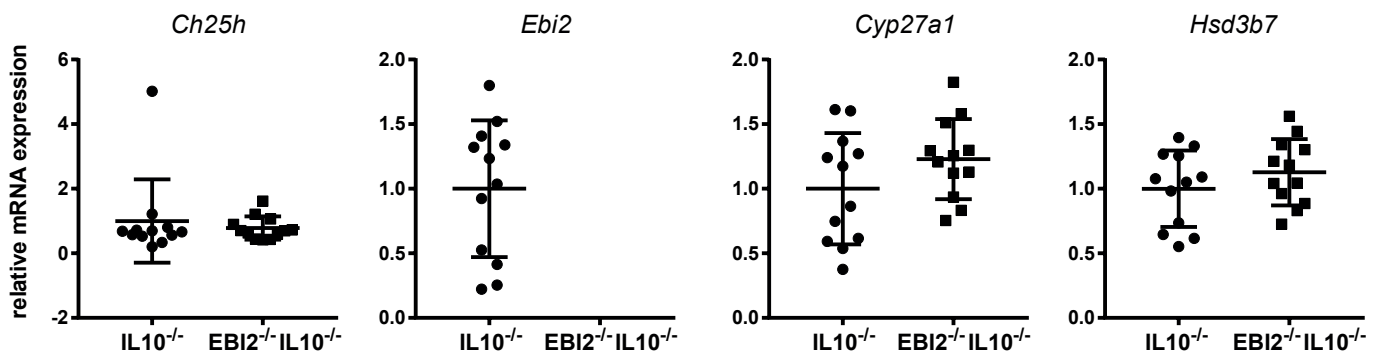
**b**



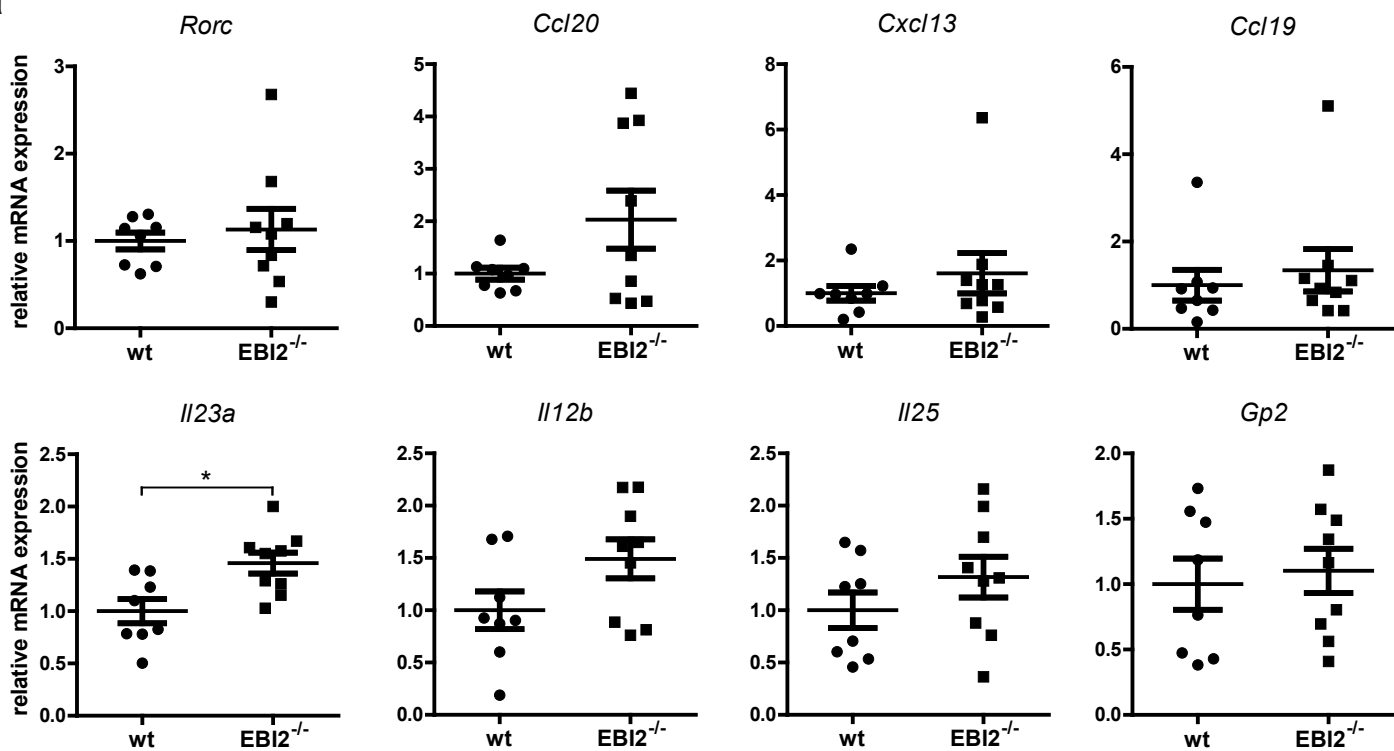
**c**



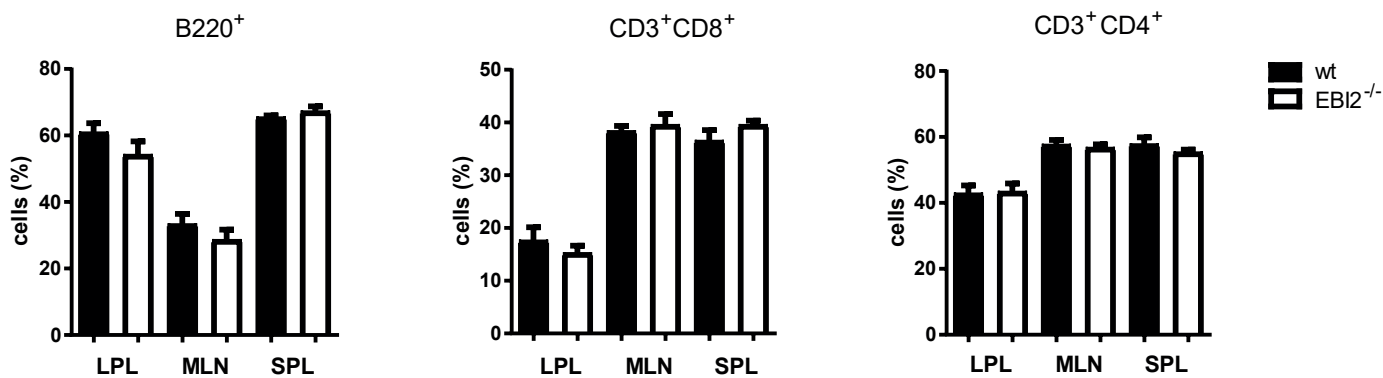
**d**



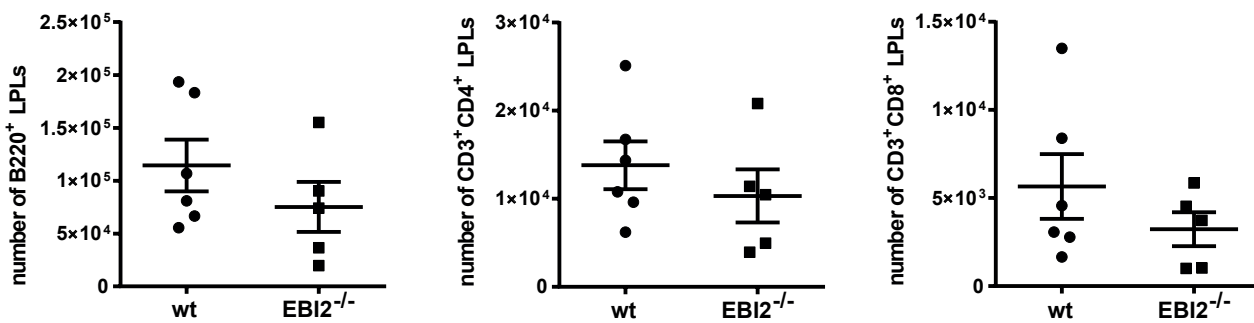
**a**



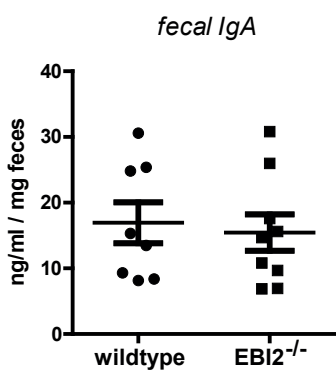
**b**



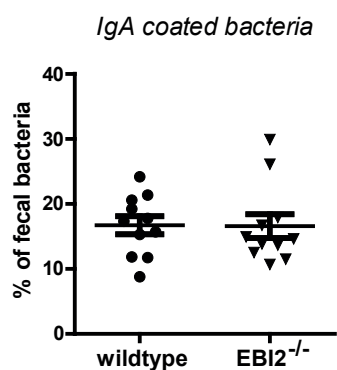
**c**



**d**

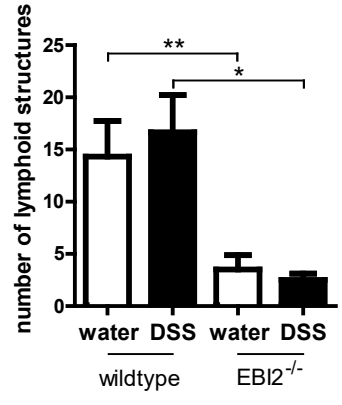


**e**

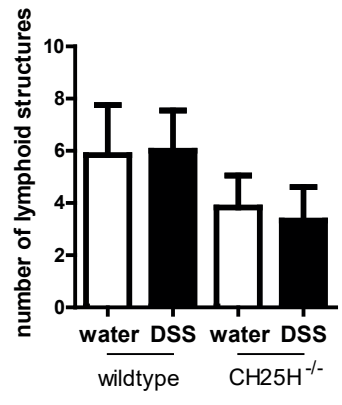


Supplementary Figure 7

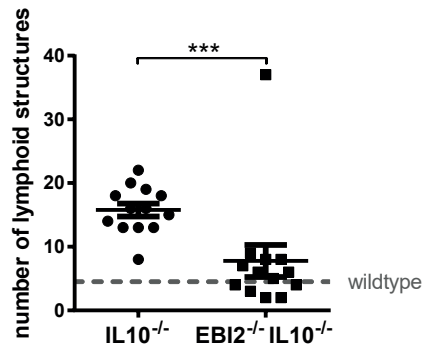
**a**



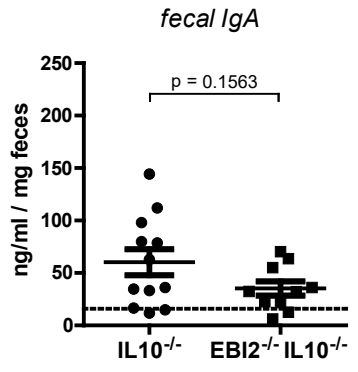
**b**



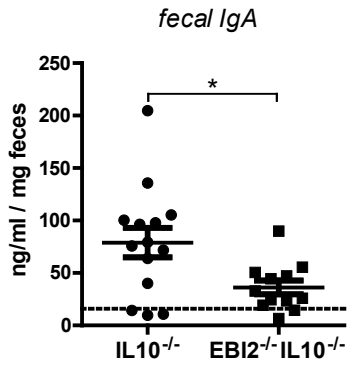
**a**



**b**



**c**



## **Supplementary Figure Legends**

### **Supplementary Figure S1: Expression of oxysterol processing enzymes and pro-inflammatory genes in colon tissue and EB12 surface expression in PBMCs upon TNF treatment**

**(a)** Data from a human whole genome microarray (GEO data sets: GDS3268) was analyzed regarding mRNA expression levels of *CYP27A1* and *HSD3B7* in non-inflamed colon tissue of healthy volunteers (n=63) and non-inflamed (n=61) and inflamed (n=62) colon tissue of UC patients. The dotted line represents the mean of healthy tissue (set to 1). **(b)** mRNA expression levels of tumor necrosis factor (*TNF*), interferon- $\gamma$  (*IFNG*), and interleukin-1 $\beta$  (*IL1B*) from rectal biopsies of UC patients (non-inflamed from patients with quiescent disease activity (n=20) and inflamed from patients with moderate to severe disease activity (n=20)) from the SIBDCS were determined by RT-PCR and normalized to GAPDH using the  $\Delta\Delta C_t$  method. **(c)** EB12 expression shown as mean fluorescence intensity ratio (MFIR) in CD19<sup>+</sup> B cells, CD4<sup>+</sup> T cells, and CD8<sup>+</sup> T cells (total, naïve, and memory; n=5) from human PBMCs at baseline (white) and after 4h TNF treatment (black) determined by FACS analysis. **(d)** Representative fluorescence histogram (from c) showing EB12 expression at baseline (red) and after TNF treatment (blue) in memory CD4<sup>+</sup> T cells determined by FACS analysis. Data is shown as mean  $\pm$  SEM. Statistical analysis: Mann-Whitney U test; \*\* = p<0.01, \*\*\* = p<0.001; \*\*\*\* = p<0.0001.

### **Supplementary Figure S2: mRNA expression levels, oxysterol levels and endoscopic assessments in murine DSS colitis**

Acute and chronic DSS colitis was induced; on day 8 (acute colitis) or 80 (chronic colitis) mice underwent colonoscopy and were sacrificed to obtain tissue samples. **(a)** mRNA expression levels of *Hsd3b7* and *Cyp27a1* from colon tissue of wildtype mice with acute colitis and water controls and **(b)** chronic colitis and water controls were determined by RT-PCR and normalized to GAPDH using the  $\Delta\Delta C_t$  method. **(c, d)** Oxysterol levels from acute DSS colitis experiments were measured by LC-MS/MS. **(c)** Oxysterol levels in colon tissue of inflamed wildtype (n=4) and inflamed CH25H<sup>-/-</sup> mice (n=3) with wildtype water controls (n=3). **(d)** Oxysterol levels in liver tissue of inflamed wildtype (n=12) and inflamed CH25H<sup>-/-</sup> mice (n=6) and respective water controls (n=12/ n=6). **(e, f)** Oxysterol levels from chronic DSS colitis. **(e)** Colon tissue from wildtype mice (DSS: n=6, water: n=6). **(f)** Liver tissue of inflamed wildtype (n=6) and inflamed CH25H<sup>-/-</sup> (n=5) mice and respective water controls (n=5/ n=6) Data from acute and chronic DSS colitis are pooled from two independent experiments each. Data shown as mean  $\pm$  SEM. Statistical analysis: Mann-Whitney U test; \* = p<0.05, \*\* = p<0.01.

### **Supplementary Figure S3: Lack of EB12 and CH25H does not affect severity of DSS colitis**

Endoscopic scoring (MEICS score) for **(a)** wildtype and EB12-deficient, and **(b)** wildtype and CH25H-deficient mice in acute DSS colitis and **(c)** for wildtype and EB12-deficient mice in chronic DSS colitis. mRNA expression levels of *Il1b* from colon tissue of wildtype and CH25H<sup>-/-</sup> mice with **(d)** acute and **(e)** chronic DSS colitis and respective water controls were determined by RT-PCR and normalized to GAPDH using the  $\Delta\Delta C_t$  method. Data from acute and chronic DSS colitis are pooled from two independent experiments each. Data shown as mean  $\pm$  SEM. Statistical analysis: Mann-Whitney U test; \* = p<0.05, \*\* = p<0.01.

**Supplementary Figure S4: Histological score, spleen weight and rectal prolapse of female EB12<sup>-/-</sup> mice in the IL-10 colitis model**

**(a)** Histological scores of HE stained colon sections of female EB12<sup>-/-</sup>IL10<sup>-/-</sup> and IL10<sup>-/-</sup> mice at the age of 200 days. **(b)** Spleen weight of female animals shown in (a) and after 120 days or prolapse occurrence. **(c)** Survival curve for onset of prolapse in female mice. Each mouse represents an independent observation from continuous breeding over >12 months. Data shown as mean ± SEM. Statistical analysis: Mann-Whitney U test; \* = p<0.05, \*\* = p<0.01.

**Supplementary Figure S5: Similar expression levels of oxysterol and inflammation related genes in the IL-10 colitis model**

mRNA expression levels were determined by RT-PCR and normalized to GAPDH using the  $\Delta\Delta C_t$  method. **(a, b)** mRNA expression levels of inflammation-related genes from colon tissue of 200 days old male mice. **(c)** mRNA expression levels of *Cyp7b1* from colon tissue of 200 days old male and female mice. **(d)** mRNA expression levels of EB12 and oxysterol-related genes from colon tissue of 200 days old male mice. Each mouse represents an independent observation from continuous breeding over >12 months. Data shown as mean ± SEM. Statistical analysis: Mann-Whitney U test; \* = p<0.05.

**Supplementary Figure S6: EB12 knockout does not affect levels of B and T cells, IgA and IgA-coated bacteria**

**(a)** mRNA expression levels of *Rorc*, *Ccl20*, *Cxcl13*, *Ccl19*, *Il23a*, *Il12b*, *Il25*, *Gp2* from whole colon tissue from 12 weeks old EB12<sup>-/-</sup> mice and wildtype littermate controls determined by RT-PCR and normalized to GAPDH using the  $\Delta\Delta C_t$  method. **(b)** Percentages of isolated CD45<sup>+</sup> cells positive for B220 (left), CD3 and CD4 (middle), and CD3 and CD8 (right) of lamina propria lymphocytes (LPL), mesenteric lymph nodes (MLN) and the spleen (SPL) of 12 weeks old EB12<sup>-/-</sup> (n=5) and wildtype (n=6) littermate mice determined by FACS analysis. **(c)** Absolute numbers of isolated CD45<sup>+</sup> cells positive for B220 (left), CD3 and CD4 (middle), and CD3 and CD8 (right) of lamina propria lymphocytes (LPL) of 12 weeks old EB12<sup>-/-</sup> (n=5) and wildtype (n=6) littermate mice determined by FACS analysis. **(d)** IgA ELISA of fecal extracts of 12 weeks old EB12<sup>-/-</sup> mice and wildtype littermate controls. **(e)** Percentage of IgA-coated bacteria of total fecal bacteria of 3-4 months old EB12<sup>-/-</sup> and wildtype littermate mice determined by bacterial FACS analysis. Data shown as mean ± SEM. Statistical analysis: Mann-Whitney U test; \* = p<0.05.

**Supplementary Figure S7: No increase in lymphoid structures in acute DSS colitis**

**(a, b):** Lymphoid structures quantified in representative HE stained colon sections of wildtype and EB12<sup>-/-</sup> and CH25H-deficient female mice **(b)** with acute DSS colitis (n=6 for all groups). Data from acute DSS colitis are pooled from two independent experiments each. Data shown as mean ± SEM. Statistical analysis: Mann-Whitney U test; \* = p<0.05, \*\* = p<0.01.

**Supplementary Figure S8: EBI2 deficiency leads to a reduced number of lymphoid structures accompanied by lower fecal IgA levels in IL10 colitis**

**(a)** Quantification of lymphoid structures in 200 days old female EBI2<sup>-/-</sup>IL10<sup>-/-</sup> and IL10<sup>-/-</sup> mice. The dotted line indicates the mean number of lymphoid structures in wildtype animals at the age of approximately 200 days. **(b, c)** IgA ELISA of fecal extracts of 200 days old male **(c)** and female **(d)** EBI2<sup>-/-</sup>IL10<sup>-/-</sup> and IL10<sup>-/-</sup> mice. The dotted line indicates the mean of wildtype mice. Data shown as mean ± SEM. Statistical analysis: Mann-Whitney U test; \* = p<0.05, \*\*\* = p<0.001.

## Supplementary Tables

<b>Disease activity</b>	<b>Quiescent N=25</b>	<b>Moderate or severe N=20</b>	<b>Comparison</b>
<b>Age</b>	43 (31-53); 24-70	34 (28-51.5); 18-61	P=0.24
<b>Gender</b>	Male: 7; female: 18	Male: 11; female: 9	P=0.12
<b>Disease duration</b>	17 (10-21.5); 8-37	14.5 (11-21); 4-34	P=0.58
<b>Extent<sup>#</sup></b>	E1: 2; E2: 2; E3: 6	E1:2; E2: 11; E3:7	P=0.19
<b>BMI<sup>##</sup></b>	22.7 (21.7-25.1); 19.7-32.3	24.4 (21.9-27.7); 19.4-34.7	P=0.30
<b>MTWAI</b>	0 (0-1); 0-1	7.5 (5-12); 4-19	P<0.0001
<b>Current anti-TNF</b>	Yes: 2; no: 23	Yes: 5; no: 15	P=0.21
<b>Past + current anti-TNF</b>	Yes: 3; no: 22	Yes: 9; no: 11	P=0.019
<b>Current immune modulator</b>	Yes: 10; no: 15	Yes: 11; no: 9	P=0.38
<b>Past + current immune modulator</b>	Yes: 13; no: 12	Yes: 18; no: 2	P=0.0091
<b>Current steroids</b>	Yes: 1; no: 24	Yes: 9; no: 11	P=0.0024
<b>Past + current steroids</b>	Yes: 9; no: 16	Yes: 18; no: 2	P=0.0003

**Supplementary Table S1: Disease characteristics and treatment of SIBDC patients.** Statistical analysis: Mann-Whitney-U test, Fisher's exact test or Chi-square test. <sup>#</sup>missing values for 10 patients for quiescent disease. <sup>##</sup>missing values for 1 patient with severe disease. MTWAI: modified Truelove and Witts activity index.

	EBI2 expression	CH25H expression	CYP7B1 expression
MTWAI	<b>0.21 (0.087-0.33)</b> <b>p=0.0018</b>	-0.19 (-0.4-0.023) p=0.09029	<b>-0.27 (-0.52--0.015)</b> <b>p=0.047</b>
Endoscopic activity	-	<b>1.63 (0.26-3)</b> <b>p=0.026</b>	<b>1.95 (0.42-3.48)</b> <b>p=0.018</b>
BMI	-	-	<b>0.23 (0.096-0.36)</b> <b>p=0.0021</b>
Past or current anti-TNF treatment	-	<b>2.23 (0.71-3.74)</b> <b>p=0.0072</b>	<b>3.16 (1.29-5.02)</b> <b>p=0.0024</b>

**Supplementary Table S2: Influence of clinical parameters on expression of EBI2 and oxysterol-producing enzymes.** Measurements reflect 35-37 UC patients. For each gene indicated, a multivariate linear regression analysis with automated parameter elimination was performed. The linear slope with 95% confidence interval and the nominal p-value is provided. Nominally significant associations are shown in bold. Parameters included into model predicting algorithms were body mass index (BMI), age, disease duration, modified truelove and Witts activity index (MTWAI), current steroid usage, past or current anti-TNF usage, endoscopic disease activity during endoscopy (none, mild, moderate, severe). Reading example: each additional point of the MTWAI increases colonic EBI2 expression by an average of 0.21.

	<i>CYP7B1</i>	<i>EBI2</i>	<i>TNF</i>	<i>IFNG</i>	<i>IL1B</i>
<i>CH25H</i>	<b>r=0.4649</b> <b>p=0.0449</b>	r=0.4167 p=0.0962	r=0.3474 p=0.1334	r=-0.09391 p=0.7109	r=0.08566 p=0.7354
<i>CYP7B1</i>	-	<b>r=0.7008</b> <b>p=0.0006</b>	<b>r=0.7218</b> <b>p=0.0003</b>	r=0.09474 p=0.6997	r=0.08359 p=0.7416
<i>EBI2</i>		-	<b>r=0.5987</b> <b>p=0.00041</b>	r=0.2684 p=0.2665	r=0.3891 p=0.1105
<i>TNF</i>			-	<b>r=0.4649</b> <b>p=0.0449</b>	r=0.2054 p=0.4136
<i>IFNG</i>				-	r=0.4167 p=0.0962

**Supplementary Table S3: Expression levels of *CYP7B1*, *EBI2* and *TNF* in inflamed tissue correlate with each other.** Measurements reflect expression levels in 20 samples of inflamed tissue from patients with moderate to severe disease activity. Significant correlations are shown in bold. Statistical analysis: Spearman R correlation.

	Average value (nmol/mg liver protein)	Inflammation DSS treatment yes vs. no	CH25H genotype k.o. vs. wt	EBI2 genotype k.o. vs. wt
7 $\alpha$ , 25-diHC	11	<b>3.1 (1.3-5)</b> <b>p=0.0015</b>	<b>-4.9 (-7.1-2.7)</b> <b>p=0.000086</b>	<b>-2.40 (-4.6-0.18)</b> <b>p=0.04</b>
7 $\alpha$ ,27-diHC	40	2.84 (-5.7-11.3) p=0.52	5.28 (-5.1-15.7) p=0.33	9.68 (-0.72-20.1) p=0.075
7 $\alpha$ ,24-diHC	46	<b>29.9 (15.1-44.7)</b> <b>p=0.00027</b>	-6.3 (-24.4-11.9) p=0.5	2.62 (-15.5-20.7) p=0.78
7 $\beta$ ,27-diHC	6.7	1.46 (-1.2-4.1) p=0.29	1.46 (-1.8-4.8) p=0.39	2.84 (-0.45-6.1) p=0.098
7 $\beta$ ,25-diHC	16	<b>8.53 (5.1-12)</b> <b>p=0.000016</b>	<b>-7.05 (-11.3 - -2.8)</b> <b>p=0.0021</b>	1.67 (-2.6-5.9) p=0.44
25-HC	442	<b>220 (92-348),</b> <b>p=0.0015</b>	<b>-215 (-371 - -58)</b> <b>p=0.01</b>	32.5 (-124-189) p=0.69
27-HC	1515	1224 (-1522-3971) p=0.39	-181 (-3545-3183) p=0.92	2803 (-561-6167) p=0.1
24S-HC	1135	<b>1257 (673-1842)</b> <b>p=0.00012</b>	-108 (-824-608) p=0.77	-215 (-930-501) p=0.56

**Supplementary Table S4: Influence of inflammation, CH25H and EBI2 genotype on the concentration of various oxysterols in liver of mice with acute DSS colitis.** Measurements reflect 48 samples, with 12 animals per condition for wildtype and 6 animals per condition for both knockouts. For each oxysterol indicated, a multivariate linear regression analysis was performed. The linear slope with 95% confidence interval and the nominal p-value is provided. Nominally significant associations are shown in bold, associations remaining significant after Bonferroni correction (correcting for 24 different tests) are shown in red. Reading example: DSS treatment increases concentration of 7 $\alpha$ , 25-diHC levels from an average of 11 nmol/mg by an average of 3.1 nmol/mg

	Average value	Genotype wt vs. EB12 <sup>-/-</sup>	Histological Score	Genotype:Histological Score
SILT	8.9	16.5 (9.6 - 23.5); p=2.9x10 <sup>-05</sup>	4.3 (2.4 - 6.3) p=7.4x10 <sup>-05</sup>	-3.4 (-6 - -0.8) p=0.015

**Supplementary Table S5: Influence of EB12 genotype and the histological score (inflammation) on the number of SILT in IL-10 colitis.** The table summarizes 49 animals (24 wildtype and 25 EB12<sup>-/-</sup> animals). A generalized linear regression model was built (p=4x10<sup>-9</sup> for predictions of the complete model). The linear slope with 95% confidence interval and the nominal p-value are provided. Reading example genotype: wildtype genotype increases the number of SILT from an average of 8.9 by 16.5. Histological scoring: One point of the histology score increases the number of SILT by 4.3. Interaction of genotype with histological score: For EB12<sup>-/-</sup> animals, each point of the histological score decreases the number of SILT by 3.4.

Epithelium		Infiltrate		Mucosa	
	Score		Score		Score
Normal morphology	0	No infiltrate	0		-
Minimal hyperplasia in <10 %	1	Around crypt base	1		-
Mild hyperplasia (~2x thicker), goblet cell loss (± cryptitis, ± erosions) in 10-30 %	2	Infiltration of L. muscularis mucosae	2	1-2 ulcerations (≤ 20 crypts in total)	1
Moderate hyperplasia (2-3x thicker), goblet cell loss (cryptitis, ±crypt abscesses) in 40-70 %	3	Marked edematous infiltration of L. muscularis mucosae	3	1-4 Ulcerations (> 20-40 crypts in total)	2
Marked hyperplasia (≥ 4x thicker), goblet cell loss (multiple crypt abscesses) in >70 %	4	Infiltration of Tela submucosa	4	Any group of ulcers that exceeds the criteria above	3

**Supplementary Table S6: Scoring system for assessment of severity of colitis in IL10<sup>-/-</sup> colitis.**

## **Supplementary Methods**

### **PBMC extraction**

PBMCs from blood samples of IBD patients and healthy volunteers were extracted by gradient centrifugation using Ficoll-Paque Plus (GE Healthcare, Chicago, USA). The mononuclear cell layer was removed and washed in RPMI (Gibco / Thermo Fisher scientific, Waltham, USA) with Penicillin, Streptomycin and Glutamine (PSG; all from Sigma-Aldrich, St. Louis, USA). Viable cells were counted using trypan blue, resuspended in FCS with 10% DMSO (Sigma-Aldrich, St. Louis, USA), frozen and kept in liquid nitrogen.

### *TNF stimulation*

PBMCs were thawed, resuspended in RPMI-PSG-10% FCS and plated for overnight resting at 37°C. 200'000 cells were stimulated with TNF (Peprotech, London, UK) in final concentration of 10 ng/ml. After 4 h cells were harvested for flow cytometry analysis.

### **LPMC extraction (human samples)**

For LPMC isolation, colon resections from patients undergoing intestinal surgery were washed and fat muscle layers dissected carefully. The tissue was washed twice in cold HBSS/2% FCS, cut into small segments, and incubated twice in HBSS/2 mM EDTA at 37°C. After washing with HBSS the remaining tissue was incubated at 37°C for 45 min in RPMI/10% FCS/0.6 mg/ml Dispase (Gibco / Thermo Fisher scientific, Waltham, USA) /0.4 mg/ml Collagenase IV (Sigma-Aldrich, St. Louis, USA). The resulting cell suspension was passed through a 70 µm cell strainer and washed with PBS. Cells were frozen in FCS with 10% DMSO (Sigma-Aldrich, St. Louis, USA) and kept in liquid nitrogen.

### **Measurement of mRNA expression**

Total RNA was isolated using RNeasy Mini kit (Qiagen, Venlo, NL) according to the manufacturer's protocol. Lysis buffer from the kit was added to snap frozen tissue pieces and samples were shredded in M tubes in a gentleMACS tissue homogenizer (both obtained from Milteny Biotec, Bergisch Gladbach, DE). On-column DNase digestion with RDD buffer (Qiagen, Venlo, NL) was performed for 15 min at room temperature. RNA concentration was assessed by absorbance at 260 and 280 nm on a NanoDrop® ND-1000 Spectrophotometer (Thermo Fisher Scientific, Waltham, USA). Complementary DNA (cDNA) synthesis was performed using a High-Capacity cDNA Reverse Transcription Kit (Applied Biosystems / Thermo Fisher Scientific, Waltham, USA) following the manufacturer's instructions. Real-time PCR was performed using FAST qPCR Master Mix for Taqman Assays (Applied Biosystems / Thermo Fisher Scientific, Waltham, USA) on a Fast 7900HT Real-Time PCR system using SDS Software or on a QuantStudio 6 Flex using QuantStudio Real-Time PCR Software (all Applied Biosystems / Thermo Fisher Scientific, Waltham, USA). Measurements were performed in triplicates, glyceraldehyde 3-phosphate dehydrogenase (GAPDH) was used as endogenous control, and results were analyzed by the  $\Delta\Delta C_t$  method. The real-time PCR included an initial enzyme activation step (5 minutes, 95°C), followed by 45 cycles comprising a denaturing (95°C, 15 seconds) and an annealing/extending (60°C, 1 minute) step. All gene expression assays used were obtained from Life Technologies (Thermo Fisher Scientific, Waltham, USA).

## Oxysterol measurements in detail

### Murine liver sample preparation:

Frozen murine colon (10 – 100 mg) or liver samples (200 – 350 mg) from DSS colitis experiments were pulverized using a CryoPrep™ CP02 (Covaris, Woburn, USA), weighed and lysed in homogenization buffer (0.9% sodium chloride) to a total weight of 1.6 g and homogenized using a Qiagen TissueLyser II (Qiagen, Venlo, NL) at 4 °C. A liquid-liquid extraction was performed on the lysate using 3 ml of methanol and 3 mL of dichloromethane to aid in the extraction of the oxysterols from the lysate. The mixture was vigorously shaken on a horizontal shaker at 4 °C for 5 minutes and centrifuged at ca. 1200 g for 8 min before the bottom organic phase was extracted. A second liquid-liquid extraction was repeated on the top aqueous phase adding 1 ml of the homogenization buffer and 2 ml dichloromethane. Both organic phases were pooled and centrifuged for 8 min to consolidate impurities, which could be easily removed from the top layer after centrifugation. This extract was dried under nitrogen and the supernatant was reconstituted with 75 µl ethanol containing 0.1 % formic acid, vortexed and, after 10 min, filtered through a 20 µL filter tip (TipOne, Starlabgroup) ready for analysis on the LC-MS/MS system.

### LC-MS/MS analysis:

The LC-MS/MS analysis was performed on a Dionex UltiMate 3000 RS with HPG Pump (Thermo Scientific, Waltham, USA), coupled with a Sciex Triple Quad™ 5500 mass spectrometer (AB Sciex, Zug, CH). For RP (reversed phase)-HPLC separation of the oxysterols, a Waters Acquity UPLC BEH C18 column (150 mm x 2.1 mm; 1.7 µm) with guard column (Brebhühler AG, Schlieren, CH) was used. The mobile phase gradient consisted of two solvents, A (H<sub>2</sub>O: MeOH 95:5 % with 0.1% formic acid) and B (MeOH: ACN (62.5:37.5 % with 0.1 % formic acid) with a flow rate of 400 µL/min. The oxysterols were separated using the following gradient: (i) linear gradient from 0.2 % to 73 % solvent B in 0.5 min; (ii) linear gradient from 73 % to 81 % in 8 min; (iii) linear gradient from 81 % to 100 % solvent B in 4 min; (iv) isocratic flow 100 % solvent B for 1 min; (v) linear gradient from 100 % to 0.2 % solvent B in 2.5 min; (vi) isocratic flow 0.2 % solvent B for 4 min. The source parameters of the Sciex Triple Quad™ 5500 were: CAD: 10, CUR: 30, GS1: 50; GS2: 60, IS: 5500, TEM: 550. Scheduled multiple reaction monitoring (sMRM) was used in positive ion mode to identify the oxysterols using their precursor and selected product ions with the following transitions: 385 → 161 and 385 → 147 (24S-, 25- and 27-OHC), 391 → 159 (d6-Internal standards), 383 → 159 and 383 → 145 (7α,-diHC and 7β,-diHC), 391 → 159 and 407 → 389 (d6- and d7-Internal standards). The two transitions for each individual oxysterol were summed together using the Sciex MultiQuant™ 3.0.2 Software Data analysis software, therefore only requiring one transition for the internal standard. Oxysterol quantification was performed using the MultiQuant™ MQ4 integration algorithm with a signal to noise ratio (S/N) ≥ 3 as limit of quantification.

## Immunofluorescent stainings of colon “Swiss rolls”

Cryosections of colon “Swiss rolls” (mounted on glass slides) were air-dried, fixed with 4 % PFA, washed with PBS and permeabilized with 0.3% Triton X-100. After washing, sections were blocked with blocking buffer (PBS, 5% BSA, 0.3% Triton X-100). Incubation with primary antibodies diluted in blocking buffer (α-CD3 and α-αSMA (Abcam, Cambridge, UK); α-CD45R–Alexa Fluor 488, clone RA3-6B2 (Life Technologies / Thermo Fisher scientific, Waltham, USA); α-CD117(c-kit), clone ACK2 (Affymetrix/eBiosciences / Thermo Fisher scientific, Waltham, USA)) was performed overnight at 4°C.

The next day sections were washed and incubated with secondary antibodies ( $\alpha$ -rabbit–Alexa Fluor 546,  $\alpha$ -rat–Alexa Fluor 546 (Life Technologies / Thermo Fisher scientific, Waltham, USA) and DAPI) for 1h at RT. After washing, tissue sections were mounted using Dako® Fluorescence Mounting Medium (Dako / Agilent, Santa Clara, USA). Zeiss Axio Scan.Z1 with ZEN blue Software (Zeiss, Oberkochen, DE) was used to scan and analyze the sections. SILT and CLP were defined according to their size and localization; CLP: composed of large lymphoid follicles between the two external muscular layers and the muscularis mucosae, SILT: smaller clusters of lymphoid cells in the lamina propria.

## **ELISA**

To quantify fecal IgA, colons were cut open, feces scraped out and transferred into Eppendorf tubes. Feces were resuspended in 500  $\mu$ l PBS and spun for 5 min at 400 g to remove coarse material. Supernatants were spun for 5 min at 8000 g to pellet bacteria. This step was repeated until samples were clear of bacterial pellets. Supernatants (containing IgA) were used as samples (1:50-1:250 (v/v) dilutions) for ELISA. Anti-mouse IgA ELISA kit (Mouse IgA Ready-SET-Go!®) was obtained from Affymetrix/eBiosciences (Thermo Fisher scientific, Waltham, USA); the assay was performed according to the manufacturer's protocol. Absorbance at 450 nm with a correction wavelength of 570 nm was measured on a Synergy2 microplate reader using Gen5 software (both obtained from BioTek, Winooski, United States). Measurements were performed in duplicates.

### **Flow cytometric analysis (mouse samples)**

For LPL isolation, colonic content was removed, colons washed in PBS and opened longitudinally. Colons were washed twice in cold HBSS/2% FCS, cut into small segments, and incubated twice in HBSS/2 mM EDTA at 37°C. After washing with HBSS the remaining tissue was incubated at 37°C for 45 min in RPMI/10% FCS/1 mg/ml Dispase (Gibco / Thermo Fisher scientific, Waltham, USA)/0.75 mg/ml Collagenase D (Roche, Basel, CH)/0.4225 mg/ml Collagenase V (Sigma-Aldrich, St. Louis, USA)/ 30 µg/ml DNase (Roche, Basel, CH). The resulting cell suspension was passed through a 70 µm cell strainer, spun at 400 g, and resuspended in PBS. To obtain single cell suspensions of mesenteric lymph nodes (MLN) and spleen, organs were minced through a 70 µm cell strainer, spun at 400 g and resuspended in PBS. Cells were stained using the following antibodies: anti-mouse CD45 (30-F11) – Pacific Blue (BioLegend, San Diego, USA), CD45R/B220 (RA3-6B2) – PE-Cy7 (BD Pharmingen / BD Biosciences, Franklin Lakes, USA), anti-mouse CD3 (17A2) – APC (BioLegend, San Diego, USA), anti-mouse CD4 (GK1.5) – APC-Cy7 (BD Biosciences, Franklin Lakes, USA), anti-mouse CD8a (53-6.7) – PerCP-Cy5.5 (eBioscience / Thermo Fisher scientific, Waltham, USA). The LIVE/DEAD Fixable Dead Stain Kit (Life technologies / Thermo Fisher scientific, Waltham, USA) was used for exclusion of dead cells and absolute cell numbers were determined using Precision Count Beads (BioLegend, San Diego, USA). Data acquisition was performed on a FACSCanto II (BD Biosciences, Franklin Lakes, USA) and FlowJo (FlowJo LLC) software was used for data analysis.

### **IgA-coated bacteria**

Bacteria were isolated by differential centrifugation from frozen fecal pellets. Pellets were resuspended in sterile filtered HBS, centrifuged for 1 min at 500 rpm and the supernatant transferred to a fresh tube. Centrifugation was repeated twice. Subsequently bacteria were centrifuged for 8 min at 8000 rpm and the pellet containing bacteria suspended in 100 µl HBS containing 3% goat serum. The suspension was adjusted to obtain an OD600 of 0.12 for 1:100 dilutions. To detect IgA-coated bacteria, 2 µl of the suspension was incubated at 1:200 dilution with anti-IgA-PE (eBiosciences / Thermo Fisher scientific, Waltham, USA) for 20 min on ice. To stain bacteria Syto9 (Life Technologies / Thermo Fisher scientific, Waltham, USA) was added at 1:1000 dilution for 10 min. Bacteria were washed with HBS containing goat serum and analyzed on a BD Fortessa flow cytometer (BD Biosciences, Franklin Lakes, USA).

**4 . Manuscript N°2: A single nucleotide polymorphism in the gene for GPR183 increases its surface expression on blood lymphocytes of patients with inflammatory bowel disease**

This manuscript was published in the British Journal of Pharmacology (2021) in a themed issue :

Oxysterols, Lifelong Health and Therapeutics. DOI:  
<https://doi.org/10.1111/bph.15395>

We describe that, in peripheral blood, GPR183 is particularly more expressed in CD4 T cells expressing chemokine receptors involved in immune cells trafficking into the inflamed intestine. In addition, the IBD-associated GPR183 SNP results in increased expression of GPR183 on B cells. The patients carrying this SNP also display an increased incidence of extra-intestinal manifestation of IBD, including psoriasis.

As first author of this manuscript, under the supervision of Professor Pot, I was involved in the design, acquisition and analysis of all the experiments involving flow cytometry on PMBCs (Figure 1-5 and S1-S6). With Professor Pot and Professor Misselwitz, I wrote the manuscript.

## RESEARCH PAPER

# A single nucleotide polymorphism in the gene for GPR183 increases its surface expression on blood lymphocytes of patients with inflammatory bowel disease

Florian Ruiz<sup>1</sup> | Annika Wyss<sup>2</sup> | Jean-Benoît Rossel<sup>3</sup> | Michael Christian Sulz<sup>4</sup> |  
 Stephan Brand<sup>4</sup> | Anja Moncsek<sup>2</sup>  | Joachim C. Mertens<sup>2</sup> | René Roth<sup>2</sup> |  
 Aurélie S. Clottu<sup>1</sup> | Emanuel Burri<sup>5</sup> | Pascal Juillerat<sup>6</sup> | Luc Biedermann<sup>2</sup> |  
 Thomas Greuter<sup>2</sup> | Gerhard Rogler<sup>2</sup> | Caroline Pot<sup>1</sup>  | Benjamin Misselwitz<sup>6</sup>  |  
 Swiss IBD Cohort Study Group

<sup>1</sup>Laboratories of Neuroimmunology, Neuroscience Research Center and Service of Neurology, Department of Clinical Neurosciences, Lausanne University Hospital and University of Lausanne, Lausanne, Switzerland

<sup>2</sup>Department of Gastroenterology and Hepatology, University Hospital Zurich, University of Zurich, Zurich, Switzerland

<sup>3</sup>Center for Primary Care and Public Health (Unisanté), University of Lausanne, Lausanne, Switzerland

<sup>4</sup>Department of Gastroenterology and Hepatology, Kantonsspital St. Gallen, St. Gallen, Switzerland

<sup>5</sup>Department of Gastroenterology and Hepatology, University Medical Clinic, Kantonsspital Baselland, Liestal, Switzerland

**Background and Purpose:** Single nucleotide polymorphism rs9557195 within the gene of the G protein-coupled receptor Epstein-Barr virus-induced gene 2 (*EBI2/GPR183*) has been associated with increased risk for inflammatory bowel diseases (IBD). GPR183 mediates the migration of intestinal immune cells and promotes colitis in animal models. Here, we study GPR183 surface expression of immune cells and associations of rs9557195 with GPR183 expression and IBD disease course.

**Experimental Approach:** We recruited 27 IBD patients (15 with ulcerative colitis [UC] and 12 with Crohn's disease [CD]) and eight healthy volunteers (HV). *GPR183* expression was measured by FACS in subtypes of peripheral blood mononuclear cells. We analysed IBD disease course in 2301 patients (1335 with CD and 966 with UC) of the Swiss IBD cohort study.

**Abbreviations:** 7 $\alpha$ ,25-diHC, 7 $\alpha$ ,25-dihydroxycholesterol; CD, Crohn's disease; EIM, extraintestinal manifestations; eQTL, expression quantitative trait loci; ER, endoplasmic reticulum; FAF2, Fas associated factor 2 (FAF2); FCS, fetal calf serum; GPR183, Epstein-Barr virus-induced G protein-coupled receptor 2; EBI2, HV, healthy volunteer; IBD, inflammatory bowel disease; MFIR, mean fluorescence intensity ratio; PBMC, peripheral blood mononuclear cells; SNP, single nucleotide polymorphism; UBAC2, Ubiquitin-associated domain-containing gene 2; UC, Ulcerative colitis.

Caroline Pot and Benjamin Misselwitz both authors contributed equally to this work and share last authorship

Members of the Swiss IBD cohort study study group: Karim Abdelrahman, Gentiana Ademi, Patrick Aepli, Amman Thomas, Claudia Anderegg, Anca-Teodora Antonino, Eva Archanioti, Eviano Arrigoni, Nurullah Aslan, Diana Bakker de Jong, Bruno Balsiger, Mamadou-Pathé Barry, Polat Bastürk, Peter Bauerfeind, Andrea Becocci, José M. Bengoa, Luc Biedermann, Janek Binek, Mirjam Blattmann, Stephan Boehm, Tujana Boldanova, Jan Borovicka, Christian P. Braegger, Stephan Brand, Francisco Bravo, Lukas Brügger, Simon Brunner, Patrick Bühler, Sabine Burk, Emanuel Burri, Matthias Butter, Sophie Buysse, Dahlia-Thao Cao, Ove Carstens, Dominique H. Criblez, Fabrizia D'Angelo, Philippe de Saussure, Lukas Degen, Joakim Delarive, Christopher Doerig, Barbara Dora, Susan Drerup, Carole Ducrey, Ali El-Wafa, Matthias Engelmann, Aude Erdmann-Voisin, Christian Felley, Markus Fliegner, Montserrat Fraga, Yannick Franc, Pascal Frei, Remus Frei, Michael Fried, Florian Froehlich, Raoul Ivano Furlano, Luca Garzoni, Martin Geyer, Marc Girardin, Delphine Golay, Ignaz Good, Ulrike Graf Bigler, Sébastien Godat, Thomas Greuter, Beat Gysi, Johannes Haarer, Marcel Halama, Janine Haldemann, Pius Heer, Benjamin Heimgartner, Beat Helbling, Peter Hengstler, Denise Herzog, Cyrill Hess, Roxane Hessler, Klaas Heyland, Thomas Hinterleitner, Claudia Hirschi, Petr Hruz, Pascal Juillerat, Ioannis Kapoglou, Stephan Kayser, Céline Keller, Carolina Khalid-de Bakker, Christina Knellwolf, Christoph Knoblauch, Henrik Köhler, Rebekka Koller, Claudia Krieger, Patrizia Künzler, Rachel Kusche, Frank Serge Lehmann, Andrew Macpherson, Michel H. Maillard, Michael Manz, Maude Martinho, Rémy Meier, Christa Meyenberger, Pamela Meyer, Pierre Michetti, Benjamin Misselwitz, Bernhard Morell, Patrick Mosler, Eleni Moschouri, Christian Mottet, Christoph Müller, Beat Müllhaupt, Leilla Musso, Michaela Neagu, Cristina Nichita, Jan Niess, Andreas Nydegger, Nicole Obialo, Cassandra Oropesa, Ulrich Peter, Daniel Petermac, Laetitia Marie Petit, Valérie Pittet, Daniel Pohl, Marc Porzner, Claudia Preissler, Nadia Raschle, Ronald Rentsch, Sophie Restellini, Jean-Pierre Richterich, Sandra Riedmüller, Branislav Risti, Marc Alain Ritz, Gerhard Rogler, Nina Röhrich, Jean-Benoît Rossel, René Roth, Vanessa Rueger, Markus Sagmeister, Gaby Saner, Riad Sarraj, Bernhard Sauter, Mikael Sawatzki, Michael Scharl, Sylvie Scharl, Martin Schelling, Susanne Schibli, Hugo Schlauri, Dominique Schluckebier, Daniela Schmid, Sybille Schmid, Jean-François Schnegg, Alain Schoepfer, Philipp Schreiner, Frank Seibold, Mariam Seirafi, Gian-Marco Semadeni, Arne Senning, Christiane Sokollik, Joachim Sommer, Johannes Spalinger, Holger Spangenberg, Philippe Stadler, Peter Staub, Dominic Staudenmann, Volker Stenz, Michael Steuerwald, Alex Straumann, Andreas Stulz, Michael Sulz, Michela Tempia-Caliera, Joël Thorens, Kaspar Truninger, Radu Tutuian, Patrick Urfer, Stephan Vavricka, Francesco Viani, Fabrizio Vinzens, Jürg Vöggtlin, Roland Von Känel, Dominique Vouillamoz, Rachel Vulliamy, Marianne Vulliamy, Paul Wiesel, Reiner Wiest, Stefanie Wöhrle, Bahtiyar Yilmaz, Samuel Zamora, Silvan Zander, Jonas Zeitz, Dorothee Zimmermann.

<sup>6</sup>Department of Visceral Surgery and Medicine, Bern University Hospital, University of Bern, Bern, Switzerland.

#### Correspondence

Caroline Pot, Laboratories of Neuroimmunology, Neuroscience Research Center and Service of Neurology, Department of Clinical Neuroscience, Lausanne University Hospital and University of Lausanne, Lausanne, Switzerland.  
Email: caroline.pot-kreis@chuv.ch

#### Funding information

Swiss National Science Foundation (SNF), Grant/Award Numbers: 323630-183987, 32473B\_156525, 33CS30\_148422, PP00P3\_157476; Hartmann-Müller Foundation; Leenaards Foundation

**Key Results:** We found increased GPR183 expression in lymphocytes expressing chemokine receptors CCR6 or CCR9, implicated in IBD and on Th17 memory T cells. The GPR183 ligand  $7\alpha,25$ -dihydroxycholesterol and the CCR6 ligand CCL20 stimulated migration of memory T cells in an additive manner. Further, IBD patients with the CC allele of rs9557195 had higher GPR183 surface expression compared to individuals with the TT allele. Swiss IBD cohort study patients carrying the rs9557195-CC allele had higher psoriasis rates compared to individuals with the TT allele.

**Conclusion and Implications:** We demonstrate increased GPR183 surface expression on T cells with a potential role in gut inflammation. An SNP of the GPR183 locus was associated with GPR183 surface expression and psoriasis rates in IBD patients. Our data suggest a pro-inflammatory role of GPR183 in IBD.

**LINKED ARTICLES:** This article is part of a themed issue on Oxysterols, Lifelong Health and Therapeutics. To view the other articles in this section visit <http://onlinelibrary.wiley.com/doi/10.1111/bph.v178.16/issuetoc>

#### KEYWORDS

GPR183/EBI2, FACS, IBD, psoriasis, SNP, UBAC2

## 1 | INTRODUCTION

The two major forms of inflammatory bowel diseases (IBD), Crohn's disease (CD) and ulcerative colitis (UC), are chronic inflammatory conditions of the human gut (Maaser et al., 2019; Sturm et al., 2019). IBD is a disease with a multifactorial pathophysiology, with contributing environmental, genetic, microbial and immunological factors. Generally, IBD is characterized by a dysregulated mucosal immune response to intestinal bacteria in genetically susceptible individuals (Khor et al., 2011; Maloy & Powrie, 2011; Uhlig & Powrie, 2018). Despite extensive efforts, the pathogenesis of IBD is still not fully understood.

Up to now, more than 240 single nucleotide polymorphisms (SNP) have been associated with susceptibility to IBD in genome-wide association studies (Jostins et al., 2012; Liu et al., 2015). However, the mechanistic impact of genetic variants on the immune system remains unknown for most SNPs and it is unclear whether a specific genotype would alter the clinical course of IBD.

One of these IBD associated SNPs, rs9557195, is located within the gene for **GPR183 (also known as Epstein-Barr virus-induced G protein-coupled receptor 2; EBI2)** (Jostins et al., 2012). GPR183 is a chemoattractant receptor and GPR183 expressing immune cells move towards a gradient of the GPR183 ligand  **$7\alpha,25$ -dihydroxycholesterol ( $7\alpha,25$ -OHC)** (Hannedouche et al., 2011; Liu et al., 2011).  $7\alpha,25$ -OHC and other oxysterols are metabolites of cholesterol oxidation that have initially been proposed to act as bile acid precursors but have been assigned new roles in immune regulation (Duc et al., 2019).  $7\alpha,25$ -OHC is produced from cholesterol by two sequential oxidation steps, hydroxylation at position 25 by the enzyme 25-hydroxylase (CH25H) (Lund et al., 1998) and  $7\alpha$ -hydroxylation of 25-HC is subsequently

### What is already known

- GPR183 is implicated in immune cell migration and pre-clinical studies suggest a role in IBD.
- Polymorphisms of the rs955719 SNP within the *GPR183* gene are associated with IBD risk.

### What does this study add

- GPR183 cooperates with chemokine receptors involved in trafficking of intestinal inflammatory cells to promote chemotaxis
- The rs955719 SNP is associated with increased *GPR183* expression and psoriasis rates in IBD patients.

### What is the clinical significance

- GPR183 might be a therapeutic target in IBD and IBD-associated psoriasis.

performed by the enzyme **cytochrome P450 family 7 subfamily B member 1 (CYP7B1)** (Martin et al., 2001). Mice lacking either GPR183, CH25H, or CYP7B1 fail to correctly position B cells, T cells and dendritic cells within secondary lymphoid organs and show defects in the generation of T cell dependent immune

responses (Baptista et al., 2019; Gatto et al., 2009, 2013; Hannedouche et al., 2011; Li et al., 2016; Liu et al., 2011; Lu et al., 2017; Misselwitz et al., 2020; Pereira et al., 2009; Yi et al., 2012; Yi & Cyster, 2013).

GPR183 has an important role for the development of the intestinal immune system and intestinal inflammation. Mice either lacking GPR183 or  $7\alpha,25$ -OHC synthesizing enzymes failed to form normal numbers of solitary intestinal lymphoid tissue, lymphoid follicles within the intestinal mucosa (Chu et al., 2018; Emgard et al., 2018; Wyss et al., 2019). For efficient induction of solitary intestinal lymphoid tissues, GPR183 needs to be expressed in innate lymphoid cells type 3 (Emgard et al., 2018). GPR183 has pro-inflammatory activities in the intestine and GPR183 knockout increased susceptibility to *Citrobacter rodentium* (Chu et al., 2018) and decreased inflammatory activity in murine anti-CD40 colitis and IL-10 colitis (Emgard et al., 2018; Wyss et al., 2019), indicating a potential role of GPR183 and oxysterols in IBD pathogenesis. However, our understanding of GPR183 and oxysterols in gut disease remains incomplete (Chu et al., 2018; Emgard et al., 2018; Misselwitz et al., 2020; Raselli, Hearn, et al., 2019; Raselli, Wyss, et al., 2019; Willinger, 2019; Wu et al., 2017; Wyss et al., 2019).

GPR183 is highly expressed on immune cells including mature B cells, CD4<sup>+</sup> T cells including follicular helper T cells, innate lymphoid cells type 3 and dendritic cells (Chiang et al., 2013; Gatto et al., 2009; Gatto et al., 2013; Li et al., 2016; Pereira et al., 2009; Suan et al., 2015). In human peripheral blood, GPR183 expression is higher in CD4<sup>+</sup> cells compared to CD8<sup>+</sup> cells or natural killer cells (Clottu et al., 2017). Further, memory T cells (CD45RA<sup>-</sup>CD4<sup>+</sup> and CD8<sup>+</sup>CD45RA<sup>-</sup>) and GPR183 expression on memory B cells (CD27<sup>+</sup>CD19<sup>+</sup>) is higher than on their naïve counterparts (Clottu et al., 2017).

Genetic evidence as well as animal and patient data have implicated T cells in IBD pathogenesis (Annunziato et al., 2007; Jostins et al., 2012; Ueno et al., 2018; Uhlig & Powrie, 2018). Critical T cell subsets include Th17 cells and nonclassical Th1 cells (Th1<sup>+</sup> cells) that combine properties of Th1 and Th17 cells (Sallusto, 2016; Ueno et al., 2018). Various partially redundant mechanisms for T cell recruitment into the gut exist and integrins as well as chemokine receptors CCR6, CCR9 and CXCR3 mediate T cell homing into the inflamed gut (Perez-Jeldres et al., 2019; Trivedi & Adams, 2018). GPR183 was shown to dimerize with CXCR5 (Barroso et al., 2012) but how GPR183 cooperates with other chemokine receptors on different immune cells remains unknown.

We studied abundance of GPR183 expression on subsets of immune cells from IBD patients and healthy volunteers and tested the impact of the allele status of rs9557195 on GPR183 surface staining and IBD disease course. We found higher GPR183 expression on CCR6 and CCR9 expressing lymphocytes as well as on Th17 cells compared to total CD4 memory T lymphocytes. Further, the CC allele of rs9557195 was associated with higher GPR183 surface expression in naïve B cells and higher psoriasis rates in patients of the Swiss IBD cohort study, suggesting a pro-inflammatory role of GPR183 in IBD.

## 2 | METHODS

### 2.1 | Recruitment of healthy volunteers and IBD patients for analysis of peripheral blood mononuclear cells

Healthy volunteers (HV) were recruited by advertisement while IBD patients were recruited from our clinical practice. We also took advantage of genotyping performed within Swiss IBD cohort study (see below): Swiss IBD cohort study patients with the rs9557195-CC genotype and the rs9557195-TT genotype, respectively, were contacted and an appointment at a study centre was made. To the best of our knowledge, the impact of the rs957195 polymorphism on GPR183 expression has not been studied before. Therefore, our study should be considered a pilot study and no power analysis could be performed. The number of patients carrying the rs9557195-CC genotype and the rs9557195-TT genotype differ in the general population; therefore, a different number of individuals were recruited into both groups (more individuals homozygous for the major allele, rs9557195-TT). All patients were compensated for travel expenses, but no additional payments were made. This multi-centre study was approved by the Ethics commissions of all Swiss counties involved (BASEC 2017-01868). All patients and HV provided written informed consent. The study was registered at [www.ClinicalTrials.gov](http://www.ClinicalTrials.gov), trial registration number: NCT03633409.

All patients answered standardized questionnaires regarding IBD disease activity including the Harvey-Bradshaw index for CD patients and the ulcerative colitis severity index for UC patients (Harvey & Bradshaw, 1980). Data regarding biomarkers were extracted from the clinical records. All subjects had 50 ml of EDTA blood withdrawn and the peripheral blood mononuclear cells were isolated by gradient centrifugation (Clottu et al., 2017) and they were frozen in 90% fetal calf serum (FCS) and 10% DMSO. FCS was purchased from Biowest (lot number SI375151810) and for consistency, the same lot of FCS was used for all experiments. In the absence of FCS, peripheral blood mononuclear cells were not viable; therefore, control experiments in the absence of FCS were not feasible.

### 2.2 | Materials

For blood sampling for PMBC's isolation, S-monovette K3 EDTA tube were purchased from Sarstedt (Nümbrecht, Germany), Ficoll-Paque plus for gradient centrifugation from GE Healthcare (UK), and dimethyl sulfoxide from Sigma-Aldrich. For flow cytometry, PBS was purchased from Bichsel (Interlaken, Switzerland). Other reagents suppliers used for flow cytometry are detailed in Section 2.3. Reagents and materials suppliers used for migration assays are detailed in Section 2.4. Reagents and materials suppliers used for quantitative PCR are detailed in Section 2.5.

## 2.3 | Flow cytometry

Cryopreserved peripheral blood mononuclear cells were thawed, counted and resuspended at  $10^6$  cells·ml<sup>-1</sup> in Roswell Park Memorial institute (RPMI) 1640, GlutaMAX (GIBCO)-completed with penicillin, streptomycin (Sigma-Aldrich) and 10% FCS and plated overnight at 37°C and 5% CO<sub>2</sub>. Cells were then collected, washed in PBS and counted again with trypan blue (GIBCO) to exclude dead cells. The cells were stained with LIVE/DEAD Fixable Dead Cell Stain Kit (Life technologies/ Thermo Fisher scientific, Waltham, USA) according to the manufacturer's instructions for 30 min in the dark at 4°C. PMBCs were washed again and incubated with antibodies diluted in PBS-1% BSA. They were first incubated with the anti-GPR183 antibody or isotype control for 30 min in the dark at 4°C, followed by washing and incubation with other antibodies. The cells were fixed and acquired the next day.

Antibodies were purchased either from BioLegend (San Diego, USA): CCR4 (L291H4, used at a concentration of 500 ng·ml<sup>-1</sup> Cat), CXCR3 (G925H7, used at a concentration of 1 µg·ml<sup>-1</sup>), CCR6 (G0343E3, used at a concentration of 1 µg·ml<sup>-1</sup>), CCR9 (LO53E8, used at a concentration of 2 µg·ml<sup>-1</sup>), CD8 (SK1, used at a concentration of 400 ng·ml<sup>-1</sup>), CD4 (SK3, used at a concentration of 400 ng·ml<sup>-1</sup>), CD45RA (HI100, used at a concentration of 1 µg·ml<sup>-1</sup>), CD27 (M-T271, used at a concentration of 1 µg·ml<sup>-1</sup>), CD19 (HIB19, used at a concentration of 1 µg·ml<sup>-1</sup>) or from BD Biosciences (Franklin Lakes, USA): PE-Streptavidin (used at a concentration of 1.25 µg·ml<sup>-1</sup>), CD3 (SK7, used at a concentration of 1 µg·ml<sup>-1</sup>), and CCR7 (150,503, used at a concentration of 500 ng·ml<sup>-1</sup>). The isotype control for mouse biotin conjugated IgG2a was acquired from R&D Systems (Minnesota, USA, Cat: IC0038, used at a concentration of 5.46 µg·ml<sup>-1</sup>). The GPR183 antibody (57C9B5C9, used at a concentration of 5.46 µg·ml<sup>-1</sup>) was kindly provided by Andreas Sailer from the Novartis Institute of Biomedical Research, Basel, Switzerland (Rutkowska et al., 2015). All of the above concentrations were used to stain 1,000,000 of cells.

The samples were analysed with an LSR II flow cytometer (BD Biosciences, Franklin Lakes, USA). FlowJo software (FlowJo LLC, RRID: SCR\_008520) was used to analyse the flow cytometry data. Fluorescence minus one (FMOs) were used to identify CXCR3<sup>+</sup>, CCR4<sup>+</sup>, CCR6<sup>+</sup> and CCR9<sup>+</sup> cells. The gating strategy is indicated in Figure S1 and is highly similar to our previous work (Clottu et al., 2017) identifying T helper subset as follows:- Th1: CXCR3<sup>+</sup>CCR4<sup>-</sup>; Th2: CXCR3<sup>-</sup>CCR4<sup>+</sup>; Th17: CXCR3<sup>-</sup>CCR6<sup>+</sup>; Th1\*: CXCR3<sup>+</sup>CCR6<sup>+</sup> (Acosta-Rodriguez et al., 2007; Sallusto, 2016). Results are provided either as the percentage of positive or negative cells or the mean fluorescence intensity ratio (MFIR), the ratio of the geometric mean of the signal after staining with the GPR183 antibody over the signal after staining with isotype control. For consistency with our previous work (Clottu et al., 2017) on GPR183, we put emphasis on MFIR.

## 2.4 | Migration assays

The migrations assays were performed as previously described (Clottu et al., 2017). Briefly, after overnight resting, PMBCs were

resuspended in DMEM (Gibco) containing minimal essential medium (MEM), vitamins (100×), non-essential amino acid solution (100×), 1.5 mM sodium pyruvate, 14 mM folic acid, 0.3 mM L-asparagine, 0.7 mM L-arginine, 2 mM L-glutamine, 100 U·ml<sup>-1</sup> penicillin-streptomycin, 14.3 mM β-mercaptoethanol, 1% BSA (all from Sigma-Aldrich) at 1.5 million cells·ml<sup>-1</sup>. Human recombinant CCL20 (Peprotech, reconstituted in PBS/0.1% BSA at 100 µg·ml<sup>-1</sup>) and 7α,25-OHC (Sigma-Aldrich, catalog no.: 700080P, reconstituted in DMSO at 10 mM) were diluted at the indicated concentration in the same medium; 240 µl of CCL20 and/or 7α,25-OHC were then loaded in the lower well of a HTS Transwell-96 well permeable support (Corning catalog no.: 3387); 240 µl of media without any added chemotactic signal was used as a negative control; 75 µl of cells with or without NIBR 189 (Avanti Polar, reconstituted in DMSO at 10 mM) were then loaded into the upper well; 75 µl of cells were loaded into the lower chamber to simulate conditions with 100% migration. The system was incubated for 3 h at 37°C and 5% CO<sub>2</sub> in an incubator. Cells from the lower wells were then collected and stained with fluorochrome-conjugated antibodies. The number of migrated cells was quantified by flow cytometry using CountBright absolute counting beads (ThermoFisher). Results are expressed as "migration ratio," that is, the number of migrated cells, divided by the mean of the controls.

## 2.5 | Quantitative PCR for UBAC2 expression

Cells were rapidly thawed (<1 min) and resuspended in 30 ml RPMI, followed by a centrifugation step. RNA was isolated from the cell pellet using the Maxwell RSC simplyRNA Cells Kit (Promega); 500 ng of RNA was transcribed to cDNA by the High Capacity cDNA Reverse Transcription Kit (Applied Biosystems). UBAC2 DNA was quantified using the UBAC2 TaqMAN Gene Expression Assay (Applied Biosystems) and normalized to GAPDH levels as a house keeping gene.

## 2.6 | Analysis of Swiss IBD cohort study patients

Clinical data from IBD patients were obtained from the Swiss IBD Cohort Study (SIBDCS), a large, prospective nation-wide registry. Swiss IBD cohort study has been approved by the local ethics committee of each participating centre (institutional review board No. EK-1316, approved on February 5, 2007 and BASEC 2018-02068 on March 9, 2020). Swiss IBD cohort study goals and methodology are described elsewhere (Pittet et al., 2009; Pittet et al., 2019). All patients provided written informed consent prior to inclusion into Swiss IBD cohort study. Analysis of patient data for the current study was approved by the scientific board of Swiss IBD cohort study.

IBD characteristics of patients were retrieved from the Swiss IBD cohort study data centre. Clinical characteristics include gender; diagnosis; age at diagnosis; maximal extent of disease in UC patients (Silverberg et al., 2005) (proctitis, left-sided colitis, pancolitis, or unknown); disease location in CD patients (Silverberg et al., 2005) (L1:

ileal disease with or without disease limitation to the cecum, L2: disease limited to the colon, L3: ileal disease with disease beyond the cecum, L4: disease of the upper gastrointestinal tract); complications; intestinal surgery; CD patients: fistula, abscess or anal fissure, surgery for fistula; current and prior treatment with anti-tumour necrosis factor (TNF) drugs and anti-TNF treatment failure, psoriasis as a side effect of side anti-TNF treatment; extraintestinal manifestations and psoriasis.

## 2.7 | SNPs of the GPR183/UBAC2 locus

Besides GPR183, the *GPR183* gene locus also comprises the gene for ubiquitin-associated domain-containing gene 2 (*UBAC2*) on the complement strand. Therefore, we considered the IBD-associated SNP rs9557195 and the Behçet's disease associated SNPs rs7999348, rs3825427, rs9513548, rs9517668 and rs9517701. Genotyping of the SNPs in the *GPR183/UBAC2* gene locus was done using MALDI-TOF MS-based SNP genotyping (Storm et al., 2003) prior to this study as a part of an analysis of the whole SIBD cohort for IBD associated SNPs and additional SNPs potentially altering IBD disease course (Lang et al., 2018).

For SNPs with strong Pearson's correlation for each pair ( $R^2 \geq 0.97$ ), the SNP with least support in the literature was excluded. The following SNPs with an  $R^2 \leq 0.52$  remained for further analysis: rs9557195, rs7999348 (whose results are also valid for rs9513584) and rs3825427 (whose results are also valid for rs9517668 and rs9517701).

The major allele was defined as wildtype; for the relevant SNPs, the following genetic polymorphisms were observed: rs9557195 homozygous wildtype (TT), heterozygous (CT) and homozygous variant (CC); rs7999348 homozygous wildtype (AA), heterozygous

(GA) and homozygous variant (GG); rs3825427 homozygous wildtype (CC), heterozygous (AC) and homozygous variant (AA).

## 2.8 | Statistical analysis

The data and statistical analysis comply with the recommendations of the *British Journal of Pharmacology* on experimental design and analysis in pharmacology (Curtis et al., 2018). These studies were not designed to have equal group sizes. Unequal group sizes were handled appropriately during the statistical analysis. Statistical analyses were performed with a minimum of five patients or HV per group. In all analyses, the declared group size corresponds to independent observations and not technical replicates. If technical replicates were used, for example, in migration assays, data presented in the manuscript represent the mean of the technical replicate for each donor. A  $P$ -value  $<0.05$  was considered significant. One outlier was removed in Figure 5b from the TT subgroup of naïve B cells using the ROUT ( $Q = 1\%$ ) method in Graphpad Prism V.8.

Differences about the association of SNP variants in relation to patient characteristics such as disease location, complications, medication, extraintestinal manifestation and psoriasis were assessed by Pearson's  $\chi^2$  test or Fisher's exact test, whatever appropriate. Continuous variables (e.g. age at diagnosis) were summarized as median, quartiles and range and the Kruskal–Wallis test was used to analyse differences between the groups. For statistical analyses, Stata software, *Release 14* was used.

Statistical analysis of flow cytometry data was performed using Graphpad Prism V.8 (RRID: SCR\_002798). The difference of GPR183 expression was analysed using unpaired or paired t-test whenever appropriate.

**TABLE 1** Summary of basic characteristics of study participants

	Healthy volunteers (N = 8)	Crohn's disease (N = 12)	Ulcerative colitis (N = 15)
Age (years)	35 (32–42.75), 30–49	42 (29.5–53), 21–73	47 (35–56), 28–63
Median (IQR), range			
Gender female (%)	5 (62.5%)	8 (66.7%)	10 (66.5%)
Harvey-Bradshaw index	-	7 (4–9), 0–12	-
Median (IQR), range			
UC severity index	-	-	4 (2.5–8), 0–14
Median (IQR), range			
Treatment			
Vedolizumab		2 (17%)	5 (33%)
Anti-TNF		6 (50%)	5 (33%)
Other		4 (33%)	5 (33%)
rs9557195			
CC		2	4
TT		7	7
CT		0	0
Unknown		3	4

## 2.9 | Nomenclature and ligands

Key protein targets and ligands in this article are hyperlinked to corresponding entries in the IUPHAR/BPS Guide to PHARMACOLOGY <http://www.guidetopharmacology.org> (Harding et al., 2018) and are permanently archived in the Concise Guide to PHARMACOLOGY 2019/20 (Alexander, Cidlowski, et al., 2019; Alexander, Fabbro, et al., 2019).

## 3 | RESULTS

### 3.1 | Study population

We recruited 27 IBD patients (15 UC patients and 12 CD patients) and eight healthy volunteers (HV, Table 1). Our study population was predominantly female (23/35, 65%) and of young to middle age (median: 42 years, range 21–73 years). Most IBD patients were treated with biologicals (vedolizumab: 7/27, 26% or anti-TNF: 11/27, 41%). Twenty IBD patients also participated in the Swiss IBD cohort study and were genotyped regarding the rs9557195 SNP as part of a larger genotyping effort within Swiss IBD cohort study.

### 3.2 | Preferential GPR183 expression in CCR6<sup>+</sup> and CCR9<sup>+</sup> CD4<sup>+</sup> memory T cells in healthy volunteers (HV)

We first tested GPR183 expression on different subsets of peripheral blood mononuclear cells (for full gating strategy, see Figure S1A) obtained from HV using an anti-GPR183 monoclonal antibody (clone 57C9B5C9) by flow cytometry (Clottu et al., 2017; Rutkowska et al., 2015). We previously showed that GPR183 is strongly expressed on memory CD4 T cells (CD45RA<sup>-</sup>CD4<sup>+</sup>) (Clottu et al., 2017). The specificity of GPR183 staining with the clone 57C9B5C9 has been previously shown as incubation of peripheral blood mononuclear cells with 7 $\alpha$ -25-OHC induces an GPR183 down-regulation (Wanke et al., 2017). Since our study population was predominantly female (65%, see above), we confirmed homogenous expression in male and female study participants in CD4<sup>+</sup> T cells, CD8<sup>+</sup> T cells and B cells (Figure S2).

We then focused on CD4<sup>+</sup> memory T cell subsets expressing chemokine receptors CCR6, CCR9 and CXCR3, which can recruit immune cells into the inflamed intestine (Figure 1a–c, Figure S3A, for full gating strategy see Figure S1B; Trivedi & Adams, 2018; Trivedi et al., 2016). We observed that GPR183 was differentially expressed in relation to chemokine receptor expression. Memory CD4<sup>+</sup> T cells expressing CCR6 and CCR9 had a significantly higher GPR183 mean fluorescence intensity ratio (MFIR) compared to total memory T cells (Figure 1b,c, Table S1). In contrast, memory CD4<sup>+</sup> T cells expressing CXCR3 or chemokine receptors CCR4 or CCR7 had similar GPR183 intensity staining compared to total memory T cells (Figure 1c). The association of CCR6, CCR9, and GPR183 expression was also significant when we used percentage of GPR183<sup>+</sup> cells (instead of MFIR) as the outcome measure (Figure 1a and Figure S3A,B).

We further tested GPR183 and CCR6 expression on different lymphocyte subsets and also observed a significantly higher GPR183 MFIR in CD8<sup>+</sup> memory T cells expressing CCR6 compared to total memory CD8<sup>+</sup> T cells (Figure 1d) and a trend for higher GPR183 expression in CCR6<sup>+</sup> B cells compared to memory B cells (Figure 1e, Table S1). In conclusion, we observed enrichment for GPR183 expression in memory lymphocytes expressing CCR6 and an increased expression on CD4 memory T cells expressing CCR9.

### 3.3 | Additive effects of 7 $\alpha$ ,25-OHC and CCL20 for the stimulation of CD4<sup>+</sup> memory T cell migration

To test, whether co-expression of GPR183 and CCR6 would be functionally relevant, we performed migration assays. Total peripheral blood mononuclear cells were loaded in a transwell system and incubated with the GPR183 ligand 7 $\alpha$ ,25-OHC, the CCR6 ligand CCL20, and a combination of both with or without the GPR183 inhibitor NIBR 189. The number of migrated cells of the various lymphocyte populations (CD4 T cells, CD8 T cells and B cells) was assessed by flow cytometry. In the absence of chemokines, CD4<sup>+</sup> cells migrated inefficiently (migration ratio of 1). However, addition of either 7 $\alpha$ ,25-OHC or CCL20 at optimal concentrations stimulated migration at least 10-fold over baseline (Figure 1f). Higher migration ratios were observed in the presence of both 7 $\alpha$ ,25-OHC and CCL20 ( $P < 0.05$ ), in line with an additive effect of both chemokines. Migration was specific to GPR183 since addition of NIBR 189 eliminated the effects of 7 $\alpha$ ,25-OHC (Figure 1f).

In CD8<sup>+</sup> T cells and B cells, migration was also most efficient in the presence of both 7 $\alpha$ ,25-OHC and CCL20. However, additive effects did not reach statistical significance (Figure S3C).

### 3.4 | Preferential GPR183 expression in CCR6<sup>+</sup> cells of IBD patients

We then evaluated abundance of GPR183 expression on lymphocytes obtained from peripheral blood mononuclear cells of patients with CD and UC. Similar to HV, we observed significantly increased GPR183 staining on CCR6 expressing CD4<sup>+</sup> memory T cells of CD and UC patients (Figure 2a). However, in contrast to HV, GPR183 expression was not significantly increased in CCR9 expressing CD4<sup>+</sup> memory T cells in IBD patients (Figure 2b). When abundance of GPR183 expression was compared in CCR9 versus CCR6 expressing memory CD4<sup>+</sup> T cells in the same donor, GPR183 expression was not significantly different from both lymphocyte subsets in HV (Figure 2c, Table S1). However, in CD and UC patients, GPR183 staining was significantly lower in CCR9<sup>+</sup> compared to CCR6<sup>+</sup> memory CD4<sup>+</sup> lymphocytes (Figure 2c, Table S1). Those results suggest that GPR183 expressing CCR9<sup>+</sup> lymphocytes have been depleted from the blood compartment in favour of a preferential homing in tissues such as the gut, as CCR9<sup>+</sup> has been described as a gut homing chemokine receptor (see Section 4).

No further differences in the other CD4 memory T cells populations according to IBD state were observed (Figure S4).

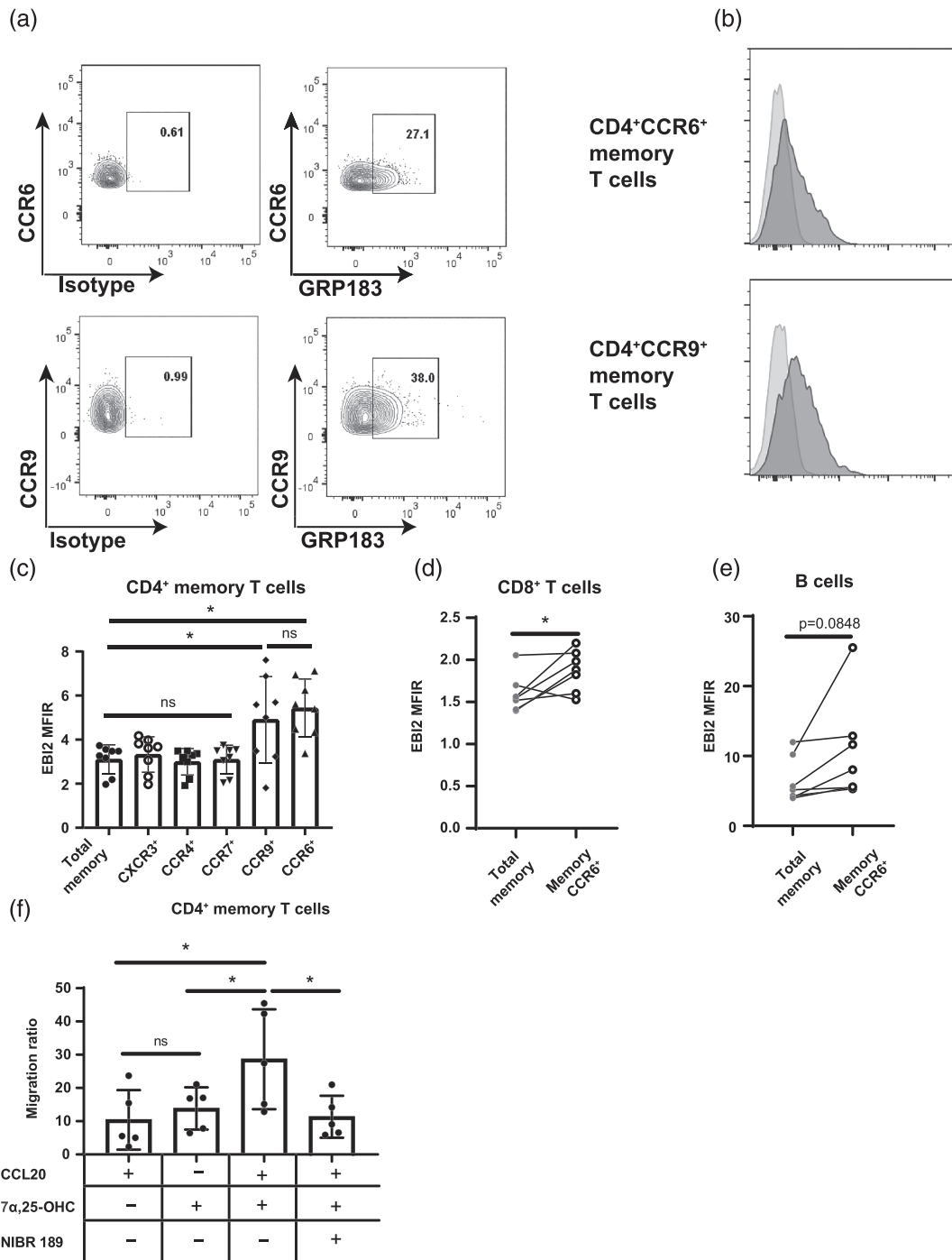


**FIGURE 1** GPR183 (EBI2) surface expression in memory lymphocytes of healthy volunteers is increased upon CCR6 and CCR9 expression. (a) Contour plot showing the frequency of isotype (left) and GPR183 (right) staining in CD4<sup>+</sup>CD45RA<sup>-</sup> memory CCR6<sup>+</sup> cells (top) and CD4<sup>+</sup>CD45RA<sup>-</sup> memory CCR9<sup>+</sup> cells (bottom). Numbers in each quadrant indicate the percentage (%) of isotype or GPR183 positive cells. (b) Histogram showing the phycoerythrin (PE) GPR183 signal of CCR6<sup>+</sup> or CCR9<sup>+</sup> cells, as indicated; the isotype control is shown in light grey. (c) GPR183 mean fluorescence intensity ratio (MFIR) in total CD4<sup>+</sup> memory T cells, CD4<sup>+</sup> memory T cells expressing CXCR3, CCR4, CCR7, CCR9 or CCR6, as indicated. MFIR is defined as the ratio between the geometric mean fluorescence intensity (MFI) of anti-GPR183 staining and the geometric MFI of the isotype control, *n* = 8. (d) GPR183 MFIR in CD8<sup>+</sup> memory T cells (CD8<sup>+</sup>CD45RA<sup>-</sup>) compared to CD8<sup>+</sup> memory T cells CCR6<sup>+</sup> and (e) in memory B cells CD19<sup>+</sup>CD27<sup>+</sup> compared to memory B cells CCR6<sup>+</sup>, *n* = 6. (f) Transwell migration assay of peripheral blood mononuclear cells (PBMCs) of five healthy volunteer comparing chemotaxis with CCL20 at 100 ng·ml<sup>-1</sup>, 7 $\alpha$ ,25-OHC at 300 nM and the GPR183 antagonist NIBR 189 at 25 nM, as indicated. The cells are quantified by flow cytometry using counting beads. The migration ratio is calculated based on the ratio between the cell concentrations in the experimental conditions and the cell concentrations using the medium only, without any added chemotactic signal as a negative control, *n* = 5. ns, not significant. \**P* < .05

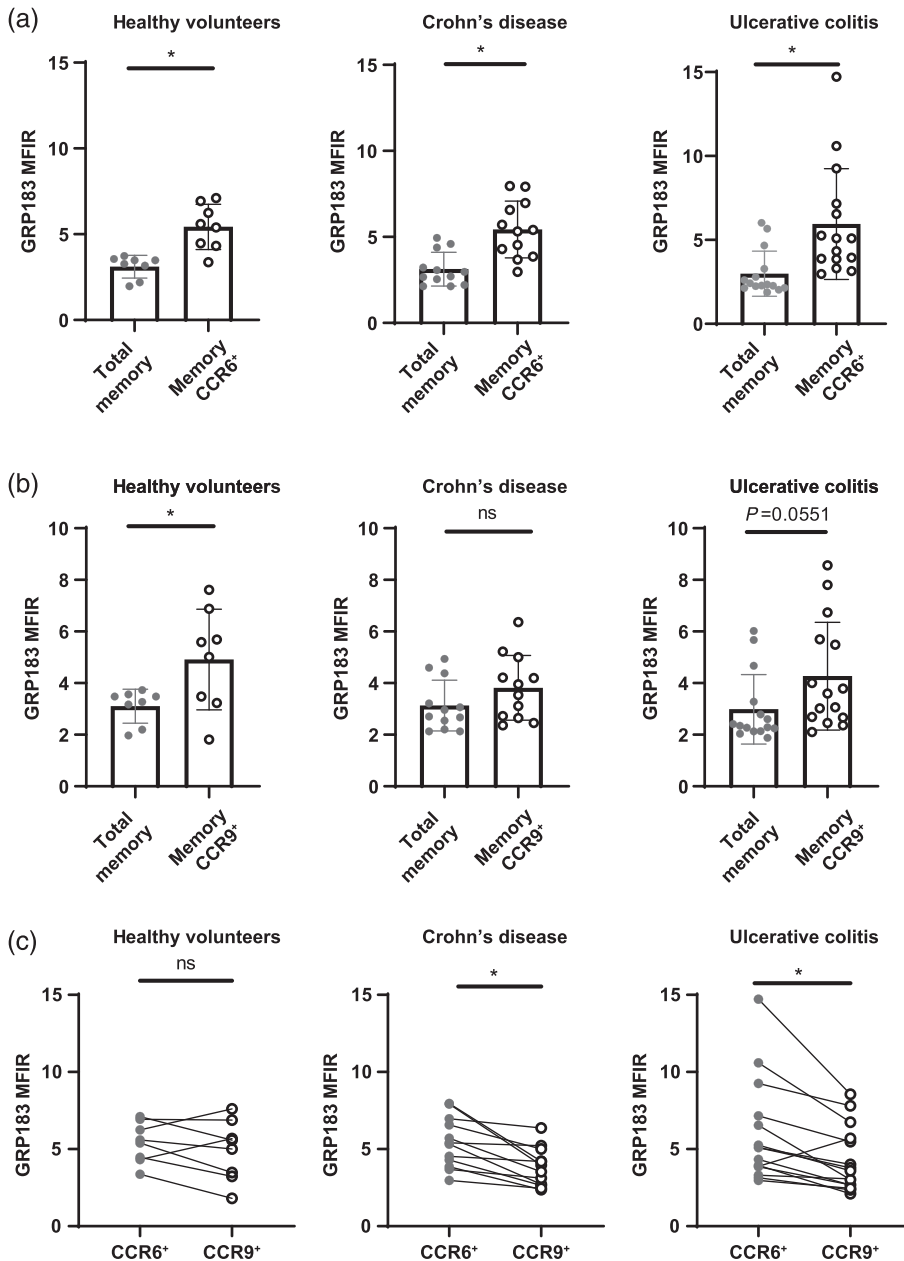


**FIGURE 2** In inflammatory bowel disease (IBD) patients, GPR83 (EBI2) surface expression in CD4<sup>+</sup> memory T cells is increased upon CCR6 but not CCR9 expression. (a) GPR183 surface staining in total CD4<sup>+</sup> memory T cells compared to CCR6 expressing CD4<sup>+</sup> memory T cells, in healthy volunteers (HV), Crohn's disease (CD) and ulcerative colitis (UC) patients, as indicated. GPR183 surface staining is indicated as the mean fluorescence intensity ratio (MFIR), the ratio between the geometric mean fluorescence intensity (MFI) of anti-GPR183 staining and the geometric MFI of the isotype control). Panel (b) as in (a), for the CCR9<sup>+</sup>CD4<sup>+</sup> memory subset. (c) Pairwise comparison of GPR183 MFIR in CCR6 and CCR9 expressing memory CD4<sup>+</sup> T cells from healthy volunteers (HV), CD and UC patients. ns, not significant; \* $P < .05$ ; HV:  $N = 8$ , CD:  $N = 12$ , UC:  $N = 15$

Furthermore, no correlation between abundance of GPR183 expression on lymphocytes and disease activity scores or biomarker levels was found (data not shown).

Subsets of patients were treated with the integrin inhibitor **vedolizumab**, which blocks immune cell homing into the gut. However, we did not find any differences in abundance of GPR183 expression according to IBD treatment neither on memory CD4<sup>+</sup>, memory CCR6<sup>+</sup>CD4<sup>+</sup>, memory CD8<sup>+</sup> or memory B cells from patients under vedolizumab, anti-TNF or under other therapies compared to HV (Figure S5A-H).

### 3.5 | Increased GPR183 expression in Th17 cells

We then evaluated GPR183 expression on different T lymphocyte subsets based on their chemokine receptor expression, namely, Th1,

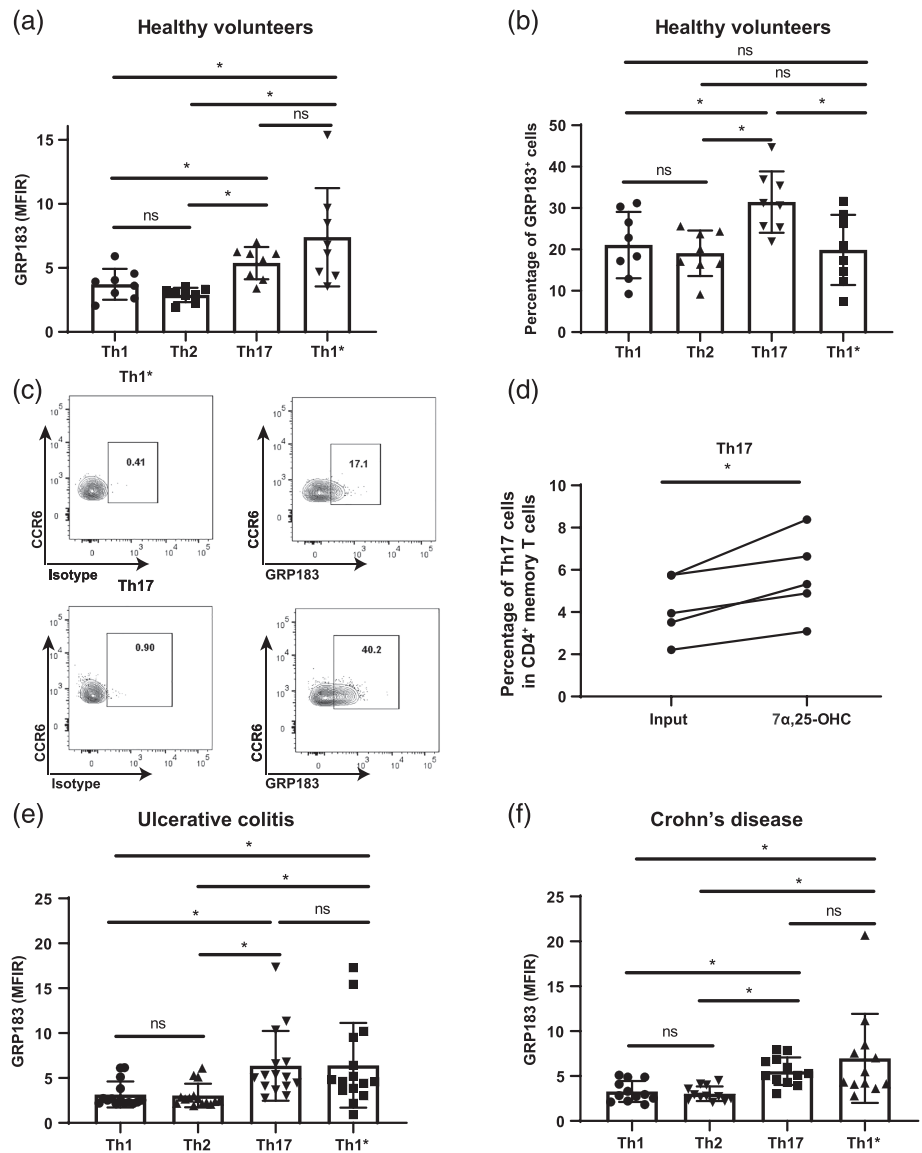
Th2, Th17 and Th1\* cells. Th1\* (also referred to as Th1/Th17 or non-classical Th1 cells) cells express transcription factors and chemokine receptors from Th1 and Th17 cells and combine properties of both cell types (Sallusto, 2016; Ueno et al., 2018). CCR6 is expressed by both Th17 (CXCR3<sup>-</sup>CCR6<sup>+</sup>) and Th1\* (CXCR3<sup>+</sup>CCR6<sup>+</sup>) cells.

Abundance of GPR183 surface staining in memory Th17 and Th1\* cells was significantly higher compared to total memory, Th1 or Th2 cells in HV (Figure 3a, Table S1). The percentage of GPR183<sup>+</sup> cells was higher in Th17 cells compared to Th1, Th2 and Th1\* (Figure 3b,c). This is in line with previous studies, demonstrating higher abundance of GPR183 surface staining in Th17 cells (Clottu et al., 2017; Wanke et al., 2017). Higher abundance of GPR183 surface staining was functionally relevant, since 7 $\alpha$ ,25-OHC induced migration resulted in enrichment of Th17 cells compared to the input (Figure 3d). No enrichment was observed for Th1, Th1\* cells or Th2 cells (Figure S6).

**FIGURE 3** The abundance of GPR183 (EBI2) surface expression is increased in Th17 and Th1\* memory cells.

(a) GPR183MFIR (ratio between the geometric mean fluorescence intensity [MFI] of anti- GPR183 staining and the geometric MFI of the isotype control) in Th1, Th2, Th17 and Th1\* cells as indicated. (b) Percentage of GPR183<sup>+</sup> cells in the Th1, Th2, Th17 and Th1\* population, as indicated.

(c) Representative contour plot of the frequency of isotype (left) and anti-GPR183 (right) in CCR6<sup>+</sup> Th1\* (top) and CCR6<sup>+</sup> Th17 cells (bottom). The number in each quadrant indicates the percentage of positive cells for the isotype or GPR183 staining as indicated,  $n = 8$ . (d) Transwell migration assay with total peripheral blood mononuclear cells (PBMCs) from five healthy volunteers showing the percentage of Th17 cells defined by flow cytometry in relation to total CD4<sup>+</sup> memory T cells in the absence of migration and after migration towards 7 $\alpha$ ,25-OHC (30 nM). The input depicts the percentage of cells before migration,  $n = 5$ . (e) As (a), only UC patients are shown. (f) as (a), only CD patients are shown. ns, not significant; \* $P < .05$



Increased amounts of GPR183 surface staining were also observed in IBD patients where GPR183 MFIR was higher in Th1\* and Th17 cells compared to Th1 and Th2 cells in UC and CD (Figure 3e,f).

### 3.6 | High GPR183 surface expression in memory CD8<sup>+</sup> T cells and memory B cells in IBD

We previously demonstrated higher GPR183 surface staining in all subsets of memory lymphocytes (CD4<sup>+</sup> and CD8<sup>+</sup> T cells as well as B cells) and compared their naïve counterparts in HV (Clottu et al., 2017). CD4<sup>+</sup> T cell subsets (data not shown) and CD8<sup>+</sup> memory T cells also depicted higher GPR183 MFIR compared to their naïve counterparts in CD and UC patients (Figure 4a). When we compared GPR183 expression in CD8<sup>+</sup> T cell subsets from different patient groups, we observed a higher GPR183 MFIR in CD compared to HV. This result was significant in total CD8<sup>+</sup> T cells as well as in naïve CD8<sup>+</sup> T cells (Figure 4b). We also note a similar trend for higher

GPR183 expression in naïve CD8<sup>+</sup> T cells in UC compared to HV (not significant; Figure 4b). Further, we confirmed significantly stronger GPR183 surface staining in memory B cells (CD27<sup>+</sup>CD19<sup>+</sup>) compared to naïve B cells in HV as well as in UC (Figure 4c) (Clottu et al., 2017), but the difference was not significant in CD. No significant differences were observed between HV, CD and UC in different B cell subsets; however, we observed that two IBD patients depicted very high GPR183 expression (Figure 4d). Those two outliers could not be identified in CD8<sup>+</sup> T cells.

### 3.7 | Increased GPR183 surface expression in IBD patients with the CC allele of rs9557195

Those results prompted us to investigate if a genetic predisposition was related to those observations. The rs9557195 SNP is located within an intron of the *GPR183* gene (Figure 5a) and has been associated with the risk for IBD (Jostins et al., 2012). Whether alleles of rs9557195 can

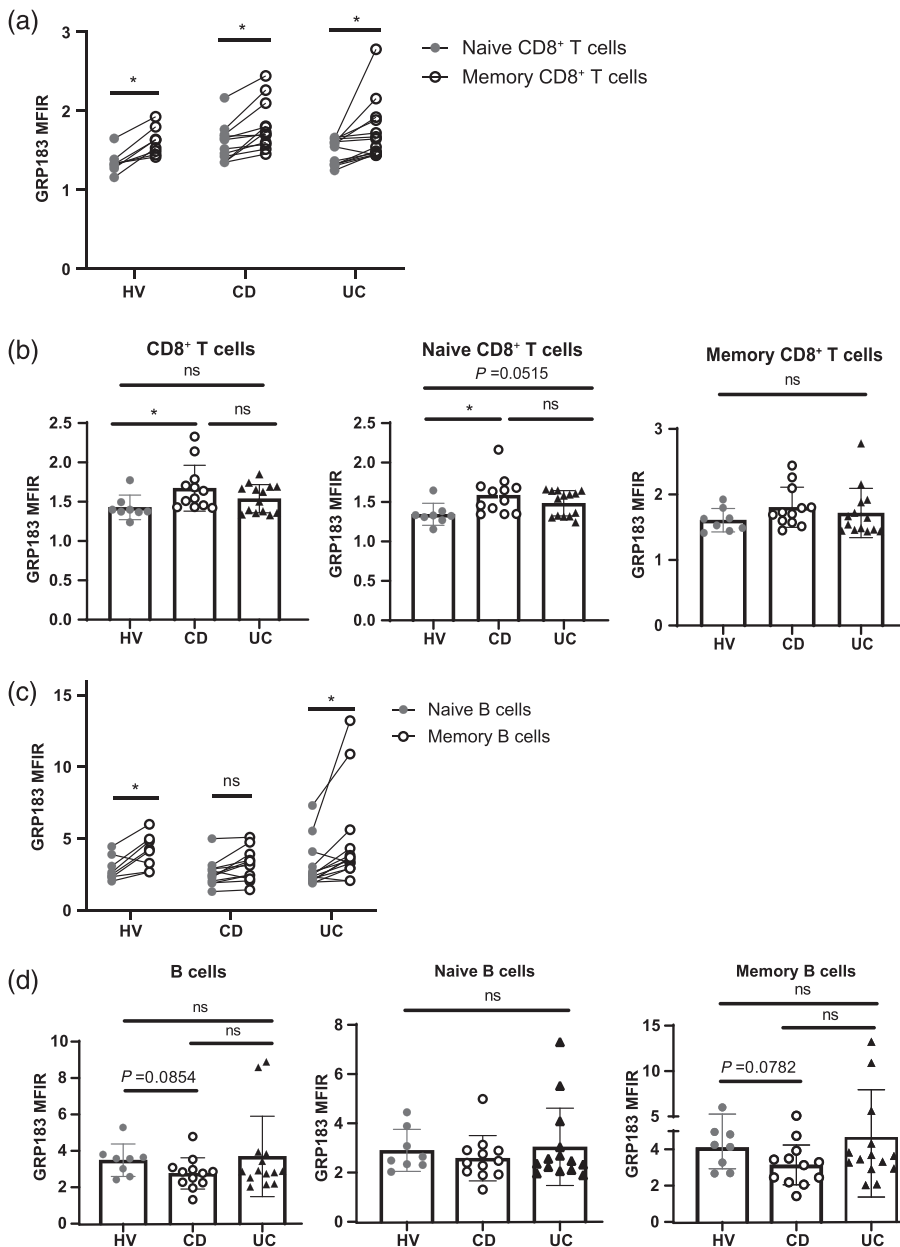


**FIGURE 4** GPR183 (EBI2) surface expression is increased in memory B and CD8<sup>+</sup> T cells. (a) Pairwise comparison of GPR183 MFIR of naïve and memory CD8<sup>+</sup> T cells from the same individual in healthy volunteers (HV), Crohn's disease (CD) and ulcerative colitis (UC) patients, as indicated. (b) Comparison of GPR183 expression in total CD8<sup>+</sup> T cells, naïve and memory CD8<sup>+</sup> T cells as indicated. Panels (c) and (d) as in (a) and (b), only the subsets of CD19<sup>+</sup> B cells are shown, healthy volunteers (HV): N = 8, CD: N = 12, UC: N = 15. ns, not significant; \* $P < .05$

affect GPR183 gene function is unclear. Of all patients, genetic testing had been performed in 20 IBD patients: six patients were homozygous for the minor C-allele (resulting genotype rs9557195-CC) and 14 patients were homozygous for the major T-allele rs9557195-TT).

In naïve B cells, we observed a significantly increased percentage of GPR183<sup>+</sup> cells in IBD patients with the CC allele compared to the TT allele (Figure 5b and representative FACS plot in Figure 5c). However, the percentage of GPR183<sup>+</sup> cells did not differ according to the rs9557195 allele state in naïve CD4<sup>+</sup> or naïve CD8<sup>+</sup> T cells (Figure 5b). Control experiments demonstrated that the percentage of naïve B cells and memory B cells in peripheral blood mononuclear cells did not differ in individuals with the rs9557195-CC and rs9557195-TT genotype (data not shown).

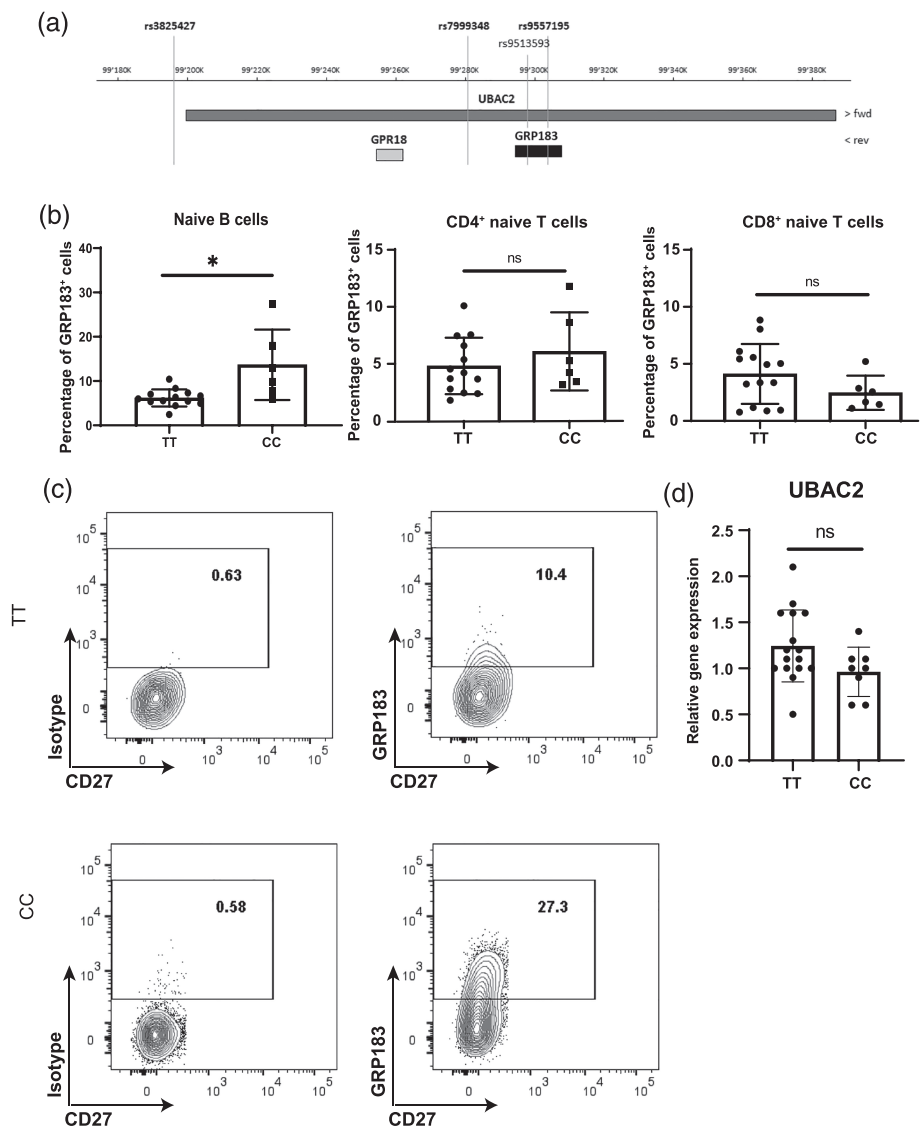
We also tested mRNA expression levels of UBAC2 according to the rs9557195 genotype. UBAC2 has a joint genomic location with

GPR183 (Figure 5a) and rs9557195 is also localized within the UBAC2 gene. However, our quantitative PCR experiments did not reveal significant differences between individuals with the CC and TT allele state of rs9557195 (Figure 5d).

### 3.8 | Distribution of rs9557195 and Behçet's disease associated alleles within Swiss IBD cohort study patients

To assess an impact of the IBD associated SNP rs9557195 on IBD disease course, we took advantage of the clinical and genetic information available for Swiss IBD cohort study patients. Of >3000 Swiss IBD cohort study patients, genetic information was available for 2304 individuals and for 2301 patients, the rs9557195 genotype

**FIGURE 5** Increased GPR183 (EB12) expression in naïve B cells of individuals with the CC allele of the GPR183 SNP rs9557195. (a) Structure of the *GPR183* gene locus. The position of the *GPR183*, *UBAC2* and *GPR18* genes as well as the inflammatory bowel disease (IBD) associated SNP rs9557195, the Behçet's disease associated SNPs rs7999348 and rs3825427 and the psoriasis associated SNP rs9513593 are indicated. (b) Percentage of GPR183<sup>+</sup> cells in peripheral blood mononuclear cells (PBMCs) of 20 individuals with IBD (11 ulcerative colitis (UC) and 9 Crohn's disease (CD)) carrying the CC and TT alleles gated on naïve B cells, CD4<sup>+</sup> naïve cells and CD8<sup>+</sup> naïve as indicated, TT: N = 13, CC: N = 6. One outlier was removed from the TT sub-group using the ROUT (Q = 1%) method of Graphpad prism. If the outlier was included P-value of the Mann-Whitney test was 0.02. (c) Scatter plot illustrating increased GPR183 expression in naïve B cells with the CC allele of rs9557195; the GPR183 PE-signal and the BV-421 CD27 signal, TT: n = 16, CC n = 8. (d) Relative expression of *UBAC2* in total peripheral blood mononuclear cells (PBMCs) from 24 IBD patients comparing *UBAC2* mRNA relative quantity between patients carrying the CC and TT measured by qPCR. *UBAC2* expression is normalized to GAPDH levels as a house keeping gene. TT = rs9557195 homozygous wildtype, CC = rs9557195 homozygous variant. \*P < .05



was known (52% male and 48% female); 1335 patients (58%) were diagnosed with CD and 966 (42%) with UC. Our study comprises a mixed cohort of patients with mild, moderate and severe disease (Table S2).

The composition of the *GPR183/UBAC2* locus is complex. The IBD associated SNP rs9557195 is positioned within an intron of *GPR183*. At the same genetic location as *GPR183* but on the reverse/complementary strand, the much larger ubiquitin-associated domain-containing gene 2 (*UBAC2*) is found (Figure 5a). Several SNPs within the *UBAC2* gene (rs9513584, rs3825427, rs9517668, rs9517701 and rs7999348) have been associated with Behçet's disease in humans (Hou et al., 2012; Sawalha et al., 2011). After reducing pairs or triplets of SNPs with strong correlation (see Section 2, Figure S7), the following three SNPs remained for further analysis: rs9557195, rs7999348 and rs3825427. Allelic frequencies of these SNPs were similar in Swiss IBD cohort study patients compared to international cohorts (Table S3).

### 3.9 | The CC genotype of the IBD SNP rs9557195 is associated with psoriasis and extraintestinal manifestation of IBD

Of 2301 Swiss IBD cohort study patients, 134 (5.8%) carried the CC genotype of the *GPR183* SNP rs9557195, 824 (35.8%) the heterozygous form (CT) and 1343 (58.4%) the homozygous wildtype allele TT. Overall, presence of the C allele was associated with younger age at IBD diagnosis (Table S2), however this difference failed to reach statistical significance. Examining clinical phenotypes including disease location, extent, surgical and medical history, and common complications in our cohort, we did not find significant associations between rs9557195 genotype and disease severity (Figure 6a,b and Table S2).

Psoriasis can complicate IBD (Cottone et al., 2019). In our study population, 129 cases of psoriasis were recorded throughout follow-up. Of patients carrying the CC genotype, 11.2% were

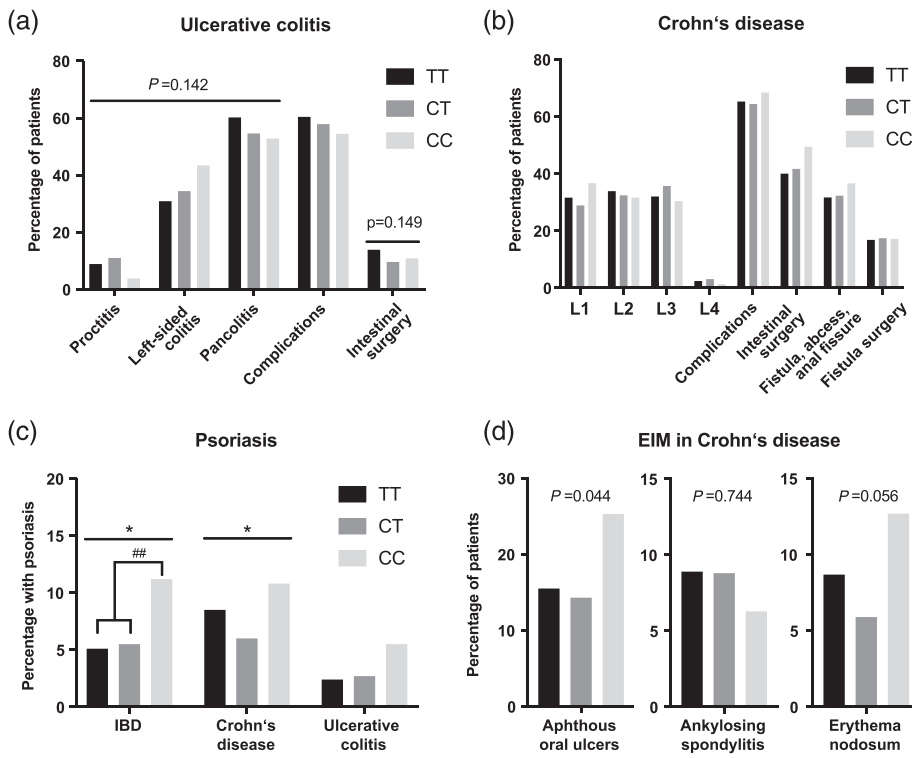


**FIGURE 6** Increased psoriasis rates in Swiss inflammatory bowel disease (IBD) cohort study patients carrying the rs9557195 CC allele. (a) Percentage of ulcerative colitis (UC) patients with the respective rs9557195 allele with the indicated disease extent, complications and intestinal surgery. (b) Percentage of Crohn's disease (CD) patients with the respective disease location according to the Montreal classification (Silverberg et al., 2005); L1: ileal, L2: colonic, L3: ileocolonic, L4: isolated upper gastrointestinal disease; intestinal surgery, fistula and fistula surgery are indicated. (c) Percentage of individuals carrying the indicated rs9557195 allele with psoriasis. (d) Percentage of IBD patients carrying the indicated rs9557195 allele with oral aphthous ulcers, ankylosing spondylitis and erythema nodosum, TT= CD: N = 767, UC: N = 576, CT= CD: N = 489, UC: N = 335, CC= CD: N = 79, UC: N = 55. Statistical analysis: Pearson  $\chi^2$  test, Fisher's exact test. TT= rs9557195 homozygous wildtype, CC= rs9557195 homozygous variant, CT =rs9557195 heterozygous variant. \* $P < .05$

diagnosed with psoriasis, compared to only 5.5% and 5.1% patients carrying the CT and TT alleles, respectively ( $P = 0.014$ , Table S4 and Figure 6c). The association between the C allele and the presence of psoriasis was even more pronounced when we merged CT and TT variants ( $P = 0.004$ ; Fisher's exact test). The rate of psoriasis was approximately twice as high for CC patients compared to CT and TT for both UC and CD patients. However, since psoriasis was diagnosed more frequently in CD than in UC (7.7% vs. 2.7%), the association of psoriasis and the CC genotype was only significant in the subgroup of CD patients (Figure 6c). In a minority of patients (26 of 126 patients: 24 with CD and two with UC), psoriasis was reported as a side effect of anti-TNF treatment; however, this side effect was not associated with the rs9557195 genotype.

Extraintestinal manifestations are common in UC and CD patients, mainly affecting peripheral and axial joints, skin and eyes, but also hepatopancreatobiliary, renal and pulmonary systems (Fagagnini et al., 2017; Larsen et al., 2010). In the CD group, aphthous oral ulcers showed a significantly different distribution between rs9557195 genotypes with 25.3% patients with aphthous oral ulcers in the CC group compared to 14.3% and 15.5% in the CT and TT group, respectively ( $P = 0.044$ ). Also, erythema nodosum tended to be more frequent in CD patients carrying the CC variant (12.7% CC vs. 5.9% CT and 8.7% TT) (Table S4 and Figure 6d).

### 3.10 | Association of the UBAC2 SNP rs799348 with extraintestinal manifestations

Alleles of rs7999348 and rs3825427, associated with the UBAC2 gene and Behçet's disease, did not differ regarding intestinal disease manifestations of IBD in an extensive association analysis (data not shown). Regarding extraintestinal manifestation we found significant associations of the risk allele G for Behçet's disease (rs7999348) with the occurrence of erythema nodosum ( $P = 0.029$ ) and ankylosing spondylitis ( $P = 0.017$ ). For rs3825427 we did not find significant associations (Table S6 and Figure S8).

## 4 | DISCUSSION

To study the role of the oxysterol receptor GPR183 in IBD, we analysed GPR183 surface expression on PBMC derived lymphocytes and the impact of alleles of the SNP rs9557195 on the clinical course of IBD. We would like to emphasize the following observations: (i) abundance of GPR183 expression is higher on immune cells expressing the IBD associated chemokine receptors CCR6 and CCR9. (ii) There is higher GPR183 surface staining on pro-inflammatory Th17 and Th1\* cells, associated with IBD. (iii)  $7\alpha,25$ -OHC and the CCR6 ligand CCL20 have additive effects on the

migration of CD4<sup>+</sup> memory T cells, (iv) IBD patients with the CC-allele of rs9557195 had higher GPR183 expression in B cells compared to patients with the TT-allele. (v) IBD patients with the CC-allele of rs9557195 had a higher psoriasis rates compared to individuals with the TT-allele. These results add to growing body of experimental and genetic evidence indicating a role of GPR183 in IBD (Chu et al., 2018; Emgard et al., 2018; Jostins et al., 2012; Misselwitz et al., 2020; Wyss et al., 2019).

#### 4.1 | GPR183 expression on CCR6 and CCR9 positive cells

A large number of chemokines and chemokine receptors can be expressed by several cell types in the colon and their expression patterns shape the distribution of immune cells in the small and large bowel in health and inflammation (Trivedi & Adams, 2018). In physiological or pathological situations, recruitment of immune cells is mediated by more than one chemokine and examples for cooperative interactions of chemokines have been reported (Verkaar et al., 2014). Strong evidence implicates GPR183 in immune cell trafficking into the gut (Chu et al., 2018; Emgard et al., 2018; Wyss et al., 2019). We demonstrate co-expression of GPR183 with two IBD associated chemokine receptors, CCR6 and CCR9, indicating cooperation and coordination of these pathways in IBD pathogenesis.

The CCR9 chemokine is expressed on 58–97% of immune cells with gut tropism (Trivedi & Adams, 2018). The only CCR9 ligand, **CCL25**, is expressed in the small bowel with a gradient of decreasing concentration from the duodenum to the ileum in health, but CCL25 is also induced in the colon upon inflammation (Trivedi et al., 2016). The CCR9-CCL25 axis promotes recruitment of many different cell types into the intestine (Trivedi & Adams, 2018) and also increases expression of additional pro-migratory receptors for intestinal homing such as **α4β7 integrin** (Miles et al., 2008), indicating cooperation.

CCR6 and its ligand CCL20 as well as CXCR3 with its ligands CXCL9/CXCL10 are also implicated in the recruitment of immune cells into the small and large intestine in inflammation; human genetic, translational and animal data implicate CCR6-CCL20 and CXCR3-CXCL9/CXCL10 in IBD pathogenesis (Jostins et al., 2012; Ostvik et al., 2013; Skovdahl et al., 2015; Trivedi & Adams, 2018). However, so far, clinical trials in IBD patients using compounds affecting CCR6, CCR9 or CXCR3 signalling have been disappointing (Biswas et al., 2019; Feagan et al., 2015; Mayer et al., 2014; Perez-Jeldres et al., 2019; Trivedi & Adams, 2018), most likely due to redundant migratory signals for immune cell recruitment into the inflamed gut. We observed co-expression of GPR183 with CCR6 and CCR9 on different subsets of memory lymphocytes from HV, in line with a joint and mutually supporting function of both chemokine receptors in the gut.

Co-expression of CCR6 and GPR183 is likely functionally relevant since in migration assays in peripheral blood mononuclear cells from HV; both the CCR6 ligand CCL20 and the GPR183 ligand 7α,25-OHC stimulated migration approximately 10-fold. Migration was increased in the presence of both ligands, in line with additive effects in health.

We similarly observed a co-expression of GPR183 and CCR6 in lymphocytes from IBD patients. Surprisingly, this was not evident for GPR183 expression in CCR9 expressing subsets. This could be the consequence of the migration of CCR9 and GPR183 expressing cells from the blood into the gut. This could be directly tested in migration experiments with the CCR9 ligand CCL25. In line with additive effects of CCR6 and/or CCR9 with GPR183 on cellular migration, we previously reported higher GPR183 expression on colonic lamina propria derived lymphocytes compared to blood lymphocytes (Wyss et al., 2019). GPR183 could thus induce or accelerate recruitment of immune cells into the gut. Such a scenario is supported by animal models of IBD and experimental autoimmune encephalomyelitis, in which inactivation of GPR183 resulted in sequestration of GPR183 expressing immune cells in mesenteric or peripheral lymph nodes (Chalmin et al., 2015; Chu et al., 2018). A non-exclusive interpretation of the role of GPR183-induced migration would be redistribution of GPR183 + lymphocytes from intestinal lymphoid tissues to inflammatory foci, as supported by mouse studies (Emgard et al., 2018; Wyss et al., 2019).

Th17 cells are crucial pro-inflammatory cells in the intestine (Sallusto, 2016). Furthermore, Th17 cells also play a central role in the pathogenesis of IBD as indicated by genetic evidence and translational data such as high concentrations of Th17 cells within the inflamed intestinal mucosa in IBD patients (Jostins et al., 2012; Ueno et al., 2018). Besides Th17 cells, Th1\* cells have been described: Th1\* cells show characteristics of Th1 cells, such as expression of CXCR3 and T-bet as well as characteristics of Th17 cells, such as expression of RORγt (NR1F3) and CCR6 (Sallusto, 2016). Such Th1\* subsets have in fact been described in the gut of CD patients (Annunziato et al., 2007). Previous studies demonstrated higher GPR183 expression on Th17 cells (Clottu et al., 2017; Wanke et al., 2017). Our study expands these findings, demonstrating preferential expression of GPR183 on Th17 and to a lesser extent on Th1\* cells, although the impact on migration was only significant in Th17 cells. Since in our study, Th17 cells are defined as CXCR3<sup>-</sup>CCR6<sup>+</sup> cells and Th1\* cells are defined as CXCR3<sup>+</sup>CCR6<sup>+</sup> cells, expression of GPR183 on Th17 and Th1\* cells is likely related to CCR6 expression. Our results are in line with a pro-inflammatory role of GPR183 and a supporting function of GPR183 for Th17 and Th1\* mediated intestinal inflammation.

#### 4.2 | A role of GPR183 in psoriasis

Clinical evidence indicates a significant co-occurrence of IBD with psoriasis and psoriasis patients have a 4-fold higher risk of developing CD (Cottone et al., 2019; Li et al., 2013). Molecular and cellular pathogenesis of IBD and psoriasis also overlap and implications GPR183 co-expression with CCR6 and CCR9 also apply to psoriasis. CCR6 and its ligand CCL20 are up-regulated in psoriasis (Homey et al., 2000); and CCR6 expression has been described in mature dendritic cells and memory T cells in psoriatic lesions (Guo et al., 2019; Kim et al., 2014) which clustered together reminiscent of secondary lymphoid organs (Kim et al., 2014). In psoriasis, higher CCR9 expression in skin biopsies was associated with poor response to anti-TNF therapy (Koga

et al., 2016). As in IBD, the Th17 - IL-23 axis plays a central role in psoriasis (Chan et al., 2006; Lee et al., 2004; Lowes et al., 2008). Th17 T cells are enriched in inflammatory lesions in IBD and psoriasis and rheumatoid arthritis and produce IL-17 and express high amounts of CCR6 (in contrast to Th1 or Th2 cells) (Pene et al., 2008). Therefore, GPR183 co-expression with CCR6 and CCR9 and preferential expression in Th17 and Th1\* cells places GPR183 in cell subtypes, which are active pro-inflammatory players in psoriasis.

Several genetic risk loci are shared between CD and psoriasis (Ellinghaus et al., 2012) and rs9513593 (in close vicinity to the IBD-associated SNP rs9557195) within the *GPR183/UBAC2* genetic locus is associated with the risk of psoriasis (Tsoi et al., 2017). We demonstrate an increased risk of psoriasis in IBD patients with the rs9557195-CC allele, suggesting that the *GPR183/UBAC2* locus is another link mediating the association of IBD and psoriasis. In line with previous data indicating clinical overlap with CD but not UC (Cottone et al., 2019; Li et al., 2013), we only observed an increased psoriasis risk in rs9557195-CC patients with CD. In our study, preferential GPR183 expression in rs9557195-CC patients was limited to B cells, possibly reflecting limited power of our analysis. However, B cells have also been implicated in the pathogenesis of psoriasis in animal and human studies (Alrefai et al., 2016; Guidelli et al., 2013; Hayashi et al., 2016; Yanaba et al., 2013) and in an animal model, expression of CCR6 on B cells supported homing into the skin (Geherin et al., 2012).

### 4.3 | The *GPR183/UBAC2* locus is associated with the risk for IBD, Behçet's disease and psoriasis

Two genes are present within the *GPR183* gene locus: *GPR183* and *UBAC2*, on the complement strand (Figure 5a). Consequently, genetic alterations within the *GPR183/UBAC2* locus might affect expression, splicing and/or function of either or even both of these genes.

In contrast to GPR183, knowledge regarding the function of the UBAC2 protein (also called phosphoglycerate dehydrogenase-like protein 1) is limited. UBAC2 is an endoplasmic reticulum membrane protein involved in protein ubiquitinylation and proteasome mediated degradation. UBAC2 is part of a protein complex in the membrane of the endoplasmic reticulum which can inhibit *Wnt/β-catenin* signalling and defects of this protein complex resulted in severe lymphocyte dysfunction (Choi et al., 2019). In another study, UBAC2 restricted trafficking of Fas associated factor 2 (FAF2, also called UBXD8) from the endoplasmic reticulum to lipid droplets (Olzmann et al., 2013). However, it remains unclear, how UBAC2 would contribute to organ inflammation.

Several studies with patients from Turkey, China and Japan associated genetic polymorphisms of the *UBAC2* gene with Behçet's disease (Hou et al., 2012; Sawalha et al., 2011; Yamazoe et al., 2017). Behçet's disease is characterized by a triple-symptom complex of oral aphthous ulcers, genital ulcers and ocular lesions. However, skin (acneiform lesions, erythema nodosum, pyoderma gangrenosum and others), joints and the gastrointestinal tract are also frequently affected (Greco et al., 2018) and clinical overlap between Behçet's

disease and IBD with extraintestinal manifestation can result in diagnostic challenges.

For two *UBAC2* associated SNPs, rs7999348 and rs3825427, previous studies have identified functional effects on *UBAC2* expression in peripheral blood mononuclear cells (Hou et al., 2012; Sawalha et al., 2011). Besides *UBAC2*, other ubiquitination-related genes (*UBASH3B*, *SUMO4*) have also been associated with Behçet's disease, suggesting a crucial role of ubiquitination in the pathogenesis of this condition (Fei et al., 2009; Hou et al., 2012; Sawalha et al., 2011). Interestingly, an expression quantitative trait loci (eQTL) study in anti-TNF resistant CD patients demonstrated elevated *UBAC2* expression in individuals with the TT allele of the IBD SNP rs9557195 in peripheral blood and the intestine (Di Narzo et al., 2016). In our study, a minor trend for higher *UBAC2* expression in individuals with the rs9557195 TT allele was also observed which did not reach statistical significance. Further, a SNP within *UBAC2/GPR18* was associated with anti-TNF non-response (Burke et al., 2018), raising the possibility of involvement of *UBAC2* also in IBD. In our study, rs7999348 was associated with extraintestinal manifestation but not with the clinical course of IBD but it remains possible that Behçet's disease associated polymorphisms mediate the risk for extraintestinal manifestation in IBD patients.

Joint localization of *UBAC2* and *GPR183* in a common genomic location might be an indication of a functional relationship. In fact, ubiquitinylation has been shown to target GPCRs for proteasomal or lysosomal degradation as a mean for desensitization or functional inactivation (Rajagopal & Shenoy, 2018; Skieterska et al., 2017). However, ubiquitinylation can have implications beyond degradation: In case of the GPCR CXCR4, ubiquitin was shown to directly bind to the receptor, mediating activation (Saini et al., 2010). Similarly, CXCR2 signalling critically depends on ubiquitinylation of the C-terminus and preventing ubiquitinylation at this position blunted CXCR2 signaling (Leclair et al., 2014). Even more interesting, ubiquitinylation can mediate biased agonisms, differential responses of the same GPCR upon interaction with different agonists (Groer et al., 2011; Skieterska et al., 2017). Further, transubiquitination refers to a process, where binding of an agonist to one receptor can mediate ubiquitinylation and degradation of another receptor (Li et al., 2008; Skieterska et al., 2017).

Activation of GPR183 by 7 $\alpha$ ,25-OHC has been shown to stimulate ubiquitinylation of Notch and inhibition of Notch signalling, resulting in endothelial-to-haematopoietic transition (Zhang et al., 2015). However, to the best of our knowledge, a functional interaction of GPR183 and *UBAC2* has not been directly addressed and any interplay will need to be clarified by future studies.

### 4.4 | Immune cell migration as a therapeutic target in IBD

Interfering in immune cell migration is a cornerstone in IBD therapy (Biswas et al., 2019; Perez-Jeldres et al., 2019) and vedolizumab, an  $\alpha$ 4 $\beta$ 7 integrin inhibitor, is a safe and effective treatment for UC and CD (Feagan et al., 2013; Sandborn et al., 2013). Previous results from our group demonstrated increased GPR183 expression in immune

cells from peripheral blood in multiple sclerosis patients treated with the  $\alpha 4$  integrin inhibitor natalizumab in a longitudinal analysis (Clottu et al., 2017). In the current cross-sectional study, no difference in GPR183 expression was observed upon vedolizumab treatment. However, it is important to stress that this result does not exclude sequestering of GPR183 expressing immune cells in peripheral blood since the natalizumab-induced GPR183 increase had only been observed in a pair-wise analysis with a longitudinal study design (Clottu et al., 2017). Future experiments will show, whether sequestration of immune cells outside the intestine by blocking the GPR183-oxysterol axis (Chu et al., 2018; Clottu et al., 2017) might be a feasible therapeutic strategy in IBD.

#### 4.5 | Strengths and limitations

Our study has several strengths and limitations. Strengths include the good clinical characterization of all IBD patients in the Swiss IBD cohort study, enabling detailed genotype phenotype association studies. Further, abundance of GPR183 expression has been tested for several subsets of IBD patients and healthy volunteers in many B and T subclasses. Limitations include the small number of IBD patients for which FACS analysis could be performed. We also did not assess GPR183 expression in intestinal cells since for ethical reasons, patients with various rs9557195 genotypes could not be recruited for endoscopies without medical justification. Moreover, genetic results were not confirmed in an independent cohort. Finally, the number of IBD patients, seemingly high at >2'000 was not sufficient to provide Bonferroni correctable significance levels for all relevant readouts.

## 5 | CONCLUSION

In conclusion, our translational experiments indicate preferential GPR183 expression in cells with a pro-inflammatory role in the intestine. We also observed additive effects of the GPR183 ligand  $7\alpha,25$ -OHC and the CCR6 ligand CCL20 on the migration of memory T cells. GPR183 expression is also higher in B cells with the CC allele of rs9557195, an IBD associated genetic polymorphism and rs9557195-CC was associated with higher psoriasis rates in IBD patients. In agreement with prior genetic and animal data, our experiments confirm GPR183 as an important inflammatory mediator and a potential drug target.

#### ACKNOWLEDGEMENTS

The authors would like to thank Andreas Sailer, Novartis Institute of Biomedical Research, Basel, Switzerland, for generously providing an GPR183(EBI2)-antibody and stimulating discussions. This work was supported by grants from the Swiss National Science Foundation (SNF) to B.M. (grant no. 32473B\_156525), to C.P. (grant no. PPO0P3\_157476) and to G.R. (for the Swiss IBD Cohort, grant no. 33CS30\_148422), a grant from the Leenaards Foundation to

C.P. and a grant from the Hartmann-Müller Foundation to B.M. F.R. holds a MD-PhD grant from the SNF (#323630-183987).

#### AUTHOR CONTRIBUTIONS

F.R., A.W., C.P. and B.M. conceived, designed and supervised the study. F.R. performed the FACS experiments and analysed FACS data, supervised by C.P. A.W., J.B.R. and B.M. were involved in the analysis of genetic data. F.R., A.W., C.P. and B.M. wrote the paper. M.C.S., S.B., A.M., J.C.M., R.R., P.J., L.B., E.B., M.G., T.G. and G.R. recruited patients and critically revised the manuscript for important intellectual content. All authors approved the final version of the manuscript.

#### CONFLICT OF INTEREST

B.M. has served at an advisory board for Gilead and Novigenix. He has received speaking fees from Vifor, MSD and Takeda and traveling fees from Vifor, Novartis, MSD, Gilead and Takeda. B.M. has received a research grant from MSD unrelated to this work. C.P. has participated in advisory boards for Biogen, Celgene, Merck, Novartis and Roche none related to this work. A.W. is currently an employee of Abbvie. G.R. has consulted to Abbvie, Augurix, BMS, Boehringer, Calypso, Celgene, FALK, Ferring, Fisher, Genentech, Gilead, Janssen, MSD, Novartis, Pfizer, Phadia, Roche, UCB, Takeda, Tillots, Vifor, Vital Solutions and Zeller; GR has received speaker's honoraria from Astra Zeneca, Abbvie, FALK, Janssen, MSD, Pfizer, Phadia, Takeda, Tillots, UCB, Vifor and Zeller; G.R. has received educational grants and research grants from Abbvie, Ardeypharm, Augurix, Calypso, FALK, Flamentera, MSD, Novartis, Pfizer, Roche, Takeda, Tillots, UCB, and Zeller. L.B. reports fees for consulting/advisory board from Abbvie, MSD, Vifor, Falk, Esocap, Calypso, Ferring, Pfizer, Shire, Takeda, Janssen, Ewopharma. M.C.S. has received consultant and/or speaker fees from Abbvie, Ferring, MSD, Janssen, Pfizer, Takeda, and UCB. P.J. has received a research grant from Vifor unrelated to this work. S.B. received fees for consulting and advisory boards and speaker's honoraria from AbbVie, Falk, Janssen-Cilag AG, MSD, Pfizer, Takeda, UCB Pharma and Vifor Pharma. R.R. has served at an advisory board for Lilly and has received travel fees from AbbVie AG. T.G. has consulting contracts with Sanofi-Regeneron and Falk Pharma GmbH, received travel grants from Falk Pharma GmbH and Vifor, and an unrestricted research grant from Novartis. E.B. received consultant and/or speaker fees from Abbvie, Janssen, MSD, Norgine, Pfizer, Takeda, and Sandoz. J.C.M. has served at advisory boards and received honoraria from Abbvie, Bayer, BMS, Eisai, Gilead, Incyte, Intercept, Ipsen, MSD, Roche, Sanofi, SigmaTau. J.C.M. received grants from Abbvie, Gilead, and Falk.

#### DECLARATION OF TRANSPARENCY AND SCIENTIFIC RIGOUR

This Declaration acknowledges that this paper adheres to the principles for transparent reporting and scientific rigour of preclinical research as stated in the BJP guidelines for [Design and Analysis](#) and as recommended by funding agencies, publishers and other organisations engaged with supporting research.

## DATA AVAILABILITY STATEMENT

The data that support the findings of this study are available from the corresponding author upon reasonable request. Some data may not be made available because of privacy or ethical restrictions.

## ORCID

Anja Moncsek  <https://orcid.org/0000-0002-1191-5842>

Caroline Pot  <https://orcid.org/0000-0002-1146-3129>

Benjamin Misselwitz  <https://orcid.org/0000-0002-8719-5175>

## REFERENCES

- Acosta-Rodriguez, E. V., Rivino, L., Geginat, J., Jarrossay, D., Gattorno, M., Lanzavecchia, A., Sallusto, F., & Napolitani, G. (2007). Surface phenotype and antigenic specificity of human interleukin 17-producing T helper memory cells. *Nature Immunology*, *8*, 639–646. <https://doi.org/10.1038/ni1467>
- Alexander, S. P. H., Cidlowski, J. A., Kelly, E., Mathie, A., Peters, J. A., Veale, E. L., Armstrong, J. F., Faccenda, E., Harding, S. D., Pawson, A. J., Sharman, J. L., Southan, C., Davies, J. A., & GTP collaborators. (2019). The concise guide to pharmacology 2019/2020: Nuclear hormones receptors. *British Journal of Pharmacology*, *176*, S229–S246. <https://doi.org/10.1111/bph.14748>
- Alexander, S. P. H., Fabbro, D., Kelly, E., Marrison, N. V., Mathie, A., Peters, J. A., & Collaborators, GTP. (2019). The concise guide to pharmacology 2019/20: Catalytic receptors. *British Journal of Pharmacology*, *176*, S247–S296. <https://doi.org/10.1111/bph.14751>
- Alrefai, H., Muhammad, K., Rudolf, R., Pham, D. A., Klein-Hessling, S., Patra, A. K., Avots, A., Bukur, V., Sahin, U., Tenzer, S., Goebeler, M., Kerstan, A., & Serfling, E. (2016). NFATc1 supports imiquimod-induced skin inflammation by suppressing IL-10 synthesis in B cells. *Nature Communications*, *7*, 11724. <https://doi.org/10.1038/ncomms11724>
- Annunziato, F., Cosmi, L., Santarlasci, V., Maggi, L., Liotta, F., Mazzinghi, B., Parente, E., Fili, L., Ferri, S., Frosali, F., Giudizi, F., Romagnani, P., Parronchi, P., Tonelli, F., Maggi, E., & Romagnani, S. (2007). Phenotypic and functional features of human Th17 cells. *The Journal of Experimental Medicine*, *204*, 1849–1861. <https://doi.org/10.1084/jem.20070663>
- Baptista, A. P., Gola, A., Huang, Y., Milanez-Almeida, P., Torabi-Parizi, P., Urban, J. F. Jr., Shapiro, V. S., Gerner, M. Y., & Germain, R. N. (2019). The chemoattractant receptor EB12 drives intranodal naive CD4(+) T cell peripheralization to promote effective adaptive immunity. *Immunity*, *50*(1188–1201), e1186.
- Barroso, R., Martinez Munoz, L., Barrondo, S., Vega, B., Holgado, B. L., Lucas, P., Baíllo, A., Sallés, J., Rodríguez-Frade, J. M., & Mellado, M. (2012). EB12 regulates CXCL13-mediated responses by heterodimerization with CXCR5. *The FASEB Journal*, *26*, 4841–4854. <https://doi.org/10.1096/fj.12-208876>
- Biswas, S., Bryant, R. V., & Travis, S. (2019). Interfering with leukocyte trafficking in Crohn's disease. *Best Practice & Research. Clinical Gastroenterology*, *38–39*, 101617. <https://doi.org/10.1016/j.bpg.2019.05.004>
- Burke, K. E., Khalili, H., Garber, J. J., Haritunians, T., McGovern, D. P. B., Xavier, R. J., & Ananthakrishnan, A. N. (2018). Genetic markers predict primary nonresponse and durable response to anti-tumor necrosis factor therapy in ulcerative colitis. *Inflammatory Bowel Diseases*, *24*, 1840–1848. <https://doi.org/10.1093/ibd/izy083>
- Chalmin, F., Rochemont, V., Lippens, C., Clottu, A., Sailer, A. W., Merkler, D., Hugues, S., & Pot, C. (2015). Oxysterols regulate encephalitogenic CD4(+) T cell trafficking during central nervous system autoimmunity. *Journal of Autoimmunity*, *56*, 45–55. <https://doi.org/10.1016/j.jaut.2014.10.001>
- Chan, J. R., Blumenschein, W., Murphy, E., Diveu, C., Wiekowski, M., Abbondanzo, S., Lucian, L., Geissler, R., Brodie, S., Kimball, A. B., Gorman, D. M., Smith, K., de Waal Malefyt, R., Kastelein, R. A., McClanahan, T. K., & Bowman, E. P. (2006). IL-23 stimulates epidermal hyperplasia via TNF and IL-20R2-dependent mechanisms with implications for psoriasis pathogenesis. *The Journal of Experimental Medicine*, *203*, 2577–2587. <https://doi.org/10.1084/jem.20060244>
- Chiang, E. Y., Johnston, R. J., & Grogan, J. L. (2013). EB12 is a negative regulator of type I interferons in plasmacytoid and myeloid dendritic cells. *PLoS One*, *8*, e83457. <https://doi.org/10.1371/journal.pone.0083457>
- Choi, J. H., Zhong, X., McAlpine, W., Liao, T. C., Zhang, D., Fang, B., Russell, J., Ludwig, S., Nair-Gill, E., Zhang, Z., Wang, K.-W., Misawa, T., Zhan, X., Choi, M., Wang, T., Li, X., Tang, M., Sun, Q., Yu, L., ... Beutler, B. (2019). LMBR1L regulates lymphopoiesis through Wnt/beta-catenin signaling. *Science*, *364*, eaau0812. <https://doi.org/10.1126/science.aau0812>
- Chu, C., Moriyama, S., Li, Z., Zhou, L., Flamar, A. L., Klose, C. S. N., Moeller, J. B., Putzel, G. G., Withers, D. R., Sonnenberg, G. F., & Artis, D. (2018). Anti-microbial functions of group 3 innate lymphoid cells in gut-associated lymphoid tissues are regulated by G-protein-coupled receptor 183. *Cell Reports*, *23*, 3750–3758. <https://doi.org/10.1016/j.celrep.2018.05.099>
- Clottu, A. S., Mathias, A., Sailer, A. W., Schlupe, M., Seebach, J. D., Du Pasquier, R., & Pot, C. (2017). EB12 expression and function: Robust in memory lymphocytes and increased by natalizumab in multiple sclerosis. *Cell Reports*, *18*, 213–224. <https://doi.org/10.1016/j.celrep.2016.12.006>
- Cottone, M., Sapienza, C., Macaluso, F. S., & Cannizzaro, M. (2019). Psoriasis and inflammatory bowel disease. *Digestive Diseases*, *37*, 451–457. <https://doi.org/10.1159/000500116>
- Curtis, M. J., Alexander, S., Cirino, G., Docherty, J. R., George, C. H., Giembycz, M. A., Hoyer, D., Insel, P. A., Izzo, A. A., Ji, Y., MacEwan, D. J., Sobey, C. G., Stanford, S. C., Teixeira, M. M., Wonnacott, S., & Ahluwalia, A. (2018). Experimental design and analysis and their reporting II: Updated and simplified guidance for authors and peer reviewers. *British Journal of Pharmacology*, *175*, 987–993. <https://doi.org/10.1111/bph.14153>
- Di Narzo, A. F., Peters, L. A., Argmann, C., Stojmirovic, A., Perrigoue, J., Li, K., Telesco, S., Kidd, B., Walker, J., Dudley, J., Cho, J., Schadt, E. E., Kasarskis, A., Curran, M., Dobrin, R., & Hao, K. (2016). Blood and intestine eQTLs from an anti-TNF-resistant Crohn's disease cohort inform IBD genetic association loci. *Clinical and Translational Gastroenterology*, *7*, e177. <https://doi.org/10.1038/ctg.2016.34>
- Duc, D., Vigne, S., & Pot, C. (2019). Oxysterols in autoimmunity. *International Journal of Molecular Sciences*, *20*, 4522. <https://doi.org/10.3390/ijms20184522>
- Ellinghaus, D., Ellinghaus, E., Nair, R. P., Stuart, P. E., Esko, T., Metspalu, A., Debrus, S., Raelson, J. V., Tejasvi, T., Belouchi, M., West, S. L., Barker, J. N., Köks, S., Kingo, K., Balschun, T., Palmieri, O., Annese, V., Gieger, C., Wichmann, H. E., ... Franke, A. (2012). Combined analysis of genome-wide association studies for Crohn disease and psoriasis identifies seven shared susceptibility loci. *American Journal of Human Genetics*, *90*, 636–647. <https://doi.org/10.1016/j.ajhg.2012.02.020>
- Emgard, J., Kammoun, H., Garcia-Cassani, B., Chesne, J., Parigi, S. M., Jacob, J. M., Cheng, H.-W., Evren, E., Das, S., Czarnecki, P., Sleiers, N., Melo-Gonzalez, F., Kvedaraitė, E., Svensson, M., Scandella, E., Hepworth, M. R., Huber, S., Ludewig, B., Peduto, L., ... Willinger, T. (2018). Oxysterol sensing through the receptor GPR183 promotes the lymphoid-tissue-inducing function of innate lymphoid cells and colonic inflammation. *Immunity*, *48*, 120, e128–132.
- Fagagnini, S., Heinrich, H., Rossel, J. B., Biedermann, L., Frei, P., Zeitz, J., Spalinger, M., Battegay, E., Zimmerli, L., Vavricka, S. R., Rogler, G., Scharl, M., & Misselwitz, B. (2017). Risk factors for gallstones and kidney stones in a cohort of patients with inflammatory bowel diseases. *PLoS One*, *12*, e0185193. <https://doi.org/10.1371/journal.pone.0185193>
- Feagan, B. G., Rutgeerts, P., Sands, B. E., Hanauer, S., Colombel, J. F., Sandborn, W. J., Van Assche, G., Axler, J., Kim, H.-J., Danese, S., Fox, I., Milch, C., Sankoh, S., Wyant, T., Xu, J., Parikh, A., & GEMINI 1 Study

- Group. (2013). Vedolizumab as induction and maintenance therapy for ulcerative colitis. *The New England Journal of Medicine*, 369, 699–710. <https://doi.org/10.1056/NEJMoa1215734>
- Feagan, B. G., Sandborn, W. J., D'Haens, G., Lee, S. D., Allez, M., Fedorak, R. N., Seidler, U., Vermeire, S., Lawrance, I. C., Maroney, A. C., Jurgensen, C. H., Heath, A., & Chang, D. J. (2015). Randomised clinical trial: Vercirnon, an oral CCR9 antagonist, vs. placebo as induction therapy in active Crohn's disease. *Alimentary Pharmacology & Therapeutics*, 42, 1170–1181. <https://doi.org/10.1111/apt.13398>
- Fei, Y., Webb, R., Cobb, B. L., Direskeneli, H., Saruhan-Direskeneli, G., & Sawalha, A. H. (2009). Identification of novel genetic susceptibility loci for Behcet's disease using a genome-wide association study. *Arthritis Research & Therapy*, 11, R66. <https://doi.org/10.1186/ar2695>
- Gatto, D., Paus, D., Basten, A., Mackay, C. R., & Brink, R. (2009). Guidance of B cells by the orphan G protein-coupled receptor EB12 shapes humoral immune responses. *Immunity*, 31, 259–269. <https://doi.org/10.1016/j.immuni.2009.06.016>
- Gatto, D., Wood, K., Caminschi, I., Murphy-Durland, D., Schofield, P., Christ, D., Karupiah, G., & Brink, R. (2013). The chemotactic receptor EB12 regulates the homeostasis, localization and immunological function of splenic dendritic cells. *Nature Immunology*, 14, 446–453. <https://doi.org/10.1038/ni.2555>
- Geherin, S. A., Fintushel, S. R., Lee, M. H., Wilson, R. P., Patel, R. T., Alt, C., Young, A. J., Hay, J. B., & Debes, G. F. (2012). The skin, a novel niche for recirculating B cells. *Journal of Immunology*, 188, 6027–6035. <https://doi.org/10.4049/jimmunol.1102639>
- Greco, A., De Virgilio, A., Ralli, M., Ciofalo, A., Mancini, P., Attanasio, G., de Vincentiis, M., & Lambiase, A. (2018). Behcet's disease: New insights into pathophysiology, clinical features and treatment options. *Autoimmunity Reviews*, 17, 567–575. <https://doi.org/10.1016/j.autrev.2017.12.006>
- Groer, C. E., Schmid, C. L., Jaeger, A. M., & Bohn, L. M. (2011). Agonist-directed interactions with specific beta-arrestins determine mu-opioid receptor trafficking, ubiquitination, and dephosphorylation. *The Journal of Biological Chemistry*, 286, 31731–31741. <https://doi.org/10.1074/jbc.M111.248310>
- Guidelli, G. M., Fioravanti, A., Rubegni, P., & Feci, L. (2013). Induced psoriasis after rituximab therapy for rheumatoid arthritis: A case report and review of the literature. *Rheumatology International*, 33, 2927–2930. <https://doi.org/10.1007/s00296-012-2581-3>
- Guo, R., Zhang, T., Meng, X., Lin, Z., Lin, J., Gong, Y., Liu, X., Yu, Y., Zhao, G., Ding, X., Chen, X., Lu, L., & Chen, X. (2019). Lymphocyte mass cytometry identifies a CD3-CD4+ cell subset with a potential role in psoriasis. *JCI Insight*, 4, e125306. <https://doi.org/10.1172/jci.insight.125306>
- Hannedouche, S., Zhang, J., Yi, T., Shen, W., Nguyen, D., Pereira, J. P., Guerini, D., Baumgarten, B. U., Roggo, S., Wen, B., Knochenmuss, R., Noël, S., Gessier, F., Kelly, L. M., Vanek, M., Laurent, S., Preuss, I., Miault, C., Christen, I., ... Sailer, A. W. (2011). Oxysterols direct immune cell migration via EB12. *Nature*, 475, 524–527. <https://doi.org/10.1038/nature10280>
- Harding, S. D., Sharman, J. L., Faccenda, E., Southan, C., Pawson, A. J., Ireland, S., Gray, A. J. G., Bruce, L., Alexander, S. P. H., Anderton, S., Bryant, C., Davenport, A. P., Doerig, C., Fabbro, D., Levi-Schaffer, F., Spedding, M., Davies, J. A., & NC-IUPHAR. (2018). The IUPHAR/BPS guide to pharmacology in 2018: Updates and expansion to encompass the new guide to immunopharmacology. *Nucleic Acids Research*, 46, D1091–D1106. <https://doi.org/10.1093/nar/gkx1121>
- Harvey, R. F., & Bradshaw, J. M. (1980). A simple index of Crohn's-disease activity. *Lancet*, 1, 514.
- Hayashi, M., Yanaba, K., Umezawa, Y., Yoshihara, Y., Kikuchi, S., Ishiui, Y., Saeki, H., & Nakagawa, H. (2016). IL-10-producing regulatory B cells are decreased in patients with psoriasis. *Journal of Dermatological Science*, 81, 93–100. <https://doi.org/10.1016/j.jdermsci.2015.11.003>
- Homey, B., Dieu-Nosjean, M. C., Wiesenborn, A., Massacrier, C., Pin, J. J., Oldham, E., Catron, D., Buchanan, M. E., Müller, A., deWaal Malefyt, R., Deng, G., Orozco, R., Ruzicka, T., Lehmann, P., Lebecque, S., Caux, C., & Zlotnik, A. (2000). Up-regulation of macrophage inflammatory protein-3 alpha/CCL20 and CC chemokine receptor 6 in psoriasis. *Journal of Immunology*, 164, 6621–6632. <https://doi.org/10.4049/jimmunol.164.12.6621>
- Hou, S., Shu, Q., Jiang, Z., Chen, Y., Li, F., Chen, F., Li, F., Chen, F., Kijlstra, A., & Yang, P. (2012). Replication study confirms the association between UBAC2 and Behcet's disease in two independent Chinese sets of patients and controls. *Arthritis Research & Therapy*, 14, R70. <https://doi.org/10.1186/ar3789>
- Jostins, L., Ripke, S., Weersma, R. K., Duerr, R. H., McGovern, D. P., Hui, K. Y., Lee, J. C., Schumm, L. P., Sharma, Y., Anderson, C. A., Essers, J., Mitrovic, M., Ning, K., Cleynen, I., Theatre, E., Spain, S. L., Raychaudhuri, S., Goyette, P., Wei, Z., ... Cho, J. H. (2012). Host-microbe interactions have shaped the genetic architecture of inflammatory bowel disease. *Nature*, 491, 119–124. <https://doi.org/10.1038/nature11582>
- Khor, B., Gardet, A., & Xavier, R. J. (2011). Genetics and pathogenesis of inflammatory bowel disease. *Nature*, 474, 307–317. <https://doi.org/10.1038/nature10209>
- Kim, T. G., Jee, H., Fuentes-Duculan, J., Wu, W. H., Byamba, D., Kim, D. S., Kim, D.-Y., Lew, D.-H., Yang, W.-I., Krueger, J. G., & Lee, M. G. (2014). Dermal clusters of mature dendritic cells and T cells are associated with the CCL20/CCR6 chemokine system in chronic psoriasis. *The Journal of Investigative Dermatology*, 134, 1462–1465. <https://doi.org/10.1038/jid.2013.534>
- Koga, A., Kajihara, I., Yamada, S., Makino, K., Ichihara, A., Aoi, J., Makino, T., Fukushima, S., Jinnin, M., & Ihn, H. (2016). Enhanced CCR9 expression levels in psoriatic skin are associated with poor clinical outcome to infliximab treatment. *The Journal of Dermatology*, 43, 522–525. <https://doi.org/10.1111/1346-8138.13178>
- Lang, B. M., Biedermann, L., van Haaften, W. T., de Valliere, C., Schuurmans, M., Begre, S., Zeitz, J., Scharl, M., Turina, M., Greuter, T., Schreiner, P., Heinrich, H., Kuntzen, T., Vavricka, S. R., Rogler, G., Beerwinkel, N., Misselwitz, B., & Swiss IBD Cohort Study Group. (2018). Genetic polymorphisms associated with smoking behaviour predict the risk of surgery in patients with Crohn's disease. *Alimentary Pharmacology & Therapeutics*, 47, 55–66. <https://doi.org/10.1111/apt.14378>
- Larsen, S., Bendtzen, K., & Nielsen, O. H. (2010). Extraintestinal manifestations of inflammatory bowel disease: Epidemiology, diagnosis, and management. *Annals of Medicine*, 42, 97–114. <https://doi.org/10.3109/07853890903559724>
- Leclair, H. M., Dubois, S. M., Azzi, S., Dwyer, J., Bidere, N., & Gavard, J. (2014). Control of CXCR2 activity through its ubiquitination on K327 residue. *BMC Cell Biology*, 15, 38. <https://doi.org/10.1186/s12860-014-0038-0>
- Lee, E., Trepicchio, W. L., Oestreicher, J. L., Pittman, D., Wang, F., Chamian, F., Dhodapkar, M., & Krueger, J. G. (2004). Increased expression of interleukin 23 p19 and p40 in lesional skin of patients with psoriasis vulgaris. *The Journal of Experimental Medicine*, 199, 125–130. <https://doi.org/10.1084/jem.20030451>
- Li, H., Armando, I., Yu, P., Escano, C., Mueller, S. C., Asico, L., Pascua, A., Lu, Q., Wang, X., Villar, V. A. M., Jones, J. E., Wang, Z., Periasamy, A., Lau, Y.-S., Soares-da-Silva, P., Creswell, K., Guillemette, G., Sibley, D. R., Eisner, G., ... Jose, P. A. (2008). Dopamine 5 receptor mediates Ang II type 1 receptor degradation via a ubiquitin-proteasome pathway in mice and human cells. *The Journal of Clinical Investigation*, 118, 2180–2189. <https://doi.org/10.1172/JCI33637>
- Li, J., Lu, E., Yi, T., & Cyster, J. G. (2016). EB12 augments Tfh cell fate by promoting interaction with IL-2-queching dendritic cells. *Nature*, 533, 110–114. <https://doi.org/10.1038/nature17947>

- Li, W. Q., Han, J. L., Chan, A. T., & Qureshi, A. A. (2013). Psoriasis, psoriatic arthritis and increased risk of incident Crohn's disease in US women. *Annals of the Rheumatic Diseases*, 72, 1200–1205. <https://doi.org/10.1136/annrheumdis-2012-202143>
- Liu, C., Yang, X. V., Wu, J., Kuei, C., Mani, N. S., Zhang, L., Yu, J., Sutton, S. W., Qin, N., Banie, H., Karlsson, L., Sun, S., & Lovenberg, T. W. (2011). Oxysterols direct B-cell migration through EBI2. *Nature*, 475, 519–523. <https://doi.org/10.1038/nature10226>
- Liu, J. Z., van Sommeren, S., Huang, H., Ng, S. C., Alberts, R., Takahashi, A., Ripke, S., Lee, J. C., Jostins, L., Shah, T., Abedian, S., Cheon, J. H., Cho, J., Dayani, N. E., Franke, L., Fuyuno, Y., Hart, A., Juyal, R. C., Juyal, G., ... Weersma, R. K. (2015). Association analyses identify 38 susceptibility loci for inflammatory bowel disease and highlight shared genetic risk across populations. *Nature Genetics*, 47, 979–986. <https://doi.org/10.1038/ng.3359>
- Lowes, M. A., Kikuchi, T., Fuentes-Duculan, J., Cardinale, I., Zaba, L. C., Haider, A. S., Bowman, E. P., & Krueger, J. G. (2008). Psoriasis vulgaris lesions contain discrete populations of Th1 and Th17 T cells. *The Journal of Investigative Dermatology*, 128, 1207–1211. <https://doi.org/10.1038/sj.jid.5701213>
- Lu, Dang, E. V., McDonald, J. G., & Cyster, J. G. (2017). Distinct oxysterol requirements for positioning naive and activated dendritic cells in the spleen. *Science Immunology*, 2, eaal5237.
- Lund, E. G., Kerr, T. A., Sakai, J., Li, W. P., & Russell, D. W. (1998). cDNA cloning of mouse and human cholesterol 25-hydroxylases, polytopic membrane proteins that synthesize a potent oxysterol regulator of lipid metabolism. *The Journal of Biological Chemistry*, 273, 34316–34327. <https://doi.org/10.1074/jbc.273.51.34316>
- Maaser, C., Sturm, A., Vavricka, S. R., Kucharzik, T., Fiorino, G., Annese, V., Calabrese, E., Baumgart, D. C., Bettenworth, D., Nunes, P. B., Burisch, J., Castiglione, F., Eliakim, R., Ellul, P., González-Lama, Y., Gordon, H., Halligan, S., Katsanos, K., Kopylov, U., ... European Crohn's and Colitis Organisation [ECCO] and the European Society of Gastrointestinal and Abdominal Radiology [ESGAR]. (2019). ECCO-ESGAR guideline for diagnostic assessment in IBD part 1: Initial diagnosis, monitoring of known IBD, detection of complications. *Journal of Crohn's & Colitis*, 13, 144–164. <https://doi.org/10.1093/ecco-jcc/jjy113>
- Maloy, K. J., & Powrie, F. (2011). Intestinal homeostasis and its breakdown in inflammatory bowel disease. *Nature*, 474, 298–306. <https://doi.org/10.1038/nature10208>
- Martin, C., Bean, R., Rose, K., Habib, F., & Seckl, J. (2001). cyp7b1 catalyses the 7 $\alpha$ -hydroxylation of dehydroepiandrosterone and 25-hydroxy cholesterol in rat prostate. *The Biochemical Journal*, 355, 509–515. <https://doi.org/10.1042/bj3550509>
- Mayer, L., Sandborn, W. J., Stepanov, Y., Geboes, K., Hardi, R., Yellin, M., Tao, X., Xu, L. A., Salter-Cid, L., Gujrathi, S., Aranda, R., & Luo, A. Y. (2014). Anti-IP-10 antibody (BMS-936557) for ulcerative colitis: A phase II randomised study. *Gut*, 63, 442–450. <https://doi.org/10.1136/gutjnl-2012-303424>
- Miles, A., Liaskou, E., Eksteen, B., Lalor, P. F., & Adams, D. H. (2008). CCL25 and CCL28 promote  $\alpha 4 \beta 7$ -integrin-dependent adhesion of lymphocytes to MAdCAM-1 under shear flow. *American Journal of Physiology. Gastrointestinal and Liver Physiology*, 294, G1257–G1267. <https://doi.org/10.1152/ajpgi.00266.2007>
- Misselwitz, B., Wyss, A., Raselli, T., Cerovic, V., Sailer, A. W., Krupka, N., Ruiz, F., Pot, C., & Pabst, O. (2020). The oxysterol receptor GPR183 in inflammatory bowel diseases. *British Journal of Pharmacology*.
- Olzmann, J. A., Richter, C. M., & Kopito, R. R. (2013). Spatial regulation of UBXD8 and p97/VCP controls ATGL-mediated lipid droplet turnover. *Proceedings of the National Academy of Sciences of the United States of America*, 110, 1345–1350. <https://doi.org/10.1073/pnas.1213738110>
- Ostvik, Granlund, A. V., Bugge, M., Nilsen, N. J., Torp, S. H., Waldum, H. L., Damås, J. K., Espevik, T., & Sandvik, A. K. (2013). Enhanced expression of CXCL10 in inflammatory bowel disease: Potential role of mucosal toll-like receptor 3 stimulation. *Inflammatory Bowel Diseases*, 19, 265–274. <https://doi.org/10.1002/ibd.23034>
- Pene, J., Chevalier, S., Preisser, L., Venereau, E., Guilleux, M. H., Ghannam, S., Molès, J.-P., Danger, Y., Ravon, E., Lesaux, S., Yssel, H., & Gascan, H. (2008). Chronically inflamed human tissues are infiltrated by highly differentiated Th17 lymphocytes. *Journal of Immunology*, 180, 7423–7430. <https://doi.org/10.4049/jimmunol.180.11.7423>
- Pereira, J. P., Kelly, L. M., Xu, Y., & Cyster, J. G. (2009). EBI2 mediates B cell segregation between the outer and centre follicle. *Nature*, 460, 1122–1126. <https://doi.org/10.1038/nature08226>
- Perez-Jeldres, T., Tyler, C. J., Boyer, J. D., Karuppuachamy, T., Bamias, G., Dulai, P. S., Boland, B. S., Sandborn, W. J., Patel, D. R., & Rivera-Nieves, J. (2019). Cell trafficking interference in inflammatory bowel disease: Therapeutic interventions based on basic pathogenesis concepts. *Inflammatory Bowel Diseases*, 25, 270–282. <https://doi.org/10.1093/ibd/izy269>
- Pittet, V., Juillerat, P., Mottet, C., Felley, C., Ballabeni, P., Burnand, B., Michetti, P., Vader, J.-P., & the Swiss IBD Cohort Study Group. (2009). Cohort profile: The Swiss inflammatory bowel disease cohort study (SIBDCS). *International Journal of Epidemiology*, 38, 922–931. <https://doi.org/10.1093/ije/dyn180>
- Pittet, V., Michetti, P., Mueller, C., Braegger, C. P., von Kanel, R., Schoepfer, A., Macpherson, A. J., & Rogler, G. (2019). Cohort profile update: The Swiss inflammatory bowel disease cohort study (SIBDCS). *International Journal of Epidemiology*, 48, 385–386f. <https://doi.org/10.1093/ije/dyy298>
- Rajagopal, S., & Shenoy, S. K. (2018). GPCR desensitization: Acute and prolonged phases. *Cellular Signalling*, 41, 9–16. <https://doi.org/10.1016/j.cellsig.2017.01.024>
- Raselli, T., Hearn, T., Wyss, A., Atrott, K., Peter, A., Frey-Wagner, I., Spalinger, M. R., Maggio, E. M., Sailer, A. W., Schmitt, J., Schreiner, P., Moncsek, A., Mertens, J., Scharl, M., Griffiths, W. J., Bueter, M., Geier, A., Rogler, G., Wang, Y., & Misselwitz, B. (2019). Elevated oxysterol levels in human and mouse livers reflect nonalcoholic steatohepatitis. *Journal of Lipid Research*, 60, 1270–1283. <https://doi.org/10.1194/jlr.M093229>
- Raselli, T., Wyss, A., Gonzalez Alvarado, M. N., Weder, B., Mamie, C., Spalinger, M. R., Van Haaften, W. T., Dijkstra, G., Sailer, A. W., Silva, P. H. I., Wagner, C. A., Tosevski, V., Leibl, S., Scharl, M., Rogler, G., Hausmann, M., & Misselwitz, B. (2019). The oxysterol synthesising enzyme CH25H contributes to the development of intestinal fibrosis. *Journal of Crohn's & Colitis*, 13, 1186–1200. <https://doi.org/10.1093/ecco-jcc/jjz039>
- Rutkowska, A., Preuss, I., Gessier, F., Sailer, A. W., & Dev, K. K. (2015). EBI2 regulates intracellular signaling and migration in human astrocyte. *Glia*, 63, 341–351. <https://doi.org/10.1002/glia.22757>
- Saini, V., Marchese, A., & Majetschak, M. (2010). CXC chemokine receptor 4 is a cell surface receptor for extracellular ubiquitin. *The Journal of Biological Chemistry*, 285, 15566–15576. <https://doi.org/10.1074/jbc.M110.103408>
- Sallusto, F. (2016). Heterogeneity of human CD4(+) T cells against microbes. *Annual Review of Immunology*, 34, 317–334. <https://doi.org/10.1146/annurev-immunol-032414-112056>
- Sandborn, W. J., Feagan, B. G., Rutgeerts, P., Hanauer, S., Colombel, J. F., Sands, B. E., Lukas, M., Fedorak, R. N., Lee, S., Bressler, B., Fox, I., Rosario, M., Sankoh, S., Xu, J., Stephens, K., Milch, C., Parikh, A., GEM-INI 2 Study Group, & Parikh, A. (2013). Vedolizumab as induction and maintenance therapy for Crohn's disease. *The New England Journal of Medicine*, 369, 711–721. <https://doi.org/10.1056/NEJMoa1215739>
- Sawalha, A. H., Hughes, T., Nadig, A., Yilmaz, V., Aksu, K., Keser, G., Cefle, A., Yazıcı, A., Ergen, A., Alarcón-Riquelme, M. E., Salvarani, C., Casali, B., Direskeneli, H., & Saruhan-Direskeneli, G. (2011). A putative functional variant within the UBAC2 gene is associated with increased risk of Behcet's disease. *Arthritis and Rheumatism*, 63, 3607–3612. <https://doi.org/10.1002/art.30604>

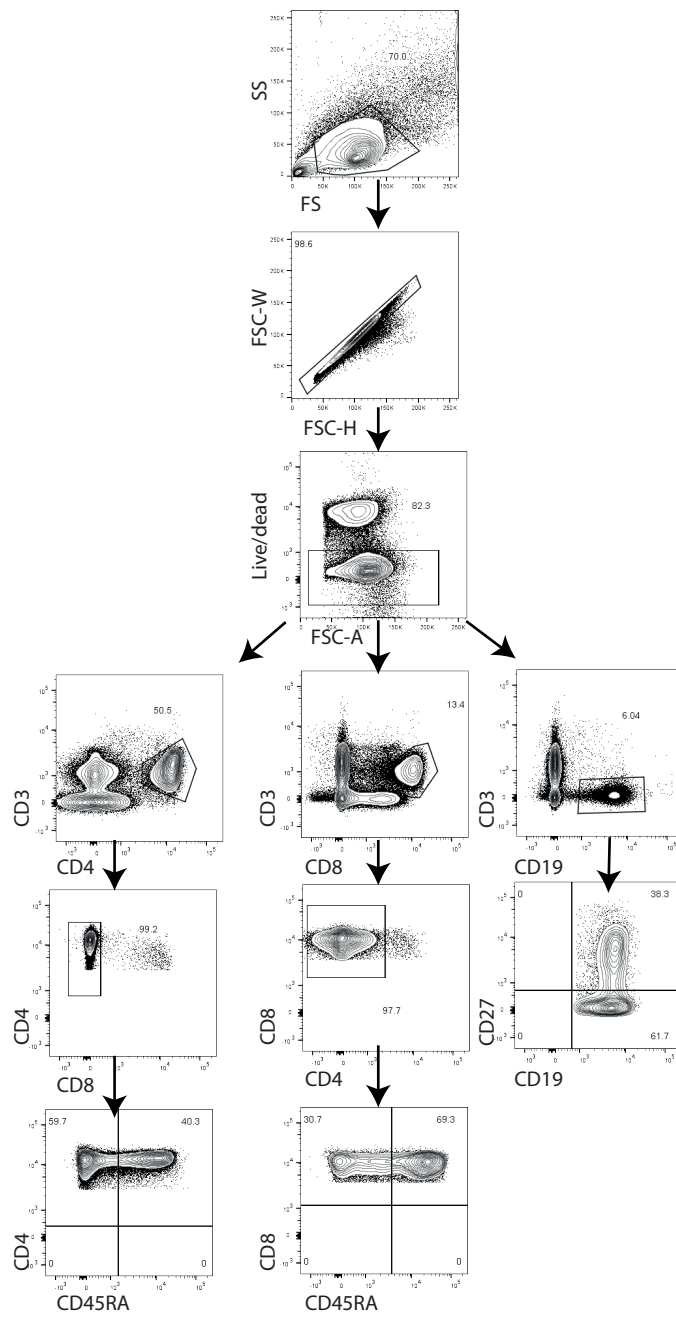
- Silverberg, M. S., Satsangi, J., Ahmad, T., Arnott, I. D., Bernstein, C. N., Brant, S. R., Caprilli, R., Colombel, J.-F., Gasche, C., Geboes, K., Jewell, D. P., Karban, A., Loftus, E. V. Jr., Peña, A. S., Riddell, R. H., Sachar, D. B., Schreiber, S., Steinhart, A. H., Targan, S. R., ... Warren, B. F. (2005). Toward an integrated clinical, molecular and serological classification of inflammatory bowel disease: Report of a working party of the 2005 Montreal World Congress of Gastroenterology. *Canadian Journal of Gastroenterology*, *19*(Suppl A), 5A–36A.
- Skieterska, K., Rondou, P., & Van Craenenbroeck, K. (2017). Regulation of G protein-coupled receptors by ubiquitination. *International Journal of Molecular Sciences*, *18*, 923.
- Skovdahl, H. K., Granlund, A., Ostvik, A. E., Bruland, T., Bakke, I., Torp, S. H., Damås, J. K., & Sandvik, A. K. (2015). Expression of CCL20 and its corresponding receptor CCR6 is enhanced in active inflammatory bowel disease, and TLR3 mediates CCL20 expression in colonic epithelial cells. *PLoS One*, *10*, e0141710. <https://doi.org/10.1371/journal.pone.0141710>
- Storm, N., Darnhofer-Patel, B., van den Boom, D., & Rodi, C. P. (2003). MALDI-TOF mass spectrometry-based SNP genotyping. *Methods in Molecular Biology*, *212*, 241–262. <https://doi.org/10.1385/1-59259-327-5:241>
- Sturm, A., Maaser, C., Calabrese, E., Annese, V., Fiorino, G., Kucharzik, T., Vavricka, S. R., Verstockt, B., van Rheeën, P., Tolan, D., Taylor, S. A., Rimola, J., Rieder, F., Limdi, J. K., Laghi, A., Krustiņš, E., Kotze, P. G., Kopylov, U., Katsanos, K., ... European Crohn's and Colitis Organisation [ECCO] and the European Society of Gastrointestinal and Abdominal Radiology [ESGAR]. (2019). ECCO-ESGAR guideline for diagnostic assessment in IBD part 2: IBD scores and general principles and technical aspects. *Journal of Crohn's & Colitis*, *13*, 273–284. <https://doi.org/10.1093/ecco-jcc/jjy114>
- Suan, D., Nguyen, A., Moran, I., Bourne, K., Hermes, J. R., Arshi, M., Hampton, H. R., Tomura, M., Miwa, Y., Kelleher, A. D., Kaplan, W., Deenick, E. K., Tangye, S. G., Brink, R., Chtanova, T., & Phan, T. G. (2015). T follicular helper cells have distinct modes of migration and molecular signatures in naive and memory immune responses. *Immunity*, *42*, 704–718. <https://doi.org/10.1016/j.immuni.2015.03.002>
- Trivedi, P. J., & Adams, D. H. (2018). Chemokines and chemokine receptors as therapeutic targets in inflammatory bowel disease; pitfalls and promise. *Journal of Crohn's & Colitis*, *12*, S641–S652. <https://doi.org/10.1093/ecco-jcc/jjy130>
- Trivedi, P. J., Bruns, T., Ward, S., Mai, M., Schmidt, C., Hirschfield, G. M., Weston, C. J., & Adams, D. H. (2016). Intestinal CCL25 expression is increased in colitis and correlates with inflammatory activity. *Journal of Autoimmunity*, *68*, 98–104. <https://doi.org/10.1016/j.jaut.2016.01.001>
- Tsoi, L. C., Stuart, P. E., Tian, C., Gudjonsson, J. E., Das, S., Zawistowski, M., Ellinghaus, E., Barker, J. N., Chandran, V., Dand, N., Duffin, K. C., Enerbäck, C., Esko, T., Franke, A., Gladman, D. D., Hoffmann, P., Kingo, K., Köks, S., Krueger, G. G., ... Elder, J. T. (2017). Large scale meta-analysis characterizes genetic architecture for common psoriasis associated variants. *Nature Communications*, *8*, 15382. <https://doi.org/10.1038/ncomms15382>
- Ueno, A., Jeffery, L., Kobayashi, T., Hibi, T., Ghosh, S., & Jijon, H. (2018). Th17 plasticity and its relevance to inflammatory bowel disease. *Journal of Autoimmunity*, *87*, 38–49. <https://doi.org/10.1016/j.jaut.2017.12.004>
- Uhlig, H. H., & Powrie, F. (2018). Translating immunology into therapeutic concepts for inflammatory bowel disease. *Annual Review of Immunology*, *36*, 755–781. <https://doi.org/10.1146/annurev-immunol-042617-053055>
- Verkaar, F., van Offenbeek, J., van der Lee, M. M. C., van Lith, L., Watts, A. O., Rops, A., Aguilar, D. C., Ziarek, J. J., van der Vlag, J., Handel, T. M., Volkman, B. F., Proudfoot, A. E. I., Vischer, H. F., Zaman, G. J. R., & Smit, M. J. (2014). Chemokine cooperativity is caused by competitive glycosaminoglycan binding. *Journal of Immunology*, *192*, 3908–3914. <https://doi.org/10.4049/jimmunol.1302159>
- Wanke, F., Moos, S., Croxford, A. L., Heinen, A. P., Graf, S., Kalt, B., Tischner, D., Zhang, J., Christen, I., Bruttger, J., Yogeve, N., Tang, Y., Zayoud, M., Israel, N., Karram, K., Reißig, S., Lacher, S. M., Reichhold, C., Mufazalov, I. A., ... Kurschus, F. C. (2017). EB12 is highly expressed in multiple sclerosis lesions and promotes early CNS migration of Encephalitogenic CD4 T cells. *Cell Reports*, *18*, 1270–1284. <https://doi.org/10.1016/j.celrep.2017.01.020>
- Willinger, T. (2019). Oxysterols in intestinal immunity and inflammation. *Journal of Internal Medicine*, *285*, 367–380. <https://doi.org/10.1111/joim.12855>
- Wu, J., McDuffie, J. E., Song, J., Harris, M. C., Raymond, H., Chen, Y., Nguyen, L., Nguyen, S., Kanerva, J., McAllister, H. M., Deng, X., Mani, N., Liu, C., & Sun, S. (2017). LC/MS/MS profiling of tissue oxysterols and its application in dextran sodium Sulphate induced mouse colitis models. *Current Topics in Medicinal Chemistry*, *17*, 2781–2790. <https://doi.org/10.2174/1568026617666170713165519>
- Wyss, A., Raselli, T., Perkins, N., Ruiz, F., Schmelczer, G., Klinke, G., Moncsek, A., Roth, R., Spalinger, M. R., Hering, L., Atrott, K., Lang, S., Frey-Wagner, I., Mertens, J. C., Scharl, M., Sailer, A. W., Pabst, O., Hersberger, M., Pot, C., ... Misselwitz, B. (2019). The EB12-oxysterol axis promotes the development of intestinal lymphoid structures and colitis. *Mucosal Immunology*, *12*, 733–745. <https://doi.org/10.1038/s41385-019-0140-x>
- Yamazoe, K., Meguro, A., Takeuchi, M., Shibuya, E., Ohno, S., & Mizuki, N. (2017). Comprehensive analysis of the association between UBAC2 polymorphisms and Behcet's disease in a Japanese population. *Scientific Reports*, *7*, 742. <https://doi.org/10.1038/s41598-017-00877-3>
- Yanaba, K., Kamata, M., Ishiura, N., Shibata, S., Asano, Y., Tada, Y., Sugaya, M., Kadono, T., Tedder, T. F., & Sato, S. (2013). Regulatory B cells suppress imiquimod-induced, psoriasis-like skin inflammation. *Journal of Leukocyte Biology*, *94*, 563–573. <https://doi.org/10.1189/jlb.1112562>
- Yi, T., & Cyster, J. G. (2013). EB12-mediated bridging channel positioning supports splenic dendritic cell homeostasis and particulate antigen capture. *eLife*, *2*, e00757. <https://doi.org/10.7554/eLife.00757>
- Yi, T., Wang, X., Kelly, L. M., An, J., Xu, Y., Sailer, A. W., Gustafsson, J.-A., Russell, D. W., & Cyster, J. G. (2012). Oxysterol gradient generation by lymphoid stromal cells guides activated B cell movement during humoral responses. *Immunity*, *37*, 535–548. <https://doi.org/10.1016/j.immuni.2012.06.015>
- Zhang, P., He, Q., Chen, D., Liu, W., Wang, L., Zhang, C., Ma, D., Li, W., Liu, B., & Liu, F. (2015). G protein-coupled receptor 183 facilitates endothelial-to-hematopoietic transition via Notch1 inhibition. *Cell Research*, *25*, 1093–1107. <https://doi.org/10.1038/cr.2015.109>

## SUPPORTING INFORMATION

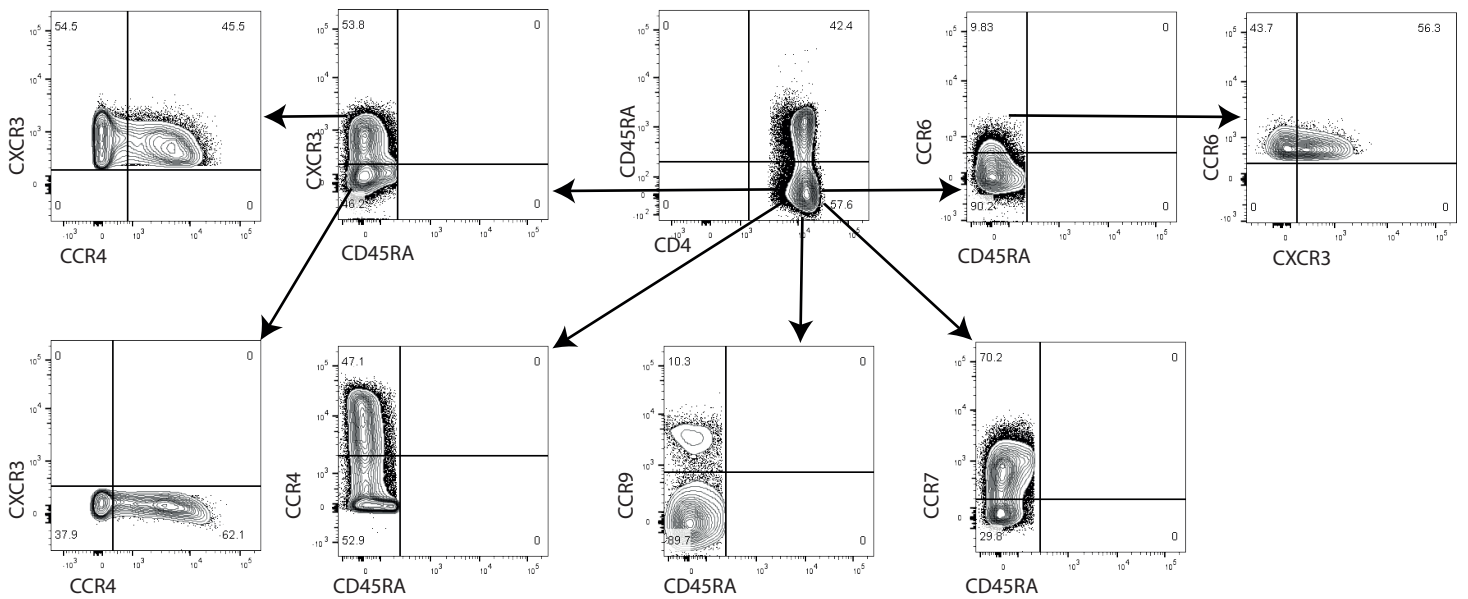
Additional supporting information may be found online in the Supporting Information section at the end of this article.

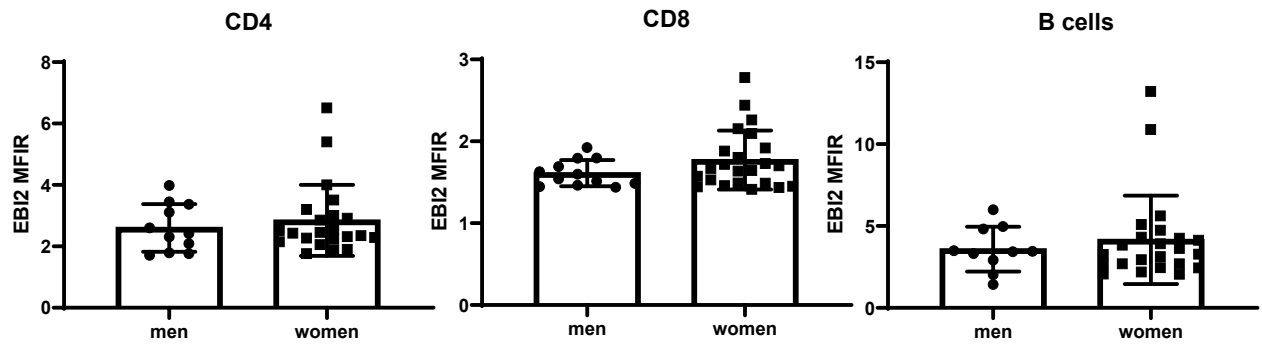
**How to cite this article:** Ruiz F, Wyss A, Rossel J-B, et al. A single nucleotide polymorphism in the gene for GPR183 increases its surface expression on blood lymphocytes of patients with inflammatory bowel disease. *Br J Pharmacol*. 2021;178:3157–3175. <https://doi.org/10.1111/bph.15395>

A

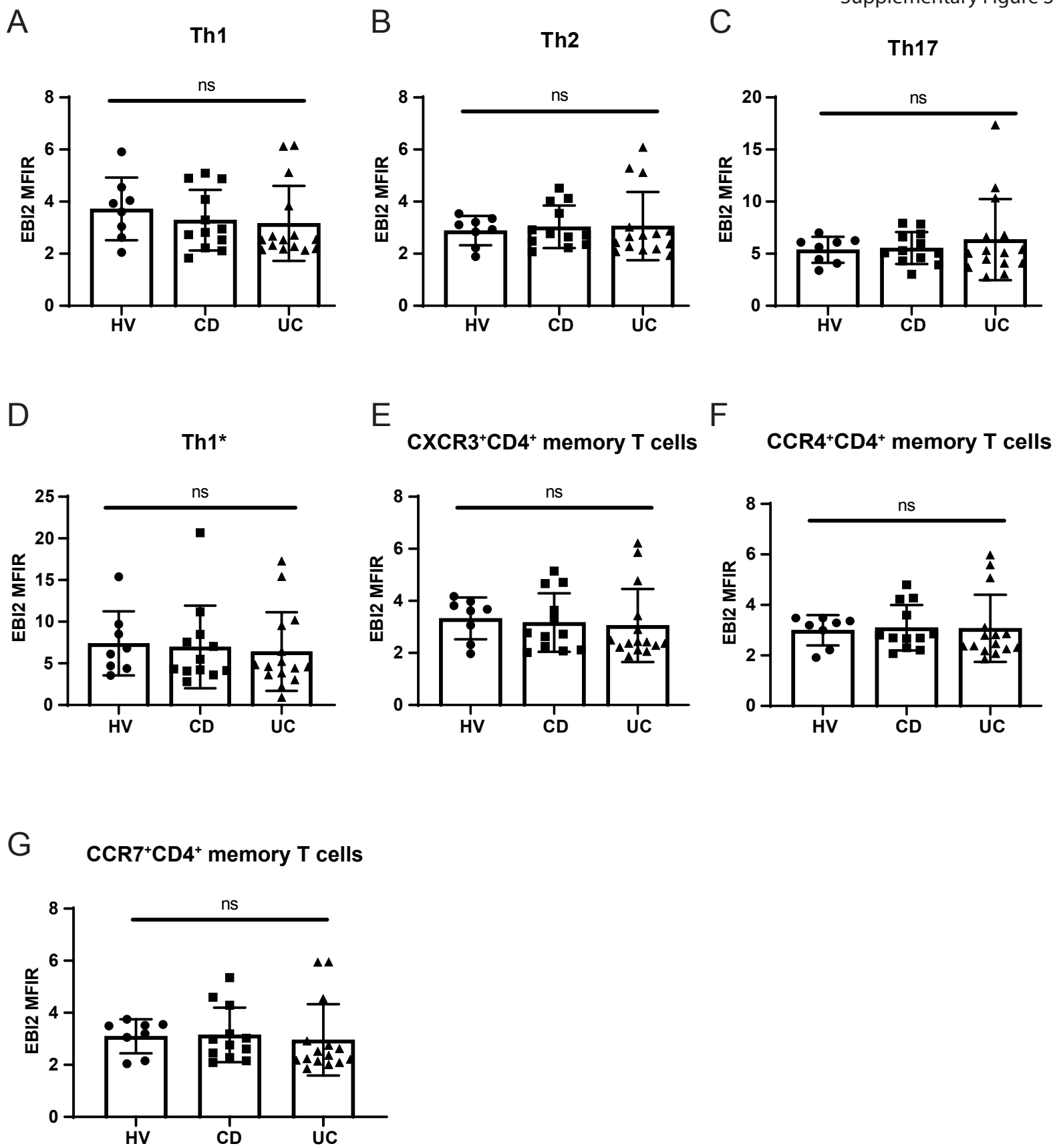


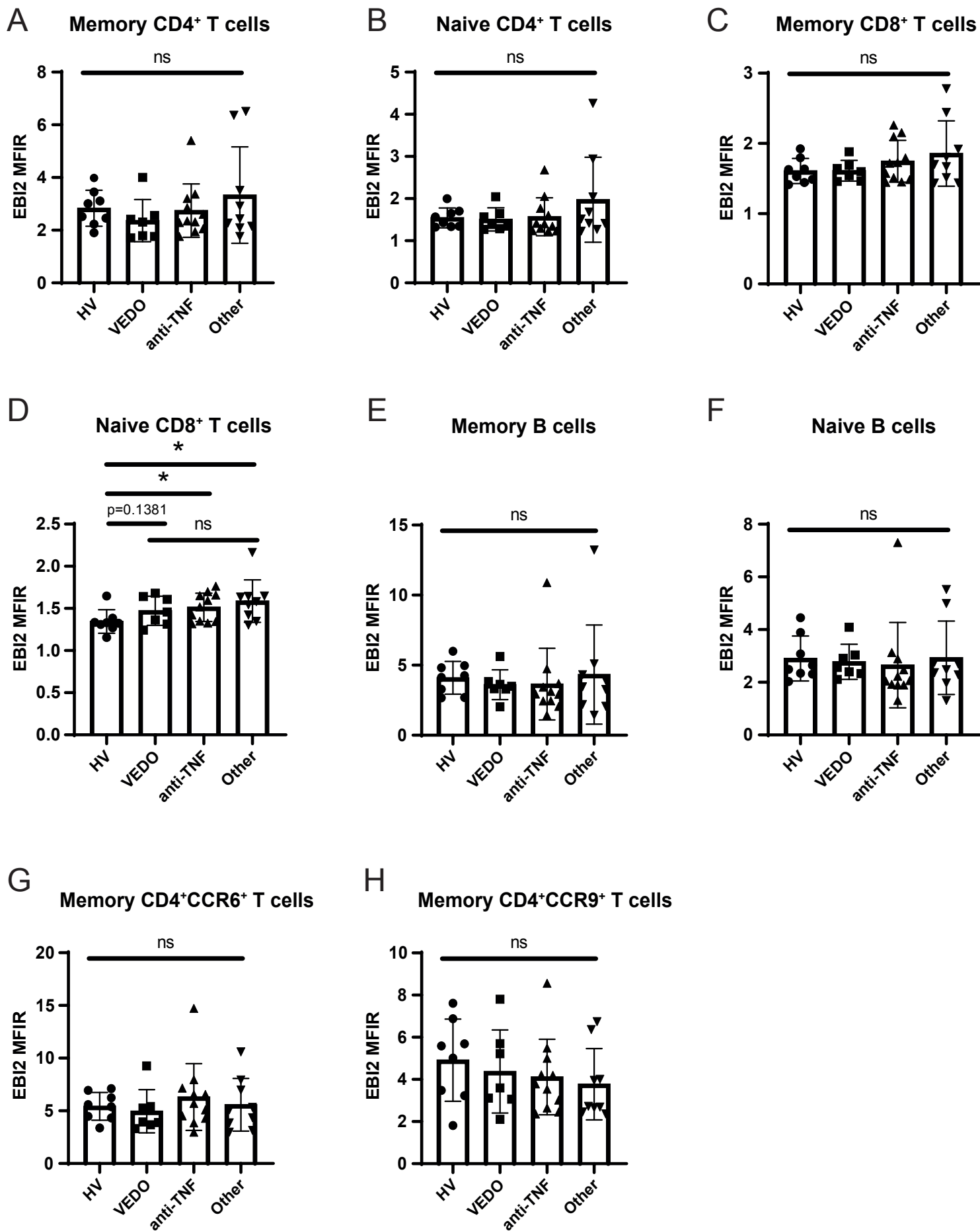
B



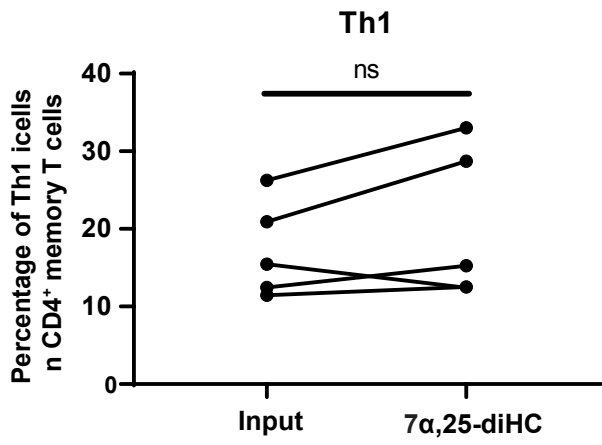




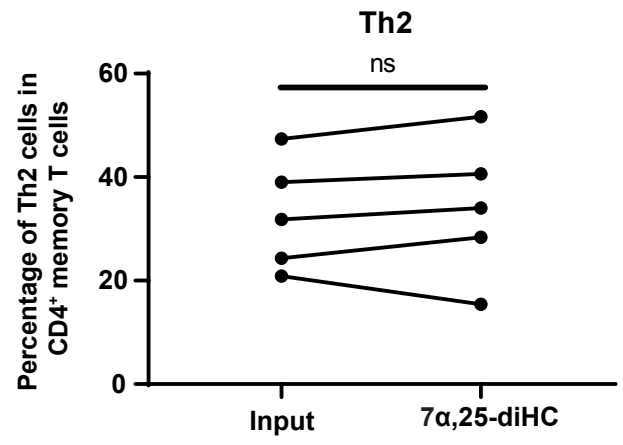




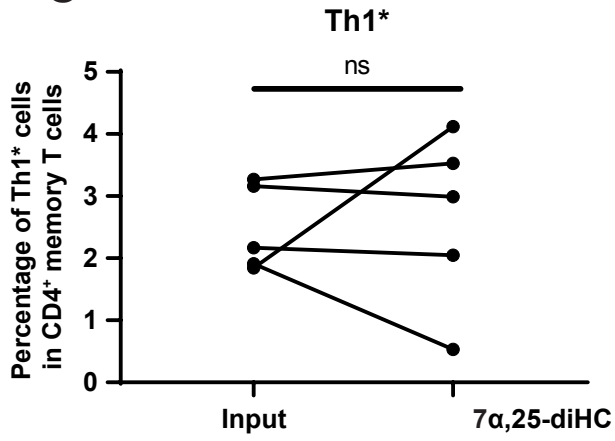
A

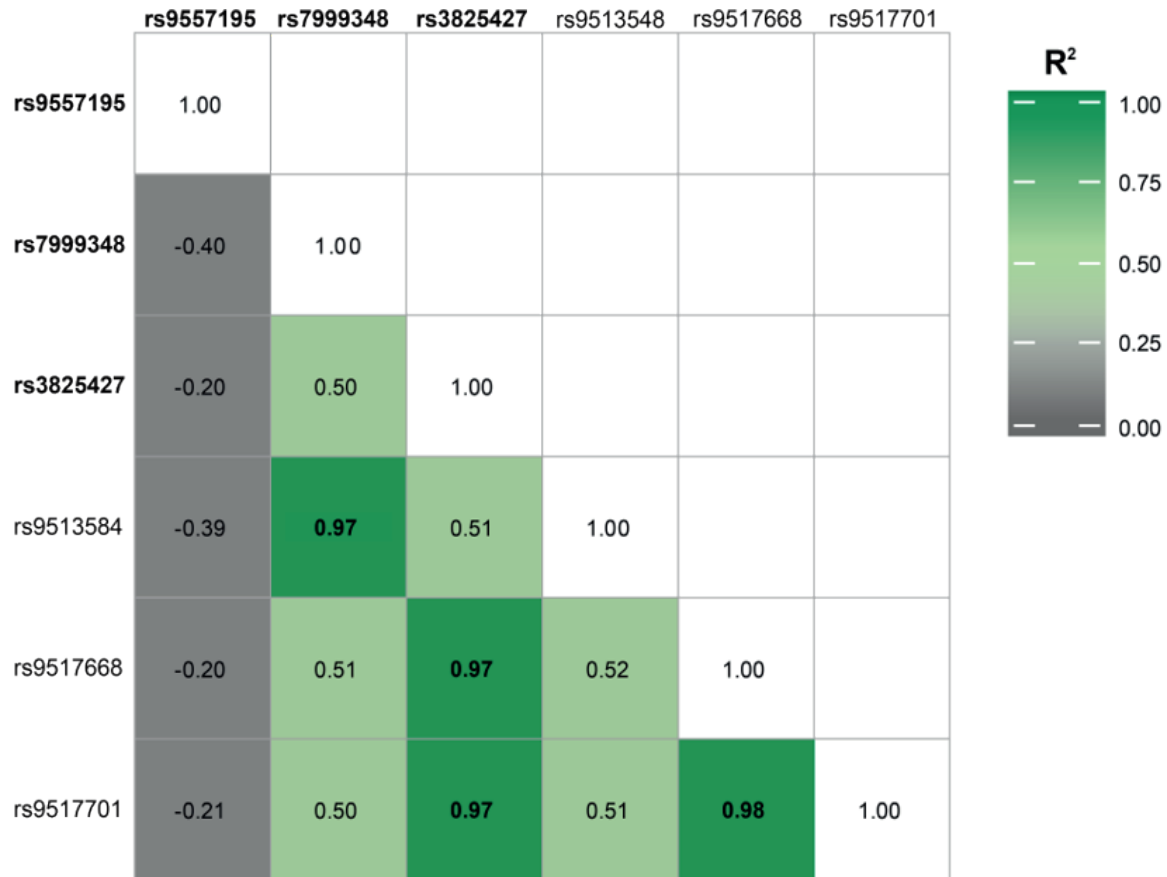


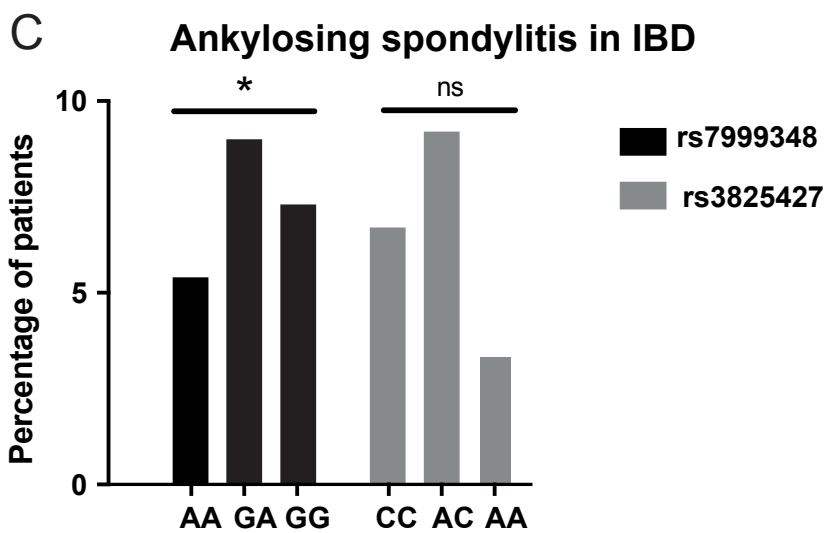
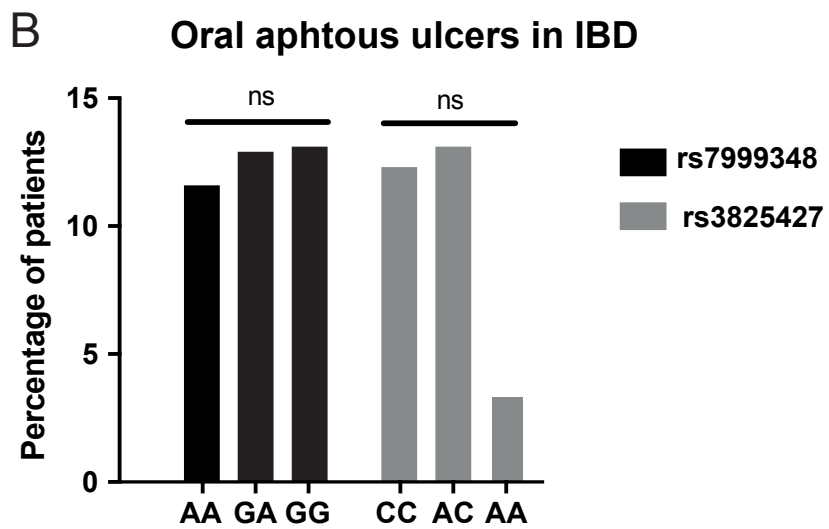
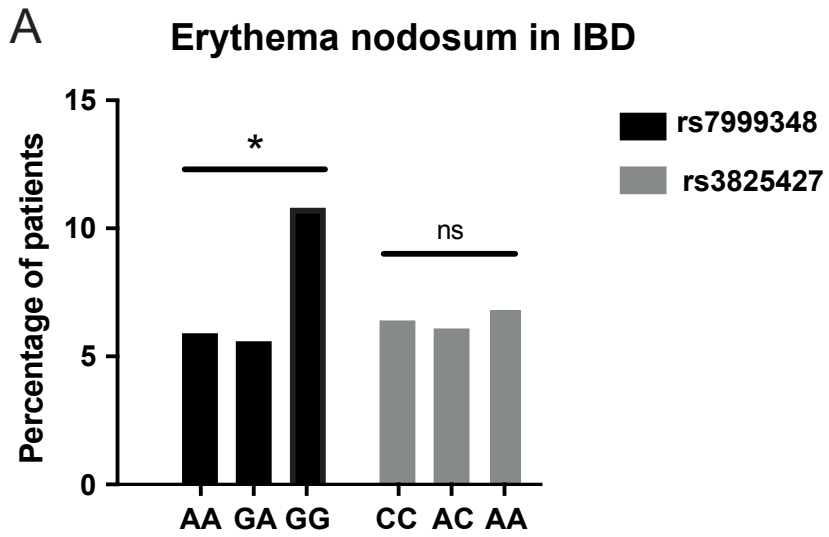
B



C







**Supplementary Figure S1: Gating strategy to define lymphocytes populations:** (A) Lymphocytes were identified using morphology (SSC-A and FSC-A) doublet and dead cells were further excluded. The different lymphocytes populations were defined as follows: CD4 naïve T cells (CD3<sup>+</sup>, CD4<sup>+</sup>, CD45RA<sup>+</sup>), CD4<sup>+</sup> memory T cells (CD3<sup>+</sup>, CD4<sup>+</sup>, CD45RA<sup>-</sup>), CD8<sup>+</sup> naïve T cells (CD8<sup>+</sup>, CD3<sup>+</sup>, CD45RA<sup>+</sup>), CD8<sup>+</sup> memory T cells (CD8<sup>+</sup>, CD3<sup>+</sup>, CD45RA<sup>-</sup>), naïve B cells (CD3<sup>-</sup>, CD19<sup>+</sup>, CD27<sup>-</sup>) memory B cells (CD3<sup>-</sup>, CD19<sup>+</sup>, CD27<sup>+</sup>). (B) CD4<sup>+</sup> memory T cells were further defined as follows: CD4<sup>+</sup> memory CXCR3<sup>+</sup>, Th1 (CXCR3<sup>+</sup>, CCR4<sup>-</sup>), CD4<sup>+</sup> memory CCR4<sup>+</sup>, Th2 (CCR4<sup>+</sup>, CXCR3<sup>-</sup>), CD4<sup>+</sup> memory CCR6<sup>+</sup>, Th17 (CXCR3<sup>-</sup>, CCR6<sup>+</sup>), Th1\* (CXCR3<sup>+</sup>, CCR6<sup>+</sup>), CD4<sup>+</sup> memory CCR9<sup>+</sup>. Fluorescence minus one was used to define positivity for the various chemokine receptors mentioned above. Central memory CD4<sup>+</sup> T cells were also assessed (CCR7<sup>+</sup>).

**Supplementary Figure S2 related to Figure 1 :** Impact of gender on EBI2 surface expression in total CD4<sup>+</sup> T cells, total CD8<sup>+</sup> T cells and B cells assessed by flow cytometry. Men n=10, women n= 23.

**Supplementary Figure S3 related to Figure 1: EBI2 expression and migration assays in subsets of CD4<sup>+</sup> T cells according to chemokine receptor expression:** (A ) Representative contour plot of EBI2 expression (right panels) vs isotype control (left panels) in memory CD4 T cells CCR6<sup>+</sup> vs CCR6<sup>-</sup>(top panels) or CCR9<sup>+</sup> vs CCR9<sup>-</sup>(bottom panel). (B) Percentage of EBI2<sup>+</sup> cells in CD4<sup>+</sup> memory T cells expressing CXCR3, CCR4, CCR7, CCR9 and CCR6, as indicated, n=8. (C) Transwell migration assay of memory CD8<sup>+</sup> and B cells of 5 healthy volunteers comparing chemotaxis with CCL20 at 100 ng/ml, 7 $\alpha$ ,25-diHC at 300nM and the EBI2 antagonist NIBR 189 at 25nM as indicated. The cells are quantified by flow cytometry using counting beads. The different lymphocyte subsets were identified using the gating strategy indicated in Supplementary Figure S1, n=5. ns: not significant; \*: p<0.05; \*\*: p<0.01; \*\*\*: p<0.001., \*\*\*\*: p<0.0001

**Supplementary Figure S4 related to Figure 2: EBI2 expression in T cell subsets does not differ in patients with UC, CD and healthy volunteers (HV).** Comparison of EBI2 MFIR between HV, CD and UC in (A) Th1 cells, (B) Th2 cells, (C) Th17 cells, (D) Th1\* cells, (E) CXCR3<sup>+</sup>CD4<sup>+</sup> memory T cells, (F) CCR4<sup>+</sup> CD4<sup>+</sup> memory T cells, (G) CCR7<sup>+</sup> CD4<sup>+</sup> memory T cells, and (H) CCR9<sup>+</sup> CD4<sup>+</sup> memory T cells. HV: n=8, CD: n=12, UC: n=15. ns: not significant.

**Supplementary Figure S5: EBI2 expression in T cell subsets in IBD patients treated with anti-TNF or vedolizumab.** EBI2 surface expression of the indicated T cell subset in healthy volunteers (HV), or IBD patients treated with vedolizumab (VEDO), anti-TNF or other/ no treatment as indicated. HV: n=8, VEDO : n=7, anti-TNF: n=11, other : n=9. ns: not significant; \*: p<0.05.

**Supplementary Figure S6 related to Figure 3: Impact of chemotaxis induced by 7 $\alpha$ ,25-diHC on the percentage of T helper populations:** (A) Percentage of Th1 cells in CD4<sup>+</sup> memory T cells in the absence of migration (input) or after migration with 7 $\alpha$ ,25-diHC (30nM). (B) as in (A) except that Th2

are shown. (C) as in (A) except that Th1\* are shown. The different lymphocyte subsets were identified using the gating strategy indicated in Supplementary Figure S1. n=5. ns: not significant.

**Supplementary Figure S7 related to Figure 5: Correlation matrix of the IBD related SNP rs9557195 and the Behçet's disease associated SNPs rs7999348, rs3825427, rs9513548, rs9517668, rs9517701 in SIBDC patients.** Statistical analysis: Pearson's correlation (pairwise).

**Supplementary Figure S8 related to Figure 6: Extraintestinal disease manifestations in according to Behçet's disease associated SNPs.** Percentage of patients carrying the indicated allele of the Behçet's disease associated SNPs rs7999348 and rs3825427 with (A) erythema nodosum, (B) aphthous oral ulcers and (C) ankylosing spondylitis. AA: n=1095, GA: n=949, GG: n=260, rs3825427 : CC : n=1853, AC : n=413, AA : n=29. \*:  $p < 0.05$ ; Statistical analysis: Pearson chi square test.

**Supplementary Table S1: Ratio of the MFIR in the cell type over a population reference.** Ratio superior to 1 is indicative of an increased MFIR in the cell type compared to the reference. ns: not significant: p-value = >0.1

Cell type	Reference	Mean of fold matched control values (SD)	p-value (cell type vs reference)	Figure
CD4 <sup>+</sup> CCR3 <sup>+</sup> memory T cells	CD4 memory T cells	1.067 (0.093)	0.0824	1C
CD4 <sup>+</sup> CCR4 <sup>+</sup> memory T cells	CD4 memory T cells	0.9686 (0.07)	ns	1C
CD4 <sup>+</sup> CCR6 <sup>+</sup> memory T cells	CD4 memory T cells	1.771 (0.33)	0.0003	1C
CD4 <sup>+</sup> CCR7 <sup>+</sup> memory T cells	CD4 memory T cells	0.9984 (0.04)	ns	1C
CD4 <sup>+</sup> CCR9 <sup>+</sup> memory T cells	CD4 memory T cells	1.548( 0.46)	0.0125	1C
Th1	CD4 memory T cells	1.191 (0.26)	0.0814	3A
Th2	CD4 memory T cells	0.9373 (0.09)	ns	3A
Th17	CD4 memory T cells	1.756 (0.33)	0.0004	3A
Th1*	CD4 memory T cells	2.364 (1.08)	0.0086	3A
CD8 <sup>+</sup> CCR6 <sup>+</sup> memory T cells	CD8 memory T cells	1.185 (0.19)	0.0452	1D
CCR6 <sup>+</sup> memory B cells	Memory B cells	1.612( 0.56)	0.028	1E
CD4 <sup>+</sup> CCR9 <sup>+</sup> memory T cells	CD4 memory CCR6+	0.89 (0.27)	ns	2C

### Ulcerative colitis patients

Cell type	Reference	Mean (SD)	p-value (cell type vs reference)	Figure
CD4 <sup>+</sup> CCR9 <sup>+</sup> memory T cells	CD4 <sup>+</sup> CCR6 <sup>+</sup> memory T cells	0.75 (0.23)	0.0011	2C
Th1	CD4 <sup>+</sup> memory T cells	1.062 (0.11)	0.0411	3E
Th2	CD4 <sup>+</sup> memory T cells	1.034 (0.08)	ns	3E
Th17	CD4 <sup>+</sup> memory T cells	2.052 (0.45)	<0.0001	3E
Th1*	CD4 <sup>+</sup> memory T cells	2.11 (1.41)	0.0085	3E

### Crohn's disease patients

Cell type	Reference	Mean (SD)	p-value (cell type vs reference)	Figure
CD4 <sup>+</sup> CCR9 <sup>+</sup> memory T cells	CD4 <sup>+</sup> CCR6 <sup>+</sup> memory T cells	0.72 (0.17)	0.0002	3C
Th1	CD4 <sup>+</sup> memory T cells	1.042 (0.13)	ns	3F
Th2	CD4 <sup>+</sup> memory T cells	0.9832 (0.09)	ns	3F
Th17	CD4 <sup>+</sup> memory T cells	1.804 (0.32)	<0.0001	3F
Th1*	CD4 <sup>+</sup> memory T cells	2.18 (1.38)	0.0127	3F

**Supplementary Table S2: Distribution of rs9557195 genotypes in IBD patients and clinical characteristics (UC and CD)**

<b>IBD patients</b>	<b>CC</b>	<b>CT</b>	<b>TT</b>	<b>p-value (Chi square)</b>
<b>Diagnosis</b>				
CD	79 (59.0%)	489 (59.3%)	767 (57.1%)	0.578
UC	55 (41.0%)	335 (40.7%)	576 (42.9%)	
<b>Gender</b>				
Male (%)	75 (56.0%)	448 (54.4%)	669 (49.8%)	0.073
Female (%)	59 (44.0%)	376 (45.6%)	674 (50.2%)	
<b>CD only:</b>				
Male (%)	46 (58.2%)	255 (52.1%)	365 (47.6%)	0.090
Female (%)	33 (41.8%)	234 (47.9%)	402 (52.4%)	
<b>UC only:</b>				
Male (%)	29 (52.7%)	193 (57.6%)	304 (52.8%)	0.356
Female (%)	26 (47.3%)	142 (42.4%)	272 (47.2%)	
<b>Age at diagnosis</b>				
Median, q25 – q75, min – max	24.5, 18.1 – 33.6, 4.2 – 67.4	25.6, 18.7 – 35.6, 1.0 – 80.1	26.5, 19.1 – 36.8, 0.5 – 81.4	0.198
<b>CD only:</b>				
Median, q25 – q75, min – max	24.5, 19.1 – 34.6, 4.2 – 67.4	24.0, 17.5 – 33.6, 1.0 – 80.1	25.2, 18.6 – 36.0, 0.5 – 81.4	0.230
<b>UC only:</b>				
Median, q25 – q75, min – max	24.4, 17.1 – 33.6, 5.7 – 61.3	29.1, 20.4 – 40.2, 3.8 – 77.9	28.6, 20.3 – 38.1, 2.9 – 79.6	0.087
<b>Maximum extent of disease – UC:</b>				
Proctitis	2 (3.8%)	36 (11.0%)	50 (8.9%)	0.142
Left-sided colitis	23 (43.4%)	112 (34.4%)	173 (30.9%)	
Pancolitis	28 (52.8%)	178 (54.6%)	337 (60.2%)	
Unknown	2	9	16	
<b>Complications</b>				
<b>UC only:</b>				
No	25 (45.5%)	141 (42.1%)	228 (39.6%)	0.584
Yes	30 (54.5%)	194 (57.9%)	348 (60.4%)	
<b>Intestinal surgery</b>				
<b>UC only:</b>				
No	49 (89.1%)	303 (90.4%)	496 (86.1%)	0.149
Yes	6 (10.9%)	32 (9.6%)	80 (13.9%)	
<b>Last disease location :</b>				
L1	29 (36.7%)	140 (28.9%)	237 (31.6%)	0.622
L2	25 (31.6%)	157 (32.4%)	254 (33.9%)	
L3	24 (30.4%)	173 (35.7%)	240 (32.0%)	
L4	1 (1.3%)	15 (3.1%)	18 (2.4%)	
Unknown	0	4	18	
<b>Complications</b>				
No	25 (31.6%)	174 (35.6%)	266 (34.7%)	0.786
Yes	54 (68.4%)	315 (64.4%)	501 (65.3%)	
<b>Intestinal surgery</b>				

No	40 (50.6%)	285 (58.3%)	460 (60.0%)	0.264
Yes	39 (49.4%)	204 (41.7%)	307 (40.0%)	
<b>Fistula, abscess or anal fissure</b>				
No	85 (63.4%)	558 (67.7%)	917 (68.3%)	0.518
Yes	49 (36.6%)	266 (32.3%)	426 (31.7%)	
<b>Surgery for fistula</b>				
No	111 (82.8%)	681 (82.6%)	1118 (83.2%)	0.935
Yes	23 (17.2%)	143 (17.4%)	225 (16.8%)	
<b>Ever treated with TNF-inhibitors</b>				
UC	18 (32.7%)	107 (31.9%)	219 (38.0%)	0.163
CD	55 (69.6%)	316 (64.6%)	468 (61.0%)	0.191
<b>At least one failure with TNF inhibitor</b>				
UC	7 (12.7%)	63 (18.8%)	108 (18.8%)	0.532
CD	25 (31.6%)	138 (28.2%)	200 (26.1%)	0.464

**Supplementary Table S3: Allele frequencies of SNPs rs9557195, rs7999348, and rs3825427 in the global and European population (controls), in patients with IBD, Behçet disease, and in the Swiss IBD cohort (SIBDC). RAF: risk allele frequency.**

	rs9557195 (C/T)	rs7999348 (G/A)	rs3825427 (A/C)
	RAF (T)	RAF (G)	RAF (A)
<b>Global Population (The Genome Aggregation Database, gnomAD)</b>	<b>0.85</b>	<b>0.44</b>	<b>0.14</b>
<b>European Population (Exome Aggregation Consortium, ExAC, 1000 Genomes)</b>	<b>0.775</b>	<b>0.285</b>	<b>0.116</b>
<b>IBD patients (4)</b>	<b>0.77</b> (cases + controls)	-	-
<b>Behçet disease (19) Turkish population</b>	-	<b>0.48 (cases)</b> <b>0.34 (controls)</b>	-
<b>Behçet disease (53) Chinese population</b>	-		<b>0.38 (cases)</b> <b>0.30 (controls)</b>
<b>SIBDC (this study)</b>	<b>0.76</b>	<b>0.32</b>	<b>0.10</b>

**Supplementary Table S4: Distribution of rs9557195 genotypes and EIM in IBD patients (UC and CD)**

<b>rs9557195</b>	<b>CC</b>	<b>CT</b>	<b>TT</b>	<b>p-value (chi square)</b>
<b>EIM at least once through-out follow-up</b>				<i>yes vs. no for each type of EIM</i>
Any one	80 (59.7%)	481 (58.4%)	746 (55.5%)	0.341
Peripheral arthritis	64 (47.8%)	382 (46.4%)	611 (45.5%)	0.842
Uveitis / Iritis	13 (9.7%)	80 (9.7%)	139 (10.3%)	0.881
Pyoderma gangrenosum	0 (0%)	13 (1.6%)	22 (1.6%)	0.331
<b><u>Erythema nodosum</u></b>	10 (7.5%)	44 (5.3%)	92 (6.9%)	0.323
<b><u>Aphthous oral ulcers</u></b>	24 (17.9%)	100 (12.1%)	159 (11.8%)	0.123
<b><u>Ankylosing spondylitis</u></b>	9 (6.7%)	57 (6.9%)	98 (7.3%)	0.929
PSC	2 (1.5%)	21 (2.5%)	31 (2.3%)	0.748
<b>CD only:</b>				
Any one	55 (69.6%)	305 (62.4%)	461 (60.1%)	0.224
Peripheral arthritis	45 (57.0%)	249 (50.9%)	394 (51.4%)	0.602
Uveitis / Iritis	8 (10.1%)	59 (12.1%)	98 (12.8%)	0.769
Pyod. gangrenosum	0 (0%)	5 (1.0%)	12 (1.6%)	0.410
<b><u>Erythema nodosum</u></b>	10 (12.7%)	29 (5.9%)	67 (8.7%)	0.056
<b><u>Aphthous oral ulcers</u></b>	20 (25.3%)	70 (14.3%)	119 (15.5%)	<b>0.044</b>
<b><u>Ankylosing spondylitis</u></b>	5 (6.3%)	43 (8.8%)	68 (8.9%)	0.744
PSC	1 (1.3%)	5 (1.0%)	5 (0.7%)	0.704
<b>UC only:</b>				
Any one	25 (45.5%)	176 (52.5%)	285 (49.5%)	0.511
Peripheral arthritis	19 (34.5%)	133 (39.7%)	217 (37.7%)	0.705
Uveitis / Iritis	5 (9.1%)	21 (6.3%)	41 (7.1%)	0.720
Pyoderma gangrenosum	0 (0%)	8 (2.4%)	10 (1.7%)	0.449
<b><u>Erythema nodosum</u></b>	0 (0%)	15 (4.5%)	25 (4.3%)	0.282
<b><u>Aphthous oral ulcers</u></b>	4 (7.3%)	30 (9.0%)	40 (6.9%)	0.543
<b><u>Ankylosing spondylitis</u></b>	4 (7.3%)	14 (4.2%)	30 (5.2%)	0.568
PSC	1 (1.8%)	16 (4.8%)	26 (4.5%)	0.611
<b>Psoriasis</b>				
No	119 (88.8%)	779 (94.5%)	1274 (94.9%)	<b>0.014</b>
Yes	15 (11.2%)	45 (5.5%)	69 (5.1%)	
<i>Psoriasis reported as a side effect</i>	2 (1.5%)	9 (1.1%)	15 (1.1%)	0.918
<b>CD only:</b>				
No	67 (84.8%)	453 (92.6%)	712 (92.8%)	<b>0.037</b>
Yes	12 (15.2%)	36 (7.4%)	55 (7.2%)	
<i>Psoriasis reported as a side effect</i>	2 (2.5%)	8 (1.6%)	14 (1.8%)	0.854
<b>UC only:</b>				
No	52 (94.5%)	326 (97.3%)	562 (97.6%)	0.416
Yes	3 (5.5%)	9 (2.7%)	14 (2.4%)	
<i>Psoriasis reported as a side effect</i>	0 (0%)	1 (0.3%)	1 (0.2%)	0.869

Supplementary Table S5: Distribution of rs7999348 genotypes and EIM in IBD patients (UC and CD)

rs7999348	GG	GA	AA	p-value (chi square)
<b>EIM at least once throughout follow-up</b>				<i>yes vs. no for each type of EIM</i>
Any one	151 (58.1%)	528 (55.6%)	628 (57.4%)	0.662
Peripheral arthritis	128 (49.2%)	431 (45.4%)	498 (45.5%)	0.515
Uveitis / Iritis	26 (10.0%)	96 (10.1%)	109 (10.0%)	0.993
<b>Pyoderma gangrenosum</b>	4 (1.5%)	14 (1.5%)	17 (1.6%)	0.990
<u><b>Erythema nodosum</b></u>	28 (10.8%)	53 (5.6%)	65 (5.9%)	<b>0.007</b>
<u><b>Aphthous oral ulcers</b></u>	34 (13.1%)	122 (12.9%)	127 (11.6%)	0.632
<u><b>Ankylosing spondylitis</b></u>	19 (7.3%)	85 (9.0%)	59 (5.4%)	<b>0.007</b>
PSC	8 (3.1%)	18 (1.9%)	28 (2.6%)	0.437
<b>CD only:</b>				
Any one	89 (64.0%)	332 (59.9%)	401 (62.3%)	0.573
Peripheral arthritis	79 (56.8%)	275 (49.6%)	335 (52.0%)	0.298
Uveitis / Iritis	19 (13.7%)	70 (12.6%)	76 (11.8%)	0.801
<b>Pyoderma gangrenosum</b>	1 (0.7%)	6 (1.1%)	10 (1.6%)	0.638
<u><b>Erythema nodosum</b></u>	19 (13.7%)	39 (7.0%)	48 (7.5%)	<b>0.029</b>
<u><b>Aphthous oral ulcers</b></u>	28 (20.1%)	91 (16.4%)	90 (14.0%)	0.153
<u><b>Ankylosing spondylitis</b></u>	12 (8.6%)	62 (11.1%)	42 (6.5%)	<b>0.017</b>
PSC	1 (0.7%)	4 (0.7%)	6 (0.9%)	0.914
<b>UC only:</b>				
Any one	62 (51.2%)	196 (49.6%)	227 (50.3%)	0.948
Peripheral arthritis	49 (40.5%)	156 (39.5%)	163 (36.1%)	0.508
Uveitis / Iritis	7 (5.8%)	26 (6.6%)	33 (7.3%)	0.813
<b>Pyoderma gangrenosum</b>	3 (2.5%)	8 (2.0%)	7 (1.6%)	0.761
<u><b>Erythema nodosum</b></u>	9 (7.4%)	14 (3.5%)	17 (3.8%)	0.147
<u><b>Aphthous oral ulcers</b></u>	6 (5.0%)	31 (7.8%)	37 (8.2%)	0.482
<u><b>Ankylosing spondylitis</b></u>	7 (5.8%)	23 (5.8%)	17 (3.8%)	0.337
PSC	7 (5.8%)	14 (3.5%)	22 (4.9%)	0.481
<b>Psoriasis</b>				
No	242 (93.1%)	901 (94.9%)	1032 (94.2%)	0.487
Yes	18 (6.9%)	48 (5.1%)	63 (5.8%)	
<i>Psoriasis reported as a side effect</i>	3 (1.2%)	9 (0.9%)	14 (1.3%)	0.779
<b>CD only:</b>				
No	124 (89.2%)	521 (94.0%)	589 (91.5%)	0.087
Yes	15 (10.8%)	33 (6.0%)	55 (8.5%)	
<i>Psoriasis reported as a side effect</i>	3 (2.2%)	8 (1.4%)	13 (2.0%)	0.714
<b>UC only:</b>				
No	118 (97.5%)	380 (96.2%)	443 (98.2%)	0.190
Yes	3 (2.5%)	15 (3.8%)	8 (1.8%)	
<i>Psoriasis reported as a side effect</i>	0 (0%)	1 (0.3%)	1 (0.2%)	0.862

Supplementary Table S6: Distribution of rs3825427 genotypes and EIM in IBD patients (UC and CD)

rs3825427	AA	AC	CC	p-value (chi square)
<b>EIM at least once through-out follow-up</b>				<i>yes vs. no at each line</i>
Any one	17 (58.6%)	225 (54.5%)	1059 (57.2%)	0.599
Peripheral arthritis	12 (41.4%)	190 (46.0%)	849 (45.8%)	0.889
Uveitis / Iritis	3 (10.3%)	39 (9.4%)	190 (10.3%)	0.884
<b>Pyoderma gangrenosum</b>	0 (0%)	6 (1.5%)	28 (1.5%)	0.799
<u><b>Erythema nodosum</b></u>	2 (6.9%)	25 (6.1%)	119 (6.4%)	0.955
<u><b>Aphthous oral ulcers</b></u>	1 (3.4%)	54 (13.1%)	228 (12.3%)	0.312
<u><b>Ankylosing spondylitis</b></u>	1 (3.4%)	38 (9.2%)	124 (6.7%)	0.148
PSC	2 (6.9%)	7 (1.7%)	45 (2.4%)	0.180
<b>CD only:</b>				
Any one	7 (46.7%)	135 (58.4%)	677 (62.3%)	0.269
Peripheral arthritis	5 (33.3%)	114 (49.4%)	567 (52.2%)	0.269
Uveitis / Iritis	0 (0%)	30 (13.0%)	135 (12.4%)	0.333
<b>Pyoderma gangrenosum</b>	0 (0%)	2 (0.9%)	15 (1.4%)	0.742
<u><b>Erythema nodosum</b></u>	1 (6.7%)	18 (7.8%)	87 (8.0%)	0.977
<u><b>Aphthous oral ulcers</b></u>	1 (6.7%)	36 (15.6%)	172 (15.8%)	0.624
<u><b>Ankylosing spondylitis</b></u>	0 (0%)	27 (11.7%)	89 (8.2%)	0.112
PSC	0 (0%)	2 (0.9%)	9 (0.8%)	0.937
<b>UC only:</b>				
Any one	10 (71.4%)	90 (49.5%)	382 (49.8%)	0.272
Peripheral arthritis	7 (50.0%)	76 (41.8%)	282 (36.8%)	0.295
Uveitis / Iritis	3 (21.4%)	9 (4.9%)	55 (7.2%)	0.057
<b>Pyoderma gangrenosum</b>	0 (0%)	4 (2.2%)	13 (1.7%)	0.791
<u><b>Erythema nodosum</b></u>	1 (7.1%)	7 (3.8%)	32 (4.2%)	0.836
<u><b>Aphthous oral ulcers</b></u>	0 (0%)	18 (9.9%)	56 (7.3%)	0.276
<u><b>Ankylosing spondylitis</b></u>	1 (7.1%)	11 (6.0%)	35 (4.6%)	0.653
PSC	2 (14.3%)	5 (2.7%)	36 (4.7%)	0.104
<b>Psoriasis</b>				
No	27 (93.1%)	387 (93.7%)	1754 (94.7%)	0.708
Yes	2 (6.9%)	26 (6.3%)	99 (5.3%)	
<i>Psoriasis reported as a side effect</i>	1 (3.4%)	2 (0.5%)	22 (1.2%)	0.216
<b>CD only:</b>				
No	13 (86.7%)	212 (91.8%)	1005 (92.5%)	0.654
Yes	2 (13.3%)	19 (8.2%)	81 (7.5%)	
<i>Psoriasis reported as a side effect</i>	1 (6.7%)	2 (0.9%)	20 (1.8%)	0.197
<b>UC only:</b>				
No	14 (100%)	175 (96.2%)	749 (97.7%)	0.430
Yes	0 (0%)	7 (3.8%)	18 (2.3%)	
<i>Psoriasis reported as a side effect</i>	0 (0%)	0 (0%)	2 (0.3%)	0.774

## **5. Manuscript N°3: Resolution of inflammation during multiple sclerosis**

This manuscript was published in Seminars in immunopathology (2019).

DOI: [10.1007/s00281-019-00765-0](https://doi.org/10.1007/s00281-019-00765-0)

It is a review describing the cellular and molecular mechanisms involved in the resolution of inflammation in MS. The review is divided into three main parts, describing the role in the resolution of inflammation in the CNS of:

- i) The immune network
- ii) The CNS resident cells
- iii) The MS treatments

I was involved in the elaboration of the plan, the figures, the writing and the revisions of this review.



# Resolution of inflammation during multiple sclerosis

F. Ruiz<sup>1</sup> · S. Vigne<sup>1</sup> · C. Pot<sup>1</sup>

Received: 15 July 2019 / Accepted: 27 September 2019 / Published online: 15 November 2019  
© The Author(s) 2019

## Abstract

Multiple sclerosis (MS) is a frequent autoimmune demyelinating disease of the central nervous system (CNS). There are three clinical forms described: relapsing-remitting multiple sclerosis (RRMS), the most common initial presentation (85%) among which, if not treated, about half will transform, into the secondary progressive multiple sclerosis (SPMS) and the primary progressive MS (PPMS) (15%) that is directly progressive without superimposed clinical relapses. Inflammation is present in all subsets of MS. The relapsing/remitting form could represent itself a particular interest for the study of inflammation resolution even though it remains incomplete in MS. Successful resolution of acute inflammation is a highly regulated process and dependent on mechanisms engaged early in the inflammatory response that are scarcely studied in MS. Moreover, recent classes of disease-modifying treatment (DMTs) that are effective against RRMS act by re-establishing the inflammatory imbalance, taking advantage of the pre-existing endogenous suppressor. In this review, we will discuss the active role of regulatory immune cells in inflammation resolution as well as the role of tissue and non-hematopoietic cells as contributors to inflammation resolution. Finally, we will explore how DMTs, more specifically induction therapies, impact the resolution of inflammation during MS.

**Keywords** Multiple sclerosis · Suppressive immune cells · Innate immune cells · Neurovascular unit · Astrocytes · Blood-brain-barrier · Induction therapies

## Introduction

Multiple sclerosis (MS) is a frequent autoimmune demyelinating disease of the central nervous system (CNS). The exact cause of MS remains elusive but it is certainly a multifactorial disease. Environmental factors, such as Epstein bar virus infection, low vitamin D status, or cigarette smoking contribute to MS development as well as genetic factors, in particular the HLA variant *HLA-DRB1\*15:01* [1]. The underlying pathophysiology of MS is only partially unraveled. Most probably, auto reactive CD4<sup>+</sup> T cells are activated in the periphery and cross the blood-brain barrier to reach the CNS, known as the

“outside-in hypothesis.” Once in the CNS, CD4<sup>+</sup> T cells are reactivated by local antigen presenting cells, which will trigger an inflammatory reaction, inducing the recruitment of other leukocytes (such as T cells, B cells, and macrophages). A second hypothesis, the “inside-out hypothesis,” suggests that MS is a primary neurodegenerative disease that triggers an autoimmune reaction. We learned from murine models of MS, in particular the experimental autoimmune encephalomyelitis (EAE) and from the treatments that are effective to constrain MS, that the outside-in hypothesis is certainly valid. Peripheral leukocyte trafficking across the blood-brain-barrier is indeed an essential step in the initiation of relapses. The infiltration of pro-inflammatory leukocytes in the CNS further triggers a disruption of the myelin sheath eventually leading to neuronal loss [2]. However, what stimulates the peripheral infiltration of leukocytes into the CNS is still matter of debate.

Predominantly, the disease starts with a relapsing remitting course (RRMS), which may later convert into a secondary progressive disease (SPMS). In a minority of cases, the patients show progression from the onset without superimposed clinical relapses (primary progressive MS, PPMS) [3]. When the disease is progressive, the majority of disease-modifying treatments (DMTs) are inefficient probably because of the

---

This article is a contribution to the special issue on Resolution of Inflammation in Chronic Diseases – Guest Editor: Markus Neurath

---

✉ C. Pot  
caroline.pot-kreis@chuv.ch

<sup>1</sup> Laboratories of Neuroimmunology, Neuroscience Research Center and Service of Neurology, Department of Clinical Neurosciences, Lausanne University Hospital and University of Lausanne, Chemin des Boveresses 155, 1066 Epalinges, Switzerland

compartmentalization of the inflammation in the CNS. RRMS is characterized by flare-ups of neurological symptoms with periods of remissions. The relapses are characterized by an infiltration of peripheral immune cells across the blood-brain barrier (BBB), and blocking leukocyte trafficking from the periphery to the CNS is effective to treat RRMS.

In this review, we will focus on the factors implicated in the resolution of inflammation and discuss how they can be impaired in MS. We will first discuss the immune mechanism involved then the importance of non-immune compartment. Finally, we will briefly explore how disease-modifying treatments impact inflammation resolution.

## Contribution of immune network to MS resolution

Suppressive immune cells, both from the adaptive and innate immunity, prevent exaggerated inflammatory responses. We will first discuss the implication of CD4<sup>+</sup> T cells, which can be subdivided based on their cytokine profiles in both pro- and anti-inflammatory subsets. Since the original classification by Mosmann and Coffman of CD4<sup>+</sup> helper T (Th) lymphocytes into Th1 and Th2 subsets [4], their repertoire has expanded: for example, Th17 cells induce immunity against extracellular bacteria and fungi. Exaggerated Th17 response promotes autoimmunity and elevated levels of IL-17 are detected in MS. However, Th17 cells are heterogeneous and under certain conditions, IL-10 secretion renders them non-pathogenic [5]. However, we will here focus on CD4<sup>+</sup> T regulatory T cell (Tregs) that are well-established players in the resolution of inflammation. Several classes of Tregs are identified: the FoxP3<sup>+</sup> regulatory T cells that consist of conventional/natural Treg (nTreg) cells and induced Tregs (iTregs) as well as the type 1 regulatory T (Tr1) cells [6]. We will then discuss the role of CD8<sup>+</sup> T cells that outnumber CD4<sup>+</sup> T cells in MS lesions and also contribute to inflammation resolution [7]. In addition, regulatory B cells (Breg) also restrain inflammation. Furthermore, innate immune cells in particular, subsets of NK cells, foamy macrophages as well as myeloid-derived suppressor cells contribute to inflammation resolution during MS [8]. Finally, the implication of pro-resolving lipid mediators (SPMs) in MS resolution will be explored. We will now discuss the implications of each of these immune cells and regulatory mechanisms in more detail.

### Role of FoxP3<sup>+</sup> regulatory T cells (Tregs)

CD4<sup>+</sup>CD25<sup>+</sup>T cells play a critical role in the regulation of CNS autoimmunity in EAE and MS (Fig. 1). Tregs influence EAE by affecting the priming, polarization, and proliferation of effector T cells in the periphery and within the CNS [9]. Transfer of Tregs in the periphery is sufficient to protect mice

from the onset and the progression of both active and spontaneous EAE, whereas their depletion exacerbates the disease [10]. In the same line, the presence of myelin proteolipid protein-specific Tregs partially explains the genetic resistance to EAE disease observed in B10.S versus SJL mice. While both mouse models harbor T cells that recognize PLP139-151 at similar frequencies upon immunization, EAE-resistant B10.S mice fail to mount a sustained proliferative response due to a higher relative frequency of PLP-specific Tregs cells in their peripheral repertoire. Indeed, depletion of CD25<sup>+</sup> cells *in vivo* restores EAE susceptibility to B10.S mice [11]. Furthermore, epigenetic modifications of the Foxp3 gene contribute to the pathogenesis of EAE [12]. Tregs are also implicated directly in the CNS at the site of inflammation resolution and can transigrate across CNS endothelium [13]. In healthy CNS, Tregs are important in promoting neuroprotection as interactions occur between the resident cells of the CNS and the infiltrating Tregs to modulate the local immune responses [14]. During neuroinflammation, the frequencies of Tregs within the CNS are elevated during the recovery phase of actively induced EAE; however, it is not clearly established if they harbor suppressive activities, at least when tested *ex-vivo* [15]. At the experimental level, treatments that increase Tregs are beneficial; however, current techniques broadly expand polyclonal Tregs but not just Ag-specific cells. Promising studies indicate that tolerogenic nanoparticles induce antigen-specific Tregs and provide protection and transferable tolerance against EAE [16]. In the same way, gene therapy-induced antigen-specific Tregs prevent development and reverses pre-existing EAE [17]. Deficiency and/or dysfunction of Tregs are observed not only in EAE but also in MS [18]. However, whether Foxp3<sup>+</sup>Tregs are deficient in the blood of MS patients has been a matter of debate for several years. To address this question, a meta-analysis regrouping 16 studies was published providing evidences that the proportion of Tregs expressing Foxp3 is indeed decreased in the peripheral blood of MS patients [19]. The assessment of Tregs directly in the CNS is however more challenging. Counter-intuitively, Foxp3<sup>+</sup>Tregs are increased in the CSF of MS patients; however, their functions are dampened in this compartment [20]. Those results are supported by genome-wide association studies (GWAS) that identified single nucleotide polymorphisms linked to Treg functions associated with an increased risk for MS disease [21].

### Role of IL-10-secreting type 1 regulatory T cells (Tr1)

In contrast to conventional Tregs, Tr1 cells do not express the transcription factor Foxp3 and only a transient expression of CD25; however, they co-expressed CD49b, LAG-3, and CD226 cell-surface markers in humans and mice [22]. C-MAF, AhR, BAFT, and IRF1 are critical transcription factors for Tr1 cell differentiation [23, 24]. Tr1 cells exert their

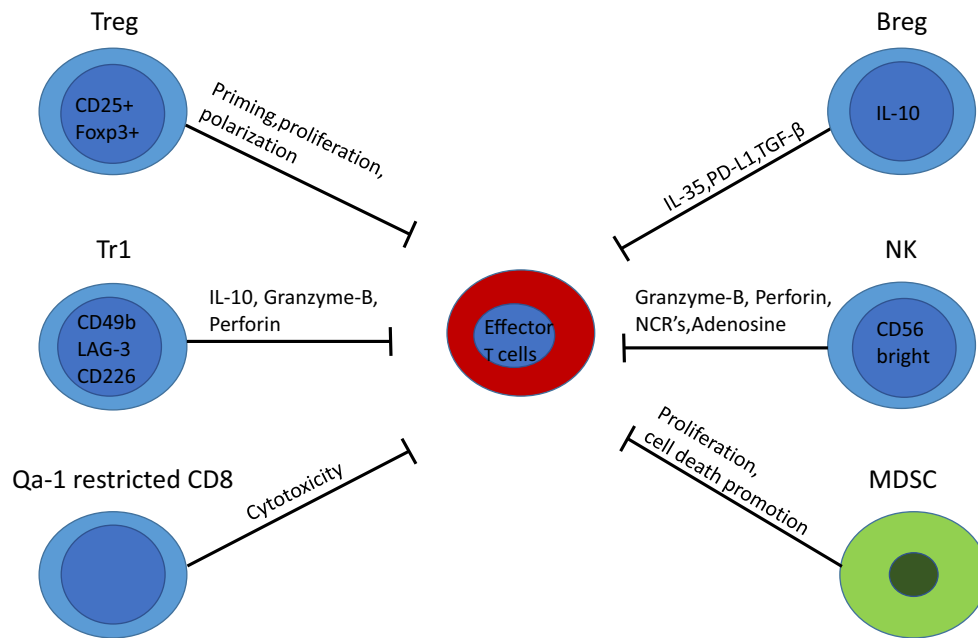


**Fig. 1** Suppressive immune cells involved in inflammation resolution. Foxp3<sup>+</sup> Treg cells affect priming, proliferation, and polarization of effector T cells both in the CNS and the periphery. Tr1 cells produce the anti-inflammatory cytokine IL-10 and kill effector cells via granzyme-B and perforin. Qa-1-restricted CD8<sup>+</sup> cells have a cytotoxic effect on

immunosuppressive effects through IL-10 expression and by killing effector cells via Granzyme-B and Perforin (Fig. 1) [6]. Several studies have reported the critical involvement of IL-10 cytokine in the suppression of EAE models associated with an increase in Tr1 cells [25]. In EAE, the transfer of *in vitro* generated OVA-specific Tr1 cells prevents the development of neurological symptoms when OVA peptide is injected intracranially [26]. Moreover, *in vivo* induction of Tr1 cells with soluble myelin basic protein (MBP) reverses ongoing disease in rats immunized with MBP [27]. Regulatory Tr1 cells regulate EAE partially through a mechanism involving IL-10 [28]. Myelin-specific Tr1 cells injected mice-mediated delay onset of EAE associated with a reduction in the severity of clinical signs [29]. Another challenge is to successfully induce regulatory T cells directly *in vivo* to avoid T cell transfer that is challenging in humans. Interestingly, nasal anti-CD3 administration can induce Tr1-like T cells *in vivo* that are further able to constrain inflammation in the progressive animal model of multiple sclerosis in an IL-10-dependent manner by regulating astrocytes and microglia function [30]. Tr1 cells also display immunosuppressive functions in the human setting. Tr1 cells isolated from MS patients display impaired IL-10 production and altered IL-10-mediated suppressive effects when compared with healthy controls [31, 32]. In this line, considering that Tr1 function is impaired in MS, some studies investigated the effect of Tr1 differentiation by tolerogenic dendritic cells (tolDCs). A phase 1b clinical trial showed the feasibility and safety of treating a patient with MS with tolDCs loaded with myelin peptides to increase IL-10 levels in PBMCs as well as the frequency of Tr1

activated CD4<sup>+</sup> T cells. Bregs secrete IL-35 and TGF- $\beta$  that suppress APC function. NK cell engagement of NCRs suppresses CD4<sup>+</sup> T cell proliferation and exerts a cytotoxic activity via the release of granzyme-B, perforin, and of the immunosuppressive adenosine. CNS-derived MDSCs suppress proliferation and promote cell death of lymphocytes

cells [33]. Furthermore, tolDCs exert some of their effects through the cytokine IL-27 that has been identified as a key inducer of Tr1 and inhibitor of Th17 during autoimmunity [6, 24]. IL-27 plays a suppressive role during EAE as demonstrated by more severe disease in IL-27R-deficient mice [34]. Furthermore, IL-27 treatment reduces the severity of EAE by a mechanism dependent on IL-10 [35]. Relevant to the human disease, the beneficial impact of IFN $\beta$ , first-line therapy for relapsing-remitting MS, is associated with IL-27 induction, which promotes the production of IL10 by dendritic cells [36]. Finally, IL-27 is expressed by astrocytes in brain biopsies of human MS lesions suggesting that IL-27 regulates T cell response also locally within the brain of MS patients [37]. Therefore, IL-27 (acting on Tr1 cells) plays a critical role in controlling autoimmunity, providing a putative target therapy.

### Role of regulatory CD8 cells

Similarly to CD4<sup>+</sup> T cells, CD8<sup>+</sup> T cells are both detrimental and protective during EAE and probably MS. After the identification of CD8 as being protective during EAE [38], the importance of the Qa-1 protein, an MHC class Ib molecule (mouse equivalent of HLA-E for human), as a key molecule in CD8-mediated suppression was highlighted [39]. Qa-1/HLA-E-restricted CD8<sup>+</sup> Tregs reduce EAE by promoting a cytotoxic activity on activated CD4<sup>+</sup> T cells (Fig. 1) [40]. By performing screening for TCR specificity, peptides specific for the TCRs of clonally expanded CD8<sup>+</sup> T cells were identified. Concomitant immunization with myelin and those peptides reduces EAE severity by

expanding CD8 T cells that limited the proliferation of myelin-specific CD4<sup>+</sup> T cells [41]. During an MS exacerbation, CD8<sup>+</sup> HLA-E-restricted show an impaired cytotoxic activity against activated myelin-specific CD4<sup>+</sup> T cells [42]. Moreover, neuroantigen-specific CD8<sup>+</sup> T cells are observed in both MS patients and healthy subjects [43] but their suppressive function is reduced during MS relapses [44]. A meta analysis evaluating the differences of frequency of CD8<sup>+</sup> Tregs between healthy volunteer and MS patients lead to the conclusion that CD8<sup>+</sup> Tregs frequency is reduced in MS patients [45]. Furthermore during EAE, while most of the expanded CD4<sup>+</sup> T cells are myelin specific, the majority of clonally expanded CD8<sup>+</sup> T cells are not activated by myelin protein [41].

### Role of regulatory B cells

Regulatory B cells (Bregs) represent a small population of B cells, which participates in immunoregulation and suppression of immune responses. Due to the limited data on the phenotype of Bregs, they are usually identified by their capacity to secrete IL-10 and are termed B10 cells (Fig. 1). Apart from their IL-10 production, Bregs exert their functions by the expression of other regulatory cytokines such as TGF $\beta$  and IL-35 or by the generation and maintenance of Tregs. The role of B cells itself remained elusive for many years, and initially, it was proposed using B cell-deficient mice, that B cells did not play a major role in the activation of encephalitogenic T cells but may solely partially contribute to the immune modulation in EAE [46]. The roles of B cells were further studied using B cell-targeted monoclonal antibodies (anti-CD20). While B cell depletion is beneficial if performed during disease activity, their depletion prior to EAE induction increases encephalitogenic T cell influx into the CNS in the MOG<sub>35-55</sub> model of EAE [47]. By using the same strategy, Ray et al. found that B cell depletion prior the onset of EAE resulted in chronic disease induced by adoptive transfer of MBP-specific encephalitogenic T cells [48]. Further studies showed that transfer of B10 cells in mice suppresses active and spontaneous EAE in different mouse strains [49, 50]. The suppressive capacity of Breg during EAE is also dependent on co-inhibitory molecules that downregulates effector T cell responses and elevated PD-L1 expression on B cells suppresses EAE [51]. In addition, IL-35 expression is also implicated in EAE recovery [52]. Finally, the presence of B cell-secreted TGF $\beta$  limits the induction phase of EAE, further demonstrating the regulatory role of B cell-derived IL-35 or TGF $\beta$  during autoimmunity [53].

In MS pathogenesis, the role of Bregs remains unclear due to several contradictory reports. The number of Bregs was reported to be reduced [54], unaltered [55], or increased [56] ending in disagreement between studies evaluating the role of Breg cells in MS. Interestingly, plasmablasts and plasma cells (that are not targeted by anti-CD20 treatment) highly express IL-10 within MS lesions [57] suggesting that these cells may ameliorate inflammation. IgA<sup>+</sup> plasma cells can be generated

in the gut and be mobilized to the CNS to further contribute to inflammation resolution in EAE and possibly in MS [58]. The controversies on Bregs are certainly the consequence of variations in patient cohorts (state/form of the disease, treatments) but also due to the non-established phenotype of Bregs and may depend upon the stage of differentiation of B cells.

### Role of NK cells

In addition to regulatory lymphocytes, innate immune cells depict immune-regulatory properties. NK cells are innate lymphocytes that were initially affected with effector function properties, in particular, anti-tumoral and anti-viral [59]. However, they also display regulatory functions, more specifically the subset of human NK cells that express CD56 at high levels (CD56<sup>bright</sup> NK cells). CD56<sup>bright</sup> NK cells are a small fraction of circulating NK cells but constitute a large proportion of NK cells within lymph nodes and CSF. NK cells are detected in the CSF of both healthy and MS patients and can be considered as a CNS-specific marker, probably entering the CNS by the lymphatic vessels. NK cells can be activated by the pro-inflammatory cytokines IL-12 and IL-15 and thus are a good prototype of cells induced in the context of inflammation to promote its resolution. Interestingly, IL-27, which drives Tr1 cell generation, further enhances the anti-inflammatory functions of CD56<sup>bright</sup> NK cells [60]. In human, CD56<sup>bright</sup> NK cells control T cell responses by several different mechanisms: contact-dependent suppression via perforin and granzyme B, via engagement of natural cytotoxicity receptors (NCRs) or via the secretion of the immunosuppressive molecule adenosine (Fig. 1) [61]. Interestingly, while the numbers of NK cells are similar in control and MS patients, NK cells from MS patients depict a lack of regulatory functions [62]. In EAE, the role of NK cells is more tedious to evaluate, as murine NK cells do not express the surface marker CD56. However, expression of other markers can further identify regulatory murine NK cells. For example, enhancing regulatory NGK2<sup>+</sup> NK cells dampens EAE disease by killing T and microglia cells in the CNS in the acute phase of EAE. In MS, modulating CD56<sup>bright</sup> NK cell functions was used as a strategy to tackle inflammatory processes. Indeed, daclizumab, a drug used to treat MS and that blocked the IL-2R $\alpha$  chain (CD25), was associated with expansion and activation of CD56<sup>bright</sup> NK cells that further controlled T cell activation [63]. While daclizumab was efficient against MS flare, it was withdrawn from the market after several cases of systemic autoimmunity complications occurred [64].

### Role of foamy macrophages

Histological assessment of the resolving lesion in MS suggests that activated macrophages/microglia play a role in inflammation resolution [65]. Microglia and macrophages can

be both detrimental and beneficial during EAE and MS [8]. Of particular interest, foamy macrophage/microglia, which phagocytose myelin, are present in the resolving lesion [65] and MS lesions in general. Foamy macrophages/microglia in MS lesions express anti-inflammatory mediators such as IL-1ra, CCL18, IL-10, TGF- $\beta$ , and IL-4 [66]. CD163 is considered as a marker of anti-inflammatory M2 macrophages [67], and it was shown that macrophages in acute MS lesions strongly express CD163 [68]. When challenged with LPS, macrophages that have ingested myelin showed reduced production of the pro-inflammatory cytokines TNF $\alpha$ , IL-12p35, and IL-12/23p40 as compared to macrophages that have not ingested myelin [66]. Myelin uptake also increased the production of prostaglandin E2 and CCL18, two mediators that skew macrophages toward an M2 anti-inflammatory phenotype [69, 70]. Myelin ingestion can activate both peroxisome proliferator-activated receptor  $\beta/\delta$  (PPAR  $\beta/\delta$ ) [71] and liver X receptor (LXR) [72]. Those two nuclear receptors are activated by lipids and can repress an inflammatory phenotype [73]. It should be noted that LXR is not a purely anti-inflammatory receptor but can also promote inflammation in certain settings [74].

### Role of myeloid cells

In all MS lesions type, the macrophages/microglia outnumber the lymphocytes [75]. Like all the cells constituting the immune cell network, innate immune cells are both detrimental and beneficial during MS. Among innate immune cells, a potentially interesting subpopulation is the myeloid-derived suppressor cells (MDSCs) that could play an important role in MS (Fig. 1). MDSCs were initially discovered in cancer [76]. They are constituted of heterogeneous populations of immature myeloid cells which have the common ability to suppress T cell proliferation [77]. Their implication in MS is only starting to be investigated and is complicated by the difficulty to define MDSCs (summarized elsewhere [78]). MDSCs accumulate in the CNS during EAE, are able to suppress T cell proliferation, and promote cell death *in vitro* [79]. In addition, the ability of some blood-derived myeloid cells to suppress T cell proliferation was impaired during EAE [80]. Furthermore, those suppressive cells accumulate within the lymphoid compartment during EAE [81] and adoptive transfer of MDSCs attenuates EAE [81]. To corroborate those findings, young mice are resistant to EAE and show a higher frequency of MDSCs [82]. In patients suffering from a MS relapse, the number of circulating MDSCs is increased. Interferon- $\beta$ , a first-line treatment for MS, could act among many mechanisms by enhancing MDSC activity [83]. Studies are showing both increased and decreased frequencies of MDSCs in MS [81]. More recently, an inverted correlation between MDSCs and CD138<sup>+</sup> B cells was observed in the CSF of MS patients [84] and CD138<sup>+</sup> B cells are

positively correlated with CNS inflammation [85]. Based on RNA sequencing analysis, MDSCs could acquire their suppressive phenotype directly in the CNS. They further prevent the accumulation of B cells in the CNS and contribute to dampening the inflammatory reaction [84]. A few publications implicating MDSCs in MS resolution and their potent immune suppressive activity indicates that it is a promising field toward a better understanding of MS resolution.

### Role of TNF and related cytokine

Tumor necrosis factor (TNF) family genes are associated with MS. TNF- $\alpha$  is produced by several cell types including immune cells (macrophages or T cells) as well as CNS-specific cells (astrocytes or neurons) and can be detected in the CNS during MS [86]. It is active under two conformations: a transmembrane protein (tmTNF) and a soluble TNF (solTNF). TNF- $\alpha$  binds to two different receptors with different affinities: TNFR1, expressed on all cell types and TNFR2 mainly expressed on neurons, endothelial and immune cells [87]. SolTNF signals through TNFR1, mediating apoptosis, and chronic inflammation; tmTNF signals by binding both TNFR1 and TNFR2 and promotes resolution of inflammation [88]. TNF- $\alpha$  was initially proposed as a prototypical pro-inflammatory mediator and its expression is associated with MS disease progression [89]. However, blocking TNF- $\alpha$  pathway with lenercept, a recombinant soluble TNFR1 fusion protein strategy, failed as a treatment for MS and even lead to more exacerbations in patients treated with the drug compared to controls [90]. One possible explanation to this phenomenon is the inability of lenercept to enter the CNS [91]. However, treatments with soluble TNFR2 fusion protein (etanercept) or anti-TNF- $\alpha$  antibodies (infliximab) are also associated with the development of MS-like demyelinating lesions in patients treated for rheumatoid arthritis [92] suggesting that TNF- $\alpha$  is possibly actively involved in inflammation resolution and repair processes. First, TNF- $\alpha$  contributes to Treg expansion. Indeed, using *in vitro* coculture experiments with murine Foxp3<sup>+</sup> Tregs and effector T cells (Teffs), short-term exposure to TNF- $\alpha$  promotes Teff expansion, and a longer exposition to TNF- $\alpha$  promotes Tregs activation [93]. TNFR2-deficient mice fail to expand Tregs under septic challenge and depict a worse EAE disease course [94]. Furthermore, TNFR2 signaling contributes to tissue repair specifically in the CNS and promotes the proliferation of immature oligodendrocytes [95]. Finally, selective blockade of solTNF improves EAE outcome by enhancing remyelination and axon preservation [95]. In addition, a polymorphism in TNF-related apoptosis-induced ligand (TRAIL) gene, a type II transmembrane protein that can induce apoptosis, is observed

in MS [96]. As for TNF- $\alpha$ , the TRAIL/TRAIL-receptor pathway has double roles during neuroinflammation. First, activating TRAIL pathway induces neurotoxicity causing inflammation and cell death [97]. On the other hand, it contributes to inflammation resolution in the CNS as chronic blockade of TRAIL pathway promotes inflammation and demyelination during EAE [98]. In conclusion, the roles of TNF and TNF-related genes on inflammation resolution remain a difficult but exciting area of research in MS.

### Lipid mediators during EAE and multiple sclerosis

Specialized pro-resolving lipid mediators (SPMs) represent promising tools for the treatment of chronic inflammatory diseases. These highly potent anti-inflammatory lipids are derived metabolically from omega-3 essential fatty acids and include lipoxin a4 (LXA4) derived from arachidonic acid (AA), the D-series resolvins, protectins and maresins derived from docosahexaenoic acid (DHA), and the E-series resolvins derived from eicosapentaenoic acid (EPA). They are produced in the resolution phase of acute inflammation and have direct potent cellular responses to dampen inflammation and restore homeostasis [99]. SPMs affect both innate and adaptive immune cells by inhibiting DC maturation and function and/or modulating T and B cell phenotype and cytokine production [99]. Despite emerging data showing that SPMs might control neuroinflammation, research on these mediators in MS remains scarce. However, SPMs are produced in different tissues including the brain and cerebrospinal fluid [100] and accumulative evidence reveal that SPMs reduce neurodegenerative disease and protect neural cells in ischemic stroke or Alzheimer's disease [101, 102]. Furthermore, a connection between disease severity and lipid mediator production has been proposed as the resolving D1 and the neuroprotection D1 are increased in CSF of patients with highly active MS [103]. In contrast, bioinformatics analysis showed that the metabolites of PUFAs were downregulated in the plasma of EAE, which has also been reported in patients with MS [104]. In addition, oral administration of resolving D1 is effective in attenuating EAE disease progression by promoting Treg phenotype while attenuating the percentage of Th1/Th17 cells [104]. Similarly, the levels of resolving D1 decrease in the CSF of patients with neuromyelitis optica or MS compared to healthy patients, indicating dysfunction of resolution in MS patients [105]. Of note, researches in preclinical models and epidemiologic studies relating specific diets in the management of MS provide preliminary evidence that omega-3 fatty acid supplementation beneficially influences both EAE and MS disease [106]. These observations further strengthen the therapeutic potential of SPMs derived from omega-3 essential fatty acids in the resolution neuroinflammation.

### Contribution of non-hematopoietic component: CNS network

The CNS has been considered as an immune-privileged site for decades, based on an original finding that foreign tissue was not rejected when grafted in the CNS parenchyma [107]. The aim here is not to describe the mechanism at the origin of this immune-privilege but to discuss the putative role of non-hematopoietic cells in the resolution of inflammation. The intrinsically immuno-suppressive nature of the CNS is an important concept to consider when evoking local mechanisms that contribute to dampening an inflammatory reaction arising in the brain and spinal cord (Fig. 2a). The infiltration of peripheral leukocytes into the CNS is a key step at the origin of inflammatory cascade leading to MS relapses (Fig. 2b). In-between the blood circulation and the CNS parenchyma lies a “two-wall castle” [108] that needs to be crossed by leukocytes to trigger a relapse, the outer wall being either the highly specialized epithelial cells or endothelial cells respectively of the choroid plexus, i.e., the blood-cerebrospinal fluid barrier (BCSFB) and the CNS capillaries, i.e., blood-brain-barrier (BBB). The inner wall is called the glia limitans as is composed of astrocytic end-feet and the parenchymal basement membrane. In between those “two walls” is found the cerebrospinal fluid (CSF). Virtually, all the cellular networks constituting the CNS mediate pro-resolving mechanisms. The BBB constitutes a tightly regulated obstacle to leukocyte entry in the CNS and in itself can limit the infiltration by counter-regulatory mechanisms. The BCSFB and the CSF serve as selective gateways that shift the infiltrating leukocytes toward a pro-resolving phenotype. The astrocytes, by the production of anti-inflammatory signals and by forming a physical barrier, are key in the MS relapse resolutions (Fig. 2b). Finally, neurons besides their numerous functions are also able to modulate the phenotype of immune cells. The highly specialized tightly sealed endothelial cells of the BBB are an obstacle for inflammatory immune cell trafficking into CNS [109]. However, the BBB endothelium should not be considered as just a simple physical barrier. The regulation of its permeability results from a dynamic cellular cross-talk between endothelial cells, astrocytes, pericytes, microglial cells, and neurons. Together, these cells form the neurovascular unit (NVU) [110].

### Astrocytes

The impact of astrocytes in inflammation can be both detrimental and beneficial [111]. However, as the purpose of this review is to give an overview of the potential mechanism resolving an MS relapse, we will focus on protective mechanisms. Astrocytes produce anti-inflammatory cytokines in reaction to an inflammatory stimulus. Activation of human astrocytes by inflammatory cytokines induces the production of

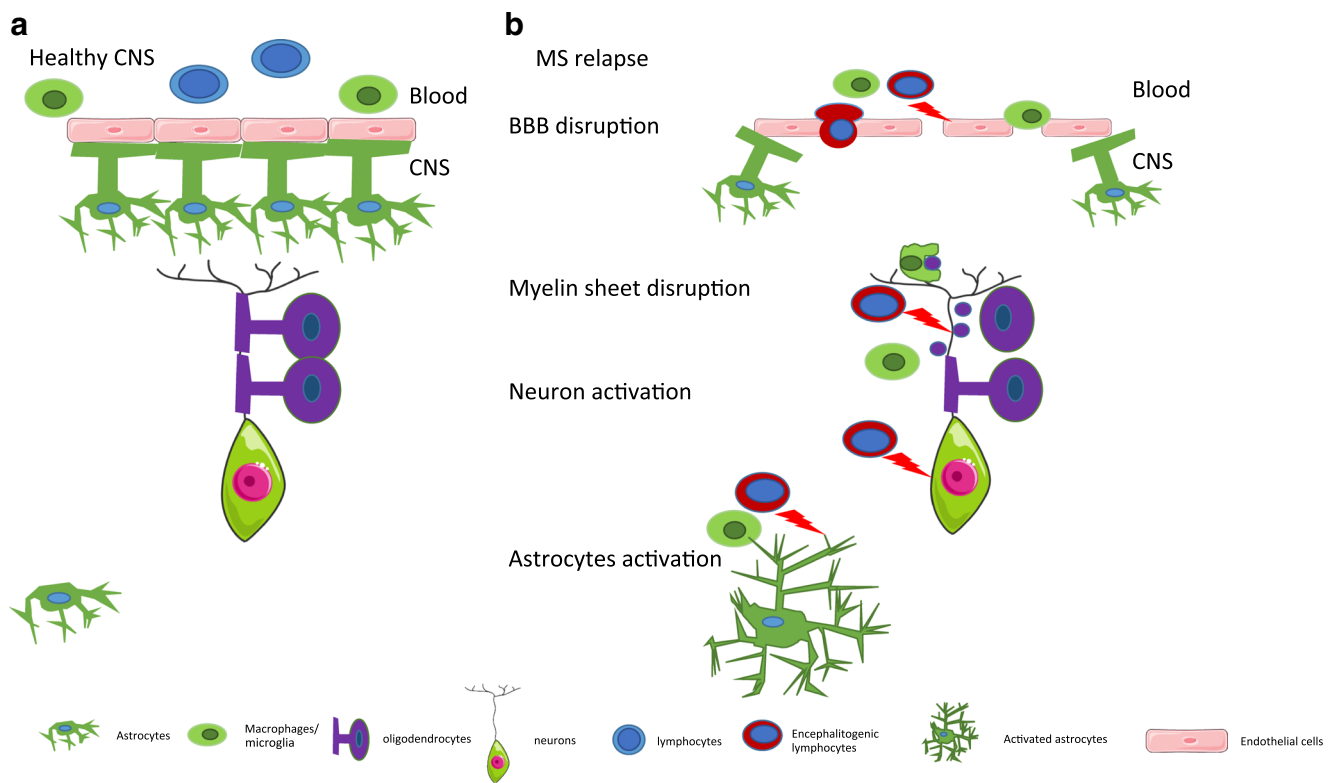


**Fig. 2** Schematic representation of the CNS at steady-state and during a relapse. **a** Healthy CNS. The endothelial cells of the BBB are ensheathed by astrocytic end-feet. The BBB is impermeable notably to leukocytes. Oligodendrocytes form the myelin layer that surrounds the axon. **b** CNS during MS. The blood-brain barrier is disrupted and the endothelial

permeability is increased. The astrocytic end-feet are detached, allowing leukocytes to transmigrate and trigger an inflammatory cascade. Inflammatory signals produced by leukocytes activate astrocytes. The myelin sheet is disrupted and phagocytes start to remove myelin debris. Neurons are further activated during the inflammatory reaction

IL-27 [112], which is further able to reduce EAE symptoms [34]. In accordance with those results, RRMS patients have increased levels of IL-27 in the CSF [37] and astrocytes show an increased immune-reactivity of the IL-27 subunit EB13 in MS lesions (Fig. 3) [37]. Furthermore, IL-6-deficient mice are resistant to EAE [113] and IL-6 activation of Gp130 in astrocytes is beneficial during EAE [114]. Using a CRE/Lox system, it has been observed that the specific depletion of gp130 in astrocytes leads to an increased EAE severity associated with a reduced number of FoxP3<sup>+</sup> CD4<sup>+</sup> Tregs cells, increased number of IL-17 and IFN- $\gamma$  producing CD4<sup>+</sup> T cells. The anti-inflammatory cytokines IL-10 and IL-4 are upregulated in activated astrocytes in MS lesions [115]. Moreover, activation of human-induced pluripotent stem cell-derived astrocytes [116] by a combination of IL-1 $\beta$  and TNF- $\alpha$  induces IL-10 secretion. Finally, the implication of a proliferation of active ligand (APRIL) was explored in MS and EAE: EAE disease is worsened in mice deficient for APRIL. APRIL is expressed in MS lesions, and stimulation of astrocytes with this molecule induces IL-10 secretion that is sufficient to reduce T cell proliferation [117].

We will now explore how the astrocytes-endothelial cellular cross-talk can regulate leukocyte trafficking in MS and

EAE. The leukocyte infiltration into the CNS during a relapse is associated with BBB disruption, and thus, restoring or maintaining the endothelial permeability could be a potential mechanism to prevent an excessive infiltration during a relapse. Astrocytes and endothelial cells cross-talk regulate and limit leukocyte infiltration. A key pathway in this cellular cross-talk is the Hedgehog pathway (Hh) [118]. Sonic-hedgehog (Shh) production by astrocytes leads to a decreased endothelial permeability. Blocking the Hh pathways during EAE leads to more severe disease and increases the number of INF- $\gamma$  and IL-17 producing T cells in the CNS. Finally, increasing amounts of Hh elements are found in MS active lesions. Netrin 1 is produced by the endothelium in response to astrocyte-derived Shh and is upregulated in MS and EAE lesions. Treatment with Netrin 1 can reduce BBB disruption and disease severity during EAE (Fig. 3) [119].

Furthermore, astrocytes limit leukocyte infiltration in the CNS by forming a physical barrier. Any kind of injury in the CNS will lead to the activation of astrocytes, which will be translated into morphological and functional changes called reactive astrogliosis [120]. Reactive astrogliosis can be both beneficial and detrimental. Thus, activated astrocytes

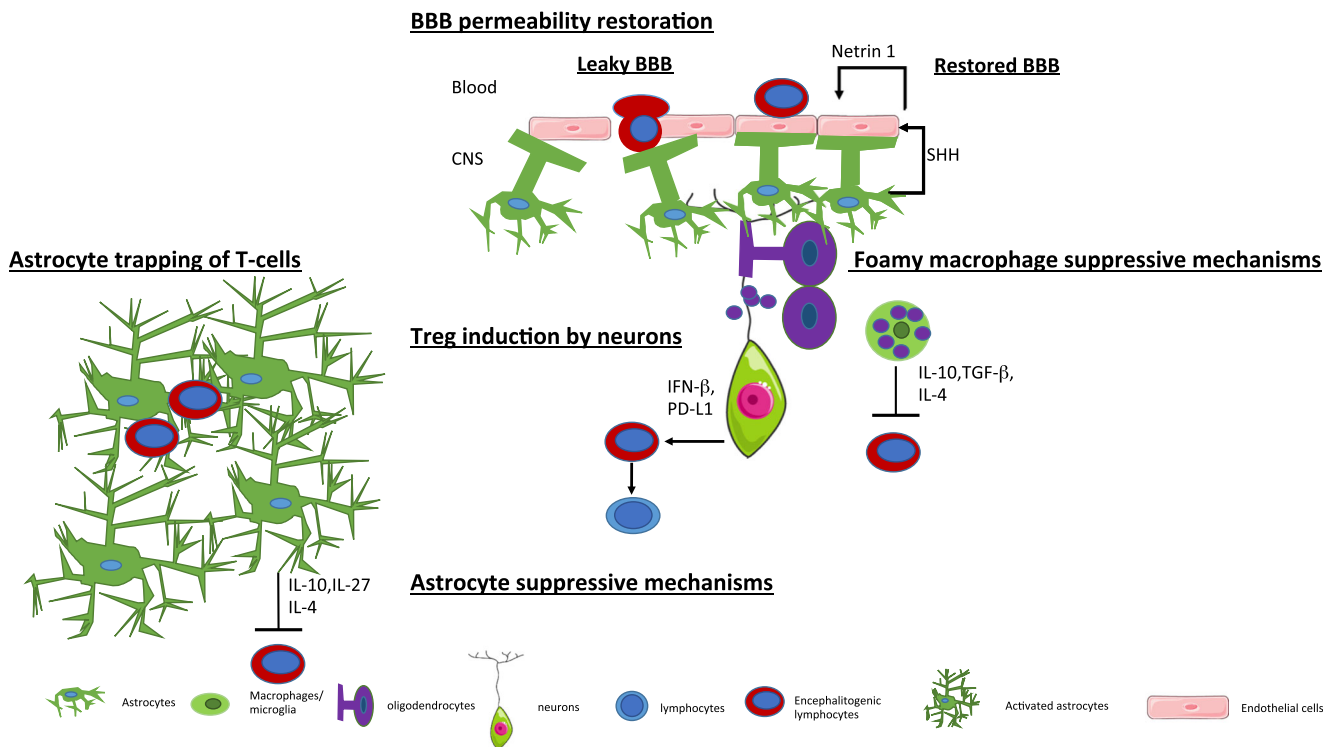


**Fig. 3** CNS network mechanism promoting resolution. BBB permeability restoration: Shh derived from astrocytes promotes Netrin 1 production by endothelial cells. This pathway reduces the BBB permeability and limits leukocyte infiltration. Astrocytes trap T-cells: activated astrocytes form a physical barrier that limits leukocyte infiltration. Astrocyte suppressive mechanisms: activated astrocytes

produce anti-inflammatory cytokines that repress encephalitogenic T cells. Treg induction by neurons: neurons can repolarize encephalitogenic T cell into FoxA1<sup>+</sup> Tregs. Foamy macrophage-suppressive mechanisms: foamy macrophages produce anti-inflammatory cytokine that contribute to inflammation resolution

attenuate the inflammatory reactions triggered by infiltrating leukocytes by forming a “scar-like perivascular barrier,” a physical barrier that prevents the spread of infiltrating cells to the adjacent CNS [121]. More recently, it has been shown that astrocytes upregulate the tight junction protein CLDN1, CLDN4, and JAM-A when activated [122]. Furthermore, activated astrocytes are able to form interconnected processes leading to a “trap” able to enclose lymphocytes (Fig. 3). This phenomenon is dependent on the expression of CLDN1, CLDN4, and JAM-A. Conditional mouse model deficient for CLDN4 in astrocytes leads to increased lesion sizes and an increased number of infiltrating CD4 T cells per mm<sup>2</sup> of lesions during EAE [122].

### Neurons actively participate in inflammation resolution during MS.

The contribution of neurons to the immune privileged site of the CNS is not well established; however, neurons harbor immunoregulatory functions. The interaction between neurons and encephalitogenic T cells induces the conversion of T cells into Foxp3<sup>+</sup> Tregs (Fig. 3) [123]. A new type of regulatory cells enriched in the CNS of a relapsing-remitting model of EAE was described [124].

The generation of these Tregs cells is dependent on the expression of IFN-β, and their suppressive functions are mediated by the co-inhibitory molecule program death ligand-1 (PDL-1) as well as the expression of the lineage-specification factor FoxA1 (or hepatocytes nuclear factor 3alpha or HNF3 alpha). PDL-1 being mentioned here, we take this opportunity to stress the role of checkpoint inhibitors. Given the increasing number of checkpoint inhibitors such as those that target the PD-1/PDL-1 pathway, notably in the field of oncology, the importance of those inhibitory signals in autoimmunity has been increasingly recognized. Altering checkpoint inhibitory pathways can trigger or worsen CNS autoimmune diseases. For an overview of the implication of those immune-checkpoint and their inhibitors in CNS autoimmune diseases, we refer the reader to the following review [125]. Using a CRE/Lox system, it has been proposed that IFN-β production by neurons is essential to generate FoxA1 Treg cells [126]. Selective depletion of IFN-β expression in neurons leads to an increased number of infiltrating cells in the spinal cord during EAE. The potential implication of neurons as active immune-modulators in MS is an interesting concept that could benefit from deeper investigations.

## Choroid plexus

The epithelial cells of the choroid plexus form the BCSFB. Like the BBB, epithelial cells of the choroid plexus are sealed together with tight junctions [127]. The barrier is thus not formed by the endothelial cells of the choroid plexus which are fenestrated [128]. So far, there is no documentation that crossing the blood-brain barrier could skew leukocytes toward an anti-inflammatory phenotype but the choroid plexus could be considered as a selective gate, facilitating the passage of regulatory cells to the CNS [129]. Moreover, once they have crossed the BCSFB, immune cells reach to cerebrospinal fluid that itself is a suppressive environment [130]. In a model of spinal cord injury, pro-resolving M2 macrophages are reaching the CNS by crossing the BCSFB rather than crossing the BBB at the site of the lesion [131]. The CSF and the choroid plexus are an M2-skewing environment, illustrated by the presence of high levels of IL-13 and TGF- $\beta$  [131]. However, the implication of the BCSFB as a selective pro-resolving gateway in the context of MS has not been investigated. So far, the evidence suggests that in this context, the choroid plexus rather serve as a primary route of entry for autoreactive lymphocytes [132]. The CCL20 chemokine ligand of CCR6 is constitutively expressed at the choroid plexus [132]. CCR6 is expressed by Th17 cells; it is suggested that during EAE, there are primary wave Th17 cells that reach the CNS by crossing the BCSFB. This primary inflammatory infiltrate would then trigger and the second wave of leukocyte infiltration that would reach the CNS via the BBB in a CCR6-independent manner [132]. It is not excluded that while choroid plexus could serve as an initial route of entry for autoreactive cells in EAE and MS; its pro-resolving nature illustrated in another context could be beneficial during the recovery phase. As Foxp3+Treg also expresses CCR6 [133] during EAE, the choroid plexus could also serve as a site for the recruitment of those cells.

## Endothelial cells in the BBB

Since leukocyte infiltration in the CNS is a tightly regulated process, multiple mechanisms are involved. One treatment strategy to target MS is to inhibit lymphocyte adhesion to the endothelium. Developmental locus-1 (DEL-1) is highly expressed in the CNS [134]. The absence of DEL-1 in the endothelium leads to an increased leukocyte function antigen 1 (LFA-1)-dependent adhesion to the endothelium. Interestingly, mutation in the gene encoding DEL-1 (EDIL3) is associated with MS [135]. DEL-1-deficient-mice display a more severe EAE than their wild-type counterpart [136]. This phenotype is associated with an increased BBB permeability and infiltration of neutrophils together with increased level of IL-17 possibly produced by CD8 T cells. DEL-1 expression is downregulated in chronic active lesions in MS and in EAE

[136]. Rather than being a simple adhesion inhibitor, DEL-1 seems to have a pro-resolution function by promoting efferocytosis, a process by which macrophages phagocytose apoptotic neutrophils and acquire a pro-resolution phenotype [137] notably by LXR activation. The implication of this pathway remains to be explored during MS.

## Impact of disease treatment on inflammation resolution

Multiple treatment strategies are available to dampen inflammation in MS. We will here discuss the potential impact of MS treatments on inflammation resolution, first with the treatment of relapse with high-dose of corticosteroids and then novel disease-modifying treatments (DMTs). We will focus on inductive therapies that induce a reset of the immune system and promote component of inflammation resolution.

### Treatment of MS relapse: glucocorticoids

MS course is influenced by the level of endogenous glucocorticoids (Gcs) that are mainly secreted from the adrenal gland in response to an activation of the hypothalamo-pituitary-adrenal (HPA) axis [138]. By interconverting active Gcs (cortisone, 11-dehydrocorticosterone), 11 $\beta$ -HSD modulates intracellular access of glucocorticoid to receptors. Type 1 11 $\beta$ -HSD (11 $\beta$ -HSD1) reactivates glucocorticoids and increases intracellular glucocorticoid concentration while type 2 11 $\beta$ -HSD (11 $\beta$ -HSD2) inactivates Gcs *in vivo*. MS patients show lower cortisol levels in the CSF during acute relapses that may be secondary to poor local activation of cortisone via 11 $\beta$ -HSD1 or to inactivation via 11 $\beta$ -HSD2. In the CNS, differential expression of 11 $\beta$ -HSD1 and 2 expressions in foamy macrophages possibly contribute to the resolution of acute inflammation in MS. The second important “neurosteroids” is the dehydroepiandrosterone (DHEA). In addition to cortisone (the natural metabolite), synthetic steroids are also substrates for the 11 $\beta$ -HSD enzymes. Synthetic Gcs have higher affinity, greater bioavailability, and are poorly metabolized, and thus persist in plasma much longer than endogenous glucocorticoids (cortisol). High-dose corticosteroid medication is thus used to shorten the duration of a relapse and to accelerate its recovery. Corticosteroids have robust anti-inflammatory properties [139], such as induction of T cell apoptosis and inhibition of BBB disruption. They further play an active role in the resolution of inflammation as they increase regulatory T (Treg) number and enhance their suppressive capacities [140]. Indeed, steroid treatment in mice increases the relative number of CD4<sup>+</sup>CD25<sup>+</sup>Treg cells, which are more resistant to GC-induced apoptosis due to a higher expression of Bcl-2 and increased levels of CTLA-4. In humans, the percentage of Treg cells in MS patients is increased after short-term GC therapy [141]. Effects on Treg cells presumably contribute to the

therapeutic efficacy of Gcs by favoring active resolution of inflammation during an MS relapse. However, glucocorticoids have no impact on the long-term MS disease course and are not considered as disease-modifying treatment (DMTs).

### Disease-modifying treatments

Disease-modifying treatments (DMTs) are divided in two main approaches: the first DMTs are efficacious through a mechanism of continuous immunosuppression; the second are induction therapies where DMTs reshape the immune system toward a new immune system less prone to disease activity. We will here focus on the second approach, not because it is more commonly used but because of its possible contribution to long-term inflammation resolution. The prototype of induction therapy is the autologous hematopoietic stem cell transplantation (aHSCT) that consists of first mobilization of CD34<sup>+</sup> hematopoietic stem cells, then an immunoablative conditioning followed by HSC transplantation. aHSCT enables recalibration of the immune system and restores the predominance of anti-inflammatory regulating factors over inflammatory effectors. These mechanisms may explain induction of long-lasting suppression of some autoimmune diseases by aHSCT with the development of a tolerant environment. Tregs are both quantitatively and qualitatively modified in MS patients after aHSCT (review in [142]). The effect of aHSCT on Bregs has not been evaluated in MS but Bregs are increased when aHSCT is performed in patients suffering from systemic sclerosis [143]. Increased PD-1 inhibitory signaling is another possible immunoregulatory mechanism by which aHSCT restores immune tolerance in MS patients with early expansion of PD-1<sup>+</sup>CD8<sup>+</sup>T cells and of PD-1-expressing CD19<sup>+</sup> B cells. PD-1/PDL pathways play a role in MS and in mouse model of EAE, blockade of PDL1 or PDL2 accelerates disease course and severity [144]. An association between PD-1 deficiency and MS progression is reported: PD-1 expression is higher on MBP-specific CD4<sup>+</sup> and CD8<sup>+</sup> T cells during remission compared to acute relapses [145].

In addition, alemtuzumab leads to a “reset of the immune system.” This treatment administered as a pulsed therapy targets CD52<sup>+</sup> cells and depletes T, B, and NK cells followed by an immune reconstitution. Alemtuzumab increased the anti-inflammatory IL-10 and TGF- $\beta$  cytokine levels within 6 months of treatment and further increase Treg percentage and function after 24 months post-treatment [146]. However, alemtuzumab increases the percentage of repopulated naïve/immature B cells and possibly the hyper-population of naïve B cell population regenerating before Tregs induce systemic loss of immune-tolerance and secondary autoimmunity that can be severe and limits its use in the clinic [147]. Finally, cladribine can be

considered as an inductive therapy. It is a purine analog, a pro-drug whose metabolite selectively accumulates in lymphocytes inducing specific lymphocyte depletion. Cladribine therapy may have a profile of immune-reconstitution closer to aHSCT compared to alemtuzumab [147].

### Open questions and concluding remarks

It is legitimate to argue that an inflammatory misbalance is at the origin of MS. Research on pro-inflammatory mechanisms in MS has been largely studied; however, the potential mechanisms that actively participate in resolving inflammation were scarcely evaluated. In fact, autoimmune diseases in general could come as much from an excess of inflammation as from a deficit of pro-resolutive mechanism or as a combination of both. For example, even if it is purely speculative, the DEL-1 mutation associated with MS [135] could result in a loss of function leading to enhanced leukocyte adhesion and transmigration across the BBB while at the same time, it could contribute to disrupting efferocytosis, an important process for inflammation resolution [148]. In MS, the lack of full resolution of inflammation probably participates to persistent chronic inflammation. For this reason, the comparison of immune responses between MS and other self-limited inflammatory diseases of the CNS like ADEM or viral encephalitis could help in understanding the specific mechanisms that lead to chronic inflammation. A first response to this question was addressed in pediatric neuroinflammatory diseases [149]. By comparing both abnormal effector and regulatory T cells, subsets in children with either MS or monophasic inflammatory CNS disorders, the authors could identify specific abnormalities in MS but not in other self-limited diseases. Only children with MS presented with both an exaggerated pro-inflammatory response of CD8<sup>+</sup> Teff cells that were resistant to suppression to Tregs as well as deficient suppressive capacities of Tregs (more specifically CD4<sup>+</sup>CD25<sup>hi</sup>CD127<sup>low</sup>Foxp3<sup>+</sup> Tregs) [149].

Furthermore, the resolution of inflammation is the results of a complex collaboration between the network of peripheral and resident immune cells together with the local cells of the CNS. Along the same lines, it is important to develop new models that specifically mimic inflammatory processes that take place in MS. Interestingly, an alternative rat EAE model that induces focal cortical demyelinating lesions could highlight that rapid resolution of inflammation contributes to more efficient remyelination [150]. A better understanding of this endogenous pro-resolutive mechanism could lead to novel therapeutic approaches. Notably, the use of SPMs for relapse treatment could be a promising new therapeutic approach also in MS. Similarly, favoring astrocytic reaction that prevents the

spread of the lesion could reduce the potential disability induced by a relapse. Favoring and accelerating inflammation resolution could be beneficial in terms of preventing the accumulation of disability that we see in RRMS patients.

In conclusion, the understanding of the immunopathogenic mechanisms involved in resolution of inflammation in MS remains an important research field. Thus, a better understanding of resolution of inflammation in MS could result in interesting alternative approaches toward improvement in the treatments of MS patients.

**Acknowledgements** The authors thank P. Dubois-Ferriere for proofreading the manuscript.

**Funding information** This work was supported by the Swiss National Science Foundation (no. PP00P3\_157476 to CP) and the Leenaards foundation. FR holds a MD-PhD grant from the Swiss National Science Foundation (no. 323630-183987 to FR).

### Compliance with ethical standards

**Conflict of interest** The authors declare that they have no conflict of interest.

**Open Access** This article is distributed under the terms of the Creative Commons Attribution 4.0 International License (<http://creativecommons.org/licenses/by/4.0/>), which permits unrestricted use, distribution, and reproduction in any medium, provided you give appropriate credit to the original author(s) and the source, provide a link to the Creative Commons license, and indicate if changes were made.

### References

- Dendrou CA, Fugger L, Friese MA (2015) Immunopathology of multiple sclerosis. *Nat Rev Immunol* 15:545–558
- Trapp BD, Nave KA (2008) Multiple sclerosis: an immune or neurodegenerative disorder? *Annu Rev Neurosci* 31:247–269
- Lublin FD, Reingold SC, Cohen JA, Cutter GR, Sorensen PS, Thompson AJ, Wolinsky JS, Balcer LJ, Banwell B, Barkhof F, Bebo B Jr, Calabresi PA, Clanet M, Comi G, Fox RJ, Freedman MS, Goodman AD, Inglesse M, Kappos L, Kieseier BC, Lincoln JA, Lubetzki C, Miller AE, Montalban X, O'Connor PW, Petkau J, Pozzilli C, Rudick RA, Sormani MP, Stuve O, Waubant E, Polman CH (2014) Defining the clinical course of multiple sclerosis: the 2013 revisions. *Neurology* 83:278–286
- Mosmann TR, Cherwinski H, Bond MW, Giedlin MA, Coffman RL (1986) Two types of murine helper T cell clone. I. Definition according to profiles of lymphokine activities and secreted proteins. *J Immunol* 136:2348–2357
- Wu X, Tian J, Wang S (2018) Insight into non-pathogenic Th17 cells in autoimmune diseases. *Front Immunol* 9:1112
- Pot C, Apetoh L, Kuchroo VK (2011) Type 1 regulatory T cells (Tr1) in autoimmunity. *Semin Immunol* 23:202–208
- Salou M, Garcia A, Michel L, Gainche-Salmon A, Loussoam D, Nicol B, Guillot F, Hulin P, Nedellec S, Baron D, Ramstein G, Soullillou JP, Brouard S, Nicot AB, Degauque N, Laplaud DA (2015) Expanded CD8 T-cell sharing between periphery and CNS in multiple sclerosis. *Ann Clin Transl Neurol* 2:609–622
- Grajchen E, Hendriks JJA, Bogie JFJ (2018) The physiology of foamy phagocytes in multiple sclerosis. *Acta Neuropathol Commun* 6:124
- Koutouros M, Berer K, Kawakami N, Wekerle H, Krishnamoorthy G (2014) Treg cells mediate recovery from EAE by controlling effector T cell proliferation and motility in the CNS. *Acta Neuropathol Commun* 2:163
- Montero E, Nussbaum G, Kaye JF, Perez R, Lage A, Ben-Nun A, Cohen IR (2004) Regulation of experimental autoimmune encephalomyelitis by CD4+, CD25+ and CD8+ T cells: analysis using depleting antibodies. *J Autoimmun* 23:1–7
- Reddy J, Illes Z, Zhang X, Encinas J, Pyrdol J, Nicholson L, Sobel RA, Wucherpfennig KW, Kuchroo VK (2004) Myelin proteolipid protein-specific CD4+CD25+ regulatory cells mediate genetic resistance to experimental autoimmune encephalomyelitis. *Proc Natl Acad Sci U S A* 101:15434–15439
- Noori-Zadeh A, Mesbah-Namin SA, Saboor-Yaraghi AA (2017) Epigenetic and gene expression alterations of FOXP3 in the T cells of EAE mouse model of multiple sclerosis. *J Neurol Sci* 375:203–208
- Schneider-Hohendorf T, Stenner MP, Weidenfeller C, Zozulya AL, Simon OJ, Schwab N, Wiendl H (2010) Regulatory T cells exhibit enhanced migratory characteristics, a feature impaired in patients with multiple sclerosis. *Eur J Immunol* 40:3581–3590
- Beers DR, Henkel JS, Zhao W, Wang J, Huang A, Wen S, Liao B, Appel SH (2011) Endogenous regulatory T lymphocytes ameliorate amyotrophic lateral sclerosis in mice and correlate with disease progression in patients with amyotrophic lateral sclerosis. *Brain* 134:1293–1314
- Kom T, Reddy J, Gao W, Bettelli E, Awasthi A, Petersen TR, Backstrom BT, Sobel RA, Wucherpfennig KW, Strom TB, Oukka M, Kuchroo VK (2007) Myelin-specific regulatory T cells accumulate in the CNS but fail to control autoimmune inflammation. *Nat Med* 13:423–431
- LaMothe RA, Kolte PN, Vo T, Ferrari JD, Gelsing TC, Wong J, Chan VT, Ahmed S, Srinivasan A, Deitemeyer P, Maldonado RA, Kishimoto TK (2018) Tolerogenic nanoparticles induce antigen-specific regulatory T cells and provide therapeutic efficacy and transferrable tolerance against experimental autoimmune encephalomyelitis. *Front Immunol* 9:281
- Keeler GD, Kumar S, Palaschak B, Silverberg EL, Markusic DM, Jones NT, Hoffman BE (2018) Gene therapy-induced antigen-specific Tregs inhibit neuro-inflammation and reverse disease in a mouse model of multiple sclerosis. *Mol Ther* 26:173–183
- Danikowski KM, Jayaraman S, Prabhakar BS (2017) Regulatory T cells in multiple sclerosis and myasthenia gravis. *J Neuroinflammation* 14:117
- Li YF, Zhang SX, Ma XW, Xue YL, Gao C, Li XY, Xu AD (2019) The proportion of peripheral regulatory T cells in patients with multiple sclerosis: a meta-analysis. *Mult Scler Relat Disord* 28:75–80
- Feger U, Luther C, Poeschel S, Melms A, Tolosa E, Wiendl H (2007) Increased frequency of CD4+ CD25+ regulatory T cells in the cerebrospinal fluid but not in the blood of multiple sclerosis patients. *Clin Exp Immunol* 147:412–418
- Lowther DE, Hafler DA (2012) Regulatory T cells in the central nervous system. *Immunol Rev* 248:156–169
- Gagliani N, Magnani CF, Huber S, Gianolini ME, Pala M, Liconalimon P, Guo B, Herbert DR, Bullfone A, Trentini F, Di Serio C, Bacchetta R, Andreani M, Brockmann L, Gregori S, Flavell RA, Roncarolo MG (2013) Coexpression of CD49b and LAG-3 identifies human and mouse T regulatory type 1 cells. *Nat Med* 19:739–746
- Apetoh L, Quintana FJ, Pot C, Joller N, Xiao S, Kumar D, Burns EJ, Sherr DH, Weiner HL, Kuchroo VK (2010) The aryl hydrocarbon receptor interacts with c-Maf to promote the differentiation

- of type 1 regulatory T cells induced by IL-27. *Nat Immunol* 11: 854–861
24. Pot C, Jin H, Awasthi A, Liu SM, Lai CY, Madan R, Sharpe AH, Karp CL, Miaw SC, Ho IC, Kuchroo VK (2009) Cutting edge: IL-27 induces the transcription factor c-Maf, cytokine IL-21, and the costimulatory receptor ICOS that coordinately act together to promote differentiation of IL-10-producing Tr1 cells. *J Immunol* 183: 797–801
  25. Beebe AM, Cua DJ, de Waal Malefyt R (2002) The role of interleukin-10 in autoimmune disease: systemic lupus erythematosus (SLE) and multiple sclerosis (MS). *Cytokine Growth Factor Rev* 13:403–412
  26. Barrat FJ, Cua DJ, Boonstra A, Richards DF, Crain C, Savelkoul HF, de Waal-Malefyt R, Coffman RL, Hawrylowicz CM, O'Garra A (2002) In vitro generation of interleukin 10-producing regulatory CD4(+) T cells is induced by immunosuppressive drugs and inhibited by T helper type 1 (Th1)- and Th2-inducing cytokines. *J Exp Med* 195:603–616
  27. Wildbaum G, Netzer N, Karin N (2002) Tr1 cell-dependent active tolerance blunts the pathogenic effects of determinant spreading. *J Clin Invest* 110:701–710
  28. Zhang X, Koldzic DN, Izikson L, Reddy J, Nazareno RF, Sakaguchi S, Kuchroo VK, Weiner HL (2004) IL-10 is involved in the suppression of experimental autoimmune encephalomyelitis by CD25+CD4+ regulatory T cells. *Int Immunol* 16:249–256
  29. Raverdeau M, Christofi M, Malara A, Wilk MM, Misiak A, Kuffova L, Yu T, McGinley AM, Quinn SM, Massilamany C, Reddy J, Forrester JV, Mills KH. 2019. Retinoic acid-induced autoantigen-specific type 1 regulatory T cells suppress autoimmunity. *EMBO Rep* 20
  30. Mayo L, Cunha AP, Madi A, Beynon V, Yang Z, Alvarez JI, Prat A, Sobel RA, Kobzik L, Lassmann H, Quintana FJ, Weiner HL (2016) IL-10-dependent Tr1 cells attenuate astrocyte activation and ameliorate chronic central nervous system inflammation. *Brain* 139:1939–1957
  31. Astier AL, Meiffren G, Freeman S, Hafler DA (2006) Alterations in CD46-mediated Tr1 regulatory T cells in patients with multiple sclerosis. *J Clin Invest* 116:3252–3257
  32. Martinez-Forero I, Garcia-Munoz R, Martinez-Pasamar S, Inoges S, Lopez-Diaz de Cerio A, Palacios R, Sepulcre J, Moreno B, Gonzalez Z, Fernandez-Diez B, Melero I, Bendandi M, Villoslada P (2008) IL-10 suppressor activity and ex vivo Tr1 cell function are impaired in multiple sclerosis. *Eur J Immunol* 38: 576–586
  33. Zubizarreta I, Florez-Grau G, Vila G, Cabezon R, Espana C, Andorra M, Saiz A, Llufrui S, Sepulveda M, Sola-Valls N, Martinez-Lapiscina EH, Pulido-Valdeolivas I, Casanova B, Martinez Gines M, Tellez N, Oreja-Guevara C, Espanol M, Trias E, Cid J, Juan M, Lozano M, Blanco Y, Steinman L, Benitez-Ribas D, Villoslada P (2019) Immune tolerance in multiple sclerosis and neuromyelitis optica with peptide-loaded tolerogenic dendritic cells in a phase 1b trial. *Proc Natl Acad Sci U S A* 116:8463–8470
  34. Batten M, Li J, Yi S, Kljavin NM, Danilenko DM, Lucas S, Lee J, de Sauvage FJ, Ghilardi N (2006) Interleukin 27 limits autoimmune encephalomyelitis by suppressing the development of interleukin 17-producing T cells. *Nat Immunol* 7:929–936
  35. Do J, Kim D, Kim S, Valentin-Torres A, Dvorina N, Jang E, Nagarajavel V, DeSilva TM, Li X, Ting AH, Vignali DAA, Stohlman SA, Baldwin WM 3rd, Min B (2017) Treg-specific IL-27 $\alpha$  deletion uncovers a key role for IL-27 in Treg function to control autoimmunity. *Proc Natl Acad Sci U S A* 114: 10190–10195
  36. Sweeney CM, Lonergan R, Basdeo SA, Kinsella K, Dungan LS, Higgins SC, Kelly PJ, Costelloe L, Tubridy N, Mills KH, Fletcher JM (2011) IL-27 mediates the response to IFN- $\beta$  therapy in multiple sclerosis patients by inhibiting Th17 cells. *Brain Behav Immun* 25:1170–1181
  37. Lalive PH, Kreutzfeldt M, Devergne O, Metz I, Bruck W, Merkler D, Pot C (2017) Increased interleukin-27 cytokine expression in the central nervous system of multiple sclerosis patients. *J Neuroinflammation* 14:144
  38. Koh DR, Fung-Leung WP, Ho A, Gray D, Acha-Orbea H, Mak TW (1992) Less mortality but more relapses in experimental allergic encephalomyelitis in CD8 $^{-/-}$  mice. *Science* 256:1210–1213
  39. Noble A, Zhao ZS, Cantor H (1998) Suppression of immune responses by CD8 cells. II. Qa-1 on activated B cells stimulates CD8 cell suppression of T helper 2 responses. *J Immunol* 160:566–571
  40. Hu D, Ikizawa K, Lu L, Sanchirico ME, Shinohara ML, Cantor H (2004) Analysis of regulatory CD8 T cells in Qa-1-deficient mice. *Nat Immunol* 5:516–523
  41. Saligrama N, Zhao F, Sikora MJ, Serratelli WS, Fernandes RA, Louis DM, Yao W, Ji X, Idoyaga J, Mahajan VB, Steinmetz LM, Chien YH, Hauser SL, Oksenberg JR, Garcia KC, Davis MM (2019) Opposing T cell responses in experimental autoimmune encephalomyelitis. *Nature* 572:481–487
  42. Correale J, Villa A (2008) Isolation and characterization of CD8+ regulatory T cells in multiple sclerosis. *J Neuroimmunol* 195:121–134
  43. Crawford MP, Yan SX, Ortega SB, Mehta RS, Hewitt RE, Price DA, Stastny P, Douek DC, Koup RA, Racke MK, Karandikar NJ (2004) High prevalence of autoreactive, neuroantigen-specific CD8+ T cells in multiple sclerosis revealed by novel flow cytometric assay. *Blood* 103:4222–4231
  44. Baughman EJ, Mendoza JP, Ortega SB, Ayers CL, Greenberg BM, Frohman EM, Karandikar NJ (2011) Neuroantigen-specific CD8+ regulatory T-cell function is deficient during acute exacerbation of multiple sclerosis. *J Autoimmun* 36:115–124
  45. Seidkhani-Nahal A, Noori-Zadeh A, Bakhtiyari S, Khosravi A (2019) Frequency of CD8(+) regulatory T cells in the multiple sclerosis patients: a systematic review and meta-analysis. *Acta Neurol Belg* 119:61–68
  46. Wolf SD, Dittel BN, Hardardottir F, Janeway CA Jr (1996) Experimental autoimmune encephalomyelitis induction in genetically B cell-deficient mice. *J Exp Med* 184:2271–2278
  47. Matsushita T, Yanaba K, Bouaziz JD, Fujimoto M, Tedder TF (2008) Regulatory B cells inhibit EAE initiation in mice while other B cells promote disease progression. *J Clin Invest* 118: 3420–3430
  48. Ray A, Mann MK, Basu S, Dittel BN (2011) A case for regulatory B cells in controlling the severity of autoimmune-mediated inflammation in experimental autoimmune encephalomyelitis and multiple sclerosis. *J Neuroimmunol* 230:1–9
  49. Fillatreau S, Sweeney CH, McGeachy MJ, Gray D, Anderton SM (2002) B cells regulate autoimmunity by provision of IL-10. *Nat Immunol* 3:944–950
  50. Mann MK, Maresz K, Shriver LP, Tan Y, Dittel BN (2007) B cell regulation of CD4+CD25+ T regulatory cells and IL-10 via B7 is essential for recovery from experimental autoimmune encephalomyelitis. *J Immunol* 178:3447–3456
  51. Khan AR, Hams E, Floudas A, Sparwasser T, Weaver CT, Fallon PG (2015) PD-L1hi B cells are critical regulators of humoral immunity. *Nat Commun* 6:5997
  52. Shen P, Roch T, Lampropoulou V, O'Connor RA, Stervbo U, Hilgenberg E, Ries S, Dang VD, Jaimes Y, Daridon C, Li R, Jouneau L, Boudinot P, Wilantri S, Sakwa I, Miyazaki Y, Leech MD, McPherson RC, Wirtz S, Neurath M, Hoehlig K, Meinel E, Grutzkau A, Grun JR, Horn K, Kuhl AA, Domer T, Bar-Or A, Kaufmann SHE, Anderton SM, Fillatreau S (2014) IL-35-producing B cells are critical regulators of immunity during autoimmune and infectious diseases. *Nature* 507:366–370

53. Bjarnadottir K, Benkhoucha M, Merkler D, Weber MS, Payne NL, Bernard CCA, Molnarfi N, Lalive PH (2016) B cell-derived transforming growth factor-beta1 expression limits the induction phase of autoimmune neuroinflammation. *Sci Rep* 6:34594
54. Knippenberg S, Peelen E, Smolders J, Thewissen M, Menheere P, Cohen Tervaert JW, Hupperts R, Damoiseaux J (2011) Reduction in IL-10 producing B cells (Breg) in multiple sclerosis is accompanied by a reduced naive/memory Breg ratio during a relapse but not in remission. *J Neuroimmunol* 239:80–86
55. Michel L, Chesneau M, Manceau P, Genty A, Garcia A, Salou M, Elong Ngono A, Pallier A, Jacq-Foucher M, Lefrère F, Wiertelowski S, Soullillou J-P, Degauque N, Laplaud D-A, Brouard S (2014) Unaltered regulatory B-cell frequency and function in patients with multiple sclerosis. *Clin Immunol* 155:198–208
56. de Andres C, Tejera-Alhambra M, Alonso B, Valor L, Teijeiro R, Ramos-Medina R, Mateos D, Faure F, Sanchez-Ramon S (2014) New regulatory CD19(+)/CD25(+) B-cell subset in clinically isolated syndrome and multiple sclerosis relapse. Changes after glucocorticoids. *J Neuroimmunol* 270:37–44
57. Machado-Santos J, Saji E, Troscher AR, Paunovic M, Liblau R, Gabriely G, Bien CG, Bauer J, Lassmann H (2018) The compartmentalized inflammatory response in the multiple sclerosis brain is composed of tissue-resident CD8+ T lymphocytes and B cells. *Brain* 141:2066–2082
58. Rojas OL, Probstel AK, Porfilio EA, Wang AA, Charabati M, Sun T, Lee DSW, Galicia G, Ramaglia V, Ward LA, Leung LYT, Najafi G, Khaleghi K, Garcillan B, Li A, Besla R, Naouar I, Cao EY, Chiaranunt P, Burrows K, Robinson HG, Allanach JR, Yam J, Luck H, Campbell DJ, Allman D, Brooks DG, Tomura M, Baumann R, Zamvil SS, Bar-Or A, Horwitz MS, Winer DA, Mortha A, Mackay F, Prat A, Osborne LC, Robbins C, Baranzini SE, Gommerman JL (2019) Recirculating intestinal IgA-producing cells regulate neuroinflammation via IL-10. *Cell* 176:610–24 e18
59. Caligiuri MA (2008) Human natural killer cells. *Blood* 112:461–469
60. Laroni A, Gandhi R, Beynon V, Weiner HL (2011) IL-27 imparts immunoregulatory function to human NK cell subsets. *PLoS One* 6:e26173
61. Gross CC, Schulte-Mecklenbeck A, Wiendl H, Marcenaro E, Kerlero de Rosbo N, Uccelli A, Laroni A (2016) Regulatory functions of natural killer cells in multiple sclerosis. *Front Immunol* 7:606
62. Laroni A (2019) Enhancing natural killer cells is beneficial in multiple sclerosis - Yes. *Mult Scler* 25:510–512
63. Gross CC, Schulte-Mecklenbeck A, Runzi A, Kuhlmann T, Posevitz-Fejfar A, Schwab N, Schneider-Hohendorf T, Herich S, Held K, Konjevic M, Hartwig M, Dormmair K, Hohlfeld R, Ziemssen T, Klotz L, Meuth SG, Wiendl H (2016) Impaired NK-mediated regulation of T-cell activity in multiple sclerosis is reconstituted by IL-2 receptor modulation. *Proc Natl Acad Sci U S A* 113:E2973–E2982
64. Rauer S, Stork L, Urbach H, Stathi A, Marx A, Suss P, Prinz M, Bruck W, Metz I (2018) Drug reaction with eosinophilia and systemic symptoms after daclizumab therapy. *Neurology* 91:e359–ee63
65. Raine CS (2017) Multiple sclerosis: the resolving lesion revealed. *J Neuroimmunol* 304:2–6
66. Boven LA, Van Meurs M, Van Zwam M, Wierenga-Wolf A, Hintzen RQ, Boot RG, Aerts JM, Amor S, Nieuwenhuis EE, Laman JD (2006) Myelin-laden macrophages are anti-inflammatory, consistent with foam cells in multiple sclerosis. *Brain* 129:517–526
67. Komohara Y, Hirahara J, Horikawa T, Kawamura K, Kiyota E, Sakashita N, Araki N, Takeya M (2006) AM-3K, an anti-macrophage antibody, recognizes CD163, a molecule associated with an anti-inflammatory macrophage phenotype. *J Histochem Cytochem* 54:763–771
68. Zhang Z, Zhang ZY, Schittenhelm J, Wu Y, Meyermann R, Schluesener HJ (2011) Parenchymal accumulation of CD163+ macrophages/microglia in multiple sclerosis brains. *J Neuroimmunol* 237:73–79
69. Wang Z, Brandt S, Medeiros A, Wang S, Wu H, Dent A, Serezani CH (2015) MicroRNA 21 is a homeostatic regulator of macrophage polarization and prevents prostaglandin E2-mediated M2 generation. *PLoS One* 10:e0115855
70. Schraufstatter IU, Zhao M, Khaldoyanidi SK, Discipio RG (2012) The chemokine CCL18 causes maturation of cultured monocytes to macrophages in the M2 spectrum. *Immunology* 135:287–298
71. Bogie JF, Jorissen W, Mailleux J, Nijland PG, Zelcer N, Vanmierlo T, Van Horsen J, Stinissen P, Hellings N, Hendriks JJ (2013) Myelin alters the inflammatory phenotype of macrophages by activating PPARs. *Acta Neuropathol Commun* 1:43
72. Bogie JF, Timmermans S, Huynh-Thu VA, Irrthum A, Smeets HJ, Gustafsson JA, Steffensen KR, Mulder M, Stinissen P, Hellings N, Hendriks JJ (2012) Myelin-derived lipids modulate macrophage activity by liver X receptor activation. *PLoS One* 7:e44998
73. Kidani Y, Bensing SJ (2012) Liver X receptor and peroxisome proliferator-activated receptor as integrators of lipid homeostasis and immunity. *Immunol Rev* 249:72–83
74. Vigne S, Chalmin F, Duc D, Clottu AS, Apetoh L, Lobaccaro JA, Christen I, Zhang J, Pot C (2017) IL-27-induced type 1 regulatory T-cells produce oxysterols that constrain IL-10 production. *Front Immunol* 8:1184
75. Kuhlmann T, Ludwin S, Prat A, Antel J, Bruck W, Lassmann H (2017) An updated histological classification system for multiple sclerosis lesions. *Acta Neuropathol* 133:13–24
76. Lappat EJ, Cawein M (1964) A study of the leukemoid response to transplantable a-280 tumor in mice. *Cancer Res* 24:302–311
77. Crook KR, Liu P (2014) Role of myeloid-derived suppressor cells in autoimmune disease. *World J Immunol* 4:26–33
78. Cassetta L, Bækkevold ES, Brandau S, Buijok A, Cassatella MA, Dorhoi A, Krieg C, Lin A, Lore K, Marini O, Pollard JW, Roussel M, Scapini P, Umansky V, Adema GJ (2019) Deciphering myeloid-derived suppressor cells: isolation and markers in humans, mice and non-human primates. *Cancer Immunol Immunother* 68:687–697
79. Moline-Velazquez V, Cuervo H, Vila-Del Sol V, Ortega MC, Clemente D, de Castro F (2011) Myeloid-derived suppressor cells limit the inflammation by promoting T lymphocyte apoptosis in the spinal cord of a murine model of multiple sclerosis. *Brain Pathol* 21:678–691
80. Slaney CY, Toker A, La Flamme A, Backstrom BT, Harper JL (2011) Naive blood monocytes suppress T-cell function. A possible mechanism for protection from autoimmunity. *Immunol Cell Biol* 89:7–13
81. Ioannou M, Alissafi T, Lazaridis I, Deraos G, Matsoukas J, Gravanis A, Mastorodemos V, Plaitakis A, Sharpe A, Boumpas D, Verginis P (2012) Crucial role of granulocytic myeloid-derived suppressor cells in the regulation of central nervous system autoimmune disease. *J Immunol* 188:1136–1146
82. Hertenberg D, Lehmann-Horn K, Kinzel S, Husterer V, Cravens PD, Kieseier BC, Hemmer B, Bruck W, Zamvil SS, Stuve O, Weber MS (2013) Developmental maturation of innate immune cell function correlates with susceptibility to central nervous system autoimmunity. *Eur J Immunol* 43:2078–2088
83. Melero-Jerez C, Suardiaz M, Lebron-Galan R, Marin-Banasco C, Oliver-Martos B, Machin-Diaz I, Fernandez O, de Castro F, Clemente D (2019) The presence and suppressive activity of myeloid-derived suppressor cells are potentiated after interferon-

- beta treatment in a murine model of multiple sclerosis. *Neurobiol Dis* 127:13–31
84. Knier B, Hiltensperger M, Sie C, Aly L, Lepenmetier G, Engleitner T, Garg G, Muschaweckh A, Mitsdorffer M, Koedel U, Hochst B, Knolle P, Gunzer M, Hemmer B, Rad R, Merkler D, Korn T (2018) Myeloid-derived suppressor cells control B cell accumulation in the central nervous system during autoimmunity. *Nat Immunol* 19:1341–1351
  85. Cepok S, Rosche B, Grummel V, Vogel F, Zhou D, Sayn J, Sommer N, Hartung HP, Hemmer B (2005) Short-lived plasma blasts are the main B cell effector subset during the course of multiple sclerosis. *Brain* 128:1667–1676
  86. Hofman FM, Hinton DR, Johnson K, Merrill JE (1989) Tumor necrosis factor identified in multiple sclerosis brain. *J Exp Med* 170:607–612
  87. Pegoretti V, Baron W, Laman JD, Eisel ULM (2018) Selective modulation of TNF-TNFRs signaling: insights for multiple sclerosis treatment. *Front Immunol* 9:925
  88. Probert L (2015) TNF and its receptors in the CNS: the essential, the desirable and the deleterious effects. *Neuroscience* 302:2–22
  89. Sharief MK, Hentges R (1991) Association between tumor necrosis factor-alpha and disease progression in patients with multiple sclerosis. *N Engl J Med* 325:467–472
  90. 1999. TNF neutralization in MS: results of a randomized, placebo-controlled multicenter study. The Lenercept Multiple Sclerosis Study Group and The University of British Columbia MS/MRI Analysis Group. *Neurology* 53: 457–65
  91. Robinson WH, Genovese MC, Moreland LW (2001) Demyelinating and neurologic events reported in association with tumor necrosis factor alpha antagonism: by what mechanisms could tumor necrosis factor alpha antagonists improve rheumatoid arthritis but exacerbate multiple sclerosis? *Arthritis Rheum* 44:1977–1983
  92. Sicotte NL, Voskuhl RR (2001) Onset of multiple sclerosis associated with anti-TNF therapy. *Neurology* 57:1885–1888
  93. Chen X, Baumel M, Mannel DN, Howard OM, Oppenheim JJ (2007) Interaction of TNF with TNF receptor type 2 promotes expansion and function of mouse CD4+CD25+ T regulatory cells. *J Immunol* 179:154–161
  94. Veroni C, Gabriele L, Canini I, Castiello L, Coccia E, Remoli ME, Columba-Cabezas S, Arico E, Aloisi F, Agresti C (2010) Activation of TNF receptor 2 in microglia promotes induction of anti-inflammatory pathways. *Mol Cell Neurosci* 45:234–244
  95. Madsen PM, Motti D, Karmally S, Szymkowski DE, Lambertsen KL, Bethea JR, Brambilla R (2016) Oligodendroglial TNFR2 mediates membrane TNF-dependent repair in experimental autoimmune encephalomyelitis by promoting oligodendrocyte differentiation and remyelination. *J Neurosci* 36:5128–5143
  96. Lopez-Gomez C, Fernandez O, Garcia-Leon JA, Pinto-Medel MJ, Oliver-Martos B, Ortega-Pinazo J, Suardiaz M, Garcia-Trujillo L, Guijarro-Castro C, Benito-Leon J, Prat I, Varade J, Alvarez-Lafuente R, Urcelay E, Leyva L (2011) TRAIL/TRAIL receptor system and susceptibility to multiple sclerosis. *PLoS One* 6: e21766
  97. Nitsch R, Bechmann I, Deisz RA, Haas D, Lehmann TN, Wendling U, Zipp F (2000) Human brain-cell death induced by tumour-necrosis-factor-related apoptosis-inducing ligand (TRAIL). *Lancet* 356:827–828
  98. Hilliard B, Wilmen A, Seidel C, Liu TS, Goke R, Chen Y (2001) Roles of TNF-related apoptosis-inducing ligand in experimental autoimmune encephalomyelitis. *J Immunol* 166:1314–1319
  99. Duffney PF, Falsetta ML, Rackow AR, Thatcher TH, Phipps RP, Sime PJ (2018) Key roles for lipid mediators in the adaptive immune response. *J Clin Invest* 128:2724–2731
  100. Hong S, Gronert K, Devchand PR, Moussignac RL, Serhan CN (2003) Novel docosatrienes and 17S-resolvins generated from docosahexaenoic acid in murine brain, human blood, and glial cells. Autacoids in anti-inflammation. *J Biol Chem* 278:14677–14687
  101. Marcheselli VL, Hong S, Lukiw WJ, Tian XH, Gronert K, Musto A, Hardy M, Gimenez JM, Chiang N, Serhan CN, Bazan NG (2003) Novel docosanoids inhibit brain ischemia-reperfusion-mediated leukocyte infiltration and pro-inflammatory gene expression. *J Biol Chem* 278:43807–43817
  102. Zhu M, Wang X, Hjorth E, Colas RA, Schroeder L, Granholm AC, Serhan CN, Schultzberg M (2016) Pro-resolving lipid mediators improve neuronal survival and increase Abeta42 phagocytosis. *Mol Neurobiol* 53:2733–2749
  103. Pruss H, Rosche B, Sullivan AB, Brommer B, Wengert O, Gronert K, Schwab JM (2013) Proresolution lipid mediators in multiple sclerosis - differential, disease severity-dependent synthesis - a clinical pilot trial. *PLoS One* 8:e55859
  104. Poisson LM, Suhail H, Singh J, Datta I, Denic A, Labuzek K, Hoda MN, Shankar A, Kumar A, Cerghet M, Elias S, Mohny RP, Rodriguez M, Rattan R, Mangalam AK, Giri S (2015) Untargeted plasma metabolomics identifies endogenous metabolite with drug-like properties in chronic animal model of multiple sclerosis. *J Biol Chem* 290:30697–30712
  105. Wang X, Jiao W, Lin M, Lu C, Liu C, Wang Y, Ma D, Wang X, Yin P, Feng J, Zhu J, Zhu M (2019) Resolution of inflammation in neuromyelitis optica spectrum disorders. *Mult Scler Relat Disord* 27:34–41
  106. Sedighian M, Djafarian K, Dabiri S, Abdollahi M, Shab-Bidar S (2019) Effect of omega-3 supplementation on expanded disability status scale and inflammatory cytokines in multiple sclerosis: a systematic review and meta-analysis of randomized controlled trials. *CNS Neurol Disord Drug Targets*
  107. Medawar PB (1948) Immunity to homologous grafted skin; the fate of skin homografts transplanted to the brain, to subcutaneous tissue, and to the anterior chamber of the eye. *Br J Exp Pathol* 29: 58–69
  108. Engelhardt B, Coisne C (2011) Fluids and barriers of the CNS establish immune privilege by confining immune surveillance to a two-walled castle moat surrounding the CNS castle. *Fluids Barriers CNS* 8:4
  109. Takeshita Y, Ransohoff RM (2012) Inflammatory cell trafficking across the blood-brain barrier: chemokine regulation and in vitro models. *Immunol Rev* 248:228–239
  110. Muoio V, Persson PB, Sendeski MM (2014) The neurovascular unit - concept review. *Acta Physiol (Oxf)* 210:790–798
  111. Colombo E, Farina C (2016) Astrocytes: key regulators of neuroinflammation. *Trends Immunol* 37:608–620
  112. Senecal V, Deblois G, Beauseigle D, Schneider R, Brandenburg J, Newcombe J, Moore CS, Prat A, Antel J, Arbour N (2016) Production of IL-27 in multiple sclerosis lesions by astrocytes and myeloid cells: modulation of local immune responses. *Glia* 64:553–569
  113. Okuda Y, Sakoda S, Bernard CC, Fujimura H, Saeki Y, Kishimoto T, Yanagihara T (1998) IL-6-deficient mice are resistant to the induction of experimental autoimmune encephalomyelitis provoked by myelin oligodendrocyte glycoprotein. *Int Immunol* 10: 703–708
  114. Haroon F, Drogemuller K, Handel U, Brunn A, Reinhold D, Nishanth G, Mueller W, Trautwein C, Ernst M, Deckert M, Schluter D (2011) Gp130-dependent astrocytic survival is critical for the control of autoimmune central nervous system inflammation. *J Immunol* 186:6521–6531
  115. Hulshof S, Montagne L, De Groot CJ, Van Der Valk P (2002) Cellular localization and expression patterns of interleukin-10, interleukin-4, and their receptors in multiple sclerosis lesions. *Glia* 38:24–35

116. Perriot S, Mathias A, Perriard G, Canales M, Jonkmans N, Merienne N, Meunier C, El Kassir L, Perrier AL, Laplaud DA, Schlupe M, Deglon N, Du Pasquier R (2018) Human induced pluripotent stem cell-derived astrocytes are differentially activated by multiple sclerosis-associated cytokines. *Stem Cell Rep* 11:1199–1210
117. Baert L, Benkhoucha M, Popa N, Ahmed MC, Manfroi B, Boutonnat J, Sturm N, Raguenez G, Tessier M, Casez O, Marignier R, Ahmadi M, Broisat A, Ghezzi C, Rivat C, Sonrier C, Hahne M, Baeten D, Vives RR, Lortat-Jacob H, Marche PN, Schneider P, Lassmann HP, Boucraut J, Lalive PH, Huard B (2019) A proliferation-inducing ligand-mediated anti-inflammatory response of astrocytes in multiple sclerosis. *Ann Neurol* 85:406–420
118. Alvarez JI, Dodelet-Devillers A, Kebir H, Ifergan I, Fabre PJ, Terouz S, Sabbagh M, Wosik K, Bourbonniere L, Bernard M, van Horssen J, de Vries HE, Charron F, Prat A (2011) The Hedgehog pathway promotes blood-brain barrier integrity and CNS immune quiescence. *Science* 334:1727–1731
119. Podjaski C, Alvarez JI, Bourbonniere L, Larouche S, Terouz S, Bin JM, Lecuyer MA, Saint-Laurent O, Larochelle C, Darlington PJ, Arbour N, Antel JP, Kennedy TE, Prat A (2015) Netrin 1 regulates blood-brain barrier function and neuroinflammation. *Brain* 138:1598–1612
120. Pekny M, Pekna M (2016) Reactive gliosis in the pathogenesis of CNS diseases. *Biochim Biophys Acta* 1862:483–491
121. Voskuhl RR, Peterson RS, Song B, Ao Y, Morales LB, Tiwari-Woodruff S, Sofroniew MV (2009) Reactive astrocytes form scar-like perivascular barriers to leukocytes during adaptive immune inflammation of the CNS. *J Neurosci* 29:11511–11522
122. Homg S, Therattil A, Moyon S, Gordon A, Kim K, Argaw AT, Hara Y, Mariani JN, Sawai S, Flodby P, Crandall ED, Borok Z, Sofroniew MV, Chapouly C, John GR (2017) Astrocytic tight junctions control inflammatory CNS lesion pathogenesis. *J Clin Invest* 127:3136–3151
123. Liu Y, Teige I, Birmir B, Issazadeh-Navikas S (2006) Neuron-mediated generation of regulatory T cells from encephalitogenic T cells suppresses EAE. *Nat Med* 12:518–525
124. Liu Y, Carlsson R, Comabella M, Wang J, Kosicki M, Carrion B, Hasan M, Wu X, Montalban X, Dziegiel MH, Sellebjerg F, Sorensen PS, Helin K, Issazadeh-Navikas S (2014) FoxA1 directs the lineage and immunosuppressive properties of a novel regulatory T cell population in EAE and MS. *Nat Med* 20:272–282
125. Joller N, Peters A, Anderson AC, Kuchroo VK (2012) Immune checkpoints in central nervous system autoimmunity. *Immunol Rev* 248:122–139
126. Liu Y, Marin A, Ejlerskov P, Rasmussen LM, Prinz M, Issazadeh-Navikas S (2017) Neuronal IFN-beta-induced PI3K/Akt-FoxA1 signalling is essential for generation of FoxA1(+)Treg cells. *Nat Commun* 8:14709
127. Redzic Z (2011) Molecular biology of the blood-brain and the blood-cerebrospinal fluid barriers: similarities and differences. *Fluids Barriers CNS* 8:3
128. Wolburg H, Paulus W (2010) Choroid plexus: biology and pathology. *Acta Neuropathol* 119:75–88
129. Shechter R, London A, Schwartz M (2013) Orchestrated leukocyte recruitment to immune-privileged sites: absolute barriers versus educational gates. *Nat Rev Immunol* 13:206–218
130. Gordon LB, Nolan SC, Ksander BR, Knopf PM, Harling-Berg CJ (1998) Normal cerebrospinal fluid suppresses the in vitro development of cytotoxic T cells: role of the brain microenvironment in CNS immune regulation. *J Neuroimmunol* 88:77–84
131. Shechter R, Miller O, Yovel G, Rosenzweig N, London A, Ruckh J, Kim KW, Klein E, Kalchenko V, Bendel P, Lira SA, Jung S, Schwartz M (2013) Recruitment of beneficial M2 macrophages to injured spinal cord is orchestrated by remote brain choroid plexus. *Immunity* 38:555–569
132. Reboldi A, Coisne C, Baumjohann D, Benvenuto F, Bottinelli D, Lira S, Uccelli A, Lanzavecchia A, Engelhardt B, Sallusto F (2009) C-C chemokine receptor 6-regulated entry of TH-17 cells into the CNS through the choroid plexus is required for the initiation of EAE. *Nat Immunol* 10:514–523
133. Yamazaki T, Yang XO, Chung Y, Fukunaga A, Nurieva R, Pappu B, Martin-Orozco N, Kang HS, Ma L, Panopoulos AD, Craig S, Watowich SS, Jetten AM, Tian Q, Dong C (2008) CCR6 regulates the migration of inflammatory and regulatory T cells. *J Immunol* 181:8391–8401
134. Choi EY, Chavakis E, Czabanka MA, Langer HF, Fraemohs L, Economopoulou M, Kundu RK, Orlandi A, Zheng YY, Prieto DA, Ballantyne CM, Constant SL, Aird WC, Papayannopoulou T, Gahmberg CG, Udey MC, Vajkoczy P, Quertermous T, Dimmeler S, Weber C, Chavakis T (2008) Del-1, an endogenous leukocyte-endothelial adhesion inhibitor, limits inflammatory cell recruitment. *Science* 322:1101–1104
135. Goris A, Sawcer S, Vandenbroeck K, Carton H, Billiau A, Setakis E, Compston A, Dubois B (2003) New candidate loci for multiple sclerosis susceptibility revealed by a whole genome association screen in a Belgian population. *J Neuroimmunol* 143:65–69
136. Choi EY, Lim JH, Neuwirth A, Economopoulou M, Chatzigeorgiou A, Chung KJ, Bittner S, Lee SH, Langer H, Samus M, Kim H, Cho GS, Ziemssen T, Bdeir K, Chavakis E, Koh JY, Boon L, Hosur K, Bornstein SR, Meuth SG, Hajishengallis G, Chavakis T (2015) Developmental endothelial locus-1 is a homeostatic factor in the central nervous system limiting neuroinflammation and demyelination. *Mol Psychiatry* 20:880–888
137. Kourtzelis I, Li X, Mitroulis I, Grosser D, Kajikawa T, Wang B, Grzybek M, von Renesse J, Czogalla A, Troullinaki M, Ferreira A, Doreth C, Ruppova K, Chen LS, Hosur K, Lim JH, Chung KJ, Grossklaus S, Tausche AK, Joosten LAB, Moutsopoulos NM, Wielockx B, Castrillo A, Korostoff JM, Coskun U, Hajishengallis G, Chavakis T (2019) DEL-1 promotes macrophage efferocytosis and clearance of inflammation. *Nat Immunol* 20:40–49
138. Heidbrink C, Hausler SF, Buttman M, Ossadnik M, Strik HM, Keller A, Buck D, Verbraak E, van Meurs M, Krockenberger M, Mehling M, Mittelbronn M, Laman JD, Wiendl H, Wischhusen J (2010) Reduced cortisol levels in cerebrospinal fluid and differential distribution of 11beta-hydroxysteroid dehydrogenases in multiple sclerosis: implications for lesion pathogenesis. *Brain Behav Immun* 24:975–984
139. Tischner D, Reichardt HM (2007) Glucocorticoids in the control of neuroinflammation. *Mol Cell Endocrinol* 275:62–70
140. Chen X, Murakami T, Oppenheim JJ, Howard OMZ (2004) Differential response of murine CD4+CD25+ and CD4+CD25-T cells to dexamethasone-induced cell death. *Eur J Immunol* 34:859–869
141. Navarro J, Aristimuno C, Sanchez-Ramon S, Vigil D, Martinez-Gines ML, Fernandez-Cruz E, de Andres C (2006) Circulating dendritic cells subsets and regulatory T-cells at multiple sclerosis relapse: differential short-term changes on corticosteroids therapy. *J Neuroimmunol* 176:153–161
142. Massey JC, Sutton IJ, Ma DDF, Moore JJ (2018) Regenerating immunotolerance in multiple sclerosis with autologous hematopoietic stem cell transplant. *Front Immunol* 9:410
143. Arruda LCM, Malmegrim KCR, Lima-Junior JR, Clave E, Dias JBE, Moraes DA, Douay C, Fournier I, Moins-Teisserenc H, Alberdi AJ, Covas DT, Simoes BP, Lansiaux P, Toubert A, Oliveira MC (2018) Immune rebound associates with a favorable clinical response to autologous HSCT in systemic sclerosis patients. *Blood Adv* 2:126–141

144. Salama AD, Chitnis T, Imitola J, Ansari MJ, Akiba H, Tushima F, Azuma M, Yagita H, Sayegh MH, Khoury SJ (2003) Critical role of the programmed death-1 (PD-1) pathway in regulation of experimental autoimmune encephalomyelitis. *J Exp Med* 198:71–78
145. Trabattoni D, Saresella M, Pavecchi M, Marventano I, Mendozzi L, Rovaris M, Caputo D, Borelli M, Clerici M (2009) Costimulatory pathways in multiple sclerosis: distinctive expression of PD-1 and PD-L1 in patients with different patterns of disease. *J Immunol* 183:4984–4993
146. De Mercanti S, Rolla S, Cucci A, Bardina V, Cocco E, Vladic A, Soldo-Butkovic S, Habek M, Adamec I, Horakova D, Annovazzi P, Novelli F, Durelli L, Clerico M (2016) Alemtuzumab long-term immunologic effect: Treg suppressor function increases up to 24 months. *Neurol Neuroimmunol Neuroinflamm* 3:e194
147. Baker D, Herrod SS, Alvarez-Gonzalez C, Giovannoni G, Schmierer K (2017) Interpreting lymphocyte reconstitution data from the pivotal phase 3 trials of alemtuzumab. *JAMA Neurol* 74:961–969
148. Yurdagul A Jr, Doran AC, Cai B, Fredman G, Tabas IA (2017) Mechanisms and consequences of defective efferocytosis in atherosclerosis. *Front Cardiovasc Med* 4:86
149. Mexhitaj I, Nyirenda MH, Li R, O'Mahony J, Rezk A, Rozenberg A, Moore CS, Johnson T, Sadovnick D, Collins DL, Arnold DL, Gran B, Yeh EA, Marrie RA, Banwell B, Bar-Or A (2019) Abnormal effector and regulatory T cell subsets in paediatric-onset multiple sclerosis. *Brain* 142:617–632
150. Merkler D, Ernting T, Kerschensteiner M, Bruck W, Stadelmann C (2006) A new focal EAE model of cortical demyelination: multiple sclerosis-like lesions with rapid resolution of inflammation and extensive remyelination. *Brain* 129:1972–1983

**Publisher's note** Springer Nature remains neutral with regard to jurisdictional claims in published maps and institutional affiliations.

## **6. Manuscript N°4: Endothelial-derived oxysterols regulate myeloid-derived suppressor cell expansion at the blood-brain barrier**

This manuscript was submitted to EMBO molecular medicine and was then transferred to EMBO reports where it is currently (31.05.2022) under review. In addition, the abstract of this project was selected for oral presentations in international congresses, including the 37<sup>th</sup> congress of the European committee for treatment and research in multiple sclerosis (ECTRIMS 2021) for which I was awarded a free registration and the 15<sup>th</sup> international meeting of neuroimmunology (ISNI 2021). I also received the award of the best oral presentation at European network for oxysterol research (ENOR) meeting 2019 and 2021.

It is the main manuscript of my thesis. We here describe a new floxed reporter Ch25h Knock-in mouse model. This tool enabled us to decipher the pro-inflammatory function of endothelial cells and Ch25h in experimental autoimmune encephalomyelitis. In particular, we describe the impact of Ch25h in the regulation of bioactive lipids secretion by CNS endothelial cells and their effect on the regulation of myeloid-derived suppressor cells (MDSCs). The role of these cells in MS is described in the manuscript "Resolution of inflammation during multiple sclerosis".

We propose that Ch25h expression by the endothelium restrains the expansion of MDSCs, which contributes to exacerbate EAE. Additionally, this mechanism might also be relevant in glioblastoma, where we identified a reduced expression of CH25H in tumor endothelial cells compared with peripheral healthy CNS tissue and a negative correlation between CH25H mRNA expression and MDSC infiltration. As first authors of this paper, I was involved in all the aspects of this study, including conceptualization, data acquisition, analysis, and manuscript writing.

# Endothelial-derived oxysterols regulate myeloid-derived suppressor cells at the blood-brain barrier

Ruiz Florian<sup>1</sup>, Vigne Solenne<sup>1</sup>, Peter Benjamin<sup>1</sup>, Rebeaud Jessica<sup>1</sup>, Wyss Tania<sup>2,3</sup>, Yersin Yannick<sup>1</sup>, Bressoud Valentine<sup>1</sup>, Roumain Martin<sup>4</sup>, Kowalski Camille<sup>5</sup>, Boivin Gael<sup>6</sup>, Roth Leonard<sup>7</sup>, Schwaninger Markus<sup>8</sup>, Muccioli Giulio G.<sup>4</sup>, Hugues Stephanie<sup>5</sup>, Petrova Tatiana V.<sup>2</sup>, Pot Caroline<sup>1</sup>

## Authors affiliations:

<sup>1</sup> Laboratories of Neuroimmunology, Service of neurology and Neuroscience research center, Department of Clinical Neurosciences, Lausanne University Hospital and University of Lausanne, Lausanne 1066, Switzerland

<sup>2</sup> Department of Oncology, University of Lausanne and Ludwig Institute for Cancer Research, Lausanne 1066, Switzerland

<sup>3</sup> SIB Swiss Institute of Bioinformatics, Lausanne 1015, Switzerland.

<sup>4</sup> Bioanalysis and Pharmacology of Bioactive Lipids Research Group, Louvain Drug Research Institute, UCL Louvain, Université catholique de Louvain, Brussels 1200, Belgium.

<sup>5</sup> Immunology and pathology department, Geneva University Hospital, Geneva 1211, Switzerland

<sup>6</sup> Radio-Oncology Laboratory, Department of Oncology, Lausanne University Hospital and University of Lausanne, Lausanne 1066, Switzerland

<sup>7</sup> Department of Epidemiology and Health Systems, University Center for Primary Care and Public Health (Unisanté), Lausanne 1066, Switzerland

<sup>8</sup> Institute for Experimental and Clinical Pharmacology and Toxicology, University of Lübeck, Luebeck, Germany.

Correspondence to: Caroline Pot

Full address: Laboratories of Neuroimmunology, Department of Clinical Neurosciences, Lausanne University Hospital and University of Lausanne, Chemin des Boveresses 155, 1066 Epalinges, Switzerland E-mail: [Caroline.Pot-Kreis@chuv.ch](mailto:Caroline.Pot-Kreis@chuv.ch)

**Running title:** endothelial lipids regulate inflammation

**Keywords:** Endothelial cells; Oxysterols; Experimental autoimmune encephalomyelitis; Polymorphonuclear myeloid-derived suppressor cells; Glioblastoma.

## **Abstract**

The vasculature is a key regulator of leukocyte trafficking into the central nervous system (CNS) during inflammatory diseases including multiple sclerosis. However, the impact of endothelial-derived factors on other aspects of CNS immune responses remains unknown. Bioactive lipids, in particular oxysterols downstream Cholesterol-25-hydroxylase (Ch25h) promote neuroinflammation but their functions in the CNS remain unclear. Using a floxed-reporter Ch25h knock-in mice, we traced Ch25h expression to CNS endothelial cells (ECs) and demonstrated that Ch25h-specific ablation in ECs attenuates experimental autoimmune encephalomyelitis. Mechanistically, inflamed Ch25h-deficient CNS ECs displayed altered lipid metabolism favoring polymorphonuclear myeloid-derived suppressor cells (PMN-MDSC) expansion that suppress encephalitogenic T lymphocytes. Additionally absence of Ch25h in ECs induced a transcriptomic profile reminiscent of human glioblastoma ECs. Accordingly, in human glioblastoma, we observed a reduced CH25H expression in ECs and an inverse correlation between CH25H expression and MDSCs. Finally, endothelial Ch25h-deficiency combined with mobilization of immature neutrophils into circulation resulted in nearly complete EAE protection. Our findings reveal a central role for endothelial-derived Ch25h in promoting neuroinflammation by regulating CNS expansion of immunosuppressive myeloid cell populations.

## Introduction

Central nervous system endothelial cells (CNS ECs) are critically involved in multiple sclerosis (MS) pathogenesis through their capacity to regulate leukocyte infiltration within the CNS parenchyma. Moreover, recent evidences suggest that brain microvascular endothelial cells dysfunction might be at the forefront of MS pathophysiology<sup>1</sup>. However, the molecular mechanisms throughout which CNS ECs promote MS are incompletely understood.

We and others have previously shown that cholesterol metabolites promote neuroinflammation<sup>2,3</sup>. Immunomodulatory cholesterol metabolites include the family of oxidized cholesterol derivatives oxysterols. Cholesterol 25-hydroxylase (Ch25h) is the rate-limiting enzyme for the synthesis of 25-hydroxycholesterol (25-OHC) and 7 $\alpha$ ,25-hydroxycholesterol (7 $\alpha$ ,25-diOHC)<sup>4</sup> that is the strongest ligand of the chemotactic receptor EBI2 (G-protein coupled receptor Epstein-Barr virus induced gene-2)<sup>5</sup>. Multiple sclerosis (MS) and its animal model, the experimental autoimmune encephalomyelitis (EAE), are characterized by inflammatory cell infiltrates and demyelination of CNS<sup>6</sup>. The development of MS is under the control of both genetic and environmental factors, among which viral infections, in particular exposure to Epstein-Barr virus (EBV) and adolescent obesity<sup>7</sup>. In this line, oxysterols downstream Ch25h have been proposed to favor EAE and possibly MS by driving pro-inflammatory lymphocyte trafficking in particular Th17 cells expressing the oxysterol receptor EBI2<sup>2,8,9</sup>.

We previously demonstrated that *Ch25h*-deficient mice display an attenuated EAE disease course<sup>2</sup>. Since then, independent works reported that *Ch25h* expression, together with 25-OHC and 7 $\alpha$ ,25-diOHC levels, were increased in the CNS during EAE<sup>9,10</sup>. However, the most critical cellular source of Ch25h-derived oxysterols during neuroinflammation remains debated so as the function of 25-OHC, which is a weak agonist of EBI2 and thus unlikely to drive Th17 cell chemotaxis<sup>5</sup>. Ch25h is pleiotropically expressed along the hematopoietic lineage, including macrophages and monocyte-derived dendritic cells (moDC), known to infiltrate the CNS early during EAE<sup>2</sup>. Others have proposed that microglial cells could be the source of Ch25h-derived oxysterols<sup>9</sup>. In addition, several studies using different disease mouse models and organs indicate that Ch25h is expressed by non-hematopoietic cells, such as fibroblastic reticular cells, blood endothelial cells (BECs) and lymphatic endothelial cells (LECs)<sup>11,12</sup>. Recently, the *Ch25h* gene was identified in the blood-brain barrier (BBB) dysfunction module<sup>13</sup>, a subset of 136 genes

upregulated in CNS endothelial cells of various mouse disease models associated with a BBB dysfunction.

Despite those results, the importance of ECs as source of Ch25h-derived oxysterols and the consequences of endothelial Ch25h inactivation during CNS inflammation have not been explored. Additionally, the function of Ch25h during EAE was mostly assessed in the context of immune cell trafficking<sup>2,9</sup>. In line with this, studies aiming at defining the implication of CNS ECs in neuroinflammation focus on their function in the regulation of leukocyte diapedesis. Much less is known about the impact of endothelial-secreted factors, in particular lipids and oxysterols, in the regulation of other aspects of leukocyte activity, such as their expansion or polarization.

Polymorphonuclear myeloid-derived suppressive cells (PMN-MDSC) are pathologically activated immunosuppressive neutrophils primarily studied in cancer<sup>14</sup> that have been shown to promote EAE recovery<sup>15</sup>. In cancer, the current model proposes that their emergence is controlled by two partially-overlapping phases: the first step takes place within the bone marrow and spleen and is induced by growth-factors derived from tumors while the second step is favored by pro-inflammatory signals primarily secreted by the tumor stroma<sup>16</sup>. However, little is known about the signals driving their expansion during neuroinflammation and the role of BBB ECs in their generation is virtually unexplored.

In this study, we generated a floxed-reporter *Ch25h* knock-in mice and demonstrated that endothelial-specific Ch25h deletion dampens EAE development. We further showed that *Ch25h* deficiency induces a remodeling of endothelial-secreted lipids favoring the expansion of PMN-MDSC. Accordingly, Ch25h endothelial-deficient mice display an increased infiltration of PMN-MDSC in the CNS during EAE. On the other hand, human glioblastoma (GBM) ECs displayed a reduced expression of human CH25H that is negatively correlated with MDSC expansion. Finally, the combination of Ch25h endothelial-deficiency with mature neutrophil depletion resulted in an almost complete protection from EAE and favored CNS PMN-MDSC accumulation. Altogether, our results reveal a novel function of both Ch25h and ECs in the regulation of PMN-MDSC expansion during neuroinflammation.

## Results

### Increased expression of Ch25h in blood endothelial cells promotes EAE

To identify the cellular source of the increased expression of Ch25h during EAE, we generated a floxed reporter-*Ch25h* knock-in mouse, where eGFP is used as a reporter for Ch25h (*Ch25h<sup>fl/fl</sup>* mice) (Fig. 1A). We first characterized the eGFP reporter signal in the CNS at baseline and during EAE. Ch25h-eGFP expression in CD45<sup>-</sup>Ter119<sup>-</sup>CD13<sup>-</sup>CD31<sup>+</sup> ECs from the CNS was low in non-immunized (NI) *Ch25h<sup>fl/fl</sup>* mice (Fig. 1B, top panel and 1c, gating strategy shown in Fig. S1A). Strikingly, 16 days after EAE induction, which corresponds to the peak of the disease severity, we noticed a 20-fold increase in Ch25h-eGFP signal in CNS ECs (Fig. 1B top panel and 1C). Ch25h-eGFP was not detected in other CNS resident cells (CD45<sup>-</sup>TER119<sup>-</sup>CD13<sup>-</sup>CD31<sup>-</sup> cells, Fig. S1B). Furthermore, CD45<sup>+</sup>TER119<sup>+</sup> cells, representing cells from the hematopoietic lineage and microglial cells, displayed low Ch25h-eGFP expression at baseline that was not significantly altered during EAE (Fig. S1C and S1D). Hence, our results suggest that enhanced expression Ch25h during EAE is restricted to the EC compartment.

To further study the role of *Ch25h* in ECs, we crossed the *Ch25h<sup>fl/fl</sup>* mice with VE-cadherin-CreERT2 mice that express the tamoxifen-inducible Cre recombinase in endothelial cells (*Ch25h<sup>ECKO</sup>*)<sup>17</sup>. We induced EAE two weeks after tamoxifen-induced *Ch25h* deletion and validated the robustness of the deletion in CNS ECs (Fig. 1B lower panel and 1C). We previously showed that *Ch25h* germline knockout mice develop a less severe disease compared with their wild-type counterparts<sup>2</sup>. Here, using the *Ch25h<sup>ECKO</sup>* mice, we found that *Ch25h* deletion in ECs was sufficient to delay the disease onset and to reduce its incidence, while the mean maximal score was similar between the two groups (Fig. 1D and Table 1). This phenotype is reminiscent of the one observed in germline *Ch25h* knockout mice<sup>2</sup>.

VE-cadherin-CreERT2 mice express the Cre recombinase in both lymphatic endothelial cells (LECs) and blood endothelial cells (BECs) and both cell types have been shown to express *Ch25h*<sup>11,12</sup>. In order to distinguish the role of Ch25h in these endothelial subtypes, we generated mouse strains with specific deletion of *Ch25h* in BECs and LECs by crossing *Ch25h<sup>fl/fl</sup>* mice with *Pdgfb-iCreERT*<sup>18</sup> and *Prox1-CreERT2*<sup>19</sup> lines respectively. We then compared the EAE phenotype of *Ch25h<sup>fl/fl</sup>;Pdgfb-iCRE<sup>ERT2+</sup>* mice (*Ch25h<sup>BECKO</sup>*), *Ch25h<sup>fl/fl</sup>;Prox1-CRE<sup>ERT2+</sup>* mice (*Ch25h<sup>LECKO</sup>*) and Cre negative control littermates injected with tamoxifen. *Ch25h<sup>BECKO</sup>* mice displayed a partial protection, similar to *Ch25h<sup>ECKO</sup>* mice (Fig. 1E and Table 1), whereas

inactivation of *Ch25h* in LECs had no effect on EAE phenotype (Fig. 1F and Table 1). Altogether, our results show that Ch25h expressed by BECs plays a central role in promoting EAE.

### **Ch25h deletion in CNS ECs upregulates genes related to polyunsaturated fatty acid biosynthesis and metabolism**

To gain mechanistic insights into the function of endothelial Ch25h in inflammation, we isolated and cultured primary mouse brain microvascular endothelial cells (pMBMECs) from tamoxifen-injected *Ch25h*<sup>ECKO</sup> and *Ch25h*<sup>fl/fl</sup> control mice. Confluent pMBMECs were stimulated or not with the pro-inflammatory cytokine IL-1 $\beta$ , since IL-1 signaling in ECs of the BBB plays a crucial role in driving EAE<sup>20</sup>. *Ch25h* mRNA expression was significantly upregulated by IL-1 $\beta$  stimulation (Fig. 2A). Additionally, *Ch25h* transcripts were reduced in brain ECs isolated from *Ch25h*<sup>ECKO</sup> mice as compared with *Ch25h*<sup>fl/fl</sup> ECs in accordance with the results obtained *in-vivo* during EAE. We next analyzed the transcriptome of pMBMECs at baseline conditions or upon IL-1 $\beta$  stimulation by RNA sequencing (RNAseq). Using FDR < 0.05 as cutoff and comparing *Ch25h*<sup>ECKO</sup> pMBMECs to *Ch25h*<sup>fl/fl</sup> ECs either at baseline or upon IL-1 $\beta$  stimulation, we identified 1338 differentially expressed genes, 740 of which were upregulated in *Ch25h*<sup>ECKO</sup> pMBMECs, while 598 were downregulated. More than 1/5 of these genes were altered both at baseline and upon IL-1 $\beta$  stimulation (Fig. 2B and Tables S1-S4). To identify the pathways altered in the absence of Ch25h, we performed a gene set enrichment analysis (GSEA). One of the most striking finding was that *Ch25h* deletion enhanced cell division-related gene expression independently from IL-1 $\beta$  stimulation (Fig. 2C). This is consistent with recent findings showing that Ch25h has angiostatic effects<sup>21</sup>. Interestingly, IL-1 $\beta$  stimulation enhanced the expression of genes related to extracellular matrix organization and response to wounding, which were further increased in *Ch25h*<sup>ECKO</sup> compared with *Ch25h*<sup>fl/fl</sup> pMBMECs (Fig. 2C). We also identified an enrichment in genes related to carboxylic acid biosynthetic process, which was only significantly increased when IL-1 $\beta$ -stimulated *Ch25h*<sup>ECKO</sup> pMBMECs were compared with *Ch25h*<sup>fl/fl</sup> pMBMECs, suggesting that this pathway is regulated by Ch25h specifically under inflammatory conditions (Fig. 2C). Ch25h and 25-OHC can regulate cholesterol metabolism<sup>22</sup>. However, this pathway was not significantly impacted by IL-1 $\beta$  stimulation nor *Ch25h* deletion. Downregulated pathways in *Ch25h*<sup>ECKO</sup> pMBMECs compared with control cells included, among others, innate immune response, response to virus, positive regulation of catabolic process, vasculogenesis and

type I interferon signaling pathway (Fig. 2C). As the carboxylic acid biosynthesis pathway was only enriched in IL-1 $\beta$ -stimulated *Ch25h*<sup>ECKO</sup> compared with *Ch25h*<sup>fl/fl</sup> pMBMECs, we focused our attention on genes from this gene set. Carboxylic acids include unsaturated fatty acids, which are regulators of the immune response. We thus specifically tested the enrichment of genes associated with unsaturated fatty acid biosynthesis and found that they were increased in IL-1 $\beta$ -stimulated *Ch25h*<sup>ECKO</sup> compared with *Ch25h*<sup>fl/fl</sup> pMBMECs (Fig. 2D). Intriguingly, this latter gene set included prostaglandin I<sub>2</sub> synthase (PTGIS), an enzyme that catalyzes the biosynthesis and metabolism of eicosanoids, in particular the isomerization of prostaglandin H<sub>2</sub> to prostaglandin I<sub>2</sub> (PGI<sub>2</sub>). PGI<sub>2</sub> can be secreted by vascular endothelial cells and has been shown to promote neuronal remodeling in a localized model of EAE<sup>23</sup>. We also observed an increase in fatty acid desaturase 2 (FADS2) expression, which promotes the production of anti-inflammatory lipids<sup>24</sup>. The elongase ELOVL4 and fatty acid desaturase 3 (FADS3) were also upregulated in *Ch25h*<sup>ECKO</sup> pMBMECs. We further generated a heatmap of genes implicated in the biosynthesis of unsaturated fatty acids and observed that among the above-mentioned genes, FADS2 and FADS3 were upregulated by IL-1 $\beta$  and increased in absence of Ch25h (Fig. 2E, Tables S1- S3). Next, we confirmed by RT-qPCR that FADS2, PTGIS and ELOVL4 were significantly upregulated in *Ch25h*<sup>ECKO</sup> versus *Ch25h*<sup>fl/fl</sup> pMBMECs under IL-1 $\beta$  stimulation (Fig. 2F). We then compared our RNAseq to genes differentially expressed in CNS ECs in response to EAE<sup>13</sup>, searching for matching genes after Ch25h deletion, IL-1 $\beta$  stimulation or during EAE. We found that FADS2 and PTGIS were upregulated in CNS ECs during EAE<sup>13</sup>. To confirm these results, we FACS-sorted CNS ECs from *Ch25h*<sup>ECKO</sup> and *Ch25h*<sup>fl/fl</sup> EAE mice and evaluated mRNA levels of FADS2 and PTGIS. We confirmed *in-vivo* that FADS2 mRNA transcripts were significantly higher in CNS ECs of *Ch25h*<sup>ECKO</sup> mice (Fig. 2G). Overall, during inflammation, loss of *Ch25h* in ECs alters lipid biosynthetic pathways, among which the upregulation of FADS2 that was confirmed both *in-vitro* and *in-vivo* in the CNS during EAE.

### ***Ch25h* deletion in pMBMECS during inflammation alters lipid secretion**

Ch25h is the rate-limiting enzyme for the synthesis of 25-OHC, and is also implicated in the production of 7 $\alpha$ ,25-diOHC and 7-keto-25-OHC<sup>25</sup>. Moreover, FADS2 is a key enzyme for the synthesis of a vast number of eicosanoids<sup>24</sup>. We thus reasoned that Ch25h deletion in ECs could have a broad impact on endothelial-secreted lipids. We evaluated lipid production by CNS ECs by first measuring 10 oxysterols in the supernatant of control *Ch25h*<sup>fl/fl</sup> or *Ch25h*<sup>ECKO</sup> pMBMECs

at baseline and upon IL-1 $\beta$  stimulation. Using principal component analysis (PCA), we found that IL-1 $\beta$  stimulation altered oxysterol production in *Ch25h*<sup>fl/fl</sup> but less in *Ch25h*<sup>ECKO</sup> pMBMECs (Fig. 3A). To identify which oxysterols were responsible for the observed differences, we generated a loading plot to visualize the relative contributions of each oxysterols to PC1 and PC2 (Fig. 3B). With this approach, we found that 25-OHC and 7-keto-25-OHC were the only two oxysterols that were increased (Fig. 3B). Further analysis revealed that IL-1 $\beta$  stimulation increased the production of 25-OHC and 7-keto-25OHC in *Ch25h*<sup>fl/fl</sup> pMBMECs while their production was reduced in *Ch25h*<sup>ECKO</sup> cells compared with *Ch25h*<sup>fl/fl</sup> cells (Fig. 3C). 24(S)-OHC levels increased by 1.5-fold in absence of Ch25h only in the IL-1 $\beta$  stimulated condition (Figure S2A). 27-OHC (Figure S2B) and 7 $\alpha$ -hydroxycholestenone (7 $\alpha$ -OHCnone) (Figure S2C) were reduced under inflammatory condition and Ch25h deletion increased their production by 1.5-fold while 7 $\alpha$ -OHC levels remained unchanged (Figure S2D). Oxysterols can be generated by enzymatic pathways and by cholesterol auto-oxidation. 7-ketocholesterol, a marker of cholesterol auto-oxidation levels, remained unchanged (Fig. 3C), indicating that Ch25h enzymatic activity is responsible for the observed changes.

To extend our lipidomic analysis to FADS2 downstream metabolites, we measured a panel of 100 eicosanoids in the supernatant of IL-1 $\beta$  treated or control pMBMECs (see material and methods for the full list). We retained 49 eicosanoids for further analysis as they were above detection threshold and detected in all the samples. PCA was performed to evaluate differences in eicosanoids production among conditions (Fig. 3D, left panel). PC1 alone explained 38 % of the total variance of eicosanoids and was retained to compare experimental groups. Comparison of PC1 scores for each sample in the different conditions revealed that IL-1 $\beta$  strongly altered eicosanoids production in pMBMECs (Fig. 3D left and right panel) and that Ch25h deletion altered the secretion of several lipids only in pMBMECs stimulated with IL-1 $\beta$  (Fig. 3D right panel). Using the same approach as for oxysterols, we identified a group of eicosanoids contributing to PC1 (Fig. 3E, top panel). Most of these variables belong to the prostaglandin family and the sum of their relative contribution to PC1 reached 40% (Fig. 3E, bottom panel). Specifically, prostaglandin E<sub>2</sub> (PGE<sub>2</sub>) was a strong contributor (Fig. 3E, top panel). Comparison of the concentration of prostaglandins in pMBMECs supernatants revealed that IL-1 $\beta$  increased the secretion of PGE<sub>2</sub> and of the stable metabolite of PGI<sub>2</sub> (6-keto-PGF<sub>1 $\alpha$</sub> ) (Fig. 3F). These were the two prostaglandins detected at the highest level in IL-1 $\beta$ -stimulated pMBMECs supernatant

(Fig. 3F). Most importantly, Ch25h deletion significantly increased the secretion of these two metabolites (Fig. 3F).

FADS2 is the rate limiting enzyme for the desaturation of linoleic acid into  $\gamma$ -linoleic acid which itself is a precursor of prostaglandins<sup>26</sup>. In accordance with this,  $\gamma$ -linolenic acid levels were significantly increased by IL-1 $\beta$  stimulation and further enhanced by *Ch25h* deletion (Figure S2E). We observed a similar pattern in prostaglandin F<sub>2 $\alpha$</sub>  (PGF<sub>2 $\alpha$</sub> ) and 15-hydroxyeicosatetraenoic acid (15-HETE) (Fig. S2F and S2G). 14-hydroxy docosahexaenoic acid (14-HDoHE) was only increased in *Ch25h* deficient endothelial cells stimulated by IL-1 $\beta$  (Fig. S2H) while docosahexaenoic acid levels were reduced by IL-1 $\beta$  only in *Ch25h*<sup>fl/fl</sup> samples but maintained in absence of *Ch25h* (Fig. S2I). Other eicosanoids such as eicosapentaenoic acid, arachidonic acid or linoleic acid were not affected by Ch25h deletion nor IL-1 $\beta$  stimulation (Fig. S2J-L). Prostaglandin-endoperoxide synthase 2 (PTGS2 or COX2) or prostaglandin E synthase expressions were not affected by Ch25h deletion (Table S3) in inflammatory conditions. In conclusion, Ch25h inactivation and IL-1 $\beta$  stimulation in pMBMECs alters oxysterols and eicosanoids secretion. Specifically, eicosanoid and prostaglandin precursor  $\gamma$ -linolenic acid produced by FADS2 and multiple eicosanoids were increased in *Ch25h*-deficient endothelial cells under inflammatory conditions. Thus, we propose that FADS2 upregulation induced by *Ch25h* deletion could be at the origin of the differences in eicosanoid levels described above and that Ch25h is an upstream regulator of this enzyme.

### **Increased infiltration of PMN-MDSC in the CNS of *Ch25h*<sup>ECKO</sup> mice during EAE**

We observed that PGE<sub>2</sub> production in response to IL-1 $\beta$  was potentiated in the absence of *Ch25h* in cultured ECs. Mechanistically, PGE<sub>2</sub> signaling through EP4 expands MDSC<sup>27</sup>, and PMN-MDSC are protective during EAE<sup>15</sup>. We thus hypothesized that pMBMEC-secreted lipids induced by IL-1 $\beta$ , in particular PGE<sub>2</sub> and 25-OHC, affect MDSC expansion. Using bone marrow-derived cells (BMDCs) cultivated under MDSC polarizing conditions<sup>28</sup>, we observed that addition of PGE<sub>2</sub> increased the population of CD11b<sup>+</sup>Ly6C<sup>+</sup>Ly6G<sup>+</sup> cells, representing PMN-MDSC (Fig. 4A and 4B upper panel) but decreased the population of CD11b<sup>+</sup>Ly6C<sup>high</sup>Ly6G<sup>-</sup> cells, representing monocytic-MDSC (M-MDSC) (Fig. 4A and 4B, lower panel) after 4 days of culture. Addition of 25-OHC reduced the percentage of M-MDSC to a similar extent than PGE<sub>2</sub> (Fig. 4A and 4B). Strikingly, 25-OHC almost completely abrogated PMN-MDSC expansion *in vitro* (Fig. 4A and 4B). Hence, we propose that 1) PGE<sub>2</sub> and 25-OHC exert opposed effects on

PMN-MDSC expansion and that 2) alteration of the secreted lipid profile induced by *Ch25h* deletion in ECs under inflammatory conditions favors the expansion of PMN-MDSC.

Given the importance of CD4<sup>+</sup> T cells for EAE pathophysiology and the lack of specific markers for PMN-MDSC, we first asked whether CD11b<sup>+</sup>Ly6C<sup>+</sup>Ly6G<sup>+</sup> cells isolated from the CNS of mice during EAE suppress CD4<sup>+</sup> T cell proliferation. We sorted this population from the CNS of EAE WT mice at the peak of the disease (Fig. S3) and co-cultured them with CFSE-labelled CD4<sup>+</sup> T cells isolated from the spleen and stimulated with anti-CD3/CD28 beads. CD11b<sup>+</sup>Ly6C<sup>+</sup>Ly6G<sup>+</sup> cells potently suppressed CD4<sup>+</sup> T cell proliferation even when they were cultivated at the ratio of 1:8 (Fig. 4C). Moreover, we observed that the abundance of this population was negatively correlated with proliferating Ki67<sup>+</sup>CD4<sup>+</sup>CD44<sup>+</sup> cells in the CNS during EAE (Fig. 4D). These results indicate that CNS infiltrating CD11b<sup>+</sup>Ly6C<sup>+</sup>Ly6G<sup>+</sup> cells at the peak of EAE can suppress CD4<sup>+</sup> T cells proliferation and hence can be functionally characterized as PMN-MDSC. As *Ch25h* deletion in cultured CNS ECs under inflammatory conditions induced a lipid remodeling favoring PMN-MDSC expansion, we assessed if *Ch25h*<sup>ECKO</sup> mice display an increased infiltration of PMN-MDSC in the CNS during EAE by FACS. In accordance with our *in-vitro* results, we observed that *Ch25h* deletion in ECs resulted in an increased infiltration of PMN-MDSC in the CNS (Fig. 4E and 4F) together with a reduction of CD4<sup>+</sup>CD44<sup>+</sup>Ki67<sup>+</sup>T cells (Fig. 4F). Finally, to confirm that our observations were specific to the CNS, we crossed our *Ch25h*<sup>fl/fl</sup> mice with the tamoxifen-inducible BBB-EC-specific *Slco1c1-CreERT2* mice<sup>29</sup>, allowing for CNS-specific deletion of *Ch25h* in ECs, hereafter termed *Ch25h*<sup>BBBKO</sup> mice. EAE was induced in *Ch25h*<sup>BBBKO</sup> and control mice and we observed that the sole deletion of *Ch25h* in CNS ECs was sufficient to reproduce the phenotype observed in the *Ch25h*<sup>ECKO</sup> and *Ch25h*<sup>BECKO</sup> mice (Fig. 4G). In conclusion, we found that *Ch25h* deletion in ECs promotes PMN-MDSC accumulation in the CNS and that the attenuation of EAE mediated *Ch25h* deletion is specific to the CNS.

### **CH25H is downregulated in ECs of human glioblastoma and its expression is negatively correlated with MDSC infiltration**

The transcriptomic alterations, combined with PGE2 increased production and PMN-MDSC infiltration observed in absence of *Ch25h* in ECs prompted us to speculate that *Ch25h* deletion induces a “cancer stroma-like” profile in CNS ECs that dampen neuroinflammation by inducing an immunosuppressive environment. To interrogate the function of CH25H in a human disease

setting, we thus focused our attention on cancer. Indeed, ECs are difficult to characterize in MS samples with standard approaches as they are depleted from CNS samples analyzed by single-cell RNAseq<sup>30,31,32</sup>. In addition, PGE<sub>2</sub> is increased in multiple cancers, can be produced by the tumor stroma, favors immune escape<sup>33</sup> and MDSC expansion<sup>27</sup>. Thus, we first compared our pMBMECs with ECs from human glioblastoma (GBM)<sup>34</sup> a CNS tumor whose progression is partially driven by PMN-MDSC<sup>35</sup>. Genes upregulated in GBM ECs were particularly highly expressed only in IL-1 $\beta$  stimulated *Ch25h*<sup>ECKO</sup> pMBMECs compared with the other conditions (Fig. 5A left panel). Genes downregulated in GBM ECs were also lowly expressed in IL-1 $\beta$  stimulated *Ch25h*<sup>ECKO</sup> pMBMECs (Fig. 5A right panel), indicating transcriptomic similarities of *Ch25h*<sup>ECKO</sup> pMBMECs and GBM ECs. We next asked whether *CH25H* expression was altered in ECs from human GBM and took advantage of a recent single-cell RNAseq dataset on human GBM samples enriched for CD31<sup>+</sup> cells (thus enriched for ECs)<sup>36</sup>. In this study, samples were collected from the tumors and the peripheral healthy tissues in the CNS of 4 patients. Within this dataset, we identified 20 different clusters (Fig. 5B) and ECs were identified using the venous, arterial and capillary gene signatures established by Yang et al. in one of the largest single-cell RNAseq dataset on human vascular cells<sup>30</sup>(Fig. 5B, see methods). Cluster 16 consistently showed a high proportion of cells displaying an enrichment of endothelial scores and was further here defined as ECs (Fig. 5B). We performed differential gene expression analysis between tumor ECs and ECs from the periphery of the tumor (namely healthy ECs) within all clusters and found that, within cluster 16, *CH25H* expression was significantly downregulated in the tumor ECs compared to healthy ECs located at the periphery of the tumors (Fig. 5C, Table S5). To further assess if *CH25H* downregulation in tumors affects MDSCs infiltration, we further used an algorithm that quantifies immune cell infiltration in cancers from bulk RNAseq data of the cancer genomic atlas<sup>37</sup>. We found that *CH25H* expression was negatively correlated with MDSCs in the majority of cancers including GBM (Fig. 5D and S3). Of note, *FADS2* expression displayed an opposite pattern (Fig. S4). Those results show in a human disease setting that *CH25H* is expressed by ECs and further negatively correlated with MDSCs expansion.

### **Mature neutrophil depletion promotes CNS PMN-MDSC accumulation and protects *Ch25h*<sup>ECKO</sup> during EAE**

To further confirm the impact of the immunosuppressive environment promoted by *ch25h* deletion in ECs during neuroinflammation, we here propose that PMN-MDSC expansion dampen

EAE disease. To further assess the function of PMN-MDSC in EAE, we targeted surface Ly6G high cells by combining anti-Ly6G antibody injections with a mouse anti-rat IgG2a (so called “Combo treatment”) <sup>38</sup>, a strategy aiming at depleting neutrophils and enhancing their turnover <sup>38</sup>. EAE was induced in *Ch25h*<sup>ECKO</sup> and *Ch25h*<sup>fl/fl</sup> mice and each group was then divided in two arms receiving either the isotype or the Combo treatment during the symptomatic phase of EAE. First, we confirmed that the Combo treatment was effective in depleting neutrophils during EAE, as their prevalence in the blood was strongly reduced in the Combo treated *Ch25h*<sup>fl/fl</sup> and *Ch25h*<sup>ECKO</sup> mice after 1.5 days of treatment (Fig. S5A for gating strategy and S5B). Moreover, the percentage of blood CD45<sup>+</sup>CD11b<sup>+</sup>Ly6C<sup>+</sup>Ly6G intracellular<sup>+</sup> cells was similar between *Ch25h*<sup>fl/fl</sup> and *Ch25h*<sup>ECKO</sup> mice treated with the isotype, suggesting that PMN-MDSC expansion in the absence of Ch25h is restricted to the CNS. Then, assessing EAE disease course in the four groups described above, we first observed a significantly reduced severity in *Ch25h*<sup>ECKO</sup> compared to the *Ch25h*<sup>fl/fl</sup> mice in the isotype group, indicating that the treatment with the isotype control did not impact the phenotype previously observed in *Ch25h*<sup>ECKO</sup> mice (Fig. 6A). Strikingly, the Combo treatment resulted in an almost complete EAE protection in *Ch25h*<sup>ECKO</sup> mice while it did not significantly alter the course of EAE in *Ch25h*<sup>fl/fl</sup> mice (Fig.6A). Remarkably, the incidence of EAE was reduced in the *Ch25h*<sup>ECKO</sup> combo-treated group (Fig. 6B). Moreover, we observed an increased accumulation of CD45<sup>+</sup>CD11b<sup>+</sup>Ly6C<sup>+</sup>Ly6G intracellular<sup>+</sup> granulocytes in the CNS of *Ch25h*<sup>ECKO</sup> Combo treated mice compared to *Ch25h*<sup>ECKO</sup> and *Ch25h*<sup>fl/fl</sup> isotype treated mice (Fig. 6C and D).

In addition to reducing the prevalence of circulating neutrophils in the blood, the Combo treatment altered their phenotype, as they displayed a reduced expression of CD101 and Ly6G, consistent with an immature phenotype (Fig. S5b). The reduced expression of CD101 in blood neutrophils persisted 10 days after Combo protocol initiation (Fig. 6E). Furthermore, compared to blood, most CNS infiltrating neutrophils were immature as they were negative for CD101 (Fig. 6E).

We next asked how EAE and the Combo treatment were affecting mature and immature neutrophil circulation. We found that 6 days after immunization, the blood prevalence of both immature and mature neutrophils was increased (Fig. 6F). Circulating mature neutrophils further increased at day 16 after immunization (Fig. 6F, left panel), while immature neutrophils decreased at this time point compared to day 6 but remained above the baseline level (Fig. 6F,

right panel). The combo treatment was initiated on day 14 after EAE induction and prevented the expansion of the circulating mature neutrophil pool but did not impact the blood prevalence of immature neutrophils (Fig. 6F). Those results show that the Combo protocol efficiently depletes mature neutrophils while immature neutrophils preferentially infiltrating the CNS are not strongly impacted. Neutrophil progenitors can be polarized in PMN-MDSC<sup>14</sup> that can further proliferate and acquire their suppressive phenotype directly in the CNS<sup>15</sup>. We thus propose that reducing the mature to immature neutrophil ratio favors the accumulation and conversion of immature neutrophils in PMN-MDSC in the CNS. Furthermore, Ch25h expression in endothelial cells negatively regulates the protective effect of PMN-MDSC accumulation in EAE.

## Discussion

In this study, we demonstrated that Ch25h expression is increased in CNS endothelial cells during EAE and that 25-OHC, the Ch25h-downstream metabolite promotes neuroinflammation by reducing the expansion of PMN-MDSC. Mechanistically, we propose that 25-OHC and PGE<sub>2</sub> are secreted by inflamed CNS endothelial cells and exert opposed effects on PMN-MDSC. Hence, reduced levels of 25-OHC and increased levels of PGE<sub>2</sub> resulting from Ch25h deletion in endothelial cells act together to favor PMN-MDSC expansion. Our data suggest that Ch25h expression by human GBM endothelial cells also regulate MDSC accumulation in this tumor and possibly other cancers. Depleting mature neutrophils by using a double antibody-based strategy during EAE promotes CNS PMN-MDSC accumulation in absence of endothelial Ch25h. Taken together, our results reveal a novel function for both Ch25h and ECs in the regulation of PMN-MDSC during neuroinflammation.

We observed that the sole deletion of Ch25h in endothelial cells was sufficient to reduce 25-OHC levels, suggesting that Ch25h is the main enzyme involved in 25-OHC secretion in this cell type. Indeed, Ch25h loss can be potentially compensated in other cell types such as hepatocytes by other enzymes displaying 25-hydroxylase activity (e.g., Cyp3a4, Cyp27a1 and Cyp46a1)<sup>39</sup>. However they were not produced by pMBMECs neither at baseline nor under IL-1 $\beta$  stimulation. Additionally, we previously showed that 25-OHC levels were reduced in Ch25h KO Type 1 Regulatory T-cells<sup>40</sup>. Hence, for these two cell types, Ch25h is the main 25-OHC synthesizing-enzyme.

Our *in-vitro* data indicate that inactivation of Ch25h affects local concentrations of 25-OHC and related oxysterol including 7-keto-25-OHC. Moreover, Ch25h was strongly upregulated in CNS ECs during EAE and *Ch25h*-deficient brain endothelial cells displayed alterations in eicosanoids and oxysterols secretion (other than 25-OHC and 7-keto-25-OHC) only under inflammatory condition. Finally, 25-OHC primarily acts as a paracrine or autocrine mediator and its levels are increased in inflammatory conditions. On the basis of these data, our results suggest that locally, in the CNS, during EAE, deletion of Ch25h in ECs results in: i) a reduction of the autocrine signaling of 25-OHC, favoring PGE<sub>2</sub> secretion and ii) a reduction of 25-OHC paracrine signaling. Ch25h expression by ECs regulates the PGE<sub>2</sub> to 25-OHC ratio that might be an important determinant of PMN-MDSC expansion in the inflamed CNS.

We observed that EC-derived Ch25h and 25-OHC promote inflammation during EAE. The role of Ch25h during inflammation is controversial, with reports suggesting both pro and anti-inflammatory functions<sup>2,9,11,41-47</sup>. Those discrepancies could result from the different disease models used in these studies that investigated Ch25h function in various cell compartments and organs (e.g colitis, lungs, and CNS inflammation). As for neuroinflammation, we have shown that Ch25h-deficient mice depict an attenuated EAE disease<sup>2</sup> while others have reported an exacerbation of the same EAE model<sup>45</sup> but using different Ch25h deficient-mouse strains and different controls. Indeed, in the later study, *Ch25h* heterozygous mice have been used as controls for Ch25h-deficient mice. Thus, we cannot exclude that partial deletion of Ch25h also results in a phenotype per se. Furthermore, environmental factors such as gut microbiota<sup>48</sup>, diet<sup>49</sup>, month of birth<sup>50</sup> and genetic background<sup>51</sup> can have a broad impact on EAE development and could contribute to the differences observed across different laboratories. However, our current study further supports a pro-inflammatory role for Ch25h during EAE.

We additionally found that the sole deletion of Ch25h in ECs was sufficient to dampen EAE. The cellular source of Ch25h is disputed during EAE as both moDCs<sup>2</sup> and microglial cells<sup>9</sup> have been proposed to express Ch25h. ECs express Ch25h at high levels in lymph nodes and play a role in B cell positioning during a humoral response<sup>12</sup>. In addition, Ch25h expression by ECs contributes to atherosclerosis development<sup>52</sup>. However, while Ch25h expression has been observed in ECs, and reported as upregulated in various murine models associated with a BBB dysfunction, its expression at the protein level and function during EAE had never been explored so far. Our data show that Ch25h expression in ECs plays a crucial role during EAE.

We here observed an increase in fatty acid desaturase 2 (FADS2) expression in the absence of Ch25h in ECs. FADS2 promotes the production of anti-inflammatory lipids<sup>24</sup>. These data prompted us to speculate that FADS2 increased activity contributes to the attenuated EAE phenotype observed in the absence of Ch25h in ECs. Mechanistically, 25-OHC restrains cholesterol synthesis through inhibition of Sterol Regulatory Element Binding Transcription Factor 2 (SREBP2)<sup>53</sup> and FADS2 has been described as a target of SREBP2<sup>54</sup>. We hence propose that the reduction of 25-OHC in ECs induced by Ch25h deletion increases FADS2 expression through the release of SREBP2 inhibition. Interestingly, two Single Nucleotide Polymorphisms (SNPs) within the FADS2 gene locus have been associated with a reduced risk of Multiple Sclerosis<sup>55</sup>. However, the impact of these SNPs on FADS2 activity remains unknown. Additionally, the role of FADS2 in EAE and ECs is virtually unexplored. We here establish that IL-1 $\beta$  signaling in ECs upregulates FADS2 expression and that Ch25h is an upstream regulator of this enzyme. Moreover, our results suggest that the increased activity of FADS2 in ECs favors PMN-MDSC expansion through PGE<sub>2</sub> secretion and could be a protective mechanism in EAE. In line with this, PGE<sub>2</sub> is increased in the CNS of mice during EAE<sup>56</sup> and injections of a stable form of PGE<sub>2</sub> or an agonist of its receptor E-type Prostanoid receptor 4 (EP4) protects mice from EAE<sup>57</sup>. Diet supplementation with a plant containing high levels of  $\gamma$ -linoleic acid have been shown to attenuate EAE and increase PGE<sub>2</sub> production by splenocytes in SJL mice<sup>58</sup>. As mentioned earlier, FADS2 is the rate limiting enzyme for the synthesis of  $\gamma$ -linoleic acid which is a precursor of prostaglandins<sup>26</sup>. Additional studies will be necessary to further clarify the role of FADS2 during neuroinflammation.

We discovered that Ch25h deletion in ECs resulted in an expansion of PMN-MDSC in the CNS during EAE. In mice, CD11b<sup>+</sup>Ly6C<sup>+</sup>Ly6G<sup>+</sup> population can be defined both as bona fide neutrophils and PMN-MDSC<sup>59</sup>. Hence, the expression of these markers is not sufficient to ensure the suppressive phenotype of these cells. Ly6G<sup>+</sup> cells isolated from the CNS during the recovery phase of the EAE suppress B cell proliferation<sup>15</sup>. We here show that CD11b<sup>+</sup>Ly6C<sup>+</sup>Ly6G<sup>+</sup> isolated from the CNS at the peak of the disease can also suppress CD4<sup>+</sup> T cell proliferation, suggesting that this population at this time point of EAE corresponds to PMN-MDSCs. However, it cannot be excluded that CD11b<sup>+</sup>Ly6C<sup>+</sup>Ly6G<sup>+</sup> cells are heterogeneous and contain both bona fide neutrophils and PMN-MDSC, and that the suppressive capacity of this population is dependent on the relative proportion of these two subsets. In line with this, single-

cell RNAseq analysis of Ly6G<sup>+</sup> cells isolated from the CNS in a mouse model of optic nerve injury identified three different cell clusters<sup>60</sup>, suggesting that CNS-infiltrating neutrophils is a heterogeneous population. Interestingly, the expression of arginase 1, a key enzyme in PMN-MDSC-mediated lymphocyte suppression was restricted to a cluster displaying a transcriptomic signature consistent with immature neutrophils<sup>60</sup>. These cells were CD101<sup>+</sup>, as the vast majority (up to 92%) of CD11b<sup>+</sup>Ly6C<sup>+</sup>Ly6G<sup>+</sup> cells infiltrating the CNS at the plateau/recovery phase of EAE in our study. Moreover, Ly6G<sup>+</sup> cells isolated from the CNS at the onset and the recovery phase of EAE have distinct transcriptomic profile and the PMN-MDSC transcriptomic signature seems restricted to Ly6G<sup>+</sup> cells from EAE recovery phase<sup>15</sup>. In other words, the maturation status of CNS-infiltrating neutrophils could determine if they will acquire a suppressive phenotype. When we depleted neutrophils using the “Combo protocol” at the time of the first EAE symptoms, we observed an almost complete EAE protection in *Ch25h*<sup>ECKO</sup> mice while we did not observe a significant protection in the control group. We also observed a paradoxical accumulation of CD11b<sup>+</sup>Ly6C<sup>+</sup>Ly6G<sup>+</sup> in the CNS. We propose that the increased circulation of immature neutrophils relative to mature neutrophils observed in the Combo treated group favors the accumulation of PMN-MDSC precursors in the CNS. However, we do not exclude that neutrophil depletion earlier in the disease course could explain this protection. Indeed, we previously showed that *Ch25h* KO mice display a delayed infiltration of Th17 cells in the CNS<sup>2</sup> and others have shown that Th17 cells can promote EAE by favoring neutrophil infiltration<sup>61</sup>. Hence, the protection could also be explained by a synergistic effect of a delayed Th17 cell infiltration in *Ch25h*<sup>ECKO</sup> mice and neutrophil depletion mediated by the Combo protocol. However, the striking infiltration of CD11b<sup>+</sup>Ly6C<sup>+</sup>Ly6G<sup>+</sup> cells in *Ch25h*<sup>ECKO</sup> Combo treated mice that did not display any symptoms does not support this hypothesis.

We discovered that *Ch25h* deletion in pMBMECs combined with IL-1 $\beta$  stimulation results in the acquisition of transcriptomic profile reminiscent of GBM ECs and that CH25H expression was reduced in the tumor endothelium of GBM. Moreover, it was shown that *Ch25h* is angiostatic in primary tumors<sup>21</sup> while microvascular proliferation and loss of chromosome 10 are hallmarks of GBM<sup>62</sup>. Interestingly, the CH25H locus is located in chromosome 10q<sup>63</sup> and loss of CH25H has been described in GBM<sup>64</sup>. Therefore, we propose that CH25H deletion participate in GBM pathophysiology by promoting vascular proliferation and PMN-MDSC infiltration.

Overall, our results demonstrate a novel function of Ch25h and ECs in the regulation of PMN-MDSC expansion during neuroinflammation. The fact that IL-1 $\beta$  can upregulate Ch25h in pMBMECs and that Ch25h has been described to be upregulated in CNS ECs in other disease models suggests that the same mechanisms may be relevant in other pathologies. We thus propose that targeting ECs and the Ch25h pathway could be promising approaches to target inflammatory diseases.

## **Materials and methods**

### **Mice**

Ch25h-eGFP<sup>fl/fl</sup> mice (Fig. 1A): These mice were generated by Cyagen as follow: A constitutive Knock-In (KI) with conditional knockout (KO), using a floxed reporter-ch25h knock-in, with eGFP is used as a reporter protein fused to the 3' end of Ch25h. Furthermore, the entire gene was flanked with LoxP sites, taking care to avoid promoter disruption. Linker-eGFP reporter has been inserted in the targeting cassette and is thus not expressed as a fusion protein before cre-recombination.

*Cdh5-CreERT2*, *Pdgfb-iCreERT2* mice, *Prox1-CreERT2* and *Slco1c1-CreERT2* mice were reported previously (PMID: **19144989**, doi.org/10.1002/dvg.20367, doi:10.1172/JCI58050)<sup>29</sup>. Wild-type mice were obtained from Charles-River Laboratories. All mouse strains were on pure C57BL/6 background. 8-12 weeks mice were used for all experiments. Animals were kept in a specific pathogen-free facility at the Lausanne University. All experiments were carried out in respect with guidelines from the Cantonal Veterinary Service of the state of Vaud.

### **EAE, tamoxifen injections and Combo protocol**

For induction of EAE mice were immunized with 100  $\mu$ g myelin oligodendrocyte glycoprotein peptide 35-55 (MOG<sub>35-55</sub>, (Anawa) in complete Freund's adjuvant supplemented with 5 mg/ml *Mycobacterium tuberculosis* H37Ra (BD Difco). 200  $\mu$ l of emulsion was subcutaneously injected into four sites on the flanks of mice. At days 0 and 2 after initial MOG<sub>35-55</sub> injections, mice received intravenous injection of 100ng pertussis toxin (Sigma Aldrich). Mice were weighed and scored daily using the following system: 0: no symptom, 1: tail paralysis, 2: hind limb paresis, 2.5: partial hind limb paralysis, 3: Complete hind limb paralysis, 4: forelimb paresis and complete hind paralysis, 5: moribund or dead.

For tamoxifen injections, mice between 8-10 weeks were injected intraperitoneally with tamoxifen in Koliphor (Sigma Aldrich) twice a day with a total of 2mg/mice/day for 4 consecutive days. Two weeks of washout period were performed before EAE induction.

The combo protocol was performed as described by G. Boivin et al<sup>38</sup>. Briefly, 25µg of Anti-Ly6G (clone 1A8, Bio X cell) antibody or isotype control (Rat IgG2a, Bio X cell) were injected intraperitoneally every day for 10 consecutive days, starting from the first symptoms of EAE. Every other day, mice were injected intraperitoneally with 50µg of anti-rat Kappa immunoglobulin (Clone MAR 18.5 Bio X cell) or Isotype control.

### **Isolation of leukocytes and ECs from the CNS**

For CNS preparation, mice were perfused through the left ventricle with cold PBS (Bichsel). Brains were dissected and spinal cords extruded by flushing the vertebral canal with cold PBS. CNS tissue was cut into pieces and digested for 45 min, in a DMEM containing collagenase D (2.5 mg/ml Sigma) and Dnase 1 (1 mg/ml Sigma) to give a single-cell suspension. For ECs, meninges were removed before brain enzymatic digestion with Collagenase/Dispase (2mg/ml), DNase I (10µg/ml) and N $\alpha$ -Tosyl-L-Lysin-chlormethyl keton hydrochlorid (TLCK, 0.147µg/ml). Mononuclear and ECs were isolated by passage of the tissue through a cell strainer (70 µm), followed by Percoll gradient centrifugation (70%/37% for CNS leukocytes and 37% for ECs). Leukocytes were removed from the interphase and for ECs the entire 37% Percoll suspension was collected, washed and resuspended in culture medium for further analysis.

### **Flow cytometry, cell sorting and suppression assay**

Single-cells were suspended in PBS and then stained with LIVE/DEAD fixable Red stain kit (Invitrogen) according to manufacturer instructions. For extracellular staining cells were incubated with anti-CD16/32 (Invitrogen) in PBS+ 1% BSA and then stained with anti-mouse fluorochrome-conjugated antibodies: CD45 (30-F11), CD3 (45-2C11), CD44 (IM7), CD11b (M1/70), Ly6G (1A8), Ly6C (HK 1.4), purchased from Biolegend, CD13 (123-242), CD4 (RM4-5), purchased from BD Bioscience, CD31 (390), CD101 (Moush1/101), purchased from Invitrogen, at 4°C for 30 minutes. For intracellular staining, after surface staining, cells were fixed and permeabilized using Foxp3/transcription factor staining kit (Invitrogen) according to manufacturer protocol and then incubated with anti-mouse fluorochrome-conjugated antibodies: Ki67 (SolA15, Invitrogen), Ly6G (1A8) for 30 minutes. Samples were all acquired on a LSR-II cytometer (BD Bioscience). For PMN-MDSC suppression assay, PMN-MDSC were isolated

from the CNS by FACS sorting using specific fluorochrome-conjugated antibodies. Isolated PMN-MDSC were then co-cultured at different ratios as indicated in the figure with purified CD4<sup>+</sup> T (CD4+T cell isolation Kit, Miltenyi Biotech, 1.10<sup>4</sup> cells/well) previously labeled with 5µM carboxyfluorescein succinimidyl ester (CFSE, Invitrogen). Co-culture were stimulated with plate-bound anti-CD3 /anti-CD28 antibodies (1µg/ml, BioXcell) for 72h. The proliferative levels of CFSE-CD4<sup>+</sup> T cells were evaluated by the rates and intensity of CFSE dilution measured with flow cytometry.

### **Isolation and culture of primary brain microvascular cells**

Isolation and culture of primary mouse brain microvascular endothelial cells (pMBMECs) from 7–12-week-old mice were performed as previously described<sup>65</sup>. Briefly, mice were euthanized by cervical dislocation, brains were dissected, and meninges, olfactory bulb, brainstem and thalami were removed. A minimum of 6 brains per genotype were pooled, homogenized, and resuspended in a 30 % dextran (Sigma) solution to obtain a final concentration of 15 % dextran. Samples were centrifuged, the vascular pellet was collected and then digested by incubation with Collagenase/Dispase (2mg/ml), DNase I (10µg/ml) and Nα-Tosyl-L-Lysin-chlormethyl keton hydrochlorid (TLCK, 0.147µg/ml) for 30 minutes at 37°C in a shaker incubator. Digested vessel fragments were then plated in Matrigel (Corning) coated 96 well Nunclon Delta Surface (Thermo Scientific) plates. Once confluent, cells were treated with either mouse recombinant IL-1β (R&D systems, 10ng/ml) or vehicle for 24 hours.

### **RT-qPCR**

Total RNA was extracted using the RNeasy Mini Kit (Qiagen) according to the manufacturer's protocol). cDNA was produced from RNA without amplification using the Superscript II RT (Invitrogen). PCR products were amplified with the PowerUp SYBR Green Master Mix (Applied Biosystem). Samples were analyzed on the StepOne Real-Time PCR System. GAPDH was used as reference gene and the comparative CT method was employed to evaluate relative mRNA expression. Primers were purchased from Microsynth AG (Balgach, Switzerland).

### **RNA sequencing**

*Ch25h*<sup>fl/fl</sup> and *Ch25h*<sup>ECKO</sup> mice were injected with tamoxifen. Nine brains per genotype were pooled and primary brain microvascular endothelial cells (pMBMEC) were isolated and plated in a 96-well plate (2 wells/brain). Confluent pMBMEC were left unstimulated or stimulated IL-1β for 24 hours. RNA of 3 wells was pooled to obtain 1 replicate for RNA sequencing. The

Lausanne Genomic Technologies Facility performed the RNA seq. RNA quality was assessed on a Fragment Analyzer (Agilent Technologies) and all RNAs had a RQN between 8.7 and 10. RNAseq libraries were prepared from 500 ng of total RNA with the Illumina TruSeq Stranded mRNA reagents (Illumina) using a unique dual indexing strategy, and following the official protocol automated on a Sciclone liquid handling robot (PerkinElmer). Libraries were quantified by a fluorometric method (Qubit, Life Technologies) and their quality assessed on a Fragment Analyzer (Agilent Technologies).

Cluster generation was performed with 2 nM of an equimolar pool from the resulting libraries using the Illumina HiSeq 3000/4000 SR Cluster Kit reagents and sequenced on the Illumina HiSeq 4000 using HiSeq 3000/4000 SBS Kit reagents for 150 cycles (single end). Sequencing data were demultiplexed using the bcl2fastq2 Conversion Software (version 2.20, Illumina).

### **Oxysterol measurements**

Oxysterols were analyzed using a validated HPLC-MS method<sup>66</sup>. Briefly, cell supernatants were placed in glass vials containing deuterated internal standards as well as dichloromethane, methanol (containing 10 µg of butylated hydroxytoluene) and bidistilled water (containing 20 ng ethylenediaminetetraacetic acid) (8:4:2 v/v/v). After mixing and sonication, samples were centrifuged and the organic phase was recovered and dried under a nitrogen stream. The organic residue was resuspended and pre-purified by solid phase extraction over silica. The eluate containing oxysterols was analyzed by HPLC-MS using an LTQ-Orbitrap XL MS (Thermo Fisher Scientific) coupled to an Accela HPLC system (Thermo Fisher Scientific). Chromatographic separation was performed using an Ascentis Express C-18 column (2.7 µm, 150 × 4.6 mm, Sigma), kept at 15 °C. Mobile phase was a gradient of methanol and water containing acetic acid. MS analyses were performed using an atmospheric pressure chemical ionization source in the positive mode. Data are expressed as a ratio between the signal (AUC) of the oxysterol of interest and the signal of the corresponding deuterated internal standard.

### **Eicosanoids measurements**

Supernatants (150 µL) from brain endothelial cells (cultured in IL-1β stimulated and non-stimulated conditions) were mixed with 150 µL of extraction buffer (citric acid/Na<sub>2</sub>HPO<sub>4</sub>, pH=5.6) and 10 µL of internal standard solution and extracted by solid phase extraction using an OASIS HLB LP 96-well plate 60 µm (60 mg). Wells were conditioned and equilibrated with 1 mL of methanol and 1 mL of water, respectively. Loaded samples were washed with

water/methanol (90:10 v/v) and eicosanoids were eluted with 750  $\mu$ L of methanol. Then solvent was evaporated to dryness under N<sub>2</sub> gas (TurboVap, Biotage) and final extracts were reconstituted with 75  $\mu$ L of methanol/water (6:1, v/v).

Extracted samples were analyzed by Reversed Phase Liquid Chromatography coupled to tandem mass spectrometry (RPLC - MS/MS)<sup>67</sup> in negative ionization modes using a 6495 triple quadrupole system (QqQ) interfaced with 1290 UHPLC system (Agilent Technologies). The chromatographic separation was carried out in an Acquity BEH C18, 1.7  $\mu$ m, 150 mm  $\times$  2.1 mm I.D. column (Waters, Massachusetts, US). Mobile phase was composed of A = water with 0.1 % acetic acid and B = acetonitrile/isopropanol 90:10 v/v at a flow rate of 500  $\mu$ L/min, column temperature 60 °C and sample injection volume 2  $\mu$ l. Gradient elution was performed with 80% of A as the starting condition, linearly decreased to 65% at 2.5 min, to 60% at 4.5 min, to 58% at 6 min, to 50% at 8 min, to 35% at 14 min, to 27.5% at 15.5 min, and to 0% at 16.6 min. The column was then washed with solvent B for 0.9 min and equilibrated to initial conditions. ESI source conditions were set as follows: dry gas temperature 290 °C, nebulizer 25 psi and flow 12 L/min, sheath gas temperature 400 °C and flow 12 L/min, nozzle voltage 2000 V, and capillary voltage 3000 V. Dynamic Multiple Reaction Monitoring (DMRM) was used as acquisition mode with a total cycle time of 250 ms. Optimized collision energies for each metabolite were applied<sup>67</sup>.

Raw LC-MS/MS data was processed using the Agilent Quantitative analysis software (version B.07.00, MassHunter Agilent technologies). Peak area integration was manually curated and corrected when necessary. Concentrations were calculated using the calibration curves and the ratio of MS response between the analyte and the stable isotope-labeled internal standard (IS), to correct for matrix effects.

The following metabolites were measured: 13-HODE, 9-HODE, 12(13)-EpOME, 12,13-DiHOME, 12-HETE, 15-HETE, 5-HETE, 9(10)-EpOME, 9,10,13-TriHOME, 9,10-DiHOME, 9,12,13-TriHOME, 9-HETE, 13-KODE, 9-KODE, 12-HEPE, 15-HEPE, 14-HDoHE, 17-HDoHE, 14,15-DiHETE, EKODE, Arachidonic acid, Linoleic Acid, Docosahexaenoic Acid, Eicosapentaenoic Acid, TXB<sub>2</sub>, 11B-PGF<sub>2a</sub>, 15-deoxy-PGJ<sub>2</sub>, 19,20-DiHDPA, 8-HETE, 11-HEPE, PGB<sub>2</sub>, PGD<sub>1</sub>, 12-KETE, 9-HEPE, 20-HETE, 8-HEPE, 11-HETE, 8-HETrE, 15(S)-HETrE, 20-COOH-LTB<sub>4</sub>, 5,6-DiHETrE, 15-KETE, 5-HEPE, 8-iso-PGE<sub>2</sub>, LTB<sub>3</sub>, LTB<sub>4</sub>, PGE<sub>1</sub>,6-keto-PGF<sub>1a</sub>, PGD<sub>2</sub>, PGD<sub>3</sub>, PGE<sub>2</sub>, 10,17-DiHDoHE, 11-HDoHE, $\delta$ 12-PGJ<sub>2</sub>, 17(R)-

Resolvin-D1, 11(12)-EpETrE, PGF2a,11,12 –DiHETrE, 14,15-DiHETrE, PGE3, PGJ2, Resolvin D1, Resolvin D2, 12(13)-EpODE, 12(S)-HHTrE, LTE4, 5-HETrE, 14(15)-EpETE, 14(15)-EpETrE, 6-trans-LTB4, 8,9-DiHETrE, 16(17)-EpDPE, 17(18)-EpETE, 17,18-DiHETE, 19(20)-EpDPE, 5(6)-EpETrE, 5,15-DiHETE, 5,6-DiHETE, 5-KETE, 8(9)-EpETrE, 9-HOTrE, 8-HDoHE, 9-KOTrE, 20-OH-LTB4, 13-HOTrE, 8,15-DiHETE, LTC4, 14,15-LTC4, LTD4, LXA4, LXA5, LXB4, 18-HEPE, 7,17-hydroxy DPA, 7-Maresin-1, tetranor-PGDM, 13,14-dihydro-15-keto PGE2, tetranor-PGEM, iPF2 $\alpha$ -IV, 5-iPF2 $\alpha$ -VI, 8-iso-PGF2 $\alpha$ , 8-iso-PGF3 $\alpha$ , 11-dehydro TXB2, TXB3, 11-dehydro TXB3, 4-HDoHE, 11-HEDE, 15-HEDE, 13-HOTrE( $\gamma$ ), 15-epi Lipoxin A4, TXB1, FOG9, 19-HETE, 15-OxoEDE, 14,15-LTE4.

### **Bone marrow derived cell culture and MDSC polarization**

Tibias and femurs from WT C57BL/6 were dissected, bone marrow was flushed and Red Blood Cells (RBC) lysed with RBC lysis buffer (Invitrogen) according to manufacturer protocol. 100'000 cells per well were plated in 24 wells plates and were cultivated during 4 days with mouse recombinant GM-CSF (Immunotools, 40ng/ml) mouse recombinant IL-6 (Peprotech,40ng/ml) and with either ethanol control, Prostaglandin E2 (Sigma-Aldrich,20nM) or 25-Hydroxycholesterol (Sigma-Aldrich,1 $\mu$ M). At the end of the experiment, adherent and non-adherent cells were collected and processed for flow cytometry as explained above.

### **Statistical analysis**

Data analyses and graphs were performed using GraphPad Prism software for Windows (GraphPad Software Inc., San Diego, CA, USA). A p-value < 0.05 was considered as significant. P-values of cell frequency, mRNA levels and oxysterols or prostaglandins concentrations were determined by either unpaired Student t-test or two-way ANOVA with Sidak's post hoc test as specified in the legends. Comparison of EAE clinical scores were assessed with two-way ANOVA with Sidak's post hoc test, EAE incidence with log-rank (Mantel-cox) test, Area Under Curve (AUC) was calculated with the AUC function of Graphpad Prism and p-values determined by unpaired Student t-test. Principal component Analysis (PCA) and its associated loading plot were determined using the PCA function of GraphPad Prism.

Preprocessing and statistical analysis of the RNA sequencing were performed by The Lausanne Genomic Technologies Facility with R (R version 3.6.1). For data processing, purity-filtered reads were adapter- and quality-trimmed with Cutadapt (v. 1.8, <sup>68</sup>). Reads matching to ribosomal RNA sequences were removed with fastq\_screen (v. 0.11.1). Remaining reads were further

filtered for low complexity with reaper (v. 15-065, <sup>69</sup>). Reads were aligned against the *Mus musculus* GRCm38.98 genome using STAR (v. 2.5.3a, <sup>70</sup>). The number of read counts per gene locus was summarized with htseq-count (v. 0.9.1, <sup>71</sup>) using the *Mus musculus* GRCm38.92 gene annotation. Quality of the RNAseq data alignment was assessed using RSeQC (v. 2.3.7, <sup>72</sup>). Genes with low counts were filtered out according to the rule of 1 count(s) per million (cpm) in at least 1 sample. Library sizes were scaled using TMM normalization. Subsequently, the normalized counts were transformed to cpm values, and a  $\log_2$  transformation was applied, by means of the function cpm with the parameter setting prior.counts = 1 (edgeR v 3.28.0; <sup>73</sup>). After data normalization, a quality control analysis was performed through sample density distribution plots, hierarchical clustering and sample PCA. Differential expression was computed with the R Bioconductor package limma (v. 3.42) by fitting data to a linear model. The approach limma-trend was used. Fold changes were computed and a moderated t-test was applied for pairwise comparison of selected conditions and for the interaction between the IL-1 $\beta$  treatment effect and the genotype (*Ch25h*<sup>ECKO</sup> vs *Ch25h*<sup>fl/fl</sup>) effect. P-values were adjusted globally on all resulting gene lists together, using the Benjamini-Hochberg (BH) method, which controls for the false discovery rate (FDR). Gene set enrichment analysis (GSEA) was conducted according to the method described in Subramanian et al. <sup>74</sup> against gene sets of the Gene Ontology (GO) <sup>75,76</sup> Biological Processes. Gene set enrichment analysis was performed using the clusterProfiler (v.4.0.5) <sup>77</sup> and the org.Mm.eg.db (v.3.13.0) packages within R (v.4.1.0). For each pairwise condition comparison, genes were sorted according to decreasing t-statistic, and provided to the “gseaGO” function, using parameters eps=1e-60, minGSSize=25, seed=T, and a seed set to 1234. The list of gene sets with adjusted p-value < 0.05 was manually parsed and representative GO terms were selected to create a dotplot of normalized enrichment scores using ggplot2 (v.3.3.5). Enrichment of genes altered in glioblastoma (GBM)-derived endothelial cells <sup>34</sup> was assessed using the GSVA package (v.1.40.1) <sup>78</sup>. A gene set variation analysis was performed for each individual sample with the “gsva” function, using either genes upregulated in GBM ECs (1233 genes) or downregulated in GBM ECs (540 genes) compared to normal brain ECs. Differences in single sample enrichment scores among conditions were assessed using an analysis of variance followed by Tukey Honest Significant Difference computations.

Gene set enrichment analysis (GSEA) was also performed with pre-ranked gene list function of the GSEA software from the Broad Institute <sup>74,79</sup> using the t statistic for ranking the input gene

lists. Unsaturated fatty acid biosynthetic process was assessed using the Gene Ontology biological process (GO: BP) collection.

To determine whether CH25H was differentially expressed between human tumor cells derived from GBM and normal brain cells from the periphery, we downloaded the matrices of raw counts per gene per single cell from NCBI's Gene Expression Omnibus (Accession number GSE162631<sup>36</sup>). The single cells came from 4 GBM samples and 4 periphery samples. We imported the matrices into R (v.4.1.0) and analyzed them with the Seurat package (v.4.1.0)<sup>80</sup>. We removed cells that expressed less than 500 genes and more than 10% mitochondrial gene expression, and we removed genes that were expressed in less than 10 cells, retaining a total of 92,820 cells. To remove batch effects linked to patient ID, we performed integration using the "FindIntegrationAnchors" and "IntegrateData" functions of Seurat: The 2000 most variable genes were selected for the cells from each sample individually, followed by identification of anchors and integration using default parameters (i.e. using 30 dimensions). The integrated counts were next scaled, and a UMAP was calculated using the first 20 principal components. For clustering, a shared nearest neighbor graph was constructed on 20 principal components, followed by clustering with the "FindClusters" function, with resolution=0.5, yielding 20 clusters. The "FindMarkers" function, implementing a Wilcoxon test, was used to determine whether CH25H and FADS2 were among the genes differentially expressed between periphery cells and tumor cells within each cluster.

Cluster annotation to cell types was performed using marker genes defined in Supplementary Table 6 of Yang et al 2022<sup>30</sup>. A score for the marker genes of each cell type was calculated using the "addModuleScore" of the Seurat package. The cluster with a high proportion of cells showing high scores for Artery, Capillary and Venous marker genes was identified as containing ECs (cluster 16).

### **Ethics approval**

All experiments were performed in accordance with guidelines from the Cantonal Veterinary Service of state Vaud (authorization #VD3393b).

### **Data availability**

All data, code, and materials used in the analysis are available to any researcher for purposes of reproducing or extending the analysis. All data are available in the main text or the supplementary materials.

## **Acknowledgments**

We thank R. Adams, M. Fruittiger, and T. Makinen for providing Cdh5-CreERT2, Pdgfb-iCreERT2 mice and Prox1-CreERT mouse strains, the Lausanne Genomic Technologies Facility for performing the RNA sequencing and the Lausanne University Metabolomic Unit for performing eicosanoids measurement.

## **Funding**

This work was supported by the Leenaards Foundation (to C.P., S.H. and T.P.), the Swiss National Science Foundation (PP00P3-157476 to CP), the Swiss National Science Foundation (310030-192738 to CP), the Swiss National Science Foundation (#323630-183987), MD-PhD grant to FR.

## **Competing interests**

Authors declare that they have no conflict of interests.

## **Author contributions**

Conceptualization: FR, SV, TP, SH, CP, Investigation: FR, SV, JR, TW, YY, VB, CK, GB, BP, GGM, Visualization: FR, CP, TW, LR, TP, Funding acquisition: FR, TP, SH, CP, Project administration: CP, Supervision: CP, Writing – original draft: FR, CP, Writing – review & editing: FR, GGM, SH, TP, CP

## **The Paper Explained**

### **Problem**

Multiple sclerosis remains an incurable disease and understanding its physiopathology is crucial to unravel new therapeutic targets. Endothelial cells are key regulators of leukocyte trafficking

into the central nervous system and therefore play a crucial role in driving multiple sclerosis disease activity. However, in the central nervous system, the inflamed endothelium produces immunomodulatory signals whose function goes beyond the regulation of immune cell migration and thus, could drive neuroinflammation by other mechanisms that are largely unexplored.

## **Results**

Our findings reveal that inflamed endothelial cells produces bioactive lipids that can contribute to the emergence of a “cancer-like” immunosuppressive environment. Notably, we identified that alterations of lipid metabolism in endothelial cells regulate polymorphonuclear myeloid-derived suppressor cell expansion (PMN-MDSC) during experimental autoimmune encephalomyelitis (EAE), a murine model of multiple sclerosis. Those cells are known to suppress the anti-tumor activity of lymphocytes and we identified that they suppress encephalitogenic CD4 T cell proliferation during EAE . Our findings reveal a central role for endothelial-derived bioactive lipids in driving CNS inflammation.

## **Impact**

This study reveal a novel function of endothelial cells as a source of bioactive lipids that have the ability to regulate neuroinflammation through mechanism beyond immune cell trafficking. We here identified potential new targets for MS treatment.

## References

1. Nishihara H, Perriot S, Gastfriend BD, et al. Intrinsic blood-brain barrier dysfunction contributes to multiple sclerosis pathogenesis. *Brain*. Jan 27 2022;doi:10.1093/brain/awac019
2. Chalmin F, Rochemont V, Lippens C, et al. Oxysterols regulate encephalitogenic CD4(+) T cell trafficking during central nervous system autoimmunity. *J Autoimmun*. Jan 2015;56:45-55. doi:10.1016/j.jaut.2014.10.001
3. Durfinova M, Prochazkova L, Petrlenicova D, et al. Cholesterol level correlate with disability score in patients with relapsing-remitting form of multiple sclerosis. *Neurosci Lett*. Nov 20 2018;687:304-307. doi:10.1016/j.neulet.2018.10.030
4. Mutemberezi V, Guillemot-Legrís O, Muccioli GG. Oxysterols: From cholesterol metabolites to key mediators. *Prog Lipid Res*. Oct 2016;64:152-169. doi:10.1016/j.plipres.2016.09.002
5. Liu C, Yang XV, Wu J, et al. Oxysterols direct B-cell migration through EB12. *Nature*. Jul 27 2011;475(7357):519-23. doi:10.1038/nature10226
6. Dendrou CA, Fugger L, Friese MA. Immunopathology of multiple sclerosis. *Nat Rev Immunol*. Sep 15 2015;15(9):545-58. doi:10.1038/nri3871
7. Olsson T, Barcellos LF, Alfredsson L. Interactions between genetic, lifestyle and environmental risk factors for multiple sclerosis. *Nat Rev Neurol*. Jan 2017;13(1):25-36. doi:10.1038/nrneuro.2016.187
8. Clottu AS, Mathias A, Sailer AW, et al. EB12 Expression and Function: Robust in Memory Lymphocytes and Increased by Natalizumab in Multiple Sclerosis. *Cell Rep*. Jan 3 2017;18(1):213-224. doi:10.1016/j.celrep.2016.12.006
9. Wanke F, Moos S, Croxford AL, et al. EB12 Is Highly Expressed in Multiple Sclerosis Lesions and Promotes Early CNS Migration of Encephalitogenic CD4 T Cells. *Cell Rep*. Jan 31 2017;18(5):1270-1284. doi:10.1016/j.celrep.2017.01.020
10. Mutemberezi V, Buisseret B, Masquelier J, Guillemot-Legrís O, Alhouayek M, Muccioli GG. Oxysterol levels and metabolism in the course of neuroinflammation: insights from in vitro and in vivo models. *J Neuroinflammation*. Mar 9 2018;15(1):74. doi:10.1186/s12974-018-1114-8
11. Emgard J, Kammoun H, Garcia-Cassani B, et al. Oxysterol Sensing through the Receptor GPR183 Promotes the Lymphoid-Tissue-Inducing Function of Innate Lymphoid Cells and Colonic Inflammation. *Immunity*. Jan 16 2018;48(1):120-132 e8. doi:10.1016/j.immuni.2017.11.020
12. Yi T, Wang X, Kelly LM, et al. Oxysterol gradient generation by lymphoid stromal cells guides activated B cell movement during humoral responses. *Immunity*. Sep 21 2012;37(3):535-48. doi:10.1016/j.immuni.2012.06.015
13. Munji RN, Soung AL, Weiner GA, et al. Profiling the mouse brain endothelial transcriptome in health and disease models reveals a core blood-brain barrier dysfunction module. *Nat Neurosci*. Nov 2019;22(11):1892-1902. doi:10.1038/s41593-019-0497-x
14. Veglia F, Sanseviero E, Gabrilovich DI. Myeloid-derived suppressor cells in the era of increasing myeloid cell diversity. *Nat Rev Immunol*. Feb 1 2021;doi:10.1038/s41577-020-00490-y
15. Knier B, Hiltensperger M, Sie C, et al. Myeloid-derived suppressor cells control B cell accumulation in the central nervous system during autoimmunity. *Nat Immunol*. Dec 2018;19(12):1341-1351. doi:10.1038/s41590-018-0237-5
16. Condamine T, Mastio J, Gabrilovich DI. Transcriptional regulation of myeloid-derived suppressor cells. *J Leukoc Biol*. Dec 2015;98(6):913-22. doi:10.1189/jlb.4RI0515-204R
17. Wang Y, Nakayama M, Pitulescu ME, et al. Ephrin-B2 controls VEGF-induced angiogenesis and lymphangiogenesis. *Nature*. May 27 2010;465(7297):483-6. doi:10.1038/nature09002
18. Claxton S, Kostourou V, Jadeja S, Chambon P, Hodivala-Dilke K, Fruttiger M. Efficient, inducible Cre-recombinase activation in vascular endothelium. *Genesis*. Feb 2008;46(2):74-80. doi:10.1002/dvg.20367
19. Bernier-Latmani J, Cisarovsky C, Demir CS, et al. DLL4 promotes continuous adult intestinal lacteal regeneration and dietary fat transport. *J Clin Invest*. Nov 3 2015;125(12):4572-86. doi:10.1172/JCI82045
20. Hauptmann J, Johann L, Marini F, et al. Interleukin-1 promotes autoimmune neuroinflammation by suppressing endothelial heme oxygenase-1 at the blood-brain barrier. *Acta Neuropathol*. Oct 2020;140(4):549-567. doi:10.1007/s00401-020-02187-x
21. Lu Z, Ortiz A, Verginadis, II, et al. Regulation of intercellular biomolecule transfer-driven tumor angiogenesis and responses to anticancer therapies. *J Clin Invest*. May 17 2021;131(10)doi:10.1172/JCI144225
22. Adams CM, Reitz J, De Brabander JK, et al. Cholesterol and 25-hydroxycholesterol inhibit activation of SREBPs by different mechanisms, both involving SCAP and Insigs. *J Biol Chem*. Dec 10 2004;279(50):52772-80. doi:10.1074/jbc.M410302200

23. Muramatsu R, Takahashi C, Miyake S, Fujimura H, Mochizuki H, Yamashita T. Angiogenesis induced by CNS inflammation promotes neuronal remodeling through vessel-derived prostacyclin. *Nat Med.* Nov 2012;18(11):1658-64. doi:10.1038/nm.2943
24. Liu R, Qiao S, Shen W, et al. Disturbance of Fatty Acid Desaturation Mediated by FADS2 in Mesenteric Adipocytes Contributes to Chronic Inflammation of Crohn's Disease. *J Crohns Colitis.* Nov 7 2020;14(11):1581-1599. doi:10.1093/ecco-jcc/jjaa086
25. Beck KR, Kanagaratnam S, Kratschmar DV, et al. Enzymatic interconversion of the oxysterols 7beta,25-dihydroxycholesterol and 7-keto,25-hydroxycholesterol by 11beta-hydroxysteroid dehydrogenase type 1 and 2. *J Steroid Biochem Mol Biol.* Jun 2019;190:19-28. doi:10.1016/j.jsbmb.2019.03.011
26. Nakamura MT, Nara TY. Structure, function, and dietary regulation of delta6, delta5, and delta9 desaturases. *Annu Rev Nutr.* 2004;24:345-76. doi:10.1146/annurev.nutr.24.121803.063211
27. Lu W, Yu W, He J, et al. Reprogramming immunosuppressive myeloid cells facilitates immunotherapy for colorectal cancer. *EMBO Mol Med.* Jan 11 2021;13(1):e12798. doi:10.15252/emmm.202012798
28. Marigo I, Bosio E, Solito S, et al. Tumor-induced tolerance and immune suppression depend on the C/EBPbeta transcription factor. *Immunity.* Jun 25 2010;32(6):790-802. doi:10.1016/j.immuni.2010.05.010
29. Ridder DA, Lang MF, Salinin S, et al. TAK1 in brain endothelial cells mediates fever and lethargy. *J Exp Med.* Dec 19 2011;208(13):2615-23. doi:10.1084/jem.20110398
30. Yang AC, Vest RT, Kern F, et al. A human brain vascular atlas reveals diverse mediators of Alzheimer's risk. *Nature.* Feb 14 2022;doi:10.1038/s41586-021-04369-3
31. Absinta M, Maric D, Gharagozloo M, et al. A lymphocyte-microglia-astrocyte axis in chronic active multiple sclerosis. *Nature.* Sep 2021;597(7878):709-714. doi:10.1038/s41586-021-03892-7
32. Schirmer L, Velmeshev D, Holmqvist S, et al. Neuronal vulnerability and multilineage diversity in multiple sclerosis. *Nature.* Sep 2019;573(7772):75-82. doi:10.1038/s41586-019-1404-z
33. Finetti F, Travelli C, Ercoli J, Colombo G, Buoso E, Trabalzini L. Prostaglandin E2 and Cancer: Insight into Tumor Progression and Immunity. *Biology (Basel).* Dec 1 2020;9(12)doi:10.3390/biology9120434
34. Schaffnerath J, Wyss T, He L, et al. Blood-brain barrier alterations in human brain tumors revealed by genome-wide transcriptomic profiling. *Neuro Oncol.* Dec 1 2021;23(12):2095-2106. doi:10.1093/neuonc/noab022
35. Chai E, Zhang L, Li C. LOX-1+ PMN-MDSC enhances immune suppression which promotes glioblastoma multiforme progression. *Cancer Manag Res.* 2019;11:7307-7315. doi:10.2147/CMAR.S210545
36. Xie Y, He L, Lugano R, et al. Key molecular alterations in endothelial cells in human glioblastoma uncovered through single-cell RNA sequencing. *JCI Insight.* Aug 9 2021;6(15)doi:10.1172/jci.insight.150861
37. Li T, Fu J, Zeng Z, et al. TIMER2.0 for analysis of tumor-infiltrating immune cells. *Nucleic Acids Res.* Jul 2 2020;48(W1):W509-W514. doi:10.1093/nar/gkaa407
38. Boivin G, Faget J, Ancey PB, et al. Durable and controlled depletion of neutrophils in mice. *Nat Commun.* Jun 2 2020;11(1):2762. doi:10.1038/s41467-020-16596-9
39. Honda A, Miyazaki T, Ikegami T, et al. Cholesterol 25-hydroxylation activity of CYP3A. *J Lipid Res.* Aug 2011;52(8):1509-16. doi:10.1194/jlr.M014084
40. Vigne S, Chalmin F, Duc D, et al. IL-27-Induced Type 1 Regulatory T-Cells Produce Oxysterols that Constrain IL-10 Production. *Front Immunol.* 2017;8:1184. doi:10.3389/fimmu.2017.01184
41. Dang EV, McDonald JG, Russell DW, Cyster JG. Oxysterol Restraint of Cholesterol Synthesis Prevents AIM2 Inflammasome Activation. *Cell.* Nov 16 2017;171(5):1057-1071 e11. doi:10.1016/j.cell.2017.09.029
42. Gold ES, Diercks AH, Podolsky I, et al. 25-Hydroxycholesterol acts as an amplifier of inflammatory signaling. *Proc Natl Acad Sci U S A.* Jul 22 2014;111(29):10666-71. doi:10.1073/pnas.1404271111
43. Jia J, Conlon TM, Sarker RS, et al. Cholesterol metabolism promotes B-cell positioning during immune pathogenesis of chronic obstructive pulmonary disease. *EMBO Mol Med.* May 2018;10(5)doi:10.15252/emmm.201708349
44. Madenspacher JH, Morrell ED, Gowdy KM, et al. Cholesterol 25-hydroxylase promotes efferocytosis and resolution of lung inflammation. *JCI Insight.* Jun 4 2020;5(11)doi:10.1172/jci.insight.137189
45. Reboldi A, Dang EV, McDonald JG, Liang G, Russell DW, Cyster JG. Inflammation. 25-Hydroxycholesterol suppresses interleukin-1-driven inflammation downstream of type I interferon. *Science.* Aug 8 2014;345(6197):679-84. doi:10.1126/science.1254790
46. Russo L, Muir L, Geletka L, et al. Cholesterol 25-hydroxylase (CH25H) as a promoter of adipose tissue inflammation in obesity and diabetes. *Mol Metab.* Sep 2020;39:100983. doi:10.1016/j.molmet.2020.100983
47. Wyss A, Raselli T, Perkins N, et al. The EBI2-oxysterol axis promotes the development of intestinal lymphoid structures and colitis. *Mucosal Immunol.* May 2019;12(3):733-745. doi:10.1038/s41385-019-0140-x

48. Berer K, Mues M, Koutrolos M, et al. Commensal microbiota and myelin autoantigen cooperate to trigger autoimmune demyelination. *Nature*. Oct 26 2011;479(7374):538-41. doi:10.1038/nature10554
49. Sonner JK, Keil M, Falk-Paulsen M, et al. Dietary tryptophan links encephalogenicity of autoreactive T cells with gut microbial ecology. *Nat Commun*. Oct 25 2019;10(1):4877. doi:10.1038/s41467-019-12776-4
50. Reynolds JD, Case LK, Kremtsov DN, Raza A, Bartiss R, Teuscher C. Modeling month-season of birth as a risk factor in mouse models of chronic disease: from multiple sclerosis to autoimmune encephalomyelitis. *FASEB J*. Jun 2017;31(6):2709-2719. doi:10.1096/fj.201700062
51. Sisay S, Pryce G, Jackson SJ, et al. Genetic background can result in a marked or minimal effect of gene knockout (GPR55 and CB2 receptor) in experimental autoimmune encephalomyelitis models of multiple sclerosis. *PLoS One*. 2013;8(10):e76907. doi:10.1371/journal.pone.0076907
52. Li Z, Martin M, Zhang J, et al. Kruppel-Like Factor 4 Regulation of Cholesterol-25-Hydroxylase and Liver X Receptor Mitigates Atherosclerosis Susceptibility. *Circulation*. Oct 3 2017;136(14):1315-1330. doi:10.1161/CIRCULATIONAHA.117.027462
53. Walzl S, Patankar JV, Fauler G, et al. 25-Hydroxycholesterol regulates cholesterol homeostasis in the murine CATH.a neuronal cell line. *Neurosci Lett*. Feb 28 2013;539:16-21. doi:10.1016/j.neulet.2013.01.014
54. Triki M, Rinaldi G, Planque M, et al. mTOR Signaling and SREBP Activity Increase FADS2 Expression and Can Activate Sapienate Biosynthesis. *Cell Rep*. Jun 23 2020;31(12):107806. doi:10.1016/j.celrep.2020.107806
55. Langer-Gould A, Black LJ, Waubant E, et al. Seafood, fatty acid biosynthesis genes, and multiple sclerosis susceptibility. *Mult Scler*. Oct 2020;26(12):1476-1485. doi:10.1177/1352458519872652
56. Kihara Y, Matsushita T, Kita Y, et al. Targeted lipidomics reveals mPGES-1-PGE2 as a therapeutic target for multiple sclerosis. *Proc Natl Acad Sci U S A*. Dec 22 2009;106(51):21807-12. doi:10.1073/pnas.0906891106
57. Esaki Y, Li Y, Sakata D, et al. Dual roles of PGE2-EP4 signaling in mouse experimental autoimmune encephalomyelitis. *Proc Natl Acad Sci U S A*. Jul 6 2010;107(27):12233-8. doi:10.1073/pnas.0915112107
58. Harbige LS, Layward L, Morris-Downes MM, Dumonde DC, Amor S. The protective effects of omega-6 fatty acids in experimental autoimmune encephalomyelitis (EAE) in relation to transforming growth factor-beta 1 (TGF-beta1) up-regulation and increased prostaglandin E2 (PGE2) production. *Clin Exp Immunol*. Dec 2000;122(3):445-52. doi:10.1046/j.1365-2249.2000.01399.x
59. Bronte V, Brandau S, Chen SH, et al. Recommendations for myeloid-derived suppressor cell nomenclature and characterization standards. *Nat Commun*. Jul 6 2016;7:12150. doi:10.1038/ncomms12150
60. Sas AR, Carbajal KS, Jerome AD, et al. A new neutrophil subset promotes CNS neuron survival and axon regeneration. *Nat Immunol*. Dec 2020;21(12):1496-1505. doi:10.1038/s41590-020-00813-0
61. McGinley AM, Sutton CE, Edwards SC, et al. Interleukin-17A Serves a Priming Role in Autoimmunity by Recruiting IL-1beta-Producing Myeloid Cells that Promote Pathogenic T Cells. *Immunity*. Feb 18 2020;52(2):342-356 e6. doi:10.1016/j.immuni.2020.01.002
62. Brat DJ, Van Meir EG. Glomeruloid microvascular proliferation orchestrated by VPF/VEGF: a new world of angiogenesis research. *Am J Pathol*. Mar 2001;158(3):789-96. doi:10.1016/S0002-9440(10)64025-4
63. Papassotiropoulos A, Lambert JC, Wavrant-De Vrieze F, et al. Cholesterol 25-hydroxylase on chromosome 10q is a susceptibility gene for sporadic Alzheimer's disease. *Neurodegener Dis*. 2005;2(5):233-41. doi:10.1159/000090362
64. Crespo I, Tao H, Nieto AB, et al. Amplified and homozygously deleted genes in glioblastoma: impact on gene expression levels. *PLoS One*. 2012;7(9):e46088. doi:10.1371/journal.pone.0046088
65. Coisne C, Dehouck L, Faveeuw C, et al. Mouse syngenic in vitro blood-brain barrier model: a new tool to examine inflammatory events in cerebral endothelium. *Lab Invest*. Jun 2005;85(6):734-46. doi:10.1038/labinvest.3700281
66. Mutemberezi V, Masquelier J, Guillemot-Legrès O, Muccioli GG. Development and validation of an HPLC-MS method for the simultaneous quantification of key oxysterols, endocannabinoids, and ceramides: variations in metabolic syndrome. *Anal Bioanal Chem*. Jan 2016;408(3):733-45. doi:10.1007/s00216-015-9150-z
67. Kolmert J, Fauland A, Fuchs D, et al. Lipid Mediator Quantification in Isolated Human and Guinea Pig Airways: An Expanded Approach for Respiratory Research. *Anal Chem*. Sep 4 2018;90(17):10239-10248. doi:10.1021/acs.analchem.8b01651
68. Martin M. Cutadapt removes adapter sequences from high-throughput sequencing reads. *next generation sequencing; small RNA; microRNA; adapter removal*. 2011. 2011-05-02 2011;17(1):3. doi:10.14806/ej.17.1.200
69. Davis MP, van Dongen S, Abreu-Goodger C, Bartonicek N, Enright AJ. Kraken: a set of tools for quality control and analysis of high-throughput sequence data. *Methods*. Sep 1 2013;63(1):41-9. doi:10.1016/j.ymeth.2013.06.027

70. Dobin A, Davis CA, Schlesinger F, et al. STAR: ultrafast universal RNA-seq aligner. *Bioinformatics*. Jan 1 2013;29(1):15-21. doi:10.1093/bioinformatics/bts635
71. Anders S, Pyl PT, Huber W. HTSeq--a Python framework to work with high-throughput sequencing data. *Bioinformatics*. Jan 15 2015;31(2):166-9. doi:10.1093/bioinformatics/btu638
72. Wang L, Wang S, Li W. RSeQC: quality control of RNA-seq experiments. *Bioinformatics*. Aug 15 2012;28(16):2184-5. doi:10.1093/bioinformatics/bts356
73. Robinson MD, McCarthy DJ, Smyth GK. edgeR: a Bioconductor package for differential expression analysis of digital gene expression data. *Bioinformatics*. Jan 1 2010;26(1):139-40. doi:10.1093/bioinformatics/btp616
74. Subramanian A, Tamayo P, Mootha VK, et al. Gene set enrichment analysis: a knowledge-based approach for interpreting genome-wide expression profiles. *Proc Natl Acad Sci U S A*. Oct 25 2005;102(43):15545-50. doi:10.1073/pnas.0506580102
75. Ashburner M, Ball CA, Blake JA, et al. Gene ontology: tool for the unification of biology. The Gene Ontology Consortium. *Nat Genet*. May 2000;25(1):25-9. doi:10.1038/75556
76. Gene Ontology C. The Gene Ontology resource: enriching a GOld mine. *Nucleic Acids Res*. Jan 8 2021;49(D1):D325-D334. doi:10.1093/nar/gkaa1113
77. Yu G, Wang LG, Han Y, He QY. clusterProfiler: an R package for comparing biological themes among gene clusters. *OMICS*. May 2012;16(5):284-7. doi:10.1089/omi.2011.0118
78. Hanzelmann S, Castelo R, Guinney J. GSEA: gene set variation analysis for microarray and RNA-seq data. *BMC Bioinformatics*. Jan 16 2013;14:7. doi:10.1186/1471-2105-14-7
79. Mootha VK, Lindgren CM, Eriksson KF, et al. PGC-1alpha-responsive genes involved in oxidative phosphorylation are coordinately downregulated in human diabetes. *Nat Genet*. Jul 2003;34(3):267-73. doi:10.1038/ng1180
80. Hao Y, Hao S, Andersen-Nissen E, et al. Integrated analysis of multimodal single-cell data. *Cell*. Jun 24 2021;184(13):3573-3587 e29. doi:10.1016/j.cell.2021.04.048

## Figures legends

**Figure 1 Ch25h expression in blood endothelial cells promotes EAE.** (A) Construct of *Ch25h-eGFP<sup>fl/fl</sup>* mice. (B) Flow cytometry analysis of Ch25h-eGFP reporter expression in CNS endothelial cells (CNS ECs: Live cells CD45<sup>-</sup>Ter119<sup>-</sup>CD13<sup>-</sup>CD31<sup>+</sup>). Wild-type mice were used as negative controls for eGFP signal. CNS ECs from Ch25h-eGFP (*Ch25h<sup>fl/fl</sup>*) mice and Ch25h-eGFP<sup>fl/fl</sup>-Ve-CadherinCreERT2 mice (*Ch25h<sup>ECKO</sup>*) mice where the Cre recombinase is expressed in the endothelial cells are compared. Non-immunized mice (NI) are compared with mice at the peak of EAE (day 16 after immunization). (C) Percentage of eGFP<sup>+</sup> CNS ECs in the same condition as in (B). Symbols indicate individual mice and bars indicate mean  $\pm$  SD. *Ch25h<sup>fl/fl</sup>* NI:  $n = 4$ , *Ch25h<sup>fl/fl</sup>* EAE:  $n = 5$ , *Ch25h<sup>ECKO</sup>* NI:  $n = 4$ , *Ch25h<sup>ECKO</sup>* EAE,  $n = 4$ . (D). EAE disease course in *Ch25h<sup>ECKO</sup>* and Cre negative littermates (*Ch25h<sup>fl/fl</sup>*). Top panel: EAE clinical score. Bars indicate mean  $\pm$  SEM. Bottom panel: Survival analysis of EAE, depicting disease incidence. (E) As in (D) except that *Ch25h<sup>fl/fl</sup>*-Pdgfb-iCreERT2 mice that express Cre recombinase in blood endothelial cells (*Ch25h<sup>BECKO</sup>*) are shown. (F) As in (D) except that *Ch25h<sup>fl/fl</sup>*-Prox1Cre mice that express Cre recombinase in lymphatic endothelial cells (*Ch25h<sup>LECKO</sup>*) are shown. (D-F) Representative results of 2 experiments with a minimum of  $n = 5$ /group.

ns = non-significant, \*  $P \leq 0.05$ , \*\*\*  $P \leq 0.0005$ , \*\*\*\*  $P \leq 0.00005$ . p values were determined by two-way ANOVA with Sidak's post hoc test (C and top panels D,E,F) and log-rank (mantel-cox) test (bottom panels d,e,f).

**Figure 2 Transcriptomic alterations in *Ch25h<sup>ECKO</sup>* CNS endothelial cells.** (A) RT-qPCR analysis of Ch25h expression in primary mouse brain microvascular endothelial cells (pMBMECs) isolated from *Ch25h<sup>fl/fl</sup>* and *Ch25h<sup>ECKO</sup>* mice. Cells were left unstimulated (NS) or stimulated with IL-1 $\beta$ .

$n = 5$  biological replicates/group. (B) Venn diagram of differentially expressed genes (DEG) between *Ch25h<sup>ECKO</sup>* and *Ch25h<sup>fl/fl</sup>* pMBMECs assessed by RNA sequencing comparing non-stimulated (NS) and IL-1 $\beta$  stimulated cells.  $n = 3$ /group. (C) Dot plot of gene set enrichment analysis (GSEA) showing selected pathways. NES = normalized enrichment score. (D) GSEA comparing enrichment of genes related to unsaturated fatty acid biosynthesis in *Ch25h<sup>ECKO</sup>* vs *Ch25h<sup>fl/fl</sup>* IL-1 $\beta$  stimulated pMBMECs. NES = normalized enrichment score, FDR= false discovery rate q-value. (E) Heatmap showing normalized expression (z-scores) of gene counts

from the RNAseq analysis related to the unsaturated fatty-acid biosynthetic pathway. **(F)** RT-qPCR of pMBMECs isolated from *Ch25h*<sup>ECKO</sup> and *Ch25h*<sup>fl/fl</sup> mice and stimulated with IL-1 $\beta$ . *n* = 4 biological replicates/group. **(G)** RT-qPCR of CNS endothelial cells sorted from *Ch25h*<sup>ECKO</sup> and *Ch25h*<sup>fl/fl</sup> mice during EAE (day 10 after immunization). *Ch25h*<sup>ECKO</sup> *n* = 3, *Ch25h*<sup>fl/fl</sup> *n* = 4. Bars indicate mean  $\pm$  SD. ns= non-significant, \**P* < 0.05. P values were determined by unpaired t-test.

**Figure 3 Ch25h deletion in CNS endothelial cells induces a remodeling of secreted lipid. (A)**

Principal component analysis of 10 oxysterols measured by HPLC-MS in the supernatant of pMBMECs isolated from *Ch25h*<sup>fl/fl</sup> mice and *Ch25h*<sup>ECKO</sup> mice. Cells were left unstimulated (NS) or stimulated by IL-1 $\beta$ . **(B)** Loading plot showing the contribution of oxysterols to PC1 and PC2. **(C)** 25-OHC, 7-k-25-OHC and 7-ketocholesterol concentration in the same conditions as in **(D)**. Bars represent mean  $\pm$  SD. *n* = 6 biological replicates/group except for *Ch25h*<sup>fl/fl</sup> IL-1 $\beta$  were *n* = 5. **(E) Left panel:** Principal component analysis of 49 eicosanoids measured by HPLC-MS/MS in the supernatant of pMBMECs in the same conditions as in **(A)**. *n* = 5 biological replicates/group. **Right panel:** Comparison of PC1 scores between the different conditions. **(E) Upper panel:** loading plot showing the contribution of each detected eicosanoids to PC1 and PC2. **Lower panel:** Relative contribution of prostaglandins to PC1. **(F)** Prostaglandin concentration (nM) in the supernatant of pMBMECs comparing conditions mentioned in **(A)**.

Bars represent mean  $\pm$  SD. ns= non-significant, \* *P* < 0.05, \*\* *P*  $\leq$  0.005, \*\*\*\* *P*  $\leq$  0.00005. P values were determined by two-tailed unpaired t-test (D) or by two-way ANOVA with Sidak's post hoc test (C and F).

**Figure 4 Ch25h deletion in endothelial cells favors PMN-MDSC expansion in the CNS during EAE. (A)**

Flow cytometry analysis of bone marrow-derived cells cultured in MDSC polarizing conditions treated with vehicle control (EtOH), PGE2 and 25-OHC. M-MDSC = Live cells CD11b<sup>+</sup> Ly6C<sup>high</sup> Ly6G<sup>-</sup>, PMN-MDSC = Live cells CD11b<sup>+</sup> Ly6C<sup>+</sup> Ly6G<sup>+</sup>. **(B)** Same conditions as in **(A)** except that bar graphs are shown. Symbols depict mean percentage of PMN-MDSC (upper panel) and M-MDSC (lower panel) in live cells. *n* = 5/group. **(C)** Impact of PMN-MDSC on CD4 T cell proliferation (anti CD3/CD28) assessed by CFSE dilution using flow cytometry. PMN-MDSC were FACS-sorted from the CNS of WT mice at the peak of EAE. NS=

non stimulated.  $n = 4$ /group. **(D)** Correlation of the percentage of PMN-MDSC in live cells with the percentage  $CD4^+CD44^+Ki67^+$  cells in live cells in the CNS at the peak of EAE assessed by flow cytometry.  $n = 17$  individual mice. **(E)** Flow cytometry analysis of PMN-MDSC in the CNS at the peak of EAE in  $Ch25h^{fl/fl}$  and  $Ch25h^{ECKO}$  mice. **(F)** Percentage of PMN-MDSC (left) and  $CD4^+CD44^+Ki67^+$  cells (right) in live cells of the CNS at the peak of the disease of  $Ch25h^{fl/fl}$  ( $n = 9$ ) and  $Ch25h^{ECKO}$  mice ( $n = 8$ ). Symbols depict individual mice and bars indicate mean  $\pm$  SD. Combined results of two independent experiments **(G)** EAE disease course in  $Ch25h^{BBBKO}$  mice ( $n = 11$ ) where the cre-recombinase is expressed endothelial cells of the CNS and Cre negative littermates ( $Ch25h^{fl/fl}$ :  $n = 7$  and  $Ch25h^{fl/wt}$ :  $n = 2$ ). Bars indicate mean  $\pm$  SEM. Representative results of two independent experiments.

ns= non-significant, \*  $P < 0.05$ , \*\*  $P \leq 0.005$ , \*\*\*\*  $P \leq 0.00005$ . P values were determined by two-tailed unpaired t-test (B,C and F), Spearman correlation (D) and by two-way ANOVA with Sidak's post hoc test (G).

**Figure 5 Ch25h expression is reduced in ECs of human glioblastoma (GBM).** **(A)** Dot plot showing enrichment of differentially expressed in GBM ECs, in  $Ch25h^{ECKO}$  and  $Ch25h^{fl/fl}$  pMBMECs non stimulated (NS) or stimulated with IL-1 $\beta$  assessed by RNAseq ( $n=3$ ). ssGSEA= single sample gene set enrichment analysis. **(B)** Top left panel: UMAP (uniform manifold approximation and projection) showing the 20 clusters identified in the single-cell RNAseq dataset of GBM and peri-tumoral tissue enriched in  $CD31^+$  cells from GSE162631. Top right and bottom panels: UMAP showing the score of each single-cell for the gene signatures of Arterial, Capillary and Venous blood ECs as defined by Yang et al. **(C)** Natural-log transformed normalized counts of CH25H mRNA transcripts in single cells from cluster 16, comparing ECs in GBM and ECs in the periphery. **(D)** Correlation between gene expression and MDSC infiltration in GBM assessed with the TIMER2.0 database.

ns= non-significant, \*  $P < 0.05$ , \*\*  $P \leq 0.005$ , \*\*\*\*  $P \leq 0.00005$ . See methods for the statistical analysis.

**Figure 6 CD101<sup>+</sup> neutrophils depletion protects  $Ch25h^{ECKO}$  mice from EAE and favors CNS PMN-MDSC accumulation.** **(A)** EAE disease course in  $Ch25h^{fl/fl}$  mice and  $Ch25h^{ECKO}$  mice treated with isotype control antibody or Combo protocol (Ly6G<sup>high</sup> cells depletion). Treatment

was initiated on the day of first symptoms occurrence (day 12 post-immunization). Symbols depict mean clinical score and bars mean  $\pm$  SEM. *Ch25h<sup>fl/fl</sup>* isotype:  $n = 7$ , *Ch25h<sup>ECKO</sup>* isotype:  $n = 8$ , *Ch25h<sup>fl/fl</sup>* combo:  $n = 8$ , *Ch25h<sup>ECKO</sup>* combo:  $n = 9$ . **(B)** Survival analysis in the same conditions as in **(A)**. **(C)** Representative contour plots of PMN-MDSC in the CNS at day 22 of EAE assessed by flow cytometry in the same conditions as in **(A)**. **(D)** As in **(C)** except that statistical analysis and percentage of PMN-MDSC in live cells is shown. Symbols depict individual mice and bars mean  $\pm$  SD. *Ch25h<sup>fl/fl</sup>* Isotype  $n= 4$ , *Ch25h<sup>ECKO</sup>* isotype  $n=4$ , *Ch25h<sup>fl/fl</sup>* Combo,  $n =3$ , *Ch25h<sup>ECKO</sup>* Combo  $n=4$ . **(E)** CD101 expression in blood and CNS neutrophils at day 22 of EAE in isotype and combo treated mice assessed by flow cytometry. Isotype  $n=8$ , combo  $n=7$ . Symbols depict individual mice, bars mean  $\pm$  SD. **(F)** CD101<sup>+</sup> blood neutrophils (left panel) and CD101<sup>-</sup> neutrophils (right panel) kinetic during EAE in isotype, and Combo treated mice assessed by flow cytometry. Treatment was initiated at the first symptoms of EAE (day 14 after immunization).  $n=11$ /group.

ns= non-significant, \* $P < 0.05$ , \*\*  $P \leq 0.005$ , \*\*\*  $P \leq 0.0005$  \*\*\*\*  $P \leq 0.00005$ . P values were determined by two-way ANOVA with Sidak's post hoc test (A,E,F) spearman correlation (B) and two-tailed unpaired t-test (D).

## Tables

**Table 1. Comparison of EAE disease course in *Ch25h*<sup>fl/fl</sup>, *Ch25h*<sup>ECKO</sup>, *Ch25h*<sup>BECKO</sup> and *Ch25h*<sup>LECKO</sup> mice.**

Group	Disease incidence	Mean maximum score (SD)	Mean day of onset (SD)	AUC (SEM)
<i>Ch25h</i> <sup>fl/fl</sup>	80%	3.5 ± 0.93	12.25 ± 0.89	19.55 ± 2.78
<i>Ch25h</i> <sup>ECKO</sup>	45.5% *	2.7 ± 0.67	14.4 ± 1.95 (p=0.05)	7.318 ± 2.55 *
<i>Ch25h</i> <sup>fl/fl</sup>	90%	2.94 ± 1.5	14.07 ± 1.91	23.56 ± 3.98
<i>Ch25h</i> <sup>BECKO</sup>	55.5% *	3 ± 0	14.4 ± 1.34	12.29 ± 2.67 (p= 0.08)
<i>Ch25h</i> <sup>fl/fl</sup>	71.40%	2.8 ± 0.45	14.4 ± 0.89	14.6 ± 2.7
<i>Ch25h</i> <sup>LECKO</sup>	80%	2.75 ± 0.5	14.5 ± 1.78	17.25 ± 2.73

**Table 1. Related to Figure 1. *Ch25h* deletion in blood ECs is protective during EAE.**

AUC = Area under the curve. Mean ± SD or SEM for AUC are indicated. P values were determined by unpaired student t-test or log-rank (mantel-cox) test for diseases incidence. \* : p<0.05. Representative results of two independent experiments per genotype with a minimum of n=5/group.

## Supplementary tables legends

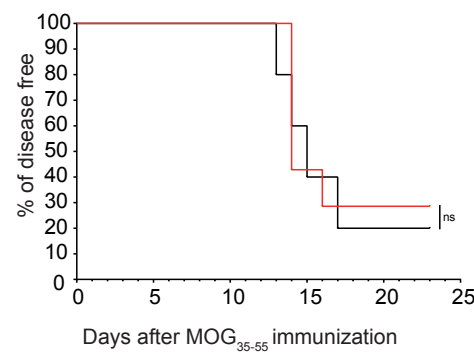
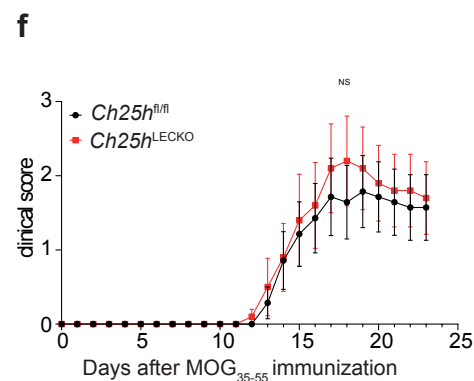
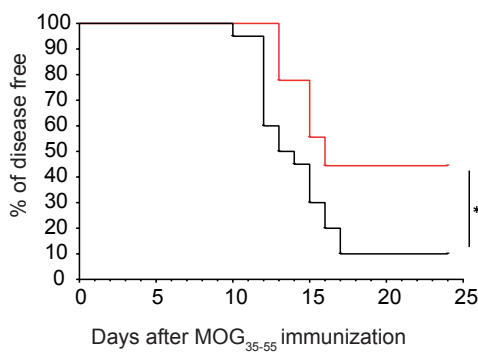
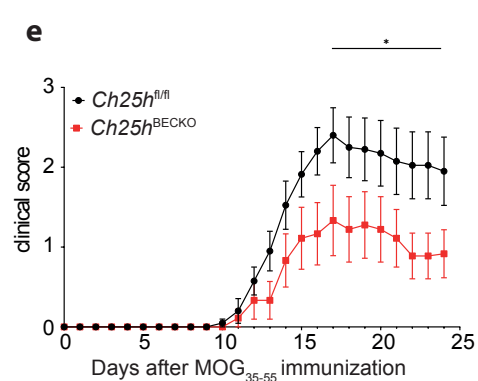
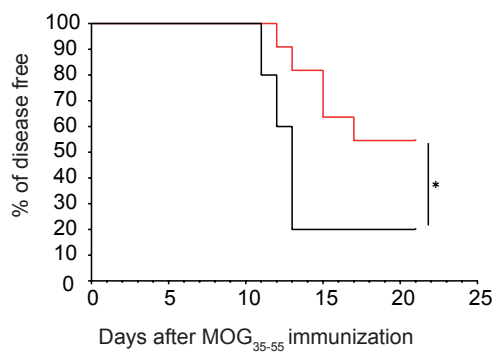
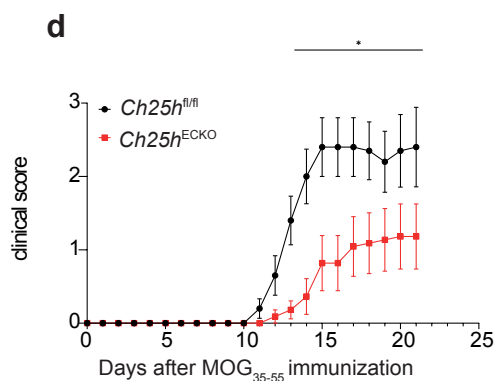
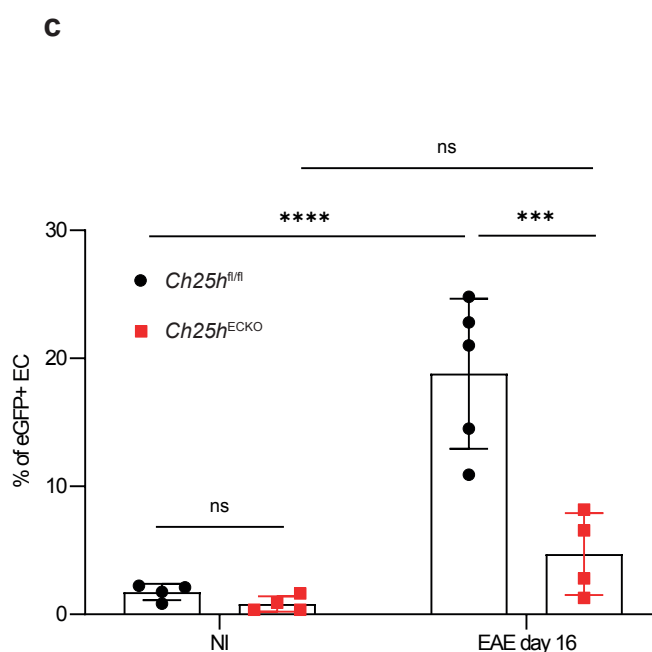
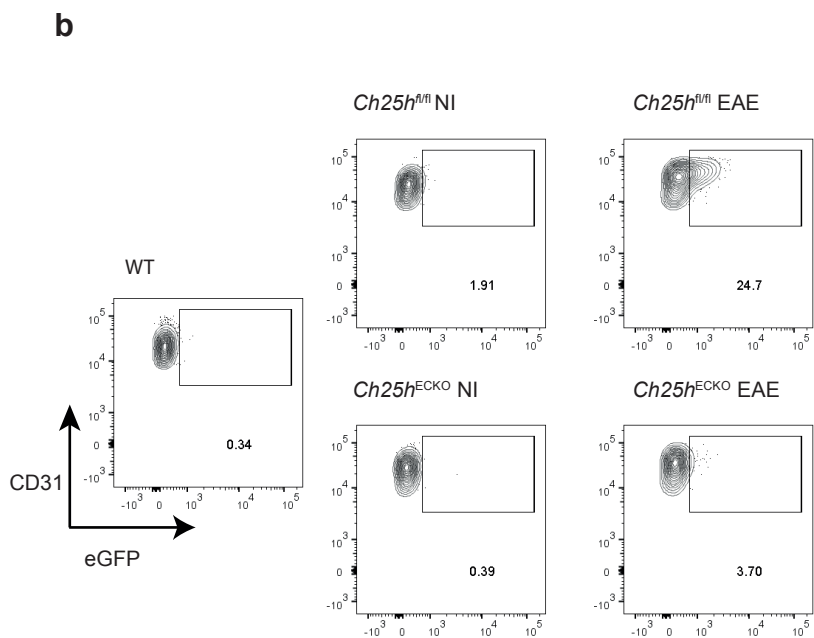
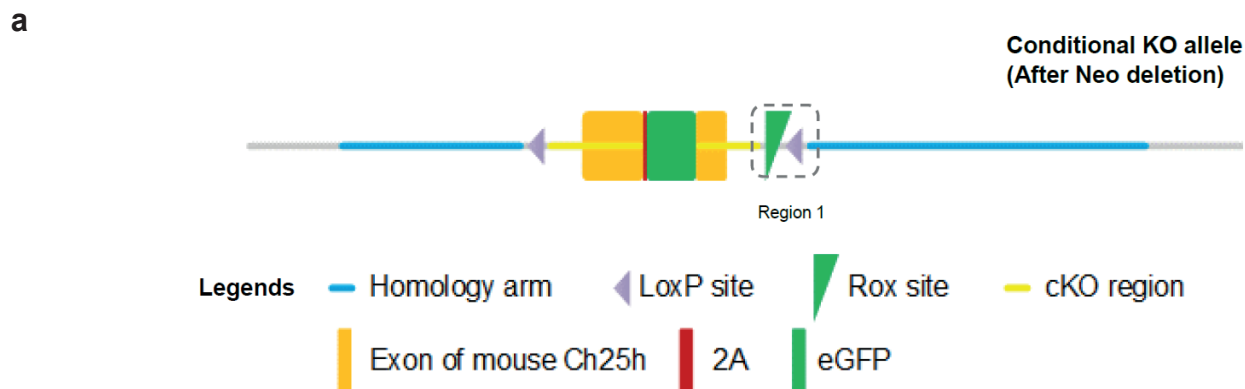
**Table S1. Related to Fig. 2. Differentially expressed genes (DEG) in *Ch25h*<sup>ECKO</sup> non stimulated vs IL-1β stimulated primary brain microvascular ECs assessed by RNA sequencing.** RNA sequencing was performed on primary brain microvascular ECs (pMBMEC) isolated from tamoxifen injected *Ch25h*<sup>fl/fl</sup> and *Ch25h*<sup>ECKO</sup> mice. Confluent cells were left unstimulated (NS) or stimulated with IL-1β. RNA seq was then performed. n=3/group.

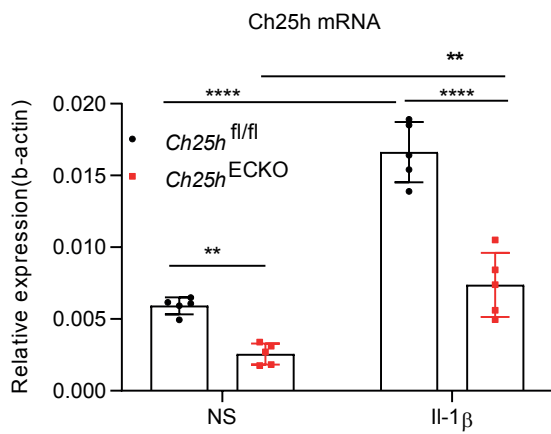
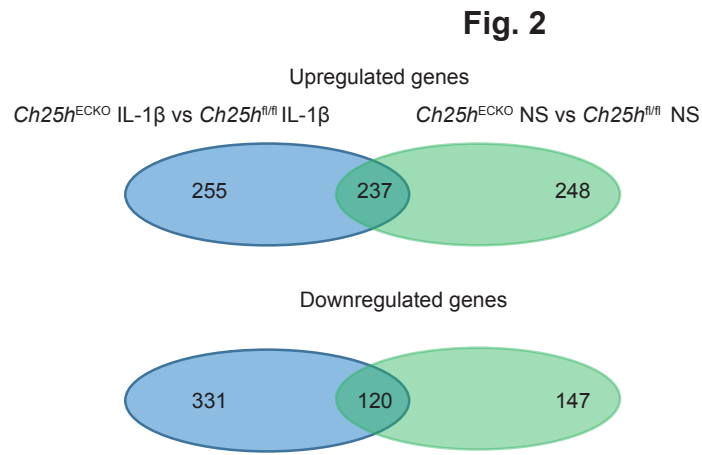
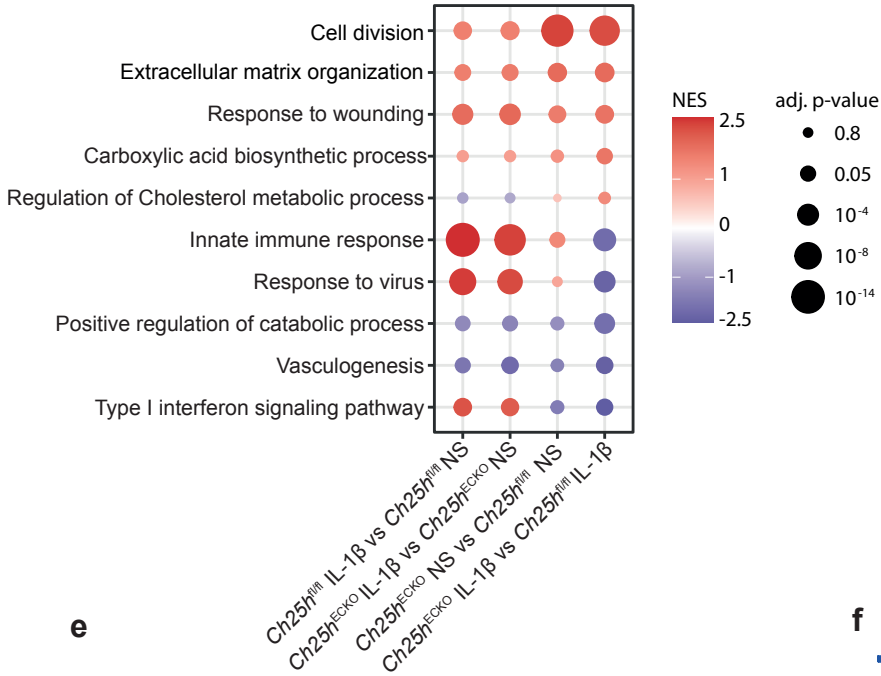
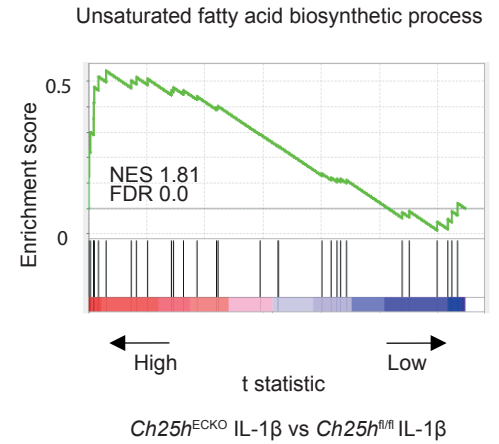
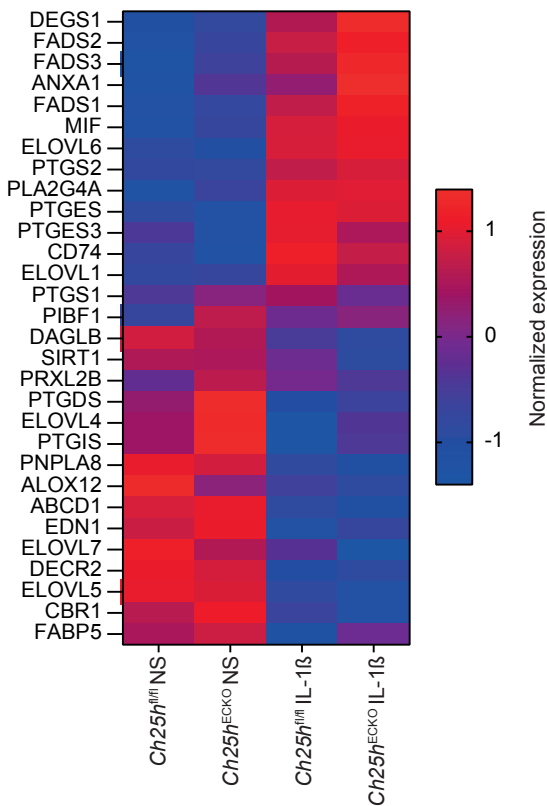
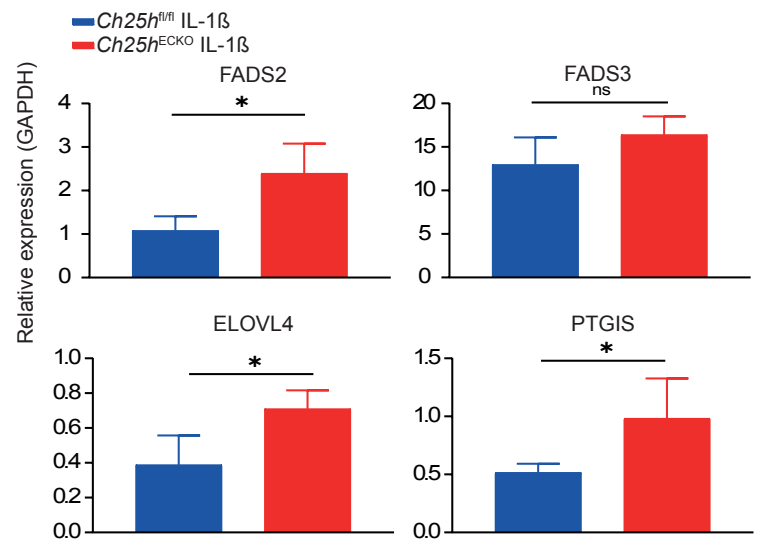
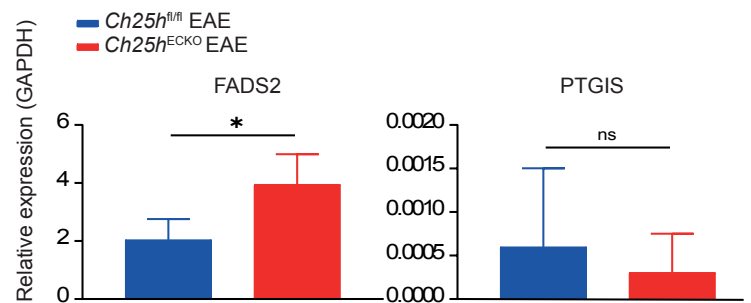
**Table S2. Related to Fig. 2. Differentially expressed genes (DEG) in *Ch25h*<sup>fl/fl</sup> non stimulated vs IL-1 $\beta$  stimulated primary brain microvascular ECs assessed by RNA sequencing.**

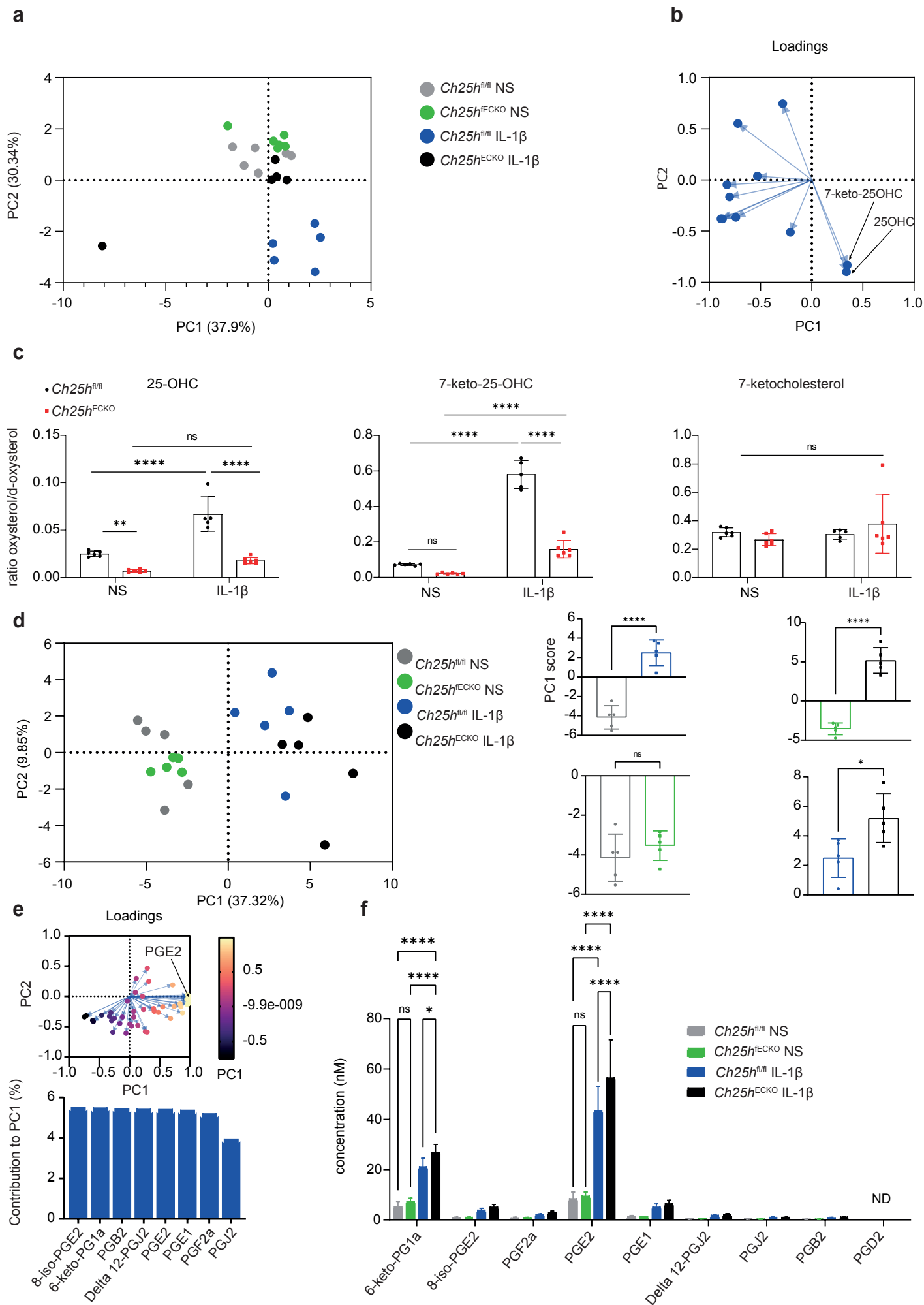
**Table S3. Related to Fig. 2. Differentially expressed genes (DEG) in *Ch25h*<sup>ECKO</sup> vs *Ch25h*<sup>fl/fl</sup> IL-1 $\beta$  stimulated primary brain microvascular ECs assessed by RNA sequencing.**

**Table S4. Related to Fig. 2. Differentially expressed genes (DEG) in *Ch25h*<sup>ECKO</sup> vs *Ch25h*<sup>fl/fl</sup> non-stimulated primary brain microvascular ECs assessed by RNA sequencing.**

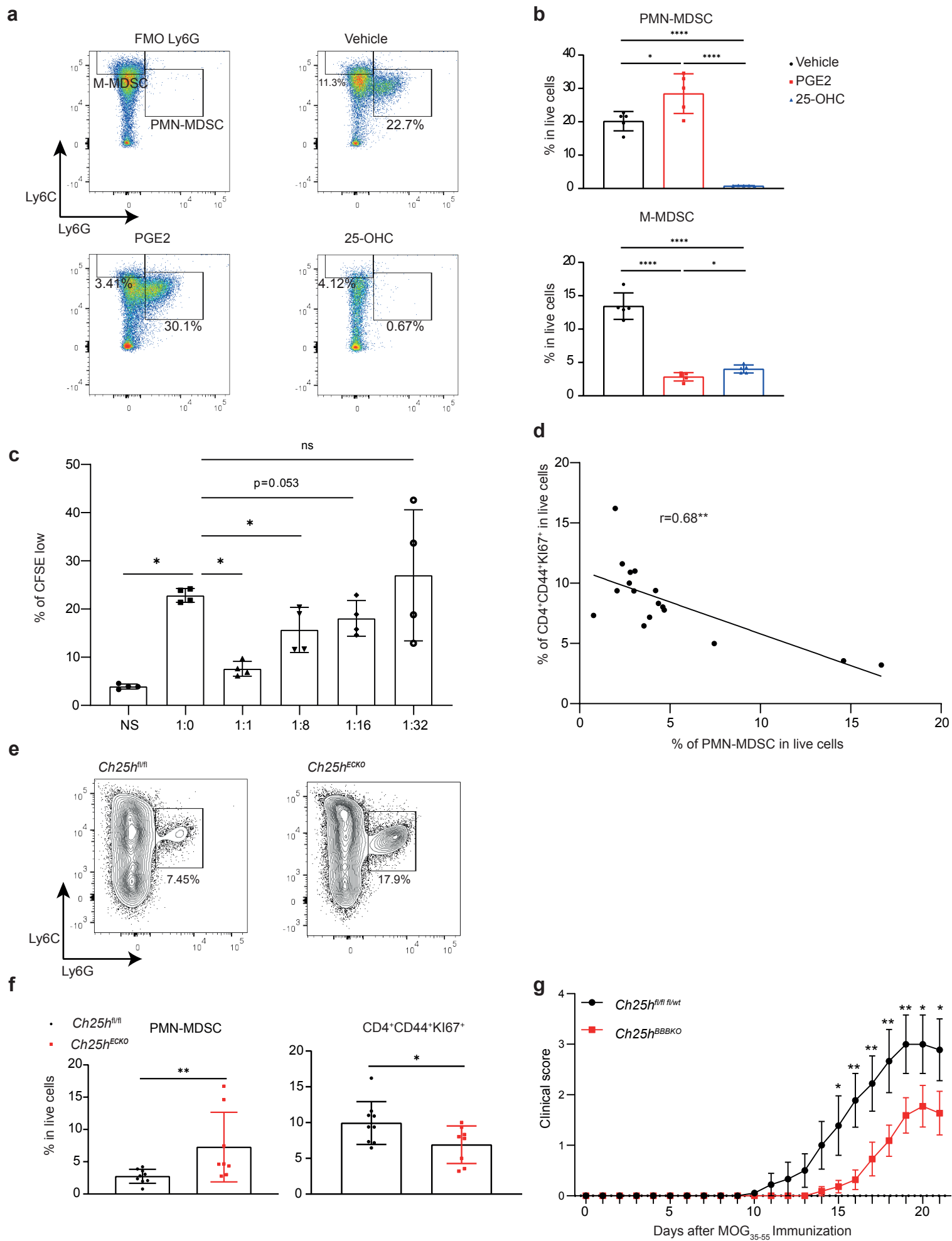
**Table S5. Related to Fig. 5. List of DEG in periphery (N) vs tumor (T) within cluster 16 from GSE16263 (output of the FindMarkers function from the Seurat package).**

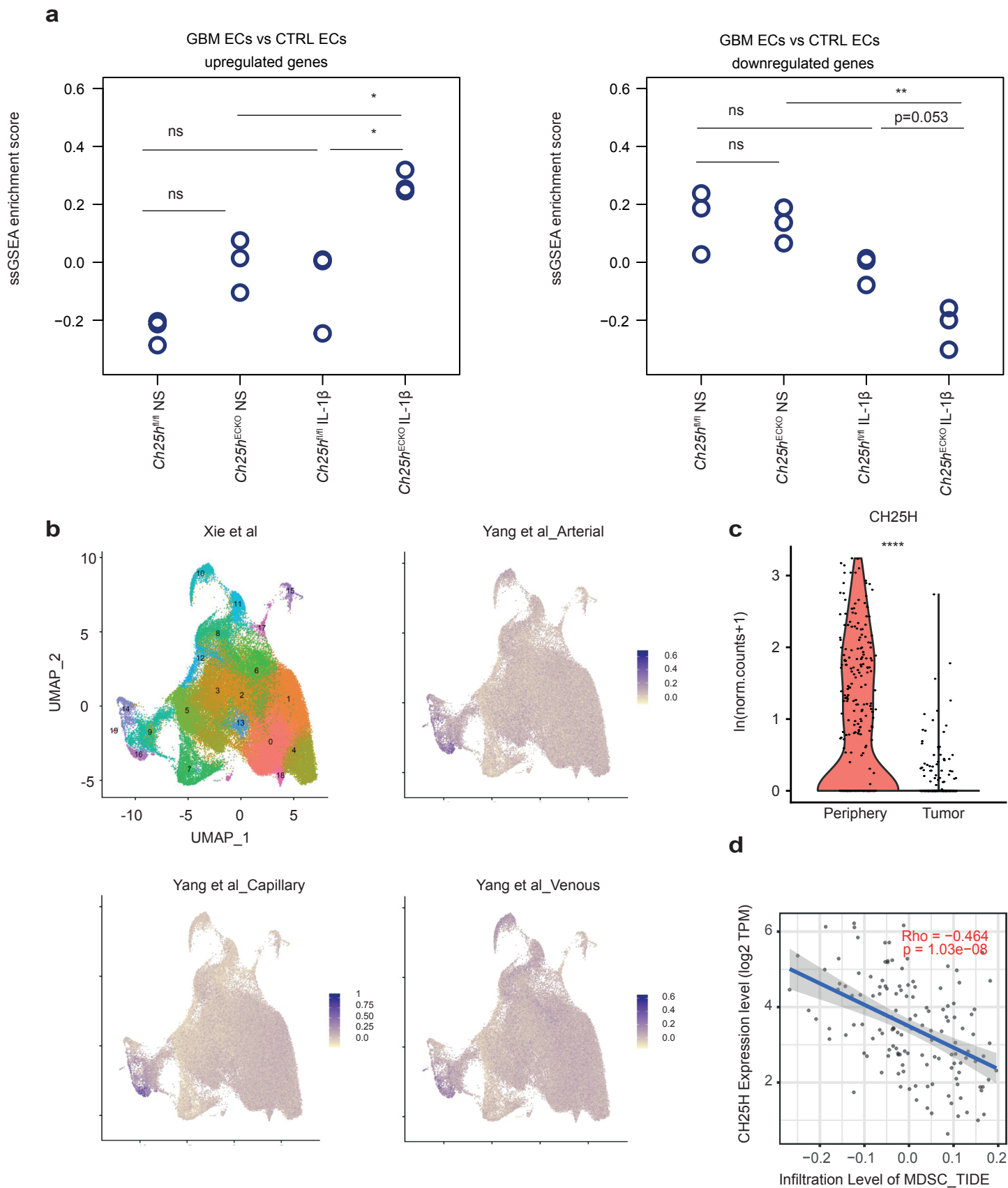


**a****b****c****d****e****f****g**

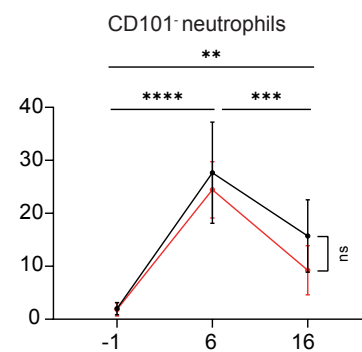
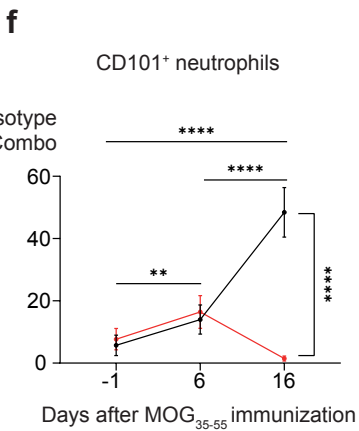
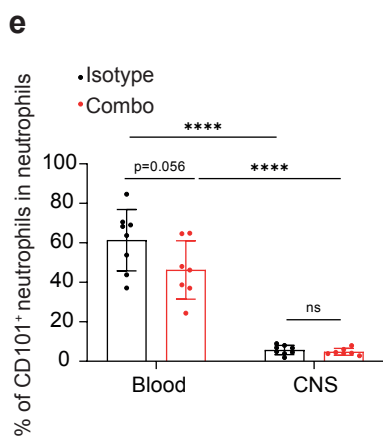
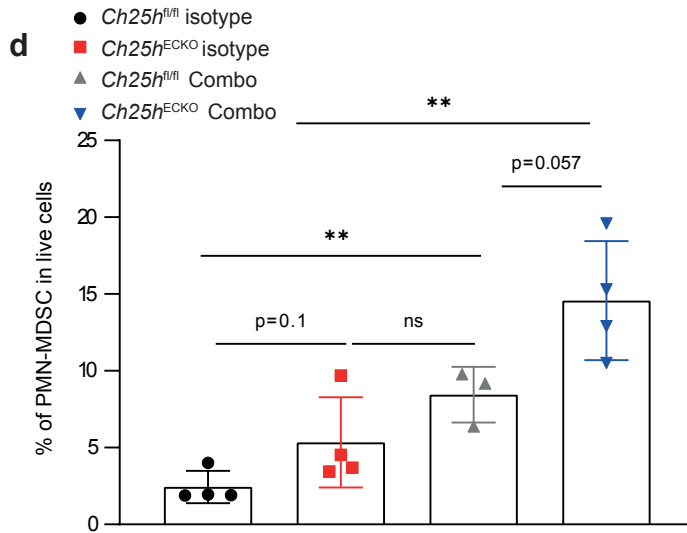
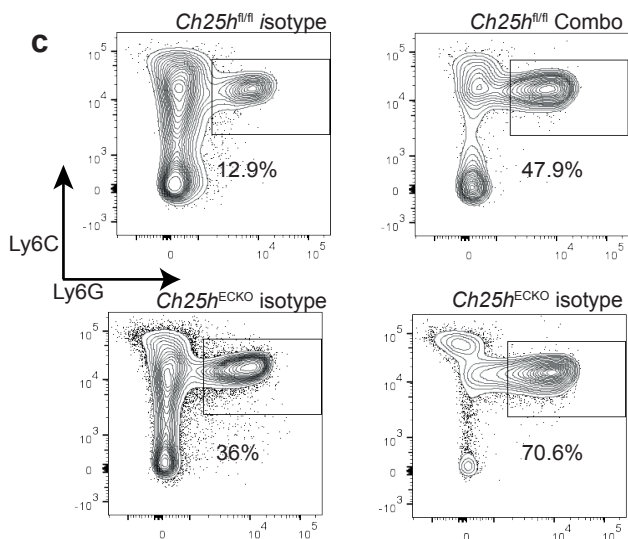
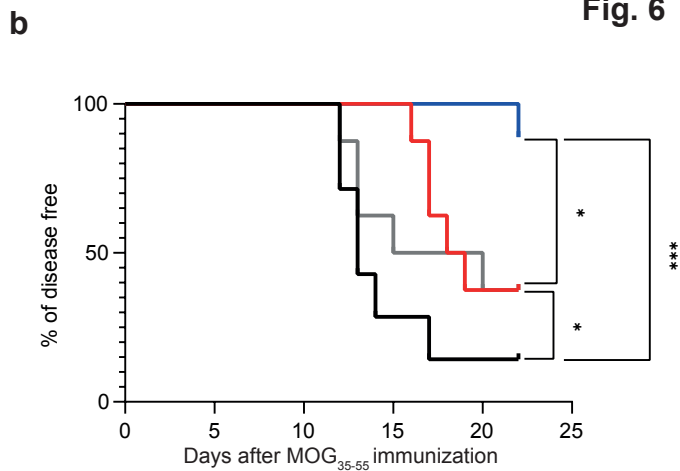
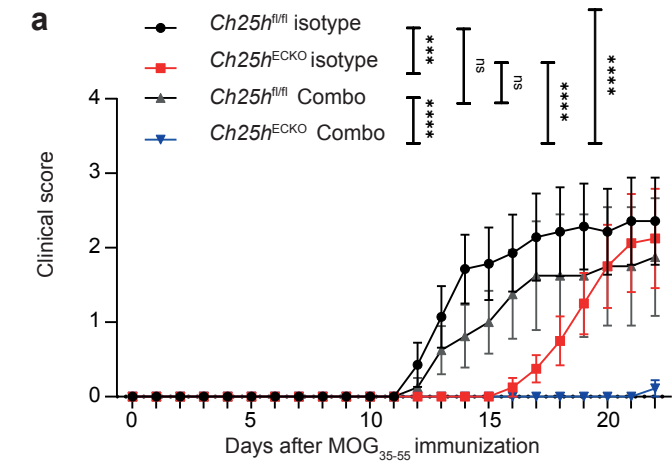


**Fig. 4**





**Fig. 6**



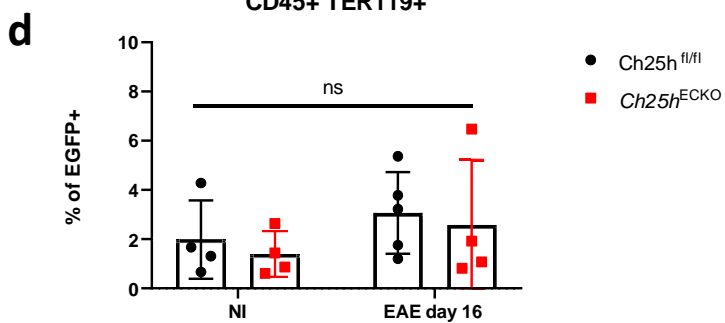
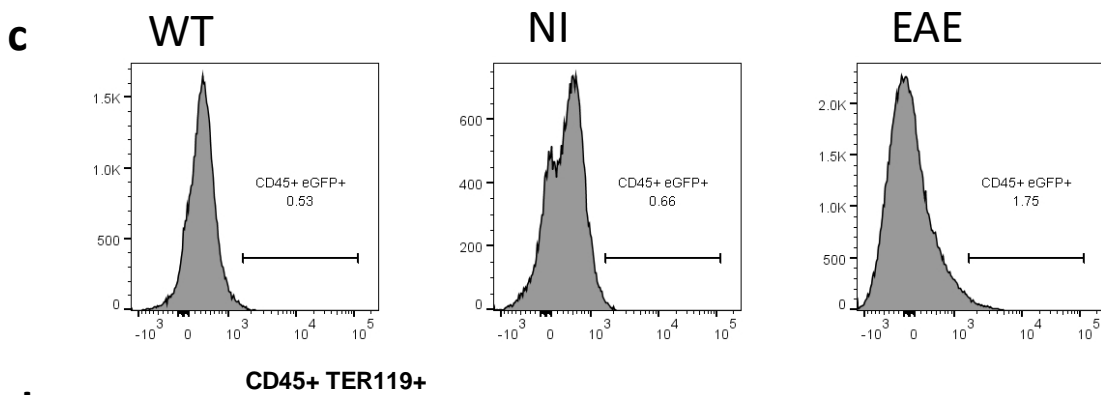
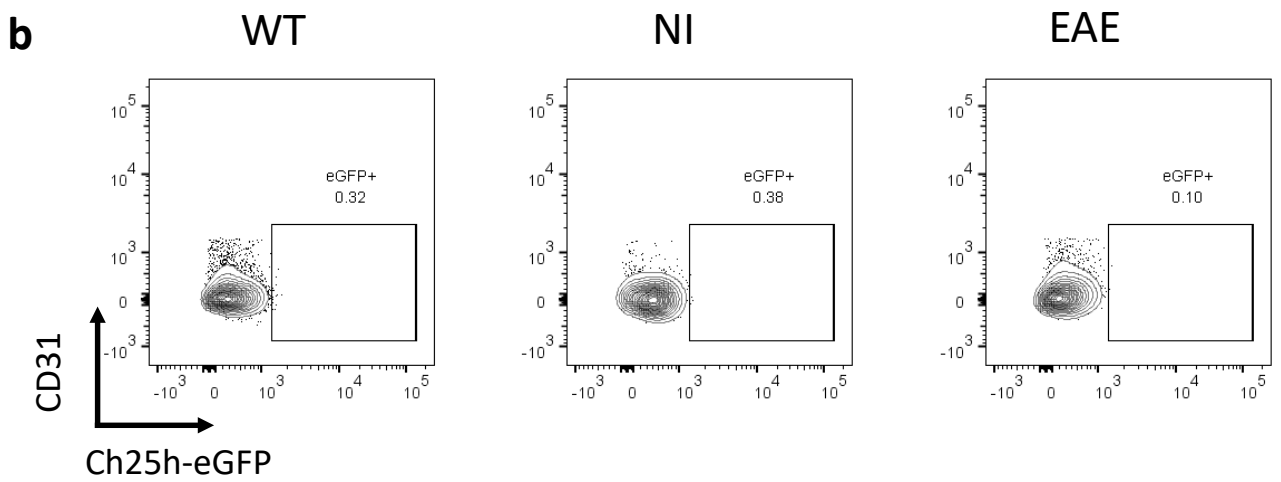
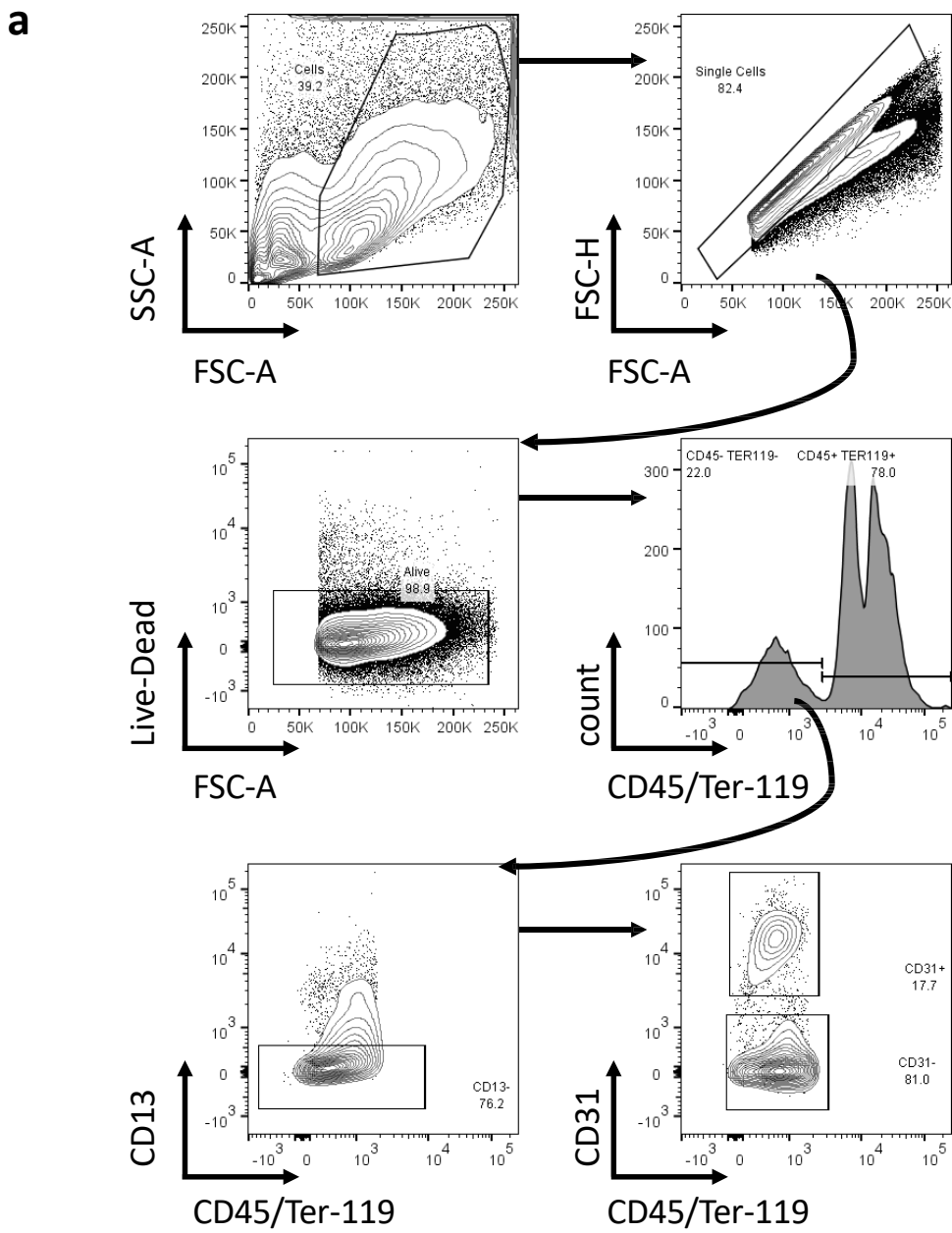


**Fig. S1. Related to Figure 1. Analysis of Ch25h-eGFP expression in the CNS.** **a)** Gating strategy for flow cytometry analysis of Ch25h-eGFP expression in cells of the CNS. Total cells were selected based on Forward Scatter (FSC-A) and side scatter plot (SSC-A). Doublet and dead cells were excluded. For endothelial cells and CNS resident cells (excluding Microglial cells), CD45<sup>-</sup>TER119<sup>-</sup> cells were selected. CD13<sup>+</sup> cells were excluded to avoid pericyte contamination. Endothelial cells were defined by CD31 expression and other CNS resident cells by the absence of CD31. Cells from the hematopoietic lineage and Microglial cells were defined by CD45 and TER119 expression. **b)** Ch25h-eGFP expression in CD45<sup>-</sup>TER119<sup>-</sup>CD13<sup>-</sup>CD31<sup>-</sup> cells. Wild type mice (WT) are compared with Ch25h-eGFP mice either non-immunized (NI) at day 16 of EAE (EAE). **c)** Histogram showing Ch25h-eGFP expression in CD45<sup>+</sup>TER119<sup>+</sup> cells in the same conditions as in **b)**. **d)** Flow cytometry analysis of Ch25h-eGFP expression in CD45<sup>+</sup>TER119<sup>+</sup> cells of the CNS isolated from *Ch25h<sup>fl/fl</sup>* and *Ch25h<sup>fl/fl</sup>-Ve-CadherinCreERT2* mice (*Ch25h<sup>ECKO</sup>*) injected with tamoxifen. Non-immunized mice (NI) are compared with mice at the peak of EAE (EAE day 16). Symbols depicts individual mice and bars indicates mean  $\pm$  SD .

ns= non significant, p values were determined by two-way ANOVA with Sidak's post hoc test.

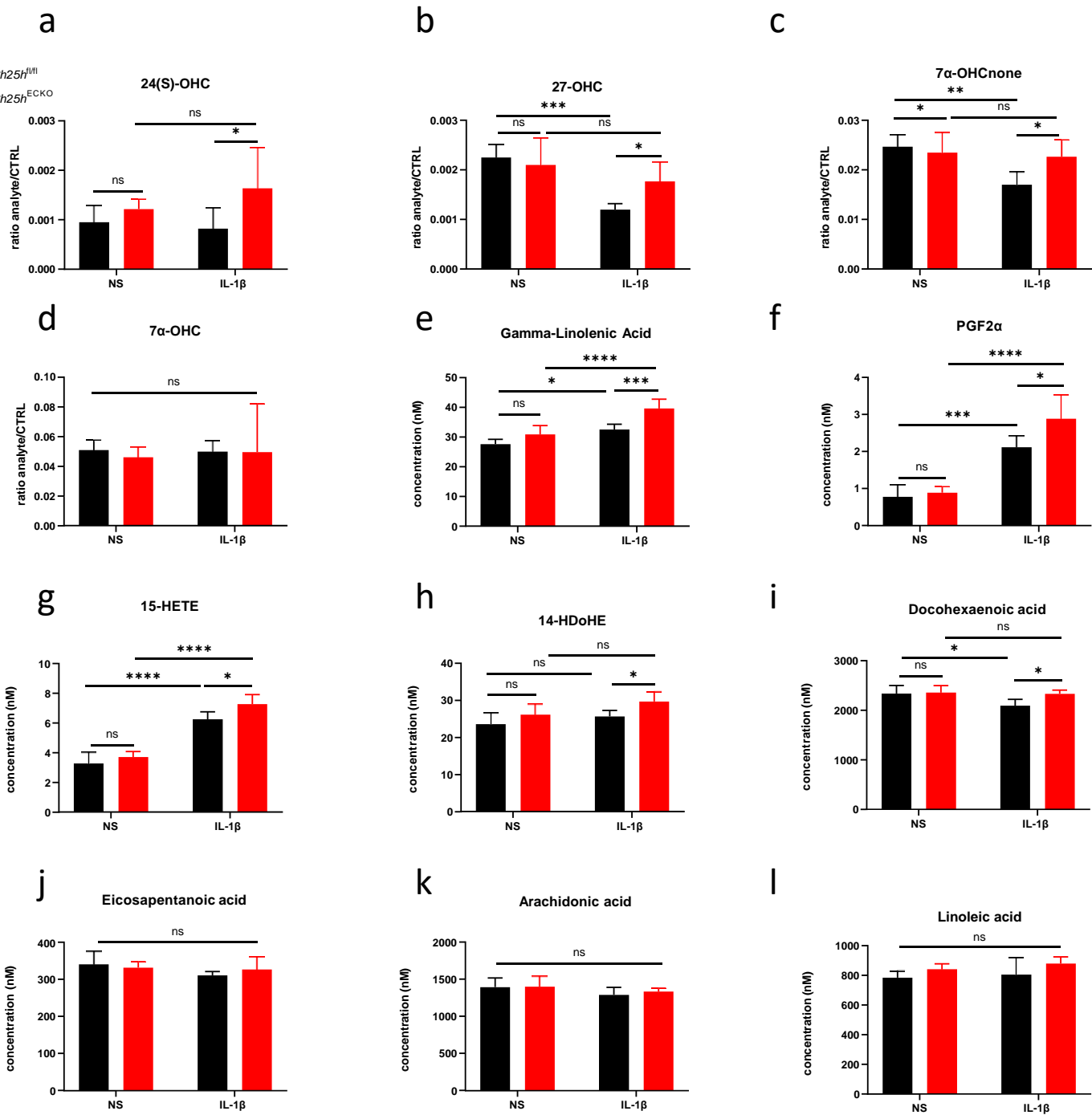


**Fig. S2. Related to figure 3. Oxysterol and eicosanoids levels in the supernatant of primary brain microvascular endothelial cells.** Primary mouse brain microvascular endothelial cells (pMBMEC) were isolated from *Ch25h<sup>fl/fl</sup>* and *Ch25h<sup>fl/fl</sup>-Ve-CadherinCreERT2* mice (*Ch25h<sup>ECKO</sup>*) injected with tamoxifen. Cells were left unstimulated (NS) or stimulated with IL-1β (10ng/mL) during 24 hours. Supernatant was then collected. Oxysterols were measured by HPLC-MS. **a)** 24(S)-Hydroxycholesterol (24(S)-OHC) levels. **b)** 27-Hydroxycholesterol (27-OHC) levels. **c)** 7α-hydroxycholestenone (7α-OHCnone) levels. **d)** 7α-hydroxycholesterol (7α-OHC) levels. n=6/group except for *Ch25h<sup>fl/fl</sup>* IL-1β n=5. **e-l)** Same conditions as in **a-d)**, except that eicosanoids were measured by Liquid Chromatography-Mass Spectrometry. **e)** gamma-linolenic acid levels. **f)** Prostaglandin F2α levels (PGF2α). **g)** 15-Hydroxyeicosatetraenoic acid levels (15-HETE). **h)** 14-hydroxy-4Z,7Z,10Z,12E,16Z,19Z-docosahexaenoic acid (14-HDoHE) levels. **i)** Docohexanoic acid levels. **j)** Eicosapentanoic acid levels. **k)** Arachidonic acid levels. **l)** Linoleic acid levels. Bars indicates mean ± SD. N=5/group. ns= non significant, \* : p<0.05, \*\*\*= p ≤ 0.0005, \*\*\*\* = p ≤ 0.00005. p values were determined by two-way ANOVA with Sidak's post hoc test.

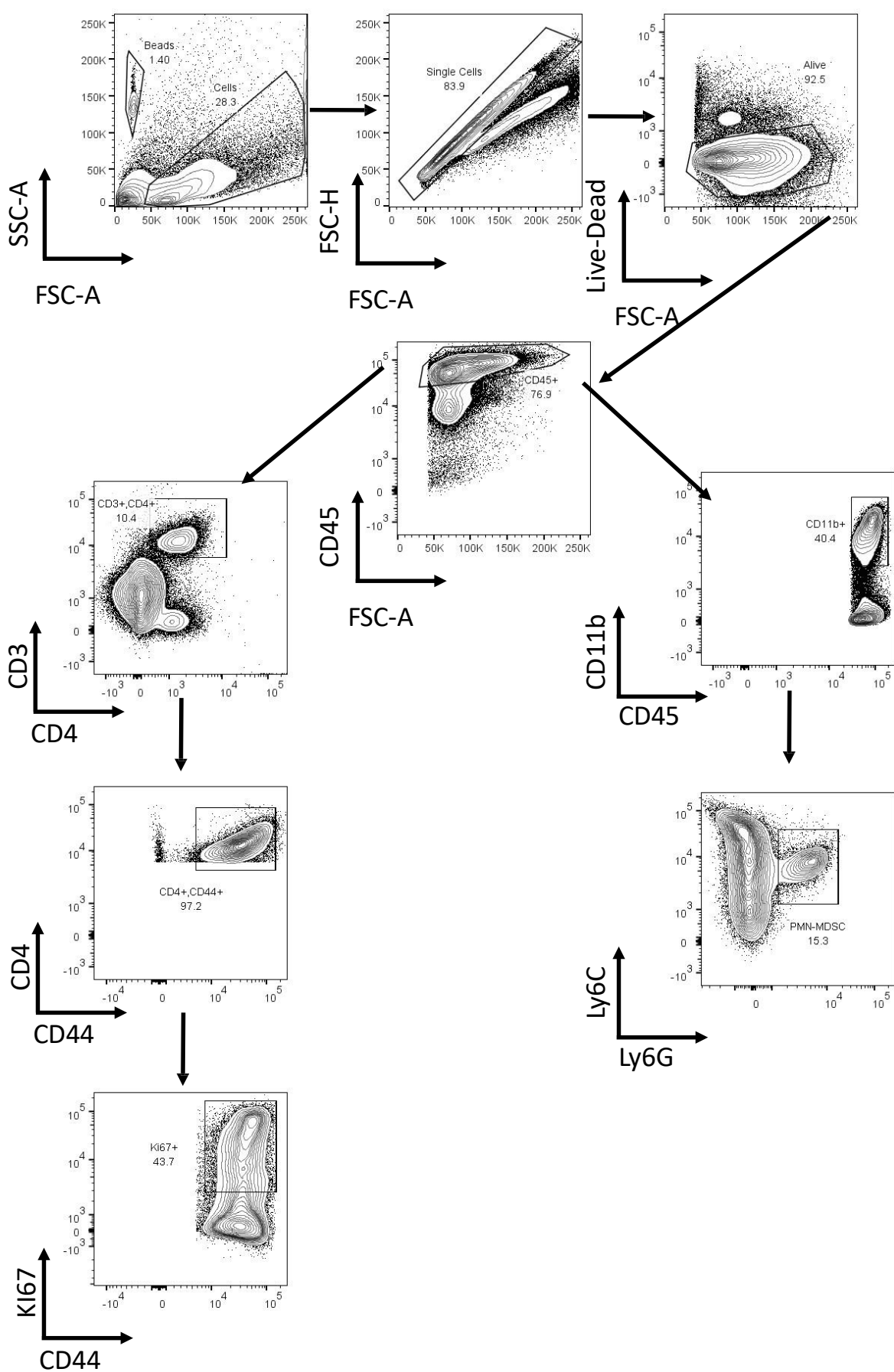


**Fig. S3. Related to figure 4. Gating strategy for CNS infiltrating leukocytes.** Total cells are selected based on Forward Scatter (FSC-A) and side scatter plot (SSC-A). Doublet and dead cells are excluded. CD45<sup>+</sup> cells are selected. Total CD11b<sup>+</sup> are selected. PMN-MDSC are defined as Ly6C<sup>int</sup>, Ly6G<sup>+</sup> Cells. CD4 T cells are selected based on CD4 and CD3 positivity. Memory CD4 T cells (CD44<sup>+</sup>) are further selected. Ki67<sup>+</sup> Cells are further selected.

## CH25H

## FADS2

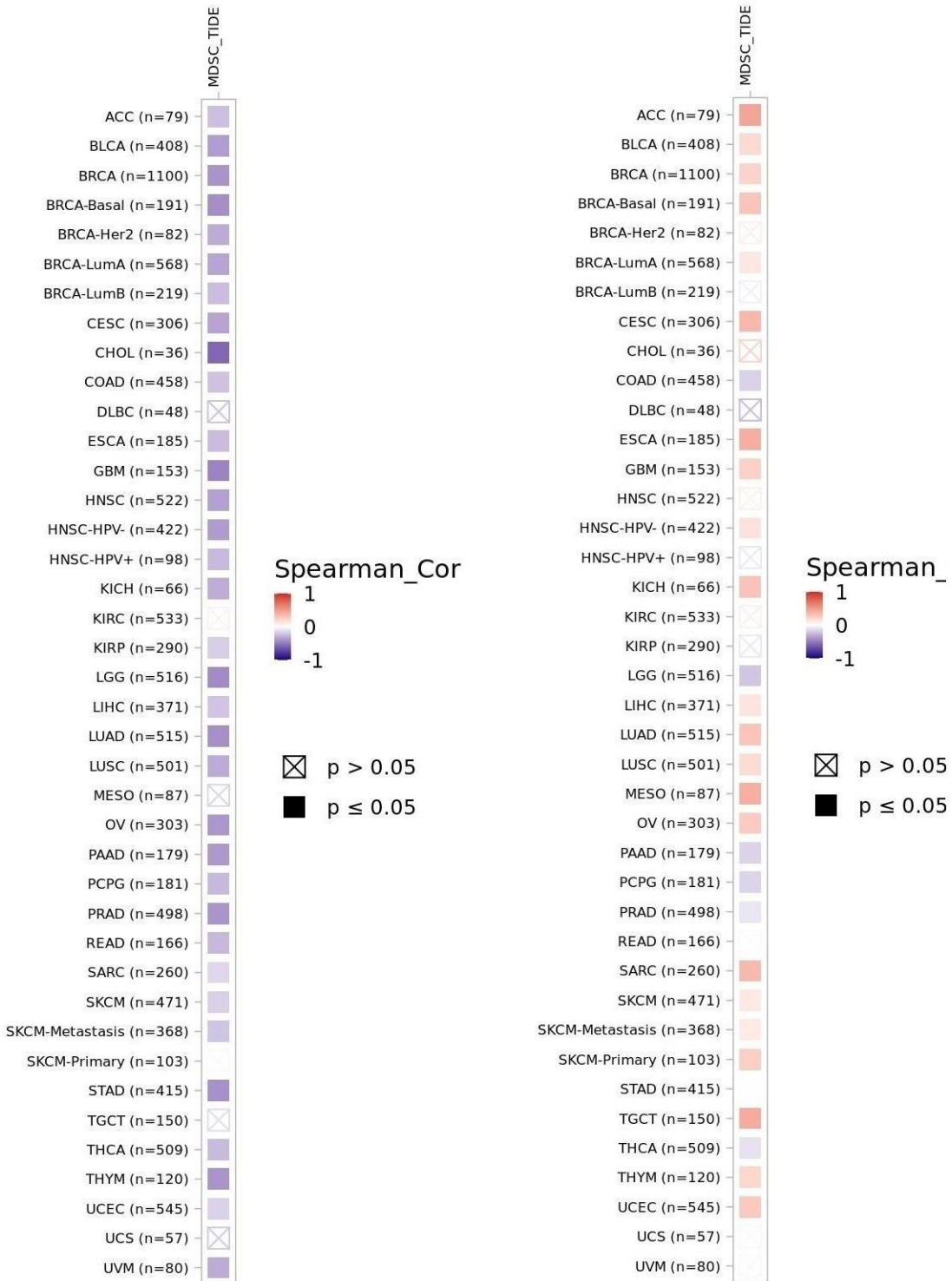
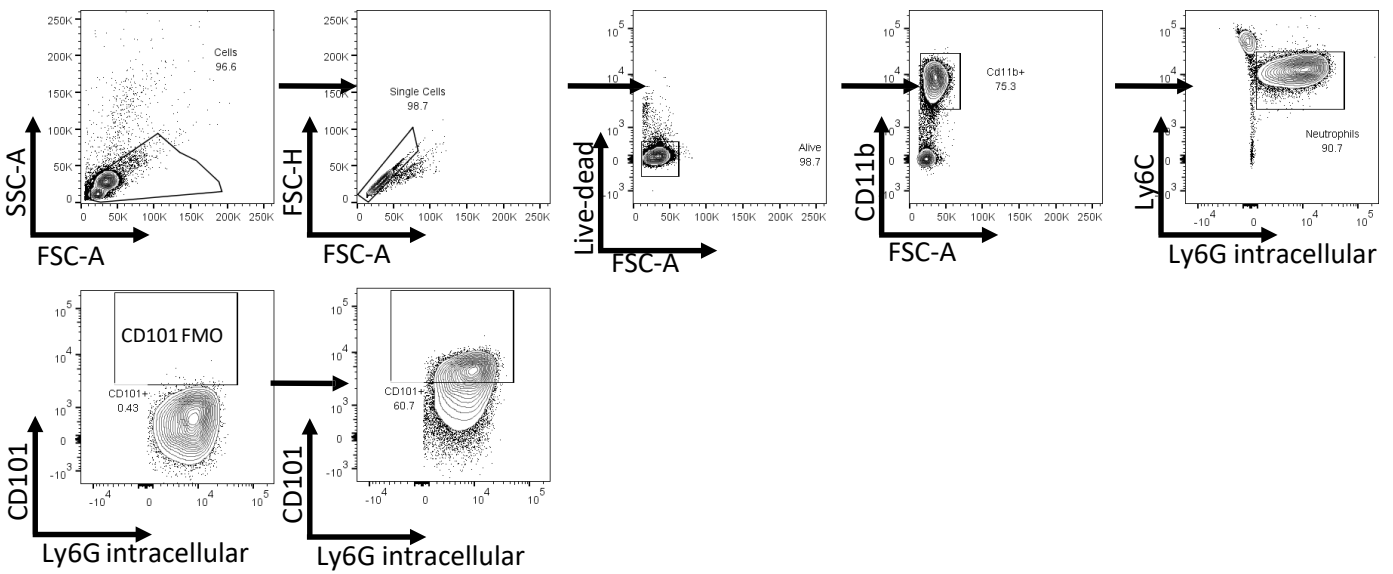


**Fig. S4. Related to figure 5. Correlation of CH25H and FADS2 expression level with Myeloid-derived suppressor cells infiltration in 40 cancers assessed with TIMER 2.0 database.** ACC: Adrenocortical Carcinoma, BLCA: Bladder Urothelial Carcinoma, CESC: Cervical and Endocervical Cancer, CHOL: Cholangiocarcinoma, COAD: Colon Adenocarcinoma, DLBC: Diffuse Large-B-cell Lymphoma, ESCA: Esophageal Carcinoma, GBM : Glioblastoma Multiforme, HNSC: Head and Neck Cancer, KICH: Kidney Chromophobe, KIRC: Kidney Renal Clear cell Carcinoma, KIRP: Kidney Renal Papillary Cell Carcinoma, LAML: Acute Myeloid Leukemia, LGG: Low Grade Glioma, LIHC: Liver Hepatocellular Carcinoma, LUAD: Lung Adenocarcinoma, LUSC: Lung Squamous Cell Carcinoma, MESO: Mesothelioma, OV; Ovarian Serous Cystadenocarcinoma, PADD: Pancreatic Adenocarcinoma, PCPG: Pheochromocytoma and Paraganglioma, PRAD: Prostate Adenocarcinoma, READ: Rectum Adenocarcinoma, SARC: Sarcoma, SKCM: Skin Cutaneous Melanoma, STAD: Stomach Adenocarcinoma, TGCT: Testicular Germ Cell Tumors, THCA: Thyroid Carcinoma, THYM: Thymoma, UCEC: Uterine Corpus Endometrial Carcinoma, UCS: Uterine Carsinosarcoma, UVM: Uveal Melanoma.

a



b

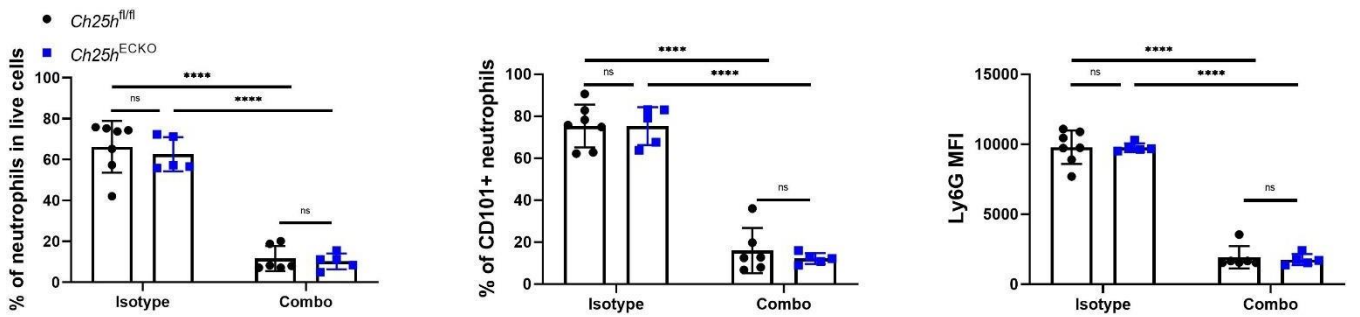


**Fig. S5. Related to figure 6. Effect of Combo treatment on circulating neutrophils. a)** Gating strategy for analysis of blood neutrophils. Total Cells are selected based on Forward Scatter (FSC-A) and side scatter plot (SSC-A). Doublet and dead cells are excluded. CD11b<sup>+</sup> cells are selected. Ly6C<sup>int</sup>, Ly6G intracellular<sup>+</sup> cells are further selected. CD101<sup>+</sup> cells are defined base on a Fluorescence minus one (FMO). **b)** EAE was performed in *Ch25h<sup>fl/fl</sup>* mice and *Ch25h<sup>ECKO</sup>* mice previously injected with tamoxifen. Mice were treated with Isotype control antibody or Combo protocol after the beginning of the first symptoms of EAE. Blood was harvested 1.5 day after treatment initiation. Neutrophils were analyzed by flow cytometry using the gating strategy defined in a). Left panel: % of neutrophils in live cells, Middle panel: % of CD101<sup>+</sup> neutrophils in neutrophils, right panel: Geometric mean fluorescence intensity of Ly6G in neutrophils. Symbols represents individual mice. Bars depicts mean ± SD.

ns= non significant, ,\*\*\*\* =  $p \leq 0.00005$ . p values were determined by two-way ANOVA with Sidak's post hoc test.

## **7. Discussion and perspectives**

In my thesis, I studied the role of the Ch25h pathway in two inflammatory diseases, IBD and the murine model of MS (EAE). I evaluated the molecular mechanisms involved to promote those two diseases. I first discovered a narrow association between GPR183 and CCR6 in IBD and then a novel function of Ch25h-derived oxysterols in the CNS that dampens the immune response. I will now discuss the perspectives that I propose for both projects.

### **Part 1: GPR183 and CCR6 a detrimental collaboration?**

#### A potential role for inflammatory imbalance and Th17-fate commitment

One of the key findings of the first part of my thesis on PBMCs obtained from IBD patients and healthy volunteers is the association of GPR183 expression with CCR6 in CD4 memory T cells. We demonstrated that CCL20 acts in an additive manner with  $7\alpha,25\text{-OHC}$  to promote CD4 memory T cell migration, suggesting that the GPR183/CCR6 co-expression is functionally relevant. We also confirmed, that memory CD4 T cells<sup>46, 76</sup>, in particular Th17 cells, display the highest expression of GPR183. Of note, CCR6 is a well-known Th17 cell marker<sup>385</sup> and is also expressed by regulatory T cells. In addition, when CCR6 KO CD4 T cells are adoptively transferred in a colitis model, the recipient mice display an exacerbated intestinal inflammation<sup>386</sup>. Thus, CCR6 is not necessarily pro-pathogenic. Previous studies indicate that in CD4 T cells, CCR6 is induced by TGF- $\beta$ , which is an important cytokine for both Th17 and regulatory T cell development<sup>387</sup>. IL-23 is a key signal for the maintenance of Th17 cells but does not impact CCR6 expression<sup>387</sup>. In contrast, IL-23

induces GPR183 expression in CD4 T cells<sup>46</sup>, suggesting that the Th17-fate commitment is associated with GPR183 induction. In addition, Foxp3<sup>+</sup> regulatory T cells have lower GPR183 expression than Foxp3<sup>-</sup> cells<sup>46</sup>. Moreover, a recent study indicates that IL-23 signaling in Th17 cells promotes their pathogenic activity during EAE<sup>388</sup>. Finally, CCL20 and 7 $\alpha$ ,25-OHC are both increased in gut inflammation<sup>47, 237, 389</sup>. Thus, these findings might have the following consequences: while CCL20 induced during inflammation could be a chemotactic signal for both regulatory T cells and Th17 cells, a combination of 7  $\alpha$ ,25-OHC and CCL20 might favor pro-pathogenic Th17 cell infiltration over regulatory T cell migration, therefore participating in the emergence of the inflammatory imbalance seen in IBD and MS. In line with this, treatment of MS patients with Natalizumab results in sequestration of GPR183 expressing CD4 memory T cells and Th17 cells in the peripheral blood suggesting that these cells are attracted in the inflamed CNS<sup>76, 390</sup>. Moreover, Natalizumab also prevents the entry of CD4 T cells into the intestine<sup>391</sup>, MS patients display increased infiltration of Th17 cells in the gut<sup>392</sup> and we have shown blocking the entry of Th17 cells in the intestine delays EAE<sup>393</sup>. Therefore, this sequestration of GPR183 expressing cells observed in MS could also be due to the effect of Natalizumab on Th17 cell trafficking in the intestine. Additionally, in a similar way that CCR7 and GPR183 collaborate to enable activated B cell positioning at the T-B boundary in lymph nodes (see section 1.4.2), co-expression of CCR6 and GPR183 might induce a differential spatial distribution of Th17 and regulatory T cells within inflamed tissues. Therefore, they might be exposed to different microenvironments and different subsets of APCs, which could further dictate if they undergo additional activation and proliferation, if they maintain or switch to a regulatory or a pro-inflammatory phenotype or if they undergo anergy.

## A role in tertiary lymphoid organs formation

Lymphoid tissues can arise before and after birth<sup>97</sup>. In particular, tertiary lymphoid organs (TLOs) are ectopic lymphoid tissues that arise postnatally in chronically inflamed organs<sup>394</sup>. Their role in the pathogenesis of inflammatory diseases remains debated but some data indicate that they are associated with a poor prognosis<sup>395</sup>.

It is interesting to note that CCR6 and GPR183 are co-expressed in cells displaying a lymphoid tissue-inducing potential such as ILC3s and Th17 cells<sup>41, 46, 76, 103, 238, 396</sup>. However, the function of these chemotactic receptors in lymphoid tissue development is not completely redundant.

GPR183 promote the formation of intestinal lymphoid tissues arising after birth at steady state and TLOs developing in inflamed tissues<sup>41, 43, 47, 103, 104</sup>. Importantly, besides positioning alterations of B cells and CD4 T cells, the number, structure, and overall development of secondary lymphoid organs that emerge in-utero do not seem to be dependent on GPR183<sup>41, 47, 86, 95, 103</sup>.

CCR6 KO mice display underdeveloped Peyer's patches<sup>397</sup>, which are secondary lymphoid organs developing prenatally<sup>97</sup> but these structures develop normally in GPR183 KO mice<sup>41</sup>. In contrast, induced bronchus-associated lymphoid tissues (iBALT) are not impacted by a defect in CCR6<sup>398</sup> but are reduced in GPR183 KO mice<sup>43</sup> although not in the same models. Therefore, GPR183 could be more particularly implicated in lymphoid tissue formation at mucosal sites arising postnatally.

The mucosal microbiota composition drastically changes after birth and it favors the development of lymphoid tissues<sup>399</sup> and of TLOs that exacerbate inflammation in the gut<sup>400</sup>. This suggests that postnatal lymphoid tissue development is microbiota

dependent. Therefore, the cross-talk between GPR183<sup>+</sup> lymphoid tissue-inducing cells and mucosal microbiota might be a driving mechanism for TLOs formation or in general for the development of lymphoid tissues after birth.

### Perspectives

All of the above-mentioned results suggest that CCR6 and GPR183 collaborate to promote lymphoid organ development and inflammation.

Future studies, combining CCR6 KO, GPR183 KO, and GPR183 and CCR6 double KO mice might enable to refine the respective role of these chemotactic receptors in inflammation and emergence of post and prenatal lymphoid tissues. By using CCR6 and GPR183 reporter mice, we could evaluate the spatial distribution and the phenotype of immune cells expressing these receptors at steady state and during gut and CNS inflammation in experimental models where TLOs are observed<sup>400, 401, 402</sup>, or in inflamed tissues. These tools combined with our Ch25h-floxed-reporter mice could enable us to refine the identity of the cellular sources of 7 $\alpha$ ,25-OHC in lymphoid organs and inflamed tissues as current data are mostly based on mRNA expression of Ch25h<sup>41, 85</sup>. Finally, the putative differential spatial location of GPR183<sup>+</sup> CCR6<sup>-</sup>, GPR183<sup>-</sup> CCR6<sup>+</sup> and GPR183<sup>+</sup> CCR6<sup>+</sup> cells and Ch25h expressing cells in inflamed tissues and lymphoid organs might inform about the different cell subsets interacting with each other. This is particularly interesting as Th17 and regulatory T cells are highly plastic<sup>194</sup> and as mentioned above GPR183 and CCR6 might be differentially expressed between these two subsets. Therefore, the identification of the cell subsets with which they interact could allow us to decipher the molecular cues governing the transition from a regulatory to pro-pathogenic phenotype and conversely.

## **Part 2: The detrimental function of Ch25h in endothelial cells**

In the main project of my thesis, we demonstrated that Ch25h expression by endothelial cells regulates PMN-MDSC expansion during EAE.

Interestingly, Lu et al demonstrated that Ch25h expression by endothelial cells is angiostatic in cancer<sup>403</sup>. The uptake of tumor-derived extracellular vesicles (TEV) by ECs increases in absence of Ch25h. This increased TEVs uptake induces the expression of angiopoietin-2 (ANGPT-2) which favors angiogenesis<sup>403</sup>.

In our RNAseq of ECs, when Ch25h expression was reduced, we did not identify alterations of ANGPT-2 expression, but we observed a robust activation of genes related to cell cycle and cell proliferation, even at steady state. This increase in TEVs uptake and activation of angiogenesis combined with our *in-vitro* data suggest that suppression of Ch25h expression in ECs could unleash their proliferative potential without the presence of tumor microenvironment. Thus, it would be important to study the effect of Ch25h deletion in ECs in another experimental paradigm than malignancies.

Lu et al observed a reduced expression of CH25H in colorectal cancer stroma compared with adjacent healthy tissue<sup>403</sup> and we were able to demonstrate that endothelial cells from glioblastoma (GBM) display a reduced expression of CH25H. Moreover, our results suggest that Ch25h inactivation and IL-1 $\beta$  stimulation in brain endothelial cells induce a transcriptomic profile reminiscent of ECs found in GBM. Of note, some common findings between GMB ECs and Ch25h-deleted ECs included increased expression genes related to extracellular matrix organization<sup>404, 405</sup>, which might indicate the acquisition of a mesenchymal phenotype. It is therefore tempting to

speculate that Ch25h in ECs functions as a checkpoint that promotes endothelial cell quiescence, restrains their proliferation, and maintains their identity.

Finally, Ch25h expression in CNS ECs is increased in stroke, epilepsy, traumatic brain injury, and EAE<sup>335</sup>, but its function in these experimental models was unknown. We demonstrated that its expression by CNS ECs is detrimental during EAE through restriction of PMN-MDSC expansion while Lu et al have shown that it restrains tumor growth by limiting angiogenesis<sup>403</sup>. This opens the possibility that angiogenesis and PMN-MDSC expansion are concomitantly induced by Ch25h deletion.

### Perspectives

The role of angiogenesis in EAE and MS pathophysiology is not clear, but it could be a detrimental process<sup>329, 330, 331</sup>, therefore the beneficial effect of Ch25h deletion that we observed in our model could be more easily explained by PMN-MDSC expansion. In addition, we have not addressed the angiostatic effect of Ch25h in the context of neuroinflammation.

However, as mentioned, it is not excluded that Ch25h ablation favors endothelial cell proliferation in another context than malignancies. These notions, combined with its negative effect on PMN-MDSC expansion and TEVs uptake suggest that it might be an attractive target in pathological paradigms where extracellular vesicle, PMN-MDSC, and angiogenesis act in concert to favor tissues healing.

For these reasons, the impact of Ch25h ablation on stroke should be evaluated. There is a substantial amount of evidence indicating that Ch25h expression is increased in the CNS during experimental models of ischemic stroke<sup>406, 407</sup>, and specifically in endothelial cells<sup>335, 408</sup>. Of note neutrophils infiltrating the CNS during ischemic stroke

are heterogeneous<sup>408</sup> and reports indicate that a subset of PMN, the so-called “N2” neutrophils might reduce the infarct volume<sup>225, 409</sup>. A recent study also describes a subset of neutrophils displaying neuro-regenerative capacities in a model of optic nerve injury that could be consistent with “N2” neutrophils<sup>410</sup>. A detrimental role of neutrophils is also described during stroke<sup>411</sup> but given their heterogeneous nature, some subsets might be beneficial, and others detrimental. Some authors have proposed that “N2 neutrophils” was just another appellation of PMN-MDSC<sup>412</sup> and therefore, these cells might be affected by 25-OHC and PGE<sub>2</sub>. Angiogenesis could also be beneficial for stroke by favoring CNS tissue regeneration after ischemia<sup>413</sup>. Finally, pre-clinical models indicate that extracellular vesicles derived from mesenchymal stem cells can enhance recovery during CNS ischemic events<sup>414, 415, 416</sup>.

Therefore, Ch25h deletion might enhance CNS tissue healing after an injury by favoring PMN-MDSC expansion and angiogenesis. In addition, Ch25h inhibition could be used as an adjuvant therapy with extracellular vesicle derived from mesenchymal stem cells as it might enhance their uptake and thus their therapeutic potential.

## **Conclusion**

During this thesis, we reinforced the degree of evidence implicating Ch25h in IBD and EAE and further refined the molecular mechanism through which this pathway promotes these two diseases. We discovered a narrow association between GPR183 and CCR6 and a novel function of Ch25h-derived oxysterols and CNS endothelial cells in PMN-MDSC regulation. Future studies are necessary to confirm the therapeutic

potential of Ch25h inhibitors and to clarify the underlying mechanisms of its pro-pathogenic or beneficial effects.

## 8. References

1. Chen, H.H. *et al.* Risk of immune-mediated inflammatory diseases in newly diagnosed ankylosing spondylitis patients: a population-based matched cohort study. *Arthritis Res Ther* **21**, 196 (2019).
2. Ruiz, F., Vigne, S. & Pot, C. Resolution of inflammation during multiple sclerosis. *Semin Immunopathol* **41**, 711-726 (2019).
3. El-Gabalawy, H., Guenther, L.C. & Bernstein, C.N. Epidemiology of immune-mediated inflammatory diseases: incidence, prevalence, natural history, and comorbidities. *J Rheumatol Suppl* **85**, 2-10 (2010).
4. McInnes, I.B. & Gravallese, E.M. Immune-mediated inflammatory disease therapeutics: past, present and future. *Nat Rev Immunol* **21**, 680-686 (2021).
5. Netea, M.G. *et al.* A guiding map for inflammation. *Nat Immunol* **18**, 826-831 (2017).
6. Gold, D.A., Caron, A., Fournier, G.P. & Summons, R.E. Paleoproterozoic sterol biosynthesis and the rise of oxygen. *Nature* **543**, 420-423 (2017).
7. Luu, W., Sharpe, L.J., Capell-Hattam, I., Gelissen, I.C. & Brown, A.J. Oxysterols: Old Tale, New Twists. *Annu Rev Pharmacol Toxicol* **56**, 447-467 (2016).
8. Wang, Y., Yutuc, E. & Griffiths, W.J. Neuro-oxysterols and neuro-sterols as ligands to nuclear receptors, GPCRs, ligand-gated ion channels and other protein receptors. *Br J Pharmacol* **178**, 3176-3193 (2021).
9. Brown, A.J. & Jessup, W. Oxysterols and atherosclerosis. *Atherosclerosis* **142**, 1-28 (1999).
10. Guillemot-Legrès, O. & Muccioli, G.G. The oxysterome and its receptors as pharmacological targets in inflammatory diseases. *Br J Pharmacol* (2021).
11. Testa, G. *et al.* Changes in brain oxysterols at different stages of Alzheimer's disease: Their involvement in neuroinflammation. *Redox Biol* **10**, 24-33 (2016).
12. Vejux, A., Namsi, A., Nury, T., Moreau, T. & Lizard, G. Biomarkers of Amyotrophic Lateral Sclerosis: Current Status and Interest of Oxysterols and Phytosterols. *Front Mol Neurosci* **11**, 12 (2018).
13. Brown, A.J., Sharpe, L.J. & Rogers, M.J. Oxysterols: From physiological tuners to pharmacological opportunities. *Br J Pharmacol* **178**, 3089-3103 (2021).
14. Russell, D.W. Oxysterol biosynthetic enzymes. *Biochim Biophys Acta* **1529**, 126-135 (2000).
15. Lund, E.G., Kerr, T.A., Sakai, J., Li, W.P. & Russell, D.W. cDNA cloning of mouse and human cholesterol 25-hydroxylases, polytopic membrane proteins that synthesize a potent oxysterol regulator of lipid metabolism. *J Biol Chem* **273**, 34316-34327 (1998).
16. Beck, K.R. *et al.* Enzymatic interconversion of the oxysterols 7 $\beta$ ,25-dihydroxycholesterol and 7-keto,25-hydroxycholesterol by 11 $\beta$ -hydroxysteroid dehydrogenase type 1 and 2. *J Steroid Biochem Mol Biol* **190**, 19-28 (2019).
17. Kandutsch, A.A. & Chen, H.W. Inhibition of cholesterol synthesis by oxygenated sterols. *Lipids* **13**, 704-707 (1978).
18. Brown, M.S. & Goldstein, J.L. Cholesterol feedback: from Schoenheimer's bottle to Scap's MELADL. *J Lipid Res* **50 Suppl**, S15-27 (2009).

19. Kandutsch, A.A., Chen, H.W. & Heiniger, H.J. Biological activity of some oxygenated sterols. *Science* **201**, 498-501 (1978).
20. Brown, A.J., Sun, L., Feramisco, J.D., Brown, M.S. & Goldstein, J.L. Cholesterol addition to ER membranes alters conformation of SCAP, the SREBP escort protein that regulates cholesterol metabolism. *Mol Cell* **10**, 237-245 (2002).
21. Yang, T. *et al.* Crucial step in cholesterol homeostasis: sterols promote binding of SCAP to INSIG-1, a membrane protein that facilitates retention of SREBPs in ER. *Cell* **110**, 489-500 (2002).
22. Luo, J., Yang, H. & Song, B.L. Mechanisms and regulation of cholesterol homeostasis. *Nat Rev Mol Cell Biol* **21**, 225-245 (2020).
23. Radhakrishnan, A., Ikeda, Y., Kwon, H.J., Brown, M.S. & Goldstein, J.L. Sterol-regulated transport of SREBPs from endoplasmic reticulum to Golgi: oxysterols block transport by binding to Insig. *Proc Natl Acad Sci U S A* **104**, 6511-6518 (2007).
24. Janowski, B.A., Willy, P.J., Devi, T.R., Falck, J.R. & Mangelsdorf, D.J. An oxysterol signalling pathway mediated by the nuclear receptor LXR alpha. *Nature* **383**, 728-731 (1996).
25. Lehmann, J.M. *et al.* Activation of the nuclear receptor LXR by oxysterols defines a new hormone response pathway. *J Biol Chem* **272**, 3137-3140 (1997).
26. Wang, B. & Tontonoz, P. Liver X receptors in lipid signalling and membrane homeostasis. *Nat Rev Endocrinol* **14**, 452-463 (2018).
27. Hamilton, B.A. *et al.* Disruption of the nuclear hormone receptor RORalpha in staggerer mice. *Nature* **379**, 736-739 (1996).
28. Lau, P. *et al.* The orphan nuclear receptor, RORalpha, regulates gene expression that controls lipid metabolism: staggerer (SG/SG) mice are resistant to diet-induced obesity. *J Biol Chem* **283**, 18411-18421 (2008).
29. Lee, I.K. *et al.* RORalpha Regulates Cholesterol Metabolism of CD8(+) T Cells for Anticancer Immunity. *Cancers (Basel)* **12** (2020).
30. Guillaumond, F., Dardente, H., Giguere, V. & Cermakian, N. Differential control of Bmal1 circadian transcription by REV-ERB and ROR nuclear receptors. *J Biol Rhythms* **20**, 391-403 (2005).
31. Ohoka, N., Kato, S., Takahashi, Y., Hayashi, H. & Sato, R. The orphan nuclear receptor RORalpha restrains adipocyte differentiation through a reduction of C/EBPbeta activity and perilipin gene expression. *Mol Endocrinol* **23**, 759-771 (2009).
32. Kumar, N. *et al.* The benzenesulfoamide T0901317 [N-(2,2,2-trifluoroethyl)-N-[4-[2,2,2-trifluoro-1-hydroxy-1-(trifluoromethyl)ethyl]phenyl]-benzenesulfonamide] is a novel retinoic acid receptor-related orphan receptor-alpha/gamma inverse agonist. *Mol Pharmacol* **77**, 228-236 (2010).
33. McDonald, J.G. & Russell, D.W. Editorial: 25-Hydroxycholesterol: a new life in immunology. *J Leukoc Biol* **88**, 1071-1072 (2010).
34. Russell, D.W. The enzymes, regulation, and genetics of bile acid synthesis. *Annu Rev Biochem* **72**, 137-174 (2003).
35. Honda, A. *et al.* Cholesterol 25-hydroxylation activity of CYP3A. *J Lipid Res* **52**, 1509-1516 (2011).

36. Schule, R. *et al.* Marked accumulation of 27-hydroxycholesterol in SPG5 patients with hereditary spastic paresis. *J Lipid Res* **51**, 819-823 (2010).
37. Willinger, T. Oxysterols in intestinal immunity and inflammation. *J Intern Med* **285**, 367-380 (2019).
38. Diczfalusy, U. *et al.* Marked upregulation of cholesterol 25-hydroxylase expression by lipopolysaccharide. *J Lipid Res* **50**, 2258-2264 (2009).
39. Bauman, D.R. *et al.* 25-Hydroxycholesterol secreted by macrophages in response to Toll-like receptor activation suppresses immunoglobulin A production. *Proc Natl Acad Sci U S A* **106**, 16764-16769 (2009).
40. Dang, E.V., McDonald, J.G., Russell, D.W. & Cyster, J.G. Oxysterol Restraint of Cholesterol Synthesis Prevents AIM2 Inflammasome Activation. *Cell* **171**, 1057-1071 e1011 (2017).
41. Emgard, J. *et al.* Oxysterol Sensing through the Receptor GPR183 Promotes the Lymphoid-Tissue-Inducing Function of Innate Lymphoid Cells and Colonic Inflammation. *Immunity* **48**, 120-132 e128 (2018).
42. Gold, E.S. *et al.* 25-Hydroxycholesterol acts as an amplifier of inflammatory signaling. *Proc Natl Acad Sci U S A* **111**, 10666-10671 (2014).
43. Jia, J. *et al.* Cholesterol metabolism promotes B-cell positioning during immune pathogenesis of chronic obstructive pulmonary disease. *EMBO Mol Med* **10** (2018).
44. Reboldi, A. *et al.* Inflammation. 25-Hydroxycholesterol suppresses interleukin-1-driven inflammation downstream of type I interferon. *Science* **345**, 679-684 (2014).
45. Russo, L. *et al.* Cholesterol 25-hydroxylase (CH25H) as a promoter of adipose tissue inflammation in obesity and diabetes. *Mol Metab* **39**, 100983 (2020).
46. Wanke, F. *et al.* EBI2 Is Highly Expressed in Multiple Sclerosis Lesions and Promotes Early CNS Migration of Encephalitogenic CD4 T Cells. *Cell Rep* **18**, 1270-1284 (2017).
47. Wyss, A. *et al.* The EBI2-oxysterol axis promotes the development of intestinal lymphoid structures and colitis. *Mucosal Immunol* **12**, 733-745 (2019).
48. Foo, C.X., Bartlett, S. & Ronacher, K. Oxysterols in the Immune Response to Bacterial and Viral Infections. *Cells* **11** (2022).
49. Park, K. & Scott, A.L. Cholesterol 25-hydroxylase production by dendritic cells and macrophages is regulated by type I interferons. *J Leukoc Biol* **88**, 1081-1087 (2010).
50. Magoro, T. *et al.* IL-1beta/TNF-alpha/IL-6 inflammatory cytokines promote STAT1-dependent induction of CH25H in Zika virus-infected human macrophages. *J Biol Chem* **294**, 14591-14602 (2019).
51. Joseph, S.B., Castrillo, A., Laffitte, B.A., Mangelsdorf, D.J. & Tontonoz, P. Reciprocal regulation of inflammation and lipid metabolism by liver X receptors. *Nat Med* **9**, 213-219 (2003).
52. Landis, M.S., Patel, H.V. & Capone, J.P. Oxysterol activators of liver X receptor and 9-cis-retinoic acid promote sequential steps in the synthesis and secretion of tumor necrosis factor-alpha from human monocytes. *J Biol Chem* **277**, 4713-4721 (2002).
53. Walcher, D. *et al.* LXR activation reduces proinflammatory cytokine expression in human CD4-positive lymphocytes. *Arterioscler Thromb Vasc Biol* **26**, 1022-1028 (2006).

54. Zhang-Gandhi, C.X. & Drew, P.D. Liver X receptor and retinoid X receptor agonists inhibit inflammatory responses of microglia and astrocytes. *J Neuroimmunol* **183**, 50-59 (2007).
55. Bottemanne, P. *et al.* 25-Hydroxycholesterol metabolism is altered by lung inflammation, and its local administration modulates lung inflammation in mice. *FASEB J* **35**, e21514 (2021).
56. Madenspacher, J.H. *et al.* Cholesterol 25-hydroxylase promotes efferocytosis and resolution of lung inflammation. *JCI Insight* **5** (2020).
57. Lee, J.H., Han, J.H., Woo, J.H. & Jou, I. 25-Hydroxycholesterol suppress IFN-gamma-induced inflammation in microglia by disrupting lipid raft formation and caveolin-mediated signaling endosomes. *Free Radic Biol Med* **179**, 252-265 (2022).
58. Jang, J. *et al.* 25-hydroxycholesterol contributes to cerebral inflammation of X-linked adrenoleukodystrophy through activation of the NLRP3 inflammasome. *Nat Commun* **7**, 13129 (2016).
59. Wong, M.Y. *et al.* 25-Hydroxycholesterol amplifies microglial IL-1beta production in an apoE isoform-dependent manner. *J Neuroinflammation* **17**, 192 (2020).
60. Tuong, Z.K. *et al.* RORalpha and 25-Hydroxycholesterol Crosstalk Regulates Lipid Droplet Homeostasis in Macrophages. *PLoS One* **11**, e0147179 (2016).
61. Spann, N.J. *et al.* Regulated accumulation of desmosterol integrates macrophage lipid metabolism and inflammatory responses. *Cell* **151**, 138-152 (2012).
62. Li, Z. *et al.* Kruppel-Like Factor 4 Regulation of Cholesterol-25-Hydroxylase and Liver X Receptor Mitigates Atherosclerosis Susceptibility. *Circulation* **136**, 1315-1330 (2017).
63. Seeley, J.J. & Ghosh, S. Molecular mechanisms of innate memory and tolerance to LPS. *J Leukoc Biol* **101**, 107-119 (2017).
64. Locati, M., Curtale, G. & Mantovani, A. Diversity, Mechanisms, and Significance of Macrophage Plasticity. *Annu Rev Pathol* **15**, 123-147 (2020).
65. Netea, M.G. *et al.* Trained immunity: A program of innate immune memory in health and disease. *Science* **352**, aaf1098 (2016).
66. Cyster, J.G., Dang, E.V., Reboldi, A. & Yi, T. 25-Hydroxycholesterols in innate and adaptive immunity. *Nat Rev Immunol* **14**, 731-743 (2014).
67. Trindade, B.C. *et al.* The cholesterol metabolite 25-hydroxycholesterol restrains the transcriptional regulator SREBP2 and limits intestinal IgA plasma cell differentiation. *Immunity* **54**, 2273-2287 e2276 (2021).
68. Takahashi, H. *et al.* Cholesterol 25-hydroxylase is a metabolic switch to constrain T cell-mediated inflammation in the skin. *Sci Immunol* **6**, eabb6444 (2021).
69. Vigne, S. *et al.* IL-27-Induced Type 1 Regulatory T-Cells Produce Oxysterols that Constrain IL-10 Production. *Front Immunol* **8**, 1184 (2017).
70. Jin, L. *et al.* Structural basis for hydroxycholesterols as natural ligands of orphan nuclear receptor RORgamma. *Mol Endocrinol* **24**, 923-929 (2010).
71. Hannedouche, S. *et al.* Oxysterols direct immune cell migration via EBI2. *Nature* **475**, 524-527 (2011).
72. Liu, C. *et al.* Oxysterols direct B-cell migration through EBI2. *Nature* **475**, 519-523 (2011).

73. Benned-Jensen, T. & Rosenkilde, M.M. Structural motifs of importance for the constitutive activity of the orphan 7TM receptor EBI2: analysis of receptor activation in the absence of an agonist. *Mol Pharmacol* **74**, 1008-1021 (2008).
74. Birkenbach, M., Josefsen, K., Yalamanchili, R., Lenoir, G. & Kieff, E. Epstein-Barr virus-induced genes: first lymphocyte-specific G protein-coupled peptide receptors. *J Virol* **67**, 2209-2220 (1993).
75. Pereira, J.P., Kelly, L.M., Xu, Y. & Cyster, J.G. EBI2 mediates B cell segregation between the outer and centre follicle. *Nature* **460**, 1122-1126 (2009).
76. Clottu, A.S. *et al.* EBI2 Expression and Function: Robust in Memory Lymphocytes and Increased by Natalizumab in Multiple Sclerosis. *Cell Rep* **18**, 213-224 (2017).
77. Gatto, D. *et al.* The chemotactic receptor EBI2 regulates the homeostasis, localization and immunological function of splenic dendritic cells. *Nat Immunol* **14**, 446-453 (2013).
78. Heinig, M. *et al.* A trans-acting locus regulates an anti-viral expression network and type 1 diabetes risk. *Nature* **467**, 460-464 (2010).
79. Shen, Z.J., Hu, J., Esnault, S., Dozmorov, I. & Malter, J.S. RNA Seq profiling reveals a novel expression pattern of TGF-beta target genes in human blood eosinophils. *Immunol Lett* **167**, 1-10 (2015).
80. Amisten, S., Braun, O.O., Bengtsson, A. & Erlinge, D. Gene expression profiling for the identification of G-protein coupled receptors in human platelets. *Thromb Res* **122**, 47-57 (2008).
81. Rutkowska, A., Preuss, I., Gessier, F., Sailer, A.W. & Dev, K.K. EBI2 regulates intracellular signaling and migration in human astrocyte. *Glia* **63**, 341-351 (2015).
82. Klejbor, I. *et al.* EBI2 is expressed in glial cells in multiple sclerosis lesions, and its knock-out modulates remyelination in the cuprizone model. *Eur J Neurosci* **54**, 5173-5188 (2021).
83. Nevius, E. *et al.* Oxysterols and EBI2 promote osteoclast precursor migration to bone surfaces and regulate bone mass homeostasis. *J Exp Med* **212**, 1931-1946 (2015).
84. Zhang, P. *et al.* G protein-coupled receptor 183 facilitates endothelial-to-hematopoietic transition via Notch1 inhibition. *Cell Res* **25**, 1093-1107 (2015).
85. Rodda, L.B. *et al.* Single-Cell RNA Sequencing of Lymph Node Stromal Cells Reveals Niche-Associated Heterogeneity. *Immunity* **48**, 1014-1028 e1016 (2018).
86. Gatto, D. & Brink, R. B cell localization: regulation by EBI2 and its oxysterol ligand. *Trends Immunol* **34**, 336-341 (2013).
87. Girard, J.P., Moussion, C. & Forster, R. HEVs, lymphatics and homeostatic immune cell trafficking in lymph nodes. *Nat Rev Immunol* **12**, 762-773 (2012).
88. Kelly, L.M., Pereira, J.P., Yi, T., Xu, Y. & Cyster, J.G. EBI2 guides serial movements of activated B cells and ligand activity is detectable in lymphoid and nonlymphoid tissues. *J Immunol* **187**, 3026-3032 (2011).
89. Coffey, F., Alabyev, B. & Manser, T. Initial clonal expansion of germinal center B cells takes place at the perimeter of follicles. *Immunity* **30**, 599-609 (2009).
90. Garside, P. *et al.* Visualization of specific B and T lymphocyte interactions in the lymph node. *Science* **281**, 96-99 (1998).

91. Li, J., Lu, E., Yi, T. & Cyster, J.G. EB12 augments Tfh cell fate by promoting interaction with IL-2-quenching dendritic cells. *Nature* **533**, 110-114 (2016).
92. Crotty, S. T Follicular Helper Cell Biology: A Decade of Discovery and Diseases. *Immunity* **50**, 1132-1148 (2019).
93. Yi, T. & Cyster, J.G. EB12-mediated bridging channel positioning supports splenic dendritic cell homeostasis and particulate antigen capture. *Elife* **2**, e00757 (2013).
94. Chappell, C.P., Draves, K.E., Giltiay, N.V. & Clark, E.A. Extrafollicular B cell activation by marginal zone dendritic cells drives T cell-dependent antibody responses. *J Exp Med* **209**, 1825-1840 (2012).
95. Baptista, A.P. *et al.* The Chemoattractant Receptor Ebi2 Drives Intranodal Naive CD4(+) T Cell Peripheralization to Promote Effective Adaptive Immunity. *Immunity* **50**, 1188-1201 e1186 (2019).
96. Neyt, K., Perros, F., GeurtsvanKessel, C.H., Hammad, H. & Lambrecht, B.N. Tertiary lymphoid organs in infection and autoimmunity. *Trends Immunol* **33**, 297-305 (2012).
97. Buettner, M. & Lochner, M. Development and Function of Secondary and Tertiary Lymphoid Organs in the Small Intestine and the Colon. *Front Immunol* **7**, 342 (2016).
98. Pitzalis, C., Jones, G.W., Bombardieri, M. & Jones, S.A. Ectopic lymphoid-like structures in infection, cancer and autoimmunity. *Nat Rev Immunol* **14**, 447-462 (2014).
99. Spits, H. *et al.* Innate lymphoid cells--a proposal for uniform nomenclature. *Nat Rev Immunol* **13**, 145-149 (2013).
100. Walker, J.A., Barlow, J.L. & McKenzie, A.N. Innate lymphoid cells--how did we miss them? *Nat Rev Immunol* **13**, 75-87 (2013).
101. Sawa, S. *et al.* Lineage relationship analysis of ROR $\gamma$ mat<sup>+</sup> innate lymphoid cells. *Science* **330**, 665-669 (2010).
102. Kanamori, Y. *et al.* Identification of novel lymphoid tissues in murine intestinal mucosa where clusters of c-kit<sup>+</sup> IL-7R<sup>+</sup> Thy1<sup>+</sup> lympho-hemopoietic progenitors develop. *J Exp Med* **184**, 1449-1459 (1996).
103. Chu, C. *et al.* Anti-microbial Functions of Group 3 Innate Lymphoid Cells in Gut-Associated Lymphoid Tissues Are Regulated by G-Protein-Coupled Receptor 183. *Cell Rep* **23**, 3750-3758 (2018).
104. Smirnova, N.F. *et al.* Inhibition of B cell-dependent lymphoid follicle formation prevents lymphocytic bronchiolitis after lung transplantation. *JCI Insight* **4** (2019).
105. Maaser, C. *et al.* ECCO-ESGAR Guideline for Diagnostic Assessment in IBD Part 1: Initial diagnosis, monitoring of known IBD, detection of complications. *J Crohns Colitis* **13**, 144-164 (2019).
106. Sturm, A. *et al.* ECCO-ESGAR Guideline for Diagnostic Assessment in IBD Part 2: IBD scores and general principles and technical aspects. *J Crohns Colitis* **13**, 273-284 (2019).
107. Larsen, S., Bendtzen, K. & Nielsen, O.H. Extraintestinal manifestations of inflammatory bowel disease: epidemiology, diagnosis, and management. *Ann Med* **42**, 97-114 (2010).
108. Molodecky, N.A. *et al.* Increasing incidence and prevalence of the inflammatory bowel diseases with time, based on systematic review. *Gastroenterology* **142**, 46-54 e42; quiz e30 (2012).

109. Zhao, M., Gonczi, L., Lakatos, P.L. & Burisch, J. The Burden of Inflammatory Bowel Disease in Europe in 2020. *J Crohns Colitis* **15**, 1573-1587 (2021).
110. Greuter, T. *et al.* Gender Differences in Inflammatory Bowel Disease. *Digestion* **101 Suppl 1**, 98-104 (2020).
111. Magro, F. *et al.* European consensus on the histopathology of inflammatory bowel disease. *J Crohns Colitis* **7**, 827-851 (2013).
112. Mowat, A.M. Anatomical basis of tolerance and immunity to intestinal antigens. *Nat Rev Immunol* **3**, 331-341 (2003).
113. Uhlig, H.H. & Powrie, F. Translating Immunology into Therapeutic Concepts for Inflammatory Bowel Disease. *Annu Rev Immunol* **36**, 755-781 (2018).
114. Maloy, K.J. & Powrie, F. Intestinal homeostasis and its breakdown in inflammatory bowel disease. *Nature* **474**, 298-306 (2011).
115. Odenwald, M.A. & Turner, J.R. The intestinal epithelial barrier: a therapeutic target? *Nat Rev Gastroenterol Hepatol* **14**, 9-21 (2017).
116. Bischoff, S.C. *et al.* Intestinal permeability--a new target for disease prevention and therapy. *BMC Gastroenterol* **14**, 189 (2014).
117. Pickard, J.M., Zeng, M.Y., Caruso, R. & Nunez, G. Gut microbiota: Role in pathogen colonization, immune responses, and inflammatory disease. *Immunol Rev* **279**, 70-89 (2017).
118. Ananthakrishnan, A.N. Epidemiology and risk factors for IBD. *Nat Rev Gastroenterol Hepatol* **12**, 205-217 (2015).
119. Jostins, L. *et al.* Host-microbe interactions have shaped the genetic architecture of inflammatory bowel disease. *Nature* **491**, 119-124 (2012).
120. Liu, J.Z. *et al.* Association analyses identify 38 susceptibility loci for inflammatory bowel disease and highlight shared genetic risk across populations. *Nat Genet* **47**, 979-986 (2015).
121. McGovern, D.P., Kugathasan, S. & Cho, J.H. Genetics of Inflammatory Bowel Diseases. *Gastroenterology* **149**, 1163-1176 e1162 (2015).
122. Hugot, J.P. *et al.* Association of NOD2 leucine-rich repeat variants with susceptibility to Crohn's disease. *Nature* **411**, 599-603 (2001).
123. Ogura, Y. *et al.* A frameshift mutation in NOD2 associated with susceptibility to Crohn's disease. *Nature* **411**, 603-606 (2001).
124. Al Nabhani, Z., Dietrich, G., Hugot, J.P. & Barreau, F. Nod2: The intestinal gate keeper. *PLoS Pathog* **13**, e1006177 (2017).
125. Strober, W., Murray, P.J., Kitani, A. & Watanabe, T. Signalling pathways and molecular interactions of NOD1 and NOD2. *Nat Rev Immunol* **6**, 9-20 (2006).
126. Cooney, R. *et al.* NOD2 stimulation induces autophagy in dendritic cells influencing bacterial handling and antigen presentation. *Nat Med* **16**, 90-97 (2010).
127. Hampe, J. *et al.* A genome-wide association scan of nonsynonymous SNPs identifies a susceptibility variant for Crohn disease in ATG16L1. *Nat Genet* **39**, 207-211 (2007).
128. Iida, T., Onodera, K. & Nakase, H. Role of autophagy in the pathogenesis of inflammatory bowel disease. *World J Gastroenterol* **23**, 1944-1953 (2017).

129. Pott, J., Kabat, A.M. & Maloy, K.J. Intestinal Epithelial Cell Autophagy Is Required to Protect against TNF-Induced Apoptosis during Chronic Colitis in Mice. *Cell Host Microbe* **23**, 191-202 e194 (2018).
130. Jandhyala, S.M. *et al.* Role of the normal gut microbiota. *World J Gastroenterol* **21**, 8787-8803 (2015).
131. Levy, M., Kolodziejczyk, A.A., Thaïss, C.A. & Elinav, E. Dysbiosis and the immune system. *Nat Rev Immunol* **17**, 219-232 (2017).
132. Glassner, K.L., Abraham, B.P. & Quigley, E.M.M. The microbiome and inflammatory bowel disease. *J Allergy Clin Immunol* **145**, 16-27 (2020).
133. Sellon, R.K. *et al.* Resident enteric bacteria are necessary for development of spontaneous colitis and immune system activation in interleukin-10-deficient mice. *Infect Immun* **66**, 5224-5231 (1998).
134. Russo, E. *et al.* Immunomodulating Activity and Therapeutic Effects of Short Chain Fatty Acids and Tryptophan Post-biotics in Inflammatory Bowel Disease. *Front Immunol* **10**, 2754 (2019).
135. Zheng, L. *et al.* Microbial-Derived Butyrate Promotes Epithelial Barrier Function through IL-10 Receptor-Dependent Repression of Claudin-2. *J Immunol* **199**, 2976-2984 (2017).
136. Hang, S. *et al.* Bile acid metabolites control TH17 and Treg cell differentiation. *Nature* **576**, 143-148 (2019).
137. Song, X. *et al.* Microbial bile acid metabolites modulate gut RORgamma(+) regulatory T cell homeostasis. *Nature* **577**, 410-415 (2020).
138. Alexeev, E.E. *et al.* Microbiota-Derived Indole Metabolites Promote Human and Murine Intestinal Homeostasis through Regulation of Interleukin-10 Receptor. *Am J Pathol* **188**, 1183-1194 (2018).
139. Morgan, X.C. *et al.* Dysfunction of the intestinal microbiome in inflammatory bowel disease and treatment. *Genome Biol* **13**, R79 (2012).
140. Torres, J. *et al.* Serum Biomarkers Identify Patients Who Will Develop Inflammatory Bowel Diseases Up to 5 Years Before Diagnosis. *Gastroenterology* **159**, 96-104 (2020).
141. Turpin, W. *et al.* Increased Intestinal Permeability Is Associated With Later Development of Crohn's Disease. *Gastroenterology* **159**, 2092-2100 e2095 (2020).
142. Wyatt, J., Vogelsang, H., Hubl, W., Waldhoer, T. & Lochs, H. Intestinal permeability and the prediction of relapse in Crohn's disease. *Lancet* **341**, 1437-1439 (1993).
143. Friedrich, M., Pohin, M. & Powrie, F. Cytokine Networks in the Pathophysiology of Inflammatory Bowel Disease. *Immunity* **50**, 992-1006 (2019).
144. Ueno, A. *et al.* Th17 plasticity and its relevance to inflammatory bowel disease. *J Autoimmun* **87**, 38-49 (2018).
145. Joossens, M. *et al.* Dysbiosis of the faecal microbiota in patients with Crohn's disease and their unaffected relatives. *Gut* **60**, 631-637 (2011).
146. Hall, A.B. *et al.* A novel Ruminococcus gnavus clade enriched in inflammatory bowel disease patients. *Genome Med* **9**, 103 (2017).

147. Henke, M.T. *et al.* Ruminococcus gnavus, a member of the human gut microbiome associated with Crohn's disease, produces an inflammatory polysaccharide. *Proc Natl Acad Sci U S A* **116**, 12672-12677 (2019).
148. Mazmanian, S.K., Round, J.L. & Kasper, D.L. A microbial symbiosis factor prevents intestinal inflammatory disease. *Nature* **453**, 620-625 (2008).
149. Caruso, R., Lo, B.C. & Nunez, G. Host-microbiota interactions in inflammatory bowel disease. *Nat Rev Immunol* **20**, 411-426 (2020).
150. Shan, Y., Lee, M. & Chang, E.B. The Gut Microbiome and Inflammatory Bowel Diseases. *Annu Rev Med* **73**, 455-468 (2022).
151. Jochum, L. & Stecher, B. Label or Concept - What Is a Pathobiont? *Trends Microbiol* **28**, 789-792 (2020).
152. Zhang, R. *et al.* Up-regulation of Gr1+CD11b+ population in spleen of dextran sulfate sodium administered mice works to repair colitis. *Inflamm Allergy Drug Targets* **10**, 39-46 (2011).
153. Tian, W.J., Wang, Q.N., Wang, X.F. & Dong, D.F. Clophosome alleviate dextran sulphate sodium-induced colitis by regulating gut immune responses and maintaining intestinal integrity in mice. *Clin Exp Pharmacol Physiol* **48**, 902-910 (2021).
154. Duerr, R.H. *et al.* A genome-wide association study identifies IL23R as an inflammatory bowel disease gene. *Science* **314**, 1461-1463 (2006).
155. Dennehy, K.M., Willment, J.A., Williams, D.L. & Brown, G.D. Reciprocal regulation of IL-23 and IL-12 following co-activation of Dectin-1 and TLR signaling pathways. *Eur J Immunol* **39**, 1379-1386 (2009).
156. Oppmann, B. *et al.* Novel p19 protein engages IL-12p40 to form a cytokine, IL-23, with biological activities similar as well as distinct from IL-12. *Immunity* **13**, 715-725 (2000).
157. Ahern, P.P. *et al.* Interleukin-23 drives intestinal inflammation through direct activity on T cells. *Immunity* **33**, 279-288 (2010).
158. McGeachy, M.J. *et al.* The interleukin 23 receptor is essential for the terminal differentiation of interleukin 17-producing effector T helper cells in vivo. *Nat Immunol* **10**, 314-324 (2009).
159. Li, J., Casanova, J.L. & Puel, A. Mucocutaneous IL-17 immunity in mice and humans: host defense vs. excessive inflammation. *Mucosal Immunol* **11**, 581-589 (2018).
160. Sivanesan, D. *et al.* IL23R (Interleukin 23 Receptor) Variants Protective against Inflammatory Bowel Diseases (IBD) Display Loss of Function due to Impaired Protein Stability and Intracellular Trafficking. *J Biol Chem* **291**, 8673-8685 (2016).
161. Zwiers, A. *et al.* Cutting edge: a variant of the IL-23R gene associated with inflammatory bowel disease induces loss of microRNA regulation and enhanced protein production. *J Immunol* **188**, 1573-1577 (2012).
162. Yen, D. *et al.* IL-23 is essential for T cell-mediated colitis and promotes inflammation via IL-17 and IL-6. *J Clin Invest* **116**, 1310-1316 (2006).
163. Feagan, B.G. *et al.* Ustekinumab as Induction and Maintenance Therapy for Crohn's Disease. *N Engl J Med* **375**, 1946-1960 (2016).
164. Sands, B.E. *et al.* Ustekinumab as Induction and Maintenance Therapy for Ulcerative Colitis. *N Engl J Med* **381**, 1201-1214 (2019).

165. Coccia, M. *et al.* IL-1beta mediates chronic intestinal inflammation by promoting the accumulation of IL-17A secreting innate lymphoid cells and CD4(+) Th17 cells. *J Exp Med* **209**, 1595-1609 (2012).
166. Shouval, D.S. *et al.* Interleukin 1beta Mediates Intestinal Inflammation in Mice and Patients With Interleukin 10 Receptor Deficiency. *Gastroenterology* **151**, 1100-1104 (2016).
167. Atreya, R. *et al.* Blockade of interleukin 6 trans signaling suppresses T-cell resistance against apoptosis in chronic intestinal inflammation: evidence in crohn disease and experimental colitis in vivo. *Nat Med* **6**, 583-588 (2000).
168. Yamamoto, M., Yoshizaki, K., Kishimoto, T. & Ito, H. IL-6 is required for the development of Th1 cell-mediated murine colitis. *J Immunol* **164**, 4878-4882 (2000).
169. Sandborn, W.J. *et al.* Certolizumab pegol for the treatment of Crohn's disease. *N Engl J Med* **357**, 228-238 (2007).
170. Stack, W.A. *et al.* Randomised controlled trial of CDP571 antibody to tumour necrosis factor-alpha in Crohn's disease. *Lancet* **349**, 521-524 (1997).
171. Kontoyiannis, D., Pasparakis, M., Pizarro, T.T., Cominelli, F. & Kollias, G. Impaired on/off regulation of TNF biosynthesis in mice lacking TNF AU-rich elements: implications for joint and gut-associated immunopathologies. *Immunity* **10**, 387-398 (1999).
172. Nenci, A. *et al.* Epithelial NEMO links innate immunity to chronic intestinal inflammation. *Nature* **446**, 557-561 (2007).
173. Bernink, J.H. *et al.* Human type 1 innate lymphoid cells accumulate in inflamed mucosal tissues. *Nat Immunol* **14**, 221-229 (2013).
174. Powell, N. *et al.* The transcription factor T-bet regulates intestinal inflammation mediated by interleukin-7 receptor+ innate lymphoid cells. *Immunity* **37**, 674-684 (2012).
175. Vonarbourg, C. *et al.* Regulated expression of nuclear receptor RORgammat confers distinct functional fates to NK cell receptor-expressing RORgammat(+) innate lymphocytes. *Immunity* **33**, 736-751 (2010).
176. Geremia, A. *et al.* IL-23-responsive innate lymphoid cells are increased in inflammatory bowel disease. *J Exp Med* **208**, 1127-1133 (2011).
177. Buonocore, S. *et al.* Innate lymphoid cells drive interleukin-23-dependent innate intestinal pathology. *Nature* **464**, 1371-1375 (2010).
178. Pearson, C. *et al.* ILC3 GM-CSF production and mobilisation orchestrate acute intestinal inflammation. *Elife* **5**, e10066 (2016).
179. Song, C. *et al.* Unique and redundant functions of NKp46+ ILC3s in models of intestinal inflammation. *J Exp Med* **212**, 1869-1882 (2015).
180. Skamnelos, A. *et al.* CD4 count remission hypothesis in patients with inflammatory bowel disease and human immunodeficiency virus infection: a systematic review of the literature. *Ann Gastroenterol* **28**, 337-346 (2015).
181. Powrie, F., Correa-Oliveira, R., Mauze, S. & Coffman, R.L. Regulatory interactions between CD45RBhigh and CD45RBlow CD4+ T cells are important for the balance between protective and pathogenic cell-mediated immunity. *J Exp Med* **179**, 589-600 (1994).
182. Boutros, C. *et al.* Safety profiles of anti-CTLA-4 and anti-PD-1 antibodies alone and in combination. *Nat Rev Clin Oncol* **13**, 473-486 (2016).

183. Nava, P. *et al.* Interferon-gamma regulates intestinal epithelial homeostasis through converging beta-catenin signaling pathways. *Immunity* **32**, 392-402 (2010).
184. Powrie, F. *et al.* Inhibition of Th1 responses prevents inflammatory bowel disease in scid mice reconstituted with CD45RBhi CD4+ T cells. *Immunity* **1**, 553-562 (1994).
185. Ito, R. *et al.* Interferon-gamma is causatively involved in experimental inflammatory bowel disease in mice. *Clin Exp Immunol* **146**, 330-338 (2006).
186. Shen, C. *et al.* Remission-inducing effect of anti-TNF monoclonal antibody in TNBS colitis: mechanisms beyond neutralization? *Inflamm Bowel Dis* **13**, 308-316 (2007).
187. Fujino, S. *et al.* Increased expression of interleukin 17 in inflammatory bowel disease. *Gut* **52**, 65-70 (2003).
188. Hueber, W. *et al.* Secukinumab, a human anti-IL-17A monoclonal antibody, for moderate to severe Crohn's disease: unexpected results of a randomised, double-blind placebo-controlled trial. *Gut* **61**, 1693-1700 (2012).
189. O'Connor, W., Jr. *et al.* A protective function for interleukin 17A in T cell-mediated intestinal inflammation. *Nat Immunol* **10**, 603-609 (2009).
190. Lee, J.S. *et al.* Interleukin-23-Independent IL-17 Production Regulates Intestinal Epithelial Permeability. *Immunity* **43**, 727-738 (2015).
191. Griseri, T. *et al.* Granulocyte Macrophage Colony-Stimulating Factor-Activated Eosinophils Promote Interleukin-23 Driven Chronic Colitis. *Immunity* **43**, 187-199 (2015).
192. Kleinschek, M.A. *et al.* Circulating and gut-resident human Th17 cells express CD161 and promote intestinal inflammation. *J Exp Med* **206**, 525-534 (2009).
193. Stadhouders, R., Lubberts, E. & Hendriks, R.W. A cellular and molecular view of T helper 17 cell plasticity in autoimmunity. *J Autoimmun* **87**, 1-15 (2018).
194. Stockinger, B. & Omenetti, S. The dichotomous nature of T helper 17 cells. *Nat Rev Immunol* **17**, 535-544 (2017).
195. Muller, S. *et al.* Activated CD4+ and CD8+ cytotoxic cells are present in increased numbers in the intestinal mucosa from patients with active inflammatory bowel disease. *Am J Pathol* **152**, 261-268 (1998).
196. Ho, J. *et al.* A CD8+/CD103high T cell subset regulates TNF-mediated chronic murine ileitis. *J Immunol* **180**, 2573-2580 (2008).
197. Liu, Y. *et al.* Phenotypic and functional characteristic of a newly identified CD8+ Foxp3-CD103+ regulatory T cells. *J Mol Cell Biol* **6**, 81-92 (2014).
198. Funderburg, N.T. *et al.* Circulating CD4(+) and CD8(+) T cells are activated in inflammatory bowel disease and are associated with plasma markers of inflammation. *Immunology* **140**, 87-97 (2013).
199. Nancey, S. *et al.* CD8+ cytotoxic T cells induce relapsing colitis in normal mice. *Gastroenterology* **131**, 485-496 (2006).
200. Boland, B.S. *et al.* Heterogeneity and clonal relationships of adaptive immune cells in ulcerative colitis revealed by single-cell analyses. *Sci Immunol* **5** (2020).
201. Smillie, C.S. *et al.* Intra- and Inter-cellular Rewiring of the Human Colon during Ulcerative Colitis. *Cell* **178**, 714-730 e722 (2019).

202. Lee, J.C. *et al.* Gene expression profiling of CD8+ T cells predicts prognosis in patients with Crohn disease and ulcerative colitis. *J Clin Invest* **121**, 4170-4179 (2011).
203. Casalegno Garduno, R. & Dabritz, J. New Insights on CD8(+) T Cells in Inflammatory Bowel Disease and Therapeutic Approaches. *Front Immunol* **12**, 738762 (2021).
204. Yacyshyn, B.R. & Meddings, J.B. CD45RO expression on circulating CD19+ B cells in Crohn's disease correlates with intestinal permeability. *Gastroenterology* **108**, 132-137 (1995).
205. Yacyshyn, B.R. & Pilarski, L.M. Expression of CD45RO on circulating CD19+ B-cells in Crohn's disease. *Gut* **34**, 1698-1704 (1993).
206. Brandtzaeg, P., Baklien, K., Fausa, O. & Hoel, P.S. Immunohistochemical characterization of local immunoglobulin formation in ulcerative colitis. *Gastroenterology* **66**, 1123-1136 (1974).
207. Macpherson, A., Khoo, U.Y., Forgacs, I., Philpott-Howard, J. & Bjarnason, I. Mucosal antibodies in inflammatory bowel disease are directed against intestinal bacteria. *Gut* **38**, 365-375 (1996).
208. Uzzan, M. *et al.* Ulcerative colitis is characterized by a plasmablast-skewed humoral response associated with disease activity. *Nat Med* (2022).
209. Castro-Dopico, T. *et al.* Anti-commensal IgG Drives Intestinal Inflammation and Type 17 Immunity in Ulcerative Colitis. *Immunity* **50**, 1099-1114 e1010 (2019).
210. Uo, M. *et al.* Mucosal CXCR4+ IgG plasma cells contribute to the pathogenesis of human ulcerative colitis through FcγR-mediated CD14 macrophage activation. *Gut* **62**, 1734-1744 (2013).
211. Martin, J.C. *et al.* Single-Cell Analysis of Crohn's Disease Lesions Identifies a Pathogenic Cellular Module Associated with Resistance to Anti-TNF Therapy. *Cell* **178**, 1493-1508 e1420 (2019).
212. Han, X. *et al.* Granulocyte-macrophage colony-stimulating factor autoantibodies in murine ileitis and progressive ileal Crohn's disease. *Gastroenterology* **136**, 1261-1271, e1261-1263 (2009).
213. Gathungu, G. *et al.* Granulocyte-macrophage colony-stimulating factor autoantibodies: a marker of aggressive Crohn's disease. *Inflamm Bowel Dis* **19**, 1671-1680 (2013).
214. Tom, M.R. *et al.* Novel CD8+ T-Cell Subsets Demonstrating Plasticity in Patients with Inflammatory Bowel Disease. *Inflamm Bowel Dis* **22**, 1596-1608 (2016).
215. Hedrich, C.M. & Bream, J.H. Cell type-specific regulation of IL-10 expression in inflammation and disease. *Immunol Res* **47**, 185-206 (2010).
216. Glocker, E.O. *et al.* Inflammatory bowel disease and mutations affecting the interleukin-10 receptor. *N Engl J Med* **361**, 2033-2045 (2009).
217. Kuhn, R., Lohler, J., Rennick, D., Rajewsky, K. & Muller, W. Interleukin-10-deficient mice develop chronic enterocolitis. *Cell* **75**, 263-274 (1993).
218. Sugimoto, K. *et al.* IL-22 ameliorates intestinal inflammation in a mouse model of ulcerative colitis. *J Clin Invest* **118**, 534-544 (2008).
219. Pickert, G. *et al.* STAT3 links IL-22 signaling in intestinal epithelial cells to mucosal wound healing. *J Exp Med* **206**, 1465-1472 (2009).

220. Kulkarni, A.B. *et al.* Transforming growth factor beta 1 null mutation in mice causes excessive inflammatory response and early death. *Proc Natl Acad Sci U S A* **90**, 770-774 (1993).
221. Sadlack, B. *et al.* Ulcerative colitis-like disease in mice with a disrupted interleukin-2 gene. *Cell* **75**, 253-261 (1993).
222. Li, M.O. & Flavell, R.A. Contextual regulation of inflammation: a duet by transforming growth factor-beta and interleukin-10. *Immunity* **28**, 468-476 (2008).
223. Chinen, T. *et al.* An essential role for the IL-2 receptor in Treg cell function. *Nat Immunol* **17**, 1322-1333 (2016).
224. Schiering, C. *et al.* The alarmin IL-33 promotes regulatory T-cell function in the intestine. *Nature* **513**, 564-568 (2014).
225. Cai, Z., Wang, S. & Li, J. Treatment of Inflammatory Bowel Disease: A Comprehensive Review. *Front Med (Lausanne)* **8**, 765474 (2021).
226. Burri, E. *et al.* Treatment Algorithm for Mild and Moderate-to-Severe Ulcerative Colitis: An Update. *Digestion* **101 Suppl 1**, 2-15 (2020).
227. Sulz, M.C. *et al.* Treatment Algorithms for Crohn's Disease. *Digestion* **101 Suppl 1**, 43-57 (2020).
228. Perrotta, C. *et al.* Five-aminosalicylic Acid: an update for the reappraisal of an old drug. *Gastroenterol Res Pract* **2015**, 456895 (2015).
229. Hayashi, R., Wada, H., Ito, K. & Adcock, I.M. Effects of glucocorticoids on gene transcription. *Eur J Pharmacol* **500**, 51-62 (2004).
230. Teng, M.W. *et al.* IL-12 and IL-23 cytokines: from discovery to targeted therapies for immune-mediated inflammatory diseases. *Nat Med* **21**, 719-729 (2015).
231. Comi, G. *et al.* Safety and efficacy of ozanimod versus interferon beta-1a in relapsing multiple sclerosis (SUNBEAM): a multicentre, randomised, minimum 12-month, phase 3 trial. *Lancet Neurol* **18**, 1009-1020 (2019).
232. Feagan, B.G. *et al.* Ozanimod induction therapy for patients with moderate to severe Crohn's disease: a single-arm, phase 2, prospective observer-blinded endpoint study. *Lancet Gastroenterol Hepatol* **5**, 819-828 (2020).
233. Feagan, B.G. *et al.* Vedolizumab as induction and maintenance therapy for ulcerative colitis. *N Engl J Med* **369**, 699-710 (2013).
234. Sandborn, W.J. *et al.* Vedolizumab as induction and maintenance therapy for Crohn's disease. *N Engl J Med* **369**, 711-721 (2013).
235. Biswas, S., Bryant, R.V. & Travis, S. Interfering with leukocyte trafficking in Crohn's disease. *Best Pract Res Clin Gastroenterol* **38-39**, 101617 (2019).
236. Perez-Jeldres, T. *et al.* Cell Trafficking Interference in Inflammatory Bowel Disease: Therapeutic Interventions Based on Basic Pathogenesis Concepts. *Inflamm Bowel Dis* **25**, 270-282 (2019).
237. Guillemot-Legris, O. *et al.* Colitis Alters Oxysterol Metabolism and is Affected by 4beta-Hydroxycholesterol Administration. *J Crohns Colitis* **13**, 218-229 (2019).
238. Ruiz, F. *et al.* A single nucleotide polymorphism in the gene for GPR183 increases its surface expression on blood lymphocytes of patients with inflammatory bowel disease. *Br J Pharmacol* **178**, 3157-3175 (2021).

239. Ingelfinger, F. *et al.* Twin study reveals non-heritable immune perturbations in multiple sclerosis. *Nature* **603**, 152-158 (2022).
240. Westerlind, H. *et al.* Modest familial risks for multiple sclerosis: a registry-based study of the population of Sweden. *Brain* **137**, 770-778 (2014).
241. International Multiple Sclerosis Genetics, C. Multiple sclerosis genomic map implicates peripheral immune cells and microglia in susceptibility. *Science* **365** (2019).
242. International Multiple Sclerosis Genetics, C. *et al.* Genetic risk and a primary role for cell-mediated immune mechanisms in multiple sclerosis. *Nature* **476**, 214-219 (2011).
243. Waubant, E. *et al.* Environmental and genetic risk factors for MS: an integrated review. *Ann Clin Transl Neurol* **6**, 1905-1922 (2019).
244. Thacker, E.L., Mirzaei, F. & Ascherio, A. Infectious mononucleosis and risk for multiple sclerosis: a meta-analysis. *Ann Neurol* **59**, 499-503 (2006).
245. Bjornevik, K. *et al.* Longitudinal analysis reveals high prevalence of Epstein-Barr virus associated with multiple sclerosis. *Science* **375**, 296-301 (2022).
246. Lanz, T.V. *et al.* Clonally expanded B cells in multiple sclerosis bind EBV EBNA1 and GlialCAM. *Nature* **603**, 321-327 (2022).
247. McGinley, M.P., Goldschmidt, C.H. & Rae-Grant, A.D. Diagnosis and Treatment of Multiple Sclerosis: A Review. *JAMA* **325**, 765-779 (2021).
248. University of California, S.F.M.S.E.T. *et al.* Long-term evolution of multiple sclerosis disability in the treatment era. *Ann Neurol* **80**, 499-510 (2016).
249. Antel, J., Antel, S., Caramanos, Z., Arnold, D.L. & Kuhlmann, T. Primary progressive multiple sclerosis: part of the MS disease spectrum or separate disease entity? *Acta Neuropathol* **123**, 627-638 (2012).
250. Collaborators, G.B.D.M.S. Global, regional, and national burden of multiple sclerosis 1990-2016: a systematic analysis for the Global Burden of Disease Study 2016. *Lancet Neurol* **18**, 269-285 (2019).
251. Goodin, D.S. The epidemiology of multiple sclerosis: insights to disease pathogenesis. *Handb Clin Neurol* **122**, 231-266 (2014).
252. Popescu, B.F., Pirko, I. & Lucchinetti, C.F. Pathology of multiple sclerosis: where do we stand? *Continuum (Minneap Minn)* **19**, 901-921 (2013).
253. Kornek, B. *et al.* Multiple sclerosis and chronic autoimmune encephalomyelitis: a comparative quantitative study of axonal injury in active, inactive, and remyelinated lesions. *Am J Pathol* **157**, 267-276 (2000).
254. Hohlfeld, R., Dormair, K., Meinl, E. & Wekerle, H. The search for the target antigens of multiple sclerosis, part 2: CD8+ T cells, B cells, and antibodies in the focus of reverse-translational research. *Lancet Neurol* **15**, 317-331 (2016).
255. Jelcic, I. *et al.* Memory B Cells Activate Brain-Homing, Autoreactive CD4(+) T Cells in Multiple Sclerosis. *Cell* **175**, 85-100 e123 (2018).
256. Wang, J. *et al.* HLA-DR15 Molecules Jointly Shape an Autoreactive T Cell Repertoire in Multiple Sclerosis. *Cell* **183**, 1264-1281 e1220 (2020).

257. Bar-Or, A. & Li, R. Cellular immunology of relapsing multiple sclerosis: interactions, checks, and balances. *Lancet Neurol* **20**, 470-483 (2021).
258. Trapp, B.D. *et al.* Cortical neuronal densities and cerebral white matter demyelination in multiple sclerosis: a retrospective study. *Lancet Neurol* **17**, 870-884 (2018).
259. Benedict, R.H.B. *et al.* Siponimod and Cognition in Secondary Progressive Multiple Sclerosis: EXPAND Secondary Analyses. *Neurology* **96**, e376-e386 (2021).
260. Montalban, X. *et al.* Ocrelizumab versus Placebo in Primary Progressive Multiple Sclerosis. *N Engl J Med* **376**, 209-220 (2017).
261. Lassmann, H. Targets of therapy in progressive MS. *Mult Scler* **23**, 1593-1599 (2017).
262. Frischer, J.M. *et al.* The relation between inflammation and neurodegeneration in multiple sclerosis brains. *Brain* **132**, 1175-1189 (2009).
263. Lassmann, H. Multiple Sclerosis Pathology. *Cold Spring Harb Perspect Med* **8** (2018).
264. Kutzelnigg, A. *et al.* Cortical demyelination and diffuse white matter injury in multiple sclerosis. *Brain* **128**, 2705-2712 (2005).
265. Kamma, E., Lasisi, W., Libner, C., Ng, H.S. & Plemel, J.R. Central nervous system macrophages in progressive multiple sclerosis: relationship to neurodegeneration and therapeutics. *J Neuroinflammation* **19**, 45 (2022).
266. Dendrou, C.A., Fugger, L. & Friese, M.A. Immunopathology of multiple sclerosis. *Nat Rev Immunol* **15**, 545-558 (2015).
267. Stys, P.K., Zamponi, G.W., van Minnen, J. & Geurts, J.J. Will the real multiple sclerosis please stand up? *Nat Rev Neurosci* **13**, 507-514 (2012).
268. Jager, A., Dardalhon, V., Sobel, R.A., Bettelli, E. & Kuchroo, V.K. Th1, Th17, and Th9 effector cells induce experimental autoimmune encephalomyelitis with different pathological phenotypes. *J Immunol* **183**, 7169-7177 (2009).
269. Cao, Y. *et al.* Functional inflammatory profiles distinguish myelin-reactive T cells from patients with multiple sclerosis. *Sci Transl Med* **7**, 287ra274 (2015).
270. Hu, D. *et al.* Transcriptional signature of human pro-inflammatory TH17 cells identifies reduced IL10 gene expression in multiple sclerosis. *Nat Commun* **8**, 1600 (2017).
271. Galli, E. *et al.* GM-CSF and CXCR4 define a T helper cell signature in multiple sclerosis. *Nat Med* **25**, 1290-1300 (2019).
272. Spath, S. *et al.* Dysregulation of the Cytokine GM-CSF Induces Spontaneous Phagocyte Invasion and Immunopathology in the Central Nervous System. *Immunity* **46**, 245-260 (2017).
273. Codarri, L. *et al.* RORgammat drives production of the cytokine GM-CSF in helper T cells, which is essential for the effector phase of autoimmune neuroinflammation. *Nat Immunol* **12**, 560-567 (2011).
274. Croxford, A.L. *et al.* The Cytokine GM-CSF Drives the Inflammatory Signature of CCR2+ Monocytes and Licenses Autoimmunity. *Immunity* **43**, 502-514 (2015).
275. Steinwede, K. *et al.* Local delivery of GM-CSF protects mice from lethal pneumococcal pneumonia. *J Immunol* **187**, 5346-5356 (2011).

276. Gonzalez-Juarrero, M. *et al.* Disruption of granulocyte macrophage-colony stimulating factor production in the lungs severely affects the ability of mice to control *Mycobacterium tuberculosis* infection. *J Leukoc Biol* **77**, 914-922 (2005).
277. Ingelfinger, F., De Feo, D. & Becher, B. GM-CSF: Master regulator of the T cell-phagocyte interface during inflammation. *Semin Immunol* **54**, 101518 (2021).
278. Ferguson, B., Matyszak, M.K., Esiri, M.M. & Perry, V.H. Axonal damage in acute multiple sclerosis lesions. *Brain* **120 ( Pt 3)**, 393-399 (1997).
279. Larochelle, C. *et al.* Pro-inflammatory T helper 17 directly harms oligodendrocytes in neuroinflammation. *Proc Natl Acad Sci U S A* **118** (2021).
280. Jordao, M.J.C. *et al.* Single-cell profiling identifies myeloid cell subsets with distinct fates during neuroinflammation. *Science* **363** (2019).
281. Hauser, S.L. *et al.* Ocrelizumab versus Interferon Beta-1a in Relapsing Multiple Sclerosis. *N Engl J Med* **376**, 221-234 (2017).
282. Li, R. *et al.* Proinflammatory GM-CSF-producing B cells in multiple sclerosis and B cell depletion therapy. *Sci Transl Med* **7**, 310ra166 (2015).
283. Krumbholz, M., Derfuss, T., Hohlfeld, R. & Meinl, E. B cells and antibodies in multiple sclerosis pathogenesis and therapy. *Nat Rev Neurol* **8**, 613-623 (2012).
284. Lassmann, H. Mechanisms of white matter damage in multiple sclerosis. *Glia* **62**, 1816-1830 (2014).
285. Sun, D. *et al.* Myelin antigen-specific CD8+ T cells are encephalitogenic and produce severe disease in C57BL/6 mice. *J Immunol* **166**, 7579-7587 (2001).
286. Bitsch, A., Schuchardt, J., Bunkowski, S., Kuhlmann, T. & Bruck, W. Acute axonal injury in multiple sclerosis. Correlation with demyelination and inflammation. *Brain* **123 ( Pt 6)**, 1174-1183 (2000).
287. Arrambide, G. *et al.* Aggressive multiple sclerosis (2): Treatment. *Mult Scler*, 1352458520924595 (2020).
288. Brusaferri, F. & Candelise, L. Steroids for multiple sclerosis and optic neuritis: a meta-analysis of randomized controlled clinical trials. *J Neurol* **247**, 435-442 (2000).
289. Gross, R.H. & Corboy, J.R. Monitoring, Switching, and Stopping Multiple Sclerosis Disease-Modifying Therapies. *Continuum (Minneap Minn)* **25**, 715-735 (2019).
290. Vollmer, T. The natural history of relapses in multiple sclerosis. *J Neurol Sci* **256 Suppl 1**, S5-13 (2007).
291. Moore, J.J. *et al.* Prospective phase II clinical trial of autologous haematopoietic stem cell transplant for treatment refractory multiple sclerosis. *J Neurol Neurosurg Psychiatry* **90**, 514-521 (2019).
292. Harding, K. *et al.* Clinical Outcomes of Escalation vs Early Intensive Disease-Modifying Therapy in Patients With Multiple Sclerosis. *JAMA Neurol* **76**, 536-541 (2019).
293. He, A. *et al.* Timing of high-efficacy therapy for multiple sclerosis: a retrospective observational cohort study. *Lancet Neurol* **19**, 307-316 (2020).
294. Ricard, N., Bailly, S., Guignabert, C. & Simons, M. The quiescent endothelium: signalling pathways regulating organ-specific endothelial normalcy. *Nat Rev Cardiol* **18**, 565-580 (2021).

295. Kalucka, J. *et al.* Single-Cell Transcriptome Atlas of Murine Endothelial Cells. *Cell* **180**, 764-779 e720 (2020).
296. Vanlandewijck, M. *et al.* A molecular atlas of cell types and zonation in the brain vasculature. *Nature* **554**, 475-480 (2018).
297. Graham, G.J., Handel, T.M. & Proudfoot, A.E.I. Leukocyte Adhesion: Reconceptualizing Chemokine Presentation by Glycosaminoglycans. *Trends Immunol* **40**, 472-481 (2019).
298. Nourshargh, S. & Alon, R. Leukocyte migration into inflamed tissues. *Immunity* **41**, 694-707 (2014).
299. Ley, K., Laudanna, C., Cybulsky, M.I. & Nourshargh, S. Getting to the site of inflammation: the leukocyte adhesion cascade updated. *Nat Rev Immunol* **7**, 678-689 (2007).
300. Engelhardt, B. & Ransohoff, R.M. Capture, crawl, cross: the T cell code to breach the blood-brain barriers. *Trends Immunol* **33**, 579-589 (2012).
301. Schwartz, A.B. *et al.* Elucidating the Biomechanics of Leukocyte Transendothelial Migration by Quantitative Imaging. *Front Cell Dev Biol* **9**, 635263 (2021).
302. Schulte, D. *et al.* Stabilizing the VE-cadherin-catenin complex blocks leukocyte extravasation and vascular permeability. *EMBO J* **30**, 4157-4170 (2011).
303. Alon, R. & van Buul, J.D. Leukocyte Breaching of Endothelial Barriers: The Actin Link. *Trends Immunol* **38**, 606-615 (2017).
304. Langen, U.H., Ayloo, S. & Gu, C. Development and Cell Biology of the Blood-Brain Barrier. *Annu Rev Cell Dev Biol* **35**, 591-613 (2019).
305. Alvarez, J.I. *et al.* The Hedgehog pathway promotes blood-brain barrier integrity and CNS immune quiescence. *Science* **334**, 1727-1731 (2011).
306. Daneman, R., Zhou, L., Kebede, A.A. & Barres, B.A. Pericytes are required for blood-brain barrier integrity during embryogenesis. *Nature* **468**, 562-566 (2010).
307. Stewart, P.A. & Wiley, M.J. Developing nervous tissue induces formation of blood-brain barrier characteristics in invading endothelial cells: a study using quail--chick transplantation chimeras. *Dev Biol* **84**, 183-192 (1981).
308. Armulik, A. *et al.* Pericytes regulate the blood-brain barrier. *Nature* **468**, 557-561 (2010).
309. Nikolakopoulou, A.M. *et al.* Pericyte loss leads to circulatory failure and pleiotrophin depletion causing neuron loss. *Nat Neurosci* **22**, 1089-1098 (2019).
310. Ben-Zvi, A. *et al.* Mfsd2a is critical for the formation and function of the blood-brain barrier. *Nature* **509**, 507-511 (2014).
311. Andreone, B.J. *et al.* Blood-Brain Barrier Permeability Is Regulated by Lipid Transport-Dependent Suppression of Caveolae-Mediated Transcytosis. *Neuron* **94**, 581-594 e585 (2017).
312. Torok, O. *et al.* Pericytes regulate vascular immune homeostasis in the CNS. *Proc Natl Acad Sci U S A* **118** (2021).
313. Sorokin, L. The impact of the extracellular matrix on inflammation. *Nat Rev Immunol* **10**, 712-723 (2010).
314. Quintana, F.J. Astrocytes to the rescue! Glia limitans astrocytic endfeet control CNS inflammation. *J Clin Invest* **127**, 2897-2899 (2017).

315. Kutuzov, N., Flyvbjerg, H. & Lauritzen, M. Contributions of the glycocalyx, endothelium, and extravascular compartment to the blood-brain barrier. *Proc Natl Acad Sci U S A* **115**, E9429-E9438 (2018).
316. Stenman, J.M. *et al.* Canonical Wnt signaling regulates organ-specific assembly and differentiation of CNS vasculature. *Science* **322**, 1247-1250 (2008).
317. Daneman, R. *et al.* Wnt/beta-catenin signaling is required for CNS, but not non-CNS, angiogenesis. *Proc Natl Acad Sci U S A* **106**, 641-646 (2009).
318. Guerit, S. *et al.* Astrocyte-derived Wnt growth factors are required for endothelial blood-brain barrier maintenance. *Prog Neurobiol* **199**, 101937 (2021).
319. Nitta, T. *et al.* Size-selective loosening of the blood-brain barrier in claudin-5-deficient mice. *J Cell Biol* **161**, 653-660 (2003).
320. Iadecola, C. The Neurovascular Unit Coming of Age: A Journey through Neurovascular Coupling in Health and Disease. *Neuron* **96**, 17-42 (2017).
321. Hong, Y. *et al.* Multiple sclerosis and stroke: a systematic review and meta-analysis. *BMC Neurol* **19**, 139 (2019).
322. Law, M. *et al.* Microvascular abnormality in relapsing-remitting multiple sclerosis: perfusion MR imaging findings in normal-appearing white matter. *Radiology* **231**, 645-652 (2004).
323. Adhya, S. *et al.* Pattern of hemodynamic impairment in multiple sclerosis: dynamic susceptibility contrast perfusion MR imaging at 3.0 T. *Neuroimage* **33**, 1029-1035 (2006).
324. Papadaki, E.Z. *et al.* White matter and deep gray matter hemodynamic changes in multiple sclerosis patients with clinically isolated syndrome. *Magn Reson Med* **68**, 1932-1942 (2012).
325. Haider, L. *et al.* The topography of demyelination and neurodegeneration in the multiple sclerosis brain. *Brain* **139**, 807-815 (2016).
326. Holley, J.E., Newcombe, J., Whatmore, J.L. & Gutowski, N.J. Increased blood vessel density and endothelial cell proliferation in multiple sclerosis cerebral white matter. *Neurosci Lett* **470**, 65-70 (2010).
327. Lin, H. *et al.* Extracellular Lactate Dehydrogenase A Release From Damaged Neurons Drives Central Nervous System Angiogenesis. *EBioMedicine* **27**, 71-85 (2018).
328. Seabrook, T.J. *et al.* Angiogenesis is present in experimental autoimmune encephalomyelitis and pro-angiogenic factors are increased in multiple sclerosis lesions. *J Neuroinflammation* **7**, 95 (2010).
329. MacMillan, C.J. *et al.* Murine experimental autoimmune encephalomyelitis is diminished by treatment with the angiogenesis inhibitors B20-4.1.1 and angiostatin (K1-3). *PLoS One* **9**, e89770 (2014).
330. MacMillan, C.J. *et al.* Bevacizumab diminishes experimental autoimmune encephalomyelitis by inhibiting spinal cord angiogenesis and reducing peripheral T-cell responses. *J Neuropathol Exp Neurol* **71**, 983-999 (2012).
331. Roscoe, W.A., Welsh, M.E., Carter, D.E. & Karlik, S.J. VEGF and angiogenesis in acute and chronic MOG((35-55)) peptide induced EAE. *J Neuroimmunol* **209**, 6-15 (2009).
332. Dore-Duffy, P., Wencel, M., Katyshev, V. & Cleary, K. Chronic mild hypoxia ameliorates chronic inflammatory activity in myelin oligodendrocyte glycoprotein (MOG) peptide induced experimental autoimmune encephalomyelitis (EAE). *Adv Exp Med Biol* **701**, 165-173 (2011).

333. Esen, N., Serkin, Z. & Dore-Duffy, P. Induction of vascular remodeling: a novel therapeutic approach in EAE. *J Neurol Sci* **333**, 88-92 (2013).
334. Zhou, T. *et al.* Microvascular endothelial cells engulf myelin debris and promote macrophage recruitment and fibrosis after neural injury. *Nat Neurosci* **22**, 421-435 (2019).
335. Munji, R.N. *et al.* Profiling the mouse brain endothelial transcriptome in health and disease models reveals a core blood-brain barrier dysfunction module. *Nat Neurosci* **22**, 1892-1902 (2019).
336. Derada Troletti, C. *et al.* Inflammation-induced endothelial to mesenchymal transition promotes brain endothelial cell dysfunction and occurs during multiple sclerosis pathophysiology. *Cell Death Dis* **10**, 45 (2019).
337. Derada Troletti, C., de Goede, P., Kamermans, A. & de Vries, H.E. Molecular alterations of the blood-brain barrier under inflammatory conditions: The role of endothelial to mesenchymal transition. *Biochim Biophys Acta* **1862**, 452-460 (2016).
338. Kovacic, J.C. *et al.* Endothelial to Mesenchymal Transition in Cardiovascular Disease: JACC State-of-the-Art Review. *J Am Coll Cardiol* **73**, 190-209 (2019).
339. Nishihara, H. *et al.* Intrinsic blood-brain barrier dysfunction contributes to multiple sclerosis pathogenesis. *Brain* (2022).
340. Spencer, J.I., Bell, J.S. & DeLuca, G.C. Vascular pathology in multiple sclerosis: reframing pathogenesis around the blood-brain barrier. *J Neurol Neurosurg Psychiatry* **89**, 42-52 (2018).
341. Halder, S.K. & Milner, R. Hypoxia in multiple sclerosis; is it the chicken or the egg? *Brain* **144**, 402-410 (2021).
342. Marchetti, L. & Engelhardt, B. Immune cell trafficking across the blood-brain barrier in the absence and presence of neuroinflammation. *Vasc Biol* **2**, H1-H18 (2020).
343. Daneman, R. *et al.* The mouse blood-brain barrier transcriptome: a new resource for understanding the development and function of brain endothelial cells. *PLoS One* **5**, e13741 (2010).
344. Bo, L. *et al.* Distribution of immunoglobulin superfamily members ICAM-1, -2, -3, and the beta 2 integrin LFA-1 in multiple sclerosis lesions. *J Neuropathol Exp Neurol* **55**, 1060-1072 (1996).
345. Cannella, B. & Raine, C.S. The adhesion molecule and cytokine profile of multiple sclerosis lesions. *Ann Neurol* **37**, 424-435 (1995).
346. Vos, C.M. *et al.* Blood-brain barrier alterations in both focal and diffuse abnormalities on postmortem MRI in multiple sclerosis. *Neurobiol Dis* **20**, 953-960 (2005).
347. Sathyanadan, K., Coisne, C., Enzmann, G., Deutsch, U. & Engelhardt, B. PSGL-1 and E/P-selectins are essential for T-cell rolling in inflamed CNS microvessels but dispensable for initiation of EAE. *Eur J Immunol* **44**, 2287-2294 (2014).
348. Doring, A., Wild, M., Vestweber, D., Deutsch, U. & Engelhardt, B. E- and P-selectin are not required for the development of experimental autoimmune encephalomyelitis in C57BL/6 and SJL mice. *J Immunol* **179**, 8470-8479 (2007).
349. Osmers, I., Bullard, D.C. & Barnum, S.R. PSGL-1 is not required for development of experimental autoimmune encephalomyelitis. *J Neuroimmunol* **166**, 193-196 (2005).

350. Steffen, B.J., Butcher, E.C. & Engelhardt, B. Evidence for involvement of ICAM-1 and VCAM-1 in lymphocyte interaction with endothelium in experimental autoimmune encephalomyelitis in the central nervous system in the SJL/J mouse. *Am J Pathol* **145**, 189-201 (1994).
351. Yednock, T.A. *et al.* Prevention of experimental autoimmune encephalomyelitis by antibodies against alpha 4 beta 1 integrin. *Nature* **356**, 63-66 (1992).
352. Leger, O.J. *et al.* Humanization of a mouse antibody against human alpha-4 integrin: a potential therapeutic for the treatment of multiple sclerosis. *Hum Antibodies* **8**, 3-16 (1997).
353. Polman, C.H. *et al.* A randomized, placebo-controlled trial of natalizumab for relapsing multiple sclerosis. *N Engl J Med* **354**, 899-910 (2006).
354. Rudick, R.A. *et al.* Natalizumab plus interferon beta-1a for relapsing multiple sclerosis. *N Engl J Med* **354**, 911-923 (2006).
355. Maria, Z., Turner, E., Agasing, A., Kumar, G. & Axtell, R.C. Pertussis Toxin Inhibits Encephalitogenic T-Cell Infiltration and Promotes a B-Cell-Driven Disease during Th17-EAE. *Int J Mol Sci* **22** (2021).
356. Robinson, D., Cockle, S., Singh, B. & Strejan, G.H. Native, but not genetically inactivated, pertussis toxin protects mice against experimental allergic encephalomyelitis. *Cell Immunol* **168**, 165-173 (1996).
357. Holman, D.W., Klein, R.S. & Ransohoff, R.M. The blood-brain barrier, chemokines and multiple sclerosis. *Biochim Biophys Acta* **1812**, 220-230 (2011).
358. Williams, J.L., Holman, D.W. & Klein, R.S. Chemokines in the balance: maintenance of homeostasis and protection at CNS barriers. *Front Cell Neurosci* **8**, 154 (2014).
359. Minten, C. *et al.* DARC shuttles inflammatory chemokines across the blood-brain barrier during autoimmune central nervous system inflammation. *Brain* **137**, 1454-1469 (2014).
360. Marchetti, L. *et al.* ACKR1 favors transcellular over paracellular T-cell diapedesis across the blood-brain barrier in neuroinflammation in vitro. *Eur J Immunol* **52**, 161-177 (2022).
361. Steiner, O. *et al.* Differential roles for endothelial ICAM-1, ICAM-2, and VCAM-1 in shear-resistant T cell arrest, polarization, and directed crawling on blood-brain barrier endothelium. *J Immunol* **185**, 4846-4855 (2010).
362. Gorina, R., Lyck, R., Vestweber, D. & Engelhardt, B. beta2 integrin-mediated crawling on endothelial ICAM-1 and ICAM-2 is a prerequisite for transcellular neutrophil diapedesis across the inflamed blood-brain barrier. *J Immunol* **192**, 324-337 (2014).
363. Haghayegh Jahromi, N. *et al.* Intercellular Adhesion Molecule-1 (ICAM-1) and ICAM-2 Differentially Contribute to Peripheral Activation and CNS Entry of Autoaggressive Th1 and Th17 Cells in Experimental Autoimmune Encephalomyelitis. *Front Immunol* **10**, 3056 (2019).
364. Bullard, D.C. *et al.* Intercellular adhesion molecule-1 expression is required on multiple cell types for the development of experimental autoimmune encephalomyelitis. *J Immunol* **178**, 851-857 (2007).
365. Calvier, L. *et al.* Reelin depletion protects against autoimmune encephalomyelitis by decreasing vascular adhesion of leukocytes. *Sci Transl Med* **12** (2020).
366. Calvier, L. *et al.* Apolipoprotein E receptor 2 deficiency decreases endothelial adhesion of monocytes and protects against autoimmune encephalomyelitis. *Sci Immunol* **6** (2021).

367. Winger, R.C., Koblinski, J.E., Kanda, T., Ransohoff, R.M. & Muller, W.A. Rapid remodeling of tight junctions during paracellular diapedesis in a human model of the blood-brain barrier. *J Immunol* **193**, 2427-2437 (2014).
368. Wimmer, I. *et al.* PECAM-1 Stabilizes Blood-Brain Barrier Integrity and Favors Paracellular T-Cell Diapedesis Across the Blood-Brain Barrier During Neuroinflammation. *Front Immunol* **10**, 711 (2019).
369. Abadier, M. *et al.* Cell surface levels of endothelial ICAM-1 influence the transcellular or paracellular T-cell diapedesis across the blood-brain barrier. *Eur J Immunol* **45**, 1043-1058 (2015).
370. Lutz, S.E. *et al.* Caveolin1 Is Required for Th1 Cell Infiltration, but Not Tight Junction Remodeling, at the Blood-Brain Barrier in Autoimmune Neuroinflammation. *Cell Rep* **21**, 2104-2117 (2017).
371. Wu, H. *et al.* Caveolin-1 Is Critical for Lymphocyte Trafficking into Central Nervous System during Experimental Autoimmune Encephalomyelitis. *J Neurosci* **36**, 5193-5199 (2016).
372. Seifert, T., Bauer, J., Weissert, R., Fazekas, F. & Storch, M.K. Differential expression of sonic hedgehog immunoreactivity during lesion evolution in autoimmune encephalomyelitis. *J Neuropathol Exp Neurol* **64**, 404-411 (2005).
373. Wang, Y., Imitola, J., Rasmussen, S., O'Connor, K.C. & Khoury, S.J. Paradoxical dysregulation of the neural stem cell pathway sonic hedgehog-Gli1 in autoimmune encephalomyelitis and multiple sclerosis. *Ann Neurol* **64**, 417-427 (2008).
374. Podjaski, C. *et al.* Netrin 1 regulates blood-brain barrier function and neuroinflammation. *Brain* **138**, 1598-1612 (2015).
375. Mulero, P. *et al.* Netrin-1 and multiple sclerosis: a new biomarker for neuroinflammation? *Eur J Neurol* **24**, 1108-1115 (2017).
376. Choi, E.Y. *et al.* Del-1, an endogenous leukocyte-endothelial adhesion inhibitor, limits inflammatory cell recruitment. *Science* **322**, 1101-1104 (2008).
377. Choi, E.Y. *et al.* Developmental endothelial locus-1 is a homeostatic factor in the central nervous system limiting neuroinflammation and demyelination. *Mol Psychiatry* **20**, 880-888 (2015).
378. Goris, A. *et al.* New candidate loci for multiple sclerosis susceptibility revealed by a whole genome association screen in a Belgian population. *J Neuroimmunol* **143**, 65-69 (2003).
379. McCandless, E.E., Wang, Q., Woerner, B.M., Harper, J.M. & Klein, R.S. CXCL12 limits inflammation by localizing mononuclear infiltrates to the perivascular space during experimental autoimmune encephalomyelitis. *J Immunol* **177**, 8053-8064 (2006).
380. McCandless, E.E. *et al.* Pathological expression of CXCL12 at the blood-brain barrier correlates with severity of multiple sclerosis. *Am J Pathol* **172**, 799-808 (2008).
381. Kohler, R.E. *et al.* Antagonism of the chemokine receptors CXCR3 and CXCR4 reduces the pathology of experimental autoimmune encephalomyelitis. *Brain Pathol* **18**, 504-516 (2008).
382. Hanes, M.S. *et al.* Dual targeting of the chemokine receptors CXCR4 and ACKR3 with novel engineered chemokines. *J Biol Chem* **290**, 22385-22397 (2015).
383. Cruz-Orengo, L. *et al.* CXCR7 influences leukocyte entry into the CNS parenchyma by controlling abluminal CXCL12 abundance during autoimmunity. *J Exp Med* **208**, 327-339 (2011).

384. Cruz-Orengo, L. *et al.* CXCR7 antagonism prevents axonal injury during experimental autoimmune encephalomyelitis as revealed by in vivo axial diffusivity. *J Neuroinflammation* **8**, 170 (2011).
385. Sallusto, F. Heterogeneity of Human CD4(+) T Cells Against Microbes. *Annu Rev Immunol* **34**, 317-334 (2016).
386. Kitamura, K., Farber, J.M. & Kelsall, B.L. CCR6 marks regulatory T cells as a colon-tropic, IL-10-producing phenotype. *J Immunol* **185**, 3295-3304 (2010).
387. Yamazaki, T. *et al.* CCR6 regulates the migration of inflammatory and regulatory T cells. *J Immunol* **181**, 8391-8401 (2008).
388. Schnell, A. *et al.* Stem-like intestinal Th17 cells give rise to pathogenic effector T cells during autoimmunity. *Cell* **184**, 6281-6298 e6223 (2021).
389. Zhang, H., Zhong, W., Zhou, G., Ding, X. & Chen, H. Expression of chemokine CCL20 in ulcerative colitis. *Mol Med Rep* **6**, 1255-1260 (2012).
390. Kivisakk, P. *et al.* Natalizumab treatment is associated with peripheral sequestration of proinflammatory T cells. *Neurology* **72**, 1922-1930 (2009).
391. Kurmaeva, E. *et al.* T cell-associated alpha4beta7 but not alpha4beta1 integrin is required for the induction and perpetuation of chronic colitis. *Mucosal Immunol* **7**, 1354-1365 (2014).
392. Cosorich, I. *et al.* High frequency of intestinal TH17 cells correlates with microbiota alterations and disease activity in multiple sclerosis. *Sci Adv* **3**, e1700492 (2017).
393. Duc, D. *et al.* Disrupting Myelin-Specific Th17 Cell Gut Homing Confers Protection in an Adoptive Transfer Experimental Autoimmune Encephalomyelitis. *Cell Rep* **29**, 378-390 e374 (2019).
394. Gago da Graca, C., van Baarsen, L.G.M. & Mebius, R.E. Tertiary Lymphoid Structures: Diversity in Their Development, Composition, and Role. *J Immunol* **206**, 273-281 (2021).
395. Pippi, E. *et al.* Tertiary Lymphoid Structures: Autoimmunity Goes Local. *Front Immunol* **9**, 1952 (2018).
396. Pikor, N.B. *et al.* Integration of Th17- and Lymphotoxin-Derived Signals Initiates Meningeal-Resident Stromal Cell Remodeling to Propagate Neuroinflammation. *Immunity* **43**, 1160-1173 (2015).
397. Varona, R. *et al.* CCR6-deficient mice have impaired leukocyte homeostasis and altered contact hypersensitivity and delayed-type hypersensitivity responses. *J Clin Invest* **107**, R37-45 (2001).
398. Rangel-Moreno, J. *et al.* The development of inducible bronchus-associated lymphoid tissue depends on IL-17. *Nat Immunol* **12**, 639-646 (2011).
399. Eberl, G. Inducible lymphoid tissues in the adult gut: recapitulation of a fetal developmental pathway? *Nat Rev Immunol* **5**, 413-420 (2005).
400. Lochner, M. *et al.* Microbiota-induced tertiary lymphoid tissues aggravate inflammatory disease in the absence of RORgamma t and LTi cells. *J Exp Med* **208**, 125-134 (2011).
401. Mitsdoerffer, M. *et al.* Formation and immunomodulatory function of meningeal B cell aggregates in progressive CNS autoimmunity. *Brain* **144**, 1697-1710 (2021).
402. Peters, A. *et al.* Th17 cells induce ectopic lymphoid follicles in central nervous system tissue inflammation. *Immunity* **35**, 986-996 (2011).

403. Lu, Z. *et al.* Regulation of intercellular biomolecule transfer-driven tumor angiogenesis and responses to anticancer therapies. *J Clin Invest* **131** (2021).
404. Schaffenrath, J. *et al.* Blood-brain barrier alterations in human brain tumors revealed by genome-wide transcriptomic profiling. *Neuro Oncol* **23**, 2095-2106 (2021).
405. Potenta, S., Zeisberg, E. & Kalluri, R. The role of endothelial-to-mesenchymal transition in cancer progression. *Br J Cancer* **99**, 1375-1379 (2008).
406. Yamaguchi, A. *et al.* Temporal expression profiling of DAMPs-related genes revealed the biphasic post-ischemic inflammation in the experimental stroke model. *Mol Brain* **13**, 57 (2020).
407. Androvic, P. *et al.* Decoding the Transcriptional Response to Ischemic Stroke in Young and Aged Mouse Brain. *Cell Rep* **31**, 107777 (2020).
408. Zheng, K. *et al.* Single-cell RNA-seq reveals the transcriptional landscape in ischemic stroke. *J Cereb Blood Flow Metab* **42**, 56-73 (2022).
409. Cuartero, M.I. *et al.* N2 neutrophils, novel players in brain inflammation after stroke: modulation by the PPARgamma agonist rosiglitazone. *Stroke* **44**, 3498-3508 (2013).
410. Sas, A.R. *et al.* A new neutrophil subset promotes CNS neuron survival and axon regeneration. *Nat Immunol* **21**, 1496-1505 (2020).
411. El Amki, M. *et al.* Neutrophils Obstructing Brain Capillaries Are a Major Cause of No-Reflow in Ischemic Stroke. *Cell Rep* **33**, 108260 (2020).
412. Veglia, F., Sanseviero, E. & Gabrilovich, D.I. Myeloid-derived suppressor cells in the era of increasing myeloid cell diversity. *Nat Rev Immunol* **21**, 485-498 (2021).
413. Rust, R. Insights into the dual role of angiogenesis following stroke. *J Cereb Blood Flow Metab* **40**, 1167-1171 (2020).
414. Chen, K.H. *et al.* Intravenous administration of xenogenic adipose-derived mesenchymal stem cells (ADMSC) and ADMSC-derived exosomes markedly reduced brain infarct volume and preserved neurological function in rat after acute ischemic stroke. *Oncotarget* **7**, 74537-74556 (2016).
415. Doepfner, T.R. *et al.* Extracellular Vesicles Improve Post-Stroke Neuroregeneration and Prevent Postischemic Immunosuppression. *Stem Cells Transl Med* **4**, 1131-1143 (2015).
416. Xin, H. *et al.* Systemic administration of exosomes released from mesenchymal stromal cells promote functional recovery and neurovascular plasticity after stroke in rats. *J Cereb Blood Flow Metab* **33**, 1711-1715 (2013).